

UCSF

UC San Francisco Electronic Theses and Dissertations

Title

Solution, gas-phase, and computational reaction profiles for heterolytic dissociation of charged substrates as models for NAD⁺ hydrolysis

Permalink

<https://escholarship.org/uc/item/8c8045w9>

Author

Buckley, Neil,

Publication Date

1995

Peer reviewed|Thesis/dissertation

**Solution, Gas-Phase, and Computational Reaction Profiles for Heterolytic
Dissociation of Charged Substrates as Models for NAD⁺ Hydrolysis**

by

Neil Buckley

DISSERTATION

Submitted in partial satisfaction of the requirements for the degree of

DOCTOR OF PHILOSOPHY

in

Pharmaceutical Chemistry

in the

GRADUATE DIVISION

of the

UNIVERSITY OF CALIFORNIA

San Francisco



**Dedicated to the memory of
Richard Allen Sneen**

Preface

The danger inherent in offering an Irishman--especially an old one with a checkered past--the chance to write a preface with no restrictions on content is that he will tell a story, certainly autobiographical and probably political. I will tell a very brief version of the story of how I came to finish my Ph.D. 32 years after I started it elsewhere that has a direct bearing on the work reported in this dissertation, and on the man to whom it is dedicated. Without this, it seems to me that the work would be incomplete. Because one of the bedevilmments of middle age is "what if," I am taking this opportunity to sum up, at least in this context, what has gone before.

As it happens, I am writing this Preface on the weekend of the 20th anniversary of the liberation of Saigon and the end of the Vietnam War, the event that fundamentally altered the political and social structure of the nation and changed all our lives utterly, just as the cultural and political structures and attitudes it spawned continue to influence the life of the nation. Despite the ardent, hopeful, and patronizing declarations of the worst cynics, Vietnam in all its aspects is still with us, unresolved and unforgotten. It is certainly still with me.

I was born eight months before Pearl Harbor, so I came of age during the 1950s, a time of general economic prosperity generally looked upon fondly as a time of tranquillity. This is of course not true. The historical period started with the Korean War in 1949 and ended with the Kennedy assassination in 1963. It was a time of great political upheaval internationally and internally. When I entered Penn State in 1959, in that first wave of working class kids admitted to universities in response to Eisenhower's National Defense Education Act strategy to increase the number and quality of scientists and engineers needed to fight the Cold War, all the disparate elements that led to the student movement in the middle 60s were in place, trying out, although few if any of us saw them clearly. By the time I

entered graduate school in 1963, however, the issues, especially racism, were fairly clear.

Independent of these events, I had an absolutely horrible academic record for my first two and a half years at Penn State. When I started doing research as part of the requirement of an undergraduate thesis project, my academic performance improved immediately. Because of a change from a semester to a term system, and a concomitant change in the curriculum, in the middle of our program, our class was given free choice of electives for two years. I took English literature classes and seminars, including graduate level work, and graduated with a formal minor in English. I went from severe academic probation to the Dean's list in one term, and finished my last year and a half with excellent grades. The overall record was mediocre, however. My research work on cyclopropyl carbocations had been very fruitful and led to a *JACS* communication that is still cited. Herman Richey, who directed my research, had faith that I could do well in graduate school and worked out a deal with Nathan Kornblum that got me admitted to the graduate program at Purdue.

I chose to continue work in physical organic, and joined the Sneen group. Sneen and Weiner had just published their first work on what became the famous Sneen ion-pair hypothesis for nucleophilic substitution reactions. The work was being carried on by John Larsen, a tall, sandy-haired Dane from Hartford who walked with a list to the left. We became fast friends (and remain so to this day). Sneen had a number of approaches to take to continue the work and examine the mechanistic possibilities in detail. The one I chose--actually, the one we agreed on; I designed the study and took it to him--involved bridgehead cations and isotope exchange in labeled benzoates, an extension of Doring's experiments on internal return. One of the other approaches involved benzyl dimethylsulfoniums,

work that was begun after I left in 1965. This is of course some of the work I did for *this* dissertation.

Between the fall of 1963 and the Spring of 1965, John Kennedy was murdered; the civil rights struggle in the South exploded: the beatings and dog attacks at the many lunch counters and, significantly, at the Selma bridge had occurred, Goodman, Schwerner, and Chaney were dead, buried in a swamp; Johnson had occupied the Dominican Republic with the First Marines; The Free Speech Movement at Berkeley had erupted; the Goldwater-Johnson campaign had polarized the nation even further; the War in Vietnam was starting to escalate and the draft had begun in earnest. I had been discharged from the Army reserve in 1964. Despite the fact that I faced no direct danger from these events, like so many of my generation I was deeply affected by them. It was necessary to be engaged, to do something, not to be complicit by being passive.

What I chose to do in 1965 seems unremarkable now, but it was a step. I applied to and was accepted in the English Graduate Program at Penn State in the belief that I might do some good and bring about change if I taught humanities and gave students an alternative based on humanistic values. That was a noble thought, but in the context of the times a very naive one. I finished what I had been doing in the lab at Purdue, moved back to central Pennsylvania, wrote up my work as an M.S. thesis, and within a week was teaching freshman composition at Penn State. Over the fall and winter of 1965-66, the war escalated and racial divisions deepened. It was soon clear that it was not sufficient to attempt to influence the course of events in traditional ways--pedagogy was too slow; the political process was (and remains) a sump of cynicism and bad compromise: we *knew* that the Tonkin Gulf incident was staged--but to engage them directly and try to stop them. It was not long before I was fully involved in the antiwar movement.

UCSF LIBRARY

This period, widely analyzed and discussed though it has been, is still largely misunderstood. What most critics of the antiwar movement fail to grasp--or to admit--is that those of us who were deeply committed and worked full time against the War had not been born angry and destructive radicals. We were in the main run-of-the-mill, average, normal working class kids with run-of-the-mill, average, normal dreams and aspirations who, given the choice, would have preferred to live out normal, calm and quiet lives and to do our work as best we could, whatever it happened to be. Because there was such a glaring disparity between what we had been taught to believe about freedom and equality and justice and what the political process yielded, we were forced by circumstance to try and change the system to become what it had always promised to be. Thus the antiwar movement in its wider context as a movement for social, racial, and economic justice was not an aberration but the direct consequence of deeply held and particularly American ideals. It was no political or philosophical error that the leading antiwar group was Students for a *Democratic* Society (SDS).

In the winter of 1967, I was asked to join the national staff of SDS. After mulling it over for a while, I decided it was the right thing to do. I resigned from my second graduate program and packed a duffel. My friend John Low drove me out to the highway, and said goodbye. I stuck out my thumb and lit out for the territory.

And so 30 years later I am about to finish a Ph.D. in chemistry. Had there not been a War in Vietnam or the need for a civil rights movement, I might have done the work I did in the early 1990s in the late 1960s. I have been told that Sneen took my leaving as a personal failure, and that in part it led to his later decline. I have no idea if this is true or not. Another of my classmates left the group about a year after I did, for different reasons. It was clearly the times,

whatever the motivation, personal or ideological. As it turned out, my work forms the basis for a refutation of the last vestige of Sneen's mechanism. In the context, I felt horrible about this, and worried that when the papers appeared he would feel further betrayed. I expressed this view in a letter to Ed Thornton, who had published work on Sneen's mechanism. He wrote back that "your [work] serves the purpose of solving a difficult scientific problem, which is what I ...and I'm sure Sneen too, were really after."

In any case, by the early 1970s Sneen's mechanism had been savaged and his ideas stolen, he claimed, by those who savaged him. He went into a personal and scientific decline. It would finally be realized that he was an alcoholic, and he was institutionalized. He stopped drinking and returned to teaching, but he was treated shabbily by the department. His last assignment before he retired, a major figure in physical organic chemistry of the modern era, was to teach organic to nursing students in a room with no blackboard. I spoke with him by phone in the middle of the afternoon one day several years ago, and he was clearly drunk. That was the last time I or any of his former student had any contact with him. He died, alone and unattended, in a clinic in Wisconsin in 1993. None of us heard of his death until last fall, when the Chemistry Department at Purdue printed a brief announcement of his death in the Newsletter. The cause of death was not listed. This dissertation is dedicated to his memory.

UCSF LIBRARY

Acknowledgments. I thank Norm Oppenheimer for having me--a singular act of courage for one so young--and for paying the bills. The labmates--Tony Handlon (who is discovering that life in the drug industry is much as I warned him it would be), Tom Xu (a good comrade who loved a good story, and who insisted that we always be *chung*, whether we wanted to be or not), Larry Wainschel (who claims that Johnny Hodges and Ornette Coleman *sound alike*), and Gary Henehan (who is from Galway, the besotted part, and has done pretty well for the son of a man who ran an abattoir)--made life *much* easier, but they all talked too much, especially Henehan, and would often *insist* on sojourning to the Courtyard for a ritual known as "Smokie Time," a phrase inherited by us through Wainschel who learned it from his low-riding colleagues at Occidental College.*

Al Burlingame and Paul Ortiz de Montellano are thanked for reading the dissertation; they are thanked much more for signing it. They are also thanked, along with Tom Scanlan, Martin Shetlar, and Dan Santi, for being members of my Orals committee.

Money: The National Institutes of Health and the State of California, through a biotechnology grant, provided funds for this work.

The computations were done on a Gateway 2000 486/66V that I bought with the 3-month salary buyout provided by the UC Benefits Program upon my retirement in Verip II--this is a very long story--which is thanked for this generous contribution. It wasn't enough, of course, but these are lean times in the postindustrial period.

The Graduate Division provided a \$1000 student research grant that was used to buy D₂O.

* There is a story here about burros and beer in Boyle Heights, but you'll have to ask Larry.

People: The kinetics took an *inordinate* amount of NMR time, and Vladimir Basus and the various curators--Kelly Hom, Jeff McDonald, and Steve Miller--and a good many regular users ignored the rules about how many hours a day I could have on the GE 300 MHz machine. Vibacker Shah, who ran ^{13}C overnight, kindly allowed me to turn off his acquisitions. Shawna Farr-Jones helped with the funny experiments that didn't work. James DeVoss helped with the ^{13}C spectra, and also talked too much.

Jim Caldwell, Randy Radmer, and Peter Kollman provided helpful insights into the computational methods used here. Dave Ferguson yelled at me a few times, but because that's the way Ferguson is, that too was helpful. The work done with Peter and Stefan Schröder led eventually to the computations done and provided some valuable insights early on. Tom Slee, who was then at Hyperchem, answered a lot of cranky questions by e-mail.

Al Burlingame and David Maltby collaborated on the gas-phase work and are thanked for their efforts. Brad Gibson and Arnie Falick spent some time explaining some of the subtleties of LSIMS and mass spec in general.

Dick Shafer, whom I've known longer than anybody on the faculty, spent an inordinate amount of time talking--and writing e-mail--about computers and software. He also had his colleague Academician A.S. Zasedatelev, Molecular Biology Institute, Leningrad, obtain azide activity data from the Soviet Archive VINITI. I am grateful to both for their help.

Ken Dill answered some questions about the hydrophobic effect and rattled off some references with no reference to written materials, which turned out to be just what he said they would be. A steel trap mind, that.

At other institutions: Charles Perrin (UCSD) was by his admission "harsh" in his review of one of the papers, but was dead on the money in what he said. Later, at my request, he came out from behind the barrier of anonymity and

corresponded about the matter; I am grateful to him for this insight and his effort. John Richard (SUNY Buffalo) read several manuscripts and exchanged letters and data, and provided one timely knock up side the head when I tried to get silly. While we disagree about a lot of this, the exchange was fruitful. Barbara Schowen (University of Kansas) very generously sent a copy of her dissertation at MIT with Swain, which was not generally available. She is thanked for this kindness. James Fishbein (Wake Forest) read several of the manuscripts upon which this dissertation is based, and even reviewed at least one (and was not kind; but then, I've been reviewing his papers for years and have not always been kind). He is thanked for his time and insight. Dennis Kevill (Northern Illinois University) generously exchanged preprints and data. Edward Thornton (Penn) made very insightful comments on a manuscript and offered advice; he even *signed* a review for *The Journal of Organic Chemistry*. Fred Menger (Emory) read several manuscripts and offered advice; he also sends along his Christmas Letter, which is much appreciated. The editors of *The Journal of Organic Chemistry*--Clayton Heathcock, Dale Boger, and Barry Carpenter--were very helpful; Heathcock, in particular, helped resolve a dicey political matter. Dick Schowen at *The Journal of the American Chemical Society* was kind as always.

Instigators: Rob Ronald (Washington State), with whom I slaved in industry, who was chair of the Faculty Search Committee in the Chemistry Department in 1986 when, with a B.S. and a lot of gall, I applied for the position, said: "Buckley, get your Ph.D. then come and talk to me. Bite the bullet." (This is an edited version.) Chris Michejda, Head of the Drug Design section at the NCI Frederick Research Facility (who knows *everybody*) after he hauled me out to the East Coast in the winter of 1987 for an interview and a talk, said: "Buckley, get your Ph.D.; otherwise, forget it. I can't get you on here without it." Dennis Deen (Associate Director, Brain Tumor Research Center, UCSF) said: "Buckley, you

can either get your Ph.D. or stay here and edit my papers for the rest of your life. Which would you prefer?" (This is *heavily* edited.). Larry Marton (then Chair of Laboratory Medicine, and Principle Investigator, Brain Tumor Research Center; later Dean, School of Medicine, University of Wisconsin), upon hearing that I was talking with another school about getting a Ph.D., said: "If you want to stay here--and you *should* want to stay here--I'll see what I can do." And he did. Lloyd Kossaloff, who was then Dean of the Graduate School, made it happen.

Friends and family:

John Troyer spent a lot of time talking about the various intricacies of computers and computations. He also house-sat several times and took care of Josie and Clawdius when Ruth and I would go on vacation. (Early on, Randy and Bonnie Radmer house-sat and took care of Dartin, Asia, Blanche, Josie and Clawdius.)

Tom Scalan was always there to listen. He made my life much easier.

John Low (III) (Dundalk Community College, Baltimore County, MD) is not a chemist. (His father John Low [II] was one hell of a scientist who invented polarized light photomicrography. A lot of that rubbed off on his son. His uncle Joseph Low was a famous illustrator who did *New Yorker* covers for Ross, among other things. A lot of *that* rubbed off on his nephew.) Next to Larsen, he is my oldest friend. We were graduate students in a Ph.D. program in English at Penn State; neither of us finished that either (although he got an M.A.). I once got him fired from a teaching job; he said it was one of the nicest things I ever did for him (considering the college and the little right-wing Indiana town it was in, it was). Over the last seven years when I would say to him "I am *sick* of this" he would say "Hey! WHAT IS THE LONG-TERM GOAL HERE?" (You could hear the hyphen, actually.)

John Larsen (Lehigh) and I go back 30 years to our youthful graduate school days. He finished and went out and got famous as a chemist (which is how it should be). For the last seven years he has read and responded to e-mail about the chemistry *daily*, rate by rate, point by point. Silly idea by not so silly idea. He has been patient *in the extreme*, constructive, full of ideas, and encouraging. He is my oldest friend.

Finally, and most of all, I thank my wife Ruth Burke, who put up with all this--most of which drove her nuts--but never for a minute let me down.

**Solution, Gas-Phase, and Computational Reaction Profiles for Heterolytic
Dissociation of Charged Substrates as Models for NAD⁺ Hydrolysis**

Abstract

Neil Buckley

Model systems were studied to provide insight into the enzyme-catalyzed cleavage of the ribosyl-nicotinamide bond. Kinetics of the solvolysis and azide substitution reactions of substituted benzyl pyridiniums in water are strictly concerted second-order reactions that do not involve ion-dipole complex intermediates. High, negative entropies of solvation of the pyridine at the transition state prevents unimolecular bond dissociation. Katritzky's suggestion (Katritzky, A.R.; Brycki, B.E. *Chem. Soc. Rev.* 1990, 19, 83-105) that ion-dipole complexes are intermediates is challenged based on the results of semi-empirical computations. Kinetics and product studies for the hydrolysis and nucleophilic substitution reactions of substituted benzyldimethylsulfoniums show that the mechanism for (4-methoxybenzyl)dimethylsulfonium is mixed S_N1/S_N2; with less electron-donating substituents, the hydrolysis and substitution reactions are S_N2. Ion-dipole complexes are not intermediates. Reactions of (4-methoxybenzyl)-dimethylsulfonium with nucleophiles only (no control of ionic strength) occur through a preassociated concerted mechanism, but not the scheme advocated by Jencks (Jencks, W.P. *Acc. Chem. Res.* 1980, 13, 161-169; *Chem. Soc. Rev.* 1981, 10, 345-375), the rationale for which is questioned. Experimental relative rates for the gas-phase dissociation of β-nicotinamide arabinosides, substituted benzyldimethylsulfoniums, and substituted benzyl pyridiniums and semi-empirically computed reaction profiles are consistent with dissociation through

ion-dipole complexes. The computed ΔH^\ddagger correlate with gas-phase k_{rel} and solution ΔH^\ddagger and ΔG^\ddagger for the arabinosides. For the benzyls, gas-phase k_{rel} correlate with σ^+ and $\delta\Delta G^\circ$ scales. Because of changes in mechanism between phases, the Hammett plots for the solution reactions are different. The ribosyl oxocarbenium ions are intrinsically more stable than the 4-methoxybenzyl carbenium ion, a solvent-equilibrated intermediate in solution. Extensive computations show that substrates with charged leaving groups that can form oxocarbenium ions react either as a function of the leaving group (pyridiniums, sulfoniums, aniliniums) or as a function of the stability of the oxocarbenium ion (water, alcohols, dialkyl ethers). The computations show that ribosides and glucosides should have the same mechanism of acid-catalyzed hydrolysis, and suggest the elements that are important for specific or general acid catalysis. The entropies of solvation of various substrates show that NAD^+ glycosylhydrolases "catalyze" an S_N1 reaction by removing the entropic barrier to dissociation.

Table of Contents

Abstract	xiv
List of Tables	xxv
List of Figures	xxvii
Chapter 1 Introduction	1
Ion Pairs	2
<i>3-Aryl-2-Butyl Systems</i>	4
<i>Winstein Scheme</i>	5
<i>Sneen Scheme</i>	6
<i>Jencks Criticism</i>	9
Stability of Oxocarbenium Ions	10
Nicotinamide Adenosine Dinucleotide (NAD⁺) and β-Nicotinamide Riboside and Arabinoside	
Hydrolysis	11
Study Design	13
<i>Benzyl Pyridiniums</i>	14
<i>Benzyl Dimethylsulfoniums</i>	14
<i>Gas-Phase Dissociation</i>	14
<i>Computational Studies of Related Reactions</i> ..	15
References and Notes	16
Chapter 2 The Solvolysis and Azide Substitution Reactions of Benzyl Pyridiniums in Water	20
Introduction	21

Experimental Section	24
<i>General</i>	24
<i>Syntheses</i>	24
<i>Kinetics</i>	25
<i>Suppression Studies</i>	26
<i>Computational Methods</i>	26
Results	27
<i>Azide Kinetics</i>	27
3'-Cyanopyridiniums.....	27
Nicotinamides.....	28
Pyridiniums.....	31
<i>D₂O Only Kinetics</i>	31
3'-Cyanopyridiniums.....	31
Nicotinamides.....	35
Other Derivatives.....	36
<i>Linear Free Energy Relations</i>	36
Hammett Plots.....	36
Bronsted Plots.....	38
<i>Product Studies</i>	39
Discussion	39
<i>Azide Reactions</i>	42
<i>Hydrolysis Reactions</i>	44
<i>Bronsted Coefficients</i>	46
<i>The Effect of Solvent</i>	50
<i>Comparison with Katritzky's IDC Mechanism</i>	51
References and Notes	60

Chapter 3	The Hydrolysis of (4-Methoxybenzyl)dimethylsulfonium Chloride.....	64
	Introduction.....	67
	Experimental Section.....	67
	<i>General</i>	67
	<i>Synthesis</i>	68
	<i>UV Kinetics</i>	68
	<i>NMR Kinetics</i>	69
	<i>Closed Vial Experiments</i>	69
	<i>Studies of the Back Reaction</i>	69
	<i>Isotope Effects</i>	70
	Results.....	70
	<i>Kinetics and Activation Values</i>	70
	<i>Suppression of Hydrolysis</i>	72
	<i>Closed Vial and Zn⁺² Experiments</i>	73
	<i>Isotope Effects</i>	75
	Discussion.....	75
	References and Notes.....	85
Chapter 4	The Nucleophilic Substitution Reactions of (4-Methoxybenzyl)dimethylsulfonium Chloride.....	89
	Introduction.....	90
	Experimental Section.....	92
	<i>Synthesis</i>	92
	<i>Trimethylsulfonium iodide</i>	92
	<i>4-Methoxybenzyl-4'-sulfobenzoate</i>	92
	<i>NMR Kinetics</i>	94

<i>Conversion of RSCN to RNCS under the</i>	
<i>Reaction Conditions</i>	94
<i>Selectivities</i>	95
Results	96
<i>Kinetics</i>	96
<i>Reaction of 1 with Nucleophiles</i>	96
<i>Reaction of 1 with Pyridine-d₅ at</i>	
<i>Constant Ionic Strength and with No</i>	
<i>Added Salt</i>	99
<i>Reaction of 1 with NaN₃ at Constant</i>	
<i>Ionic Strength</i>	100
<i>Reaction of 1 with NaN₃ with No</i>	
<i>Added Salt</i>	100
<i>Reaction of 1 with Na₂SO₃ at Constant</i>	
<i>Ionic Strength</i>	104
<i>Reaction of 1 with Na₂SO₃ with no</i>	
<i>Added Salt</i>	105
<i>Reaction of 1 with NaSCN</i>	106
<i>Hydrolysis and Selectivities of 4-methoxy-</i>	
<i>benzyl-4'-sulfobenzoate</i>	111
<i>Selectivities for 1 Under Constant Ionic</i>	
<i>Strength and with No Added Salt</i>	112
<i>Solvolysis of Trimethylsulfonium Iodide</i>	113
<i>Activation Values</i>	113
Discussion	114
<i>HSAB Dependence</i>	114

<i>Mechanisms</i>	118
<i>Salt Effects Under Control of Ionic</i>	
<i>Strength</i>	119
<i>Salt Effects with No Control of Ionic</i>	
<i>Strength</i>	119
<i>Sneen Ion-Dipole Complex Mechanism</i>	124
<i>Activation Values</i>	127
<i>The Jencks Criteria</i>	128
References and Notes	129

Chapter 5 Gas-Phase Dissociation of 2'-Substituted β -Nicotinamide

Arabinosides	133
Introduction	134
Experimental Section	134
<i>Experimental</i>	134
<i>Computational Methods</i>	135
Results	136
<i>Experimental</i>	136
<i>Computational</i>	137
<i>Methods</i>	137
<i>Activation Enthalpies</i>	139
<i>Structures of Oxocarbenium Ions and</i>	
<i>the Site of Protonation of</i>	
<i>Nicotinamide</i>	145
<i>Correlation with Solution Activation</i>	
<i>Values</i>	147

Discussion	147
<i>Mechanism of Gas-Phase Dissociation</i>	149
<i>Substituent Effects/LFERs</i>	152
<i>Mechanisms in the Two Phases</i>	154
References and Notes	155

Chapter 6 Gas-Phase Dissociation of (4-Substituted) Dimethyl-

sulfoniums and Pyridiniums	157
Introduction	158
Experimental Section	160
<i>General</i>	160
<i>Synthesis</i>	160
<i>LSIMS Spectra</i>	160
<i>Computational Methods</i>	161
Results	161
<i>LSIMS Results</i>	161
<i>Linear Free Energy Relations (LFERs)</i>	163
<i>Computational</i>	164
<i>Sulfoniums</i>	164
<i>Pyridiniums</i>	167
Discussion	169
<i>Sulfoniums</i>	172
<i>Gas-Phase Dissociation</i>	172
<i>Dissociation in Water</i>	172
<i>Pyridiniums</i>	174
<i>Gas-Phase Dissociation</i>	174
<i>Dissociation in Water</i>	174

<i>The Effect of Solvent on Mechanism</i>	176
<i>Relative Stabilities of the Ribosyl Oxocarbenium Ion and Benzyl Carbenium Ions in the Gas Phase</i>	177
<i>Model Gas-Phase Systems</i>	180
<i>Summary</i>	186
References and Notes	187

Chapter 7	A Semi-Empirical Study of the Kinetic and Thermodynamic Stabilities of Linear and Cyclic Oxo- and Thiocarbenium Ions Generated from Pyridiniums and Dimethylaniliniums	191
	Introduction	192
	Computational Methods	194
	Results	194
	Discussion	197
	<i>Linear Oxygen Compounds</i>	199
	<i>Linear Sulfur Compounds</i>	200
	<i>Unsubstituted Cyclic Compounds</i>	202
	<i>Arabinosyl-, Xylanopyranosyl-, and Glucopyranosylpyridiniums</i>	202
	<i>Estimation of the Stability of Glucosyl and Ribosyl Oxocarbenium Ions</i>	203
	<i>Activation Values and Linear Free Energy Relations (LFERs) For the Model Reactions</i>	204

<i>Activation Entropy</i>	204
<i>Taft Correlations</i>	206
<i>Bronsted Correlations</i>	207
<i>Conclusions</i>	209
References and Notes	210

Chapter 8	A Semi-empirical Study of the Kinetic and Thermo- dynamic Stabilities of Linear and Cyclic Oxo- and Thiocarbenium Ions Generated from Aldehyde Hydrates, Hemiacetals, Acetals, and Methyl Ribosides and Glucosides	214
	Introduction	215
	Methods	217
	<i>Computations</i>	217
	<i>Controls</i>	217
	Results and Discussion	219
	<i>Linear Compounds</i>	219
	<i>Formaldehyde Hydrate</i>	219
	<i>Formaldehyde Methyl Hemiacetal</i>	224
	<i>Formaldehyde Dimethyl Acetal</i>	231
	<i>Cyclic Compounds</i>	235
	<i>Five-Membered Rings</i>	235
	<i>Six-Membered Rings</i>	239
	<i>Ribofuranosides</i>	244
	<i>Methyl Glucopyranosides</i>	245
	<i>Oxygen vs. Sulfur Substrates</i>	248
	<i>Comparison of Mechanisms</i>	251

	<i>A-1 vs. A-2</i>	251
	<i>Specific vs. General-Acid Catalysis</i>	253
	<i>Aryloxy vs. Pyridinium THF Substrates</i> ..	257
	References and Notes	259
Chapter 9	Summary and Conclusions	263
	Heterolytic Cleavage of Charged Benzyl	
	Substrates	264
	Heterolytic Cleavage of the Nicotinamide-Ribosyl	
	Bond	272
	Enzyme Catalysis of NAD⁺	276
	References and Notes	278

List of Tables

Table 2.1	Second-order rate constants for the reaction 1a-e (80°C) and 2a-e (96°C) with NaN ₃ (k_2) and water (k_w).....	28
Table 2.2	Eyring activation values for the reaction of 1a-e and 1-Me with NaN ₃ at 80°C.....	29
Table 3.1	First-order rate constants k_1 (min ⁻¹) at 80°C for the hydrolysis of 1 in H ₂ O and D ₂ O at various ionic strengths....	71
Table 4.1	Reactions of nucleophiles with (4-methoxybenzyl)dimethylsulfonium, 80°C, D ₂ O.....	97
Table 4.2	First- and second-order rate constants for the reaction of 1 with NaN ₃ in D ₂ O.....	101
Table 4.3	First- and second-order rate constants for the reaction of Na ₂ SO ₃ with 1 under constant ionic strength with NaCl and Na ₂ SO ₄	105
Table 4.4	<i>Pseudo</i> -first order and second-order rate constants for the conversion of RSCN to RNCS at 80°C in H ₂ O in the presence of NaSCN.....	109
Table 4.5	Eyring activation values for (4-methoxybenzyl)dimethylsulfonium chloride and 3'-cyanopyridinium chloride derivatives at constant ionic strength $\mu = 1.7$ (NaCl).....	114
Table 5.1	Relative abundances for the gas-phase dissociation of 2'-substituted β -nicotinamide arabinosides ($M^+ = 100$).....	136
Table 5.2	Absolute AM1 enthalpies of formation (ΔH_f) for the gas-phase dissociation of 2'-substituted β -nicotinamide arabinosides.....	140

Table 5.3	Relative AM1 enthalpies of formation (ΔH_f) and activation (ΔH^\ddagger) for the gas-phase dissociation of 2'-substituted β -nicotinamide arabionsides.....	141
Table 6.1	Log $[R^+ / (R^+ + M^+)]$ for the gas-phase dissociation of (4-Y-benzyl) dimethylsulfoniums and 3-Z-pyridiniums.....	162
Table 6.2	Enthalpies of formation for the gas-phase dissociation of (4-Y-benzyl) dimethylsulfoniums (MNDO) and pyridiniums (AM1) (kcal/mol).....	165
Table 6.3	Activation enthalpies and enthalpies of reaction for the gas-phase dissociation of (4-Y-benzyl) dimethylsulfoniums (MNDO) and pyridiniums (AM1) (kcal/mol).....	165
Table 6.4	AM1 ΔH_f and ΔH_R , from the pyridiniums, of (4-Y-substituted) benzyl, norcaradienyl, and tropylium carbenium ions (kcal/mol).....	171
Table 7.1	AM1 enthalpies of activation (ΔH^\ddagger) and reaction (ΔH_R) for the dissociation of methoxymethyl and 1-oxa-cyclic pyridinium substrates.....	196
Table 7.2	Comparison of the 6-31G*, MP3/6-31G*, AM1, and PM3 ΔH_R and the experimental values for hydride and chloride exchange for α -oxo and α -thio methyl carbenium ions in the gas phase.....	197
Table 7.3	Values of ΔS^\ddagger for the hydrolysis of pyridinium substrates.....	198
Table 8.1	Semi-empirical enthalpies of reaction (kcal/mol).....	227
Table 8.2	PM3 ΔH_f , ΔH^\ddagger , and ΔH_R (kcal/mol) for 2-substituted α and β methylglucosides.....	247
Table 9.1	Relative rates for hydrolysis of benzyldimethylsulfoniums and benzylpyridiniums in D ₂ O at 70°C.....	265

List of Figures

Figure 2.1	Second-order rate plot for the reaction of 1a with NaN ₃ ($\mu = 1.7$) in D ₂ O at various temperatures.....	29
Figure 2.2	Rate plots for the reaction of 2a with NaN ₃ ($\mu = 1.7$) in D ₂ O at 96°C.....	30
Figure 2.3	Second-order Rate plots for the reaction of 2a with NaN ₃ ($\mu = 1.7$) in D ₂ O at 96°C.....	30
Figure 2.4	Reaction progress for 1a,b at 80°C in pure D ₂ O as a function of the initial molar concentration of substrate.....	32
Figure 2.5	Fit of the data for 1a from Figure 2.4 to the equation for the equilibrium $RPy^+ \rightleftharpoons ROH + Py + H_3O^+ \rightleftharpoons PyH^+$	33
Figure 2.6	Reaction progress for 0.005M 1a-d at 80°C in pure D ₂ O and with 0.005M 3-cyanopyridine added.....	34
Figure 2.7	Rate plot for the hydrolysis of 2a in 5.3M DCl at 80°C.....	35
Figure 2.8	Hammett plot for the reaction with azide (k_2) of 1a-e , 2a-e , and 3a,e at 96°C.....	36
Figure 2.9	Hammett plots for the hydrolysis in D ₂ O of 1a-e and 2a-e at 80°C and 96°C, respectively.....	37
Figure 2.10	Brønsted plot for the azide reactions of (4-methoxybenzyl) pyridiniums at 80°C.....	38
Figure 2.11	Stereodiagram (cross-eyed) of the AM1-minimized structure for 8	53
Figure 2.12	Structures obtained by manual docking of piperidine with the unminimized and AM1-minimized structures for 8	54
Figure 2.13	Ground states and ion-dipole complexes for the AM1-minimized structures for 3c and 6a	54

Figure 2.14	Stereodiagram (cross-eyed) showing the AM1-minimized structures for the ion-dipole complexes for 7 and 8	56
Figure 3.1	Plots of k_{obsd} (min^{-1}) vs [nucleophile] for the reactions of 1 with various nucleophiles measured by NMR at 80°C	66
Figure 3.2	Eyring plot for the hydrolysis of 1	72
Figure 3.3	Plots of the normalized integrated signal for the SMe_2 signal for 1 at 80°C vs. time.....	73
Figure 3.4	Plots of the fraction 1 remaining vs. the initial concentration of 1 (C_0) after heating various concentrations in sealed vials at 80°C for 40 min.....	74
Figure 3.5	Plot of k_{obsd} vs. $[\text{ZnCl}_2]$ for the hydrolysis of 1 at 80°C	74
Figure 3.6	Plot of the square of the initial concentration of 1 (from Figure 3.4) vs. the fraction remaining.....	77
Figure 3.7	Hammett plots for the hydrolysis and sulfur KIE for hydrolysis of 3- and 4-substituted BDMS^+ at 68°C	79
Figure 3.8	Plot of the product ratios vs. $[\text{NaN}_3]$ for the reaction of 1 at 80°C	83
Figure 3.9	Eyring plot for Kevill's and our data for the hydrolysis of 1 ...	84
Figure 4.1	Rate plot for the reaction of 1 with various concentrations of Na_2SO_3 in D_2O at 80°C	96
Figure 4.2	Second-order rate plot for the reaction of 1 with NaCN and NaOD at 80°C	98
Figure 4.3	Second-order rate plot for the reaction of 1 with pyridine- d_5 with and without control of ionic strength.....	100
Figure 4.4	Second-order rate plots for the reaction of 1 with NaN_3 in the range 60° - 80°C	101
Figure 4.5	Plot of k_{obsd} vs $[\text{NaN}_3]$ for 1 with no added salt (low salt).....	102

Figure 4.6	Plot of k_{obsd} vs $[\text{NaN}_3]$ for 1 with no added salt (high salt).....	102
Figure 4.7	Plot of $1/k_{\text{obsd}}$ vs. $1/[\text{nucleophile}]$ for 1 with no added salt.....	103
Figure 4.8	Plot of k_{obsd} vs. $[\text{Na}_2\text{SO}_3]$ for 1 with NaCl added.....	104
Figure 4.9	Plot of k_{obsd} vs. $[\text{Na}_2\text{SO}_3]$ for 1 with Na_2SO_4 added.....	104
Figure 4.10	Plot of k_{obsd} vs. $[\text{Na}_2\text{SO}_3]$ for 1 with no added salt.....	106
Figure 4.11	Plot of $\ln (C_t/C_o)$ vs. time for reaction of 1 with NaSCN.....	106
Figure 4.12	Plot of k_{obsd} vs. $[\text{NaSCN}]$ for 1 at 80°C with no added salt.....	107
Figure 4.13	Plot of k_{obsd} vs. $[\text{NaN}_3]$ for 4 at 80°C	112
Figure 4.14	Plot of $\log k_2$ vs. the LUMO-HOMO difference ΔE for the reaction of 1 with SO_3^- , N_3^- , SCN^- , and pyridine- d_5 at 80°C	116
Figure 4.15	Hammett plot for 1 and other benzyldimethylsulfoniums.....	117
Figure 4.16	Plot of k_{obsd} vs. the activity of NaN_3 for reaction of 1 with no control of ionic strength (low NaN_3).....	120
Figure 4.17	Plot of k_{obsd} vs. the activity of Na_2SO_3 for reaction of 1 with no control of ionic strength (low Na_2SO_3).....	120
Figure 4.18	Selectivities for the reaction of 1 with NaN_3 at 80°C with and without control of ionic strength.....	122
Figure 4.19	Selectivities for the reaction of 1 with Na_2SO_3 at 80°C with and without control of ionic strength with Na_2SO_4	124
Figure 5.1	Taft plot for the gas-phase dissociation of 2'-substituted β - nicotinamide arabinosides.....	137
Figure 5.2	PM3, AM1, and MNDO energy profiles calculated for benzyl pyridinium using Hyperchem Release 3.....	139
Figure 5.3	AM1 energy profiles for gas-phase dissociation of 1a-e	142
Figure 5.4	Plot of the experimentally determined $\log [R^+ / (R^+ + M^+)]$ vs. the AM1-calculated values of ΔH^\ddagger for gas-phase dissociation of 1a-e	143

Figure 5.5	Ground states for the 2'-H and 2'-NAc compounds.....	143
Figure 5.6	Ground state and transition state for 1b	144
Figure 5.7	Plot of ΔG^\ddagger for the hydrolysis of 1a-e vs. the AM1-calculated values of ΔH^\ddagger	146
Figure 5.8	Change in structure between the transition state and cyclization to the acylium ion within the IDC for 1d	152
Figure 6.1	Plot of the LSIMS data for 1a-e vs. the relative free energy for the gas-phase formation of <i>t</i> -cumyl carbenium ions.....	162
Figure 6.2	Plots of the LSIMS data for 2-5a-e vs. the relative free energy for the gas-phase formation of <i>t</i> -cumyl carbenium ions.....	163
Figure 6.3	Plots of the LSIMS data for 2-5a-e vs. the relative free energy for the gas-phase protonation of the respective pyridine LGs...	164
Figure 6.4	MNDO energy profiles for the gas-phase dissociation of 1a-e	166
Figure 6.5	Plots of the LSIMS data vs. the MNDO ΔH^\ddagger for 1a-e and the AM1 ΔH^\ddagger for 2a-d	167
Figure 6.6	AM1 energy profile for the gas-phase dissociation of 5a-e	168
Figure 6.7	Plots of the calculated ΔH^\ddagger vs. ΔH_R for 5a-d and 1a-e	168
Figure 6.8	Hammett plots of the gas-phase relative rates for 1a-e and the hydrolysis rate constants for various 3- and 4-substituted benzyldimethylsulfoniums.....	173
Figure 6.9	Plots of AM1 ΔH^\ddagger for bond cleavage and return to the transition state from the IDC for 2-5a	175
Figure 6.10	Hammett plots of the gas-phase relative rates for 2a-e and the hydrolysis rate constants for 2a-e and 3a-e	175
Figure 6.11	Plot of the PM3 ΔH_R for 2'-substituted THF-1-dimethylsulfoniums vs. σ_I	182

Figure 6.12	Plots of the PM3 ΔH_R vs. the relative free energy for formation of <i>t</i> -cumyl carbenium ions for various substituted benzylys with different leaving groups.....	183
Figure 6.13	Brønsted-like plots for the PM3 ΔH_R vs. the pK_a of the pyridine LG for 4-substituted benzyl compounds.....	184
Figure 6.14	Brønsted-like plots for the PM3 ΔH_R vs. the pK_a of the oxygen LG for 4-substituted benzyl compounds.....	184
Figure 7.1	AM1 energy profiles for the dissociation of $\text{MeOCH}_2\text{Py}^+$, MeOCHMePy^+ , and $\text{MeOCH}_2\text{NMe}_2\text{Ph}^+$	194
Figure 7.2	AM1 energy profiles for the dissociation of $\text{MeSCH}_2\text{Py}^+$ and MeSCHMePy^+	195
Figure 7.3	Stereodiagram (cross-eyed) of structures of the ion-dipole complex for 4 and 7 showing a bridged structure between the carbon and the sulfur.....	201
Figure 7.4	Correlations between the AM1-calculated ΔH^\ddagger and the experimental values of ΔH^\ddagger and ΔS^\ddagger for the hydrolysis of xylopyranosyl- and glucopyranosylpyridiniums and 2'-substituted β -nicotinamide arabionsides.....	206
Figure 8.1	Step-wise mechanism for the specific-acid catalyzed hydrolysis of formaldehyde methyl acetal.....	218
Figure 8.2	Structures and energies for formaldehyde hydrate.....	220
Figure 8.3	Various structures obtained upon full PM3 minimization of protonated formaldehyde hydrate by step-wise removal of the torsional angle restraints and the reaction coordinate.....	221
Figure 8.4	Full PM3 energy profile for the minimization of protonated formaldehyde hydrate after removal of the restraint on the reaction coordinate.....	223

Figure 8.5	Structures and energies for formaldehyde methyl hemiacetal..	225
Figure 8.6	PM3 structures for 60°C rotomers for protonation on the hydroxyl of formaldehyde methyl acetal.....	226
Figure 8.7	Energy profiles for dissociation of the C-O bond in the most stable ground state structures for 3, 4, and 7.....	226
Figure 8.8	The 12 60° chiral rotomers obtained by protonating the methoxy oxygen of the most stable rotomer of 2.....	229
Figure 8.9	The three stable rotomers of 5.....	231
Figure 8.10	Two chiral forms obtained by protonation of either lone pair on the oxygen of 5GG.....	232
Figure 8.11	The 12 60° rotomers obtained by protonating the methoxy oxygen of the anti form of 6.....	234
Figure 8.12	The six conformers for the protonated form of the cyclic hemiacetal of 4-hydroxybutanal.....	236
Figure 8.13	PM3 energy profiles for cleavage of 13ai, 16Aa, and 16Ea...	237
Figure 8.14	The effect of hydrogen bond formation on the stability of several conformers of 15.....	238
Figure 8.15	The six 60° rotomers for the protonated forms of equatorial 2-hydroxy-THP.....	240
Figure 8.16	The six 60° rotomers for the protonated forms of equatorial 2-methoxy-THP.....	241
Figure 8.17	Plots of PM3 ΔH^\ddagger and ΔH_R for C-O bond cleavage in 19a-d and the corresponding β -nicotinamide arabionsides vs. σ_I	245
Figure 8.18	Plots of PM3 ΔH^\ddagger and ΔH_R for C-O bond cleavage in 2'-substituted β - and α - methylglucosides.....	248
Figure 8.19	Plot of the log of the second-order rate constant for specific-acid hydrolysis of 2'-substituted β -methylglucosides.....	249

Figure 8.20	Plot of the PM3 ΔH_{k-1}^\ddagger vs. the absolute gas-phase ΔG° for the alcohols.....	258
Figure 9.1	LUMOs from the fully minimized PM3 structures for 1a , 1c , and 2a	268
Figure 9.2	Two-dimensional potential energy surfaces for gas-phase displacement reactions.....	271

Chapter 1
Introduction

UCSF LIBRARY

"Things fall apart."

Yeats

The task of physical organic chemistry is to figure out how and why they do. To this end, the paradigm reaction studied has been the heterolytic cleavage of RX and the substitution of a nucleophile Nu for X, which may or may not occur through a common intermediate.[†] Carbenium ions formed by heterolysis are the most intensively studied intermediates in organic chemistry. Yet after 60 years of detailed, sophisticated, inspired and often brilliant work--if we date the modern era from the studies of Frank Whitmore and his students at Penn State and of Ingold, Hughes and their students at the University of London in the 1930s--there are still mechanistic aspects of this relatively simple reaction that are not completely understood. Among these are the existence of ion pairs $R^+ X^-$ (or ion-dipole complexes for the reaction $RX^+ \rightarrow R^+ X^0$) and the stability of α -oxocarbenium ions.¹

Ion Pairs

Substitution reactions of RX with Nu or solvent (HOS) are characterized kinetically by two limiting reactions: the S_N1 , which is first order in RX and zero order in nucleophile, and S_N2 , which is first order in both RX and nucleophile.² These are the original Ingold designations, which he further divided into four subgroups: Type I, RX + negative Nu; Type II, RX + neutral Nu; Type III, RX^+ + negative Nu; and Type IV, RX^+ + neutral Nu.³ Under *pseudo*-first order conditions at constant ionic strength, increasing [Nu] has no effect on the rate of disappearance of RX in an S_N1 reaction, but doubling [Nu] doubles the rate of disappearance of RX in an S_N2 reaction. These are straightforward kinetic

[†] For RX, X = halides, sulfonate and carboxylate ester; for RX^+ , X = pyridine, R_2S , H_2O , ROH. etc.

consequences of ionization of RX to R⁺, which then reacts with Nu or HOS, or of direct displacement on RX by Nu.

The ionizing power of the reaction medium affects the rate. Changing the solvent from a lower to higher dielectric constant or the ionic strength of a pure solvent by increasing the concentration of added salt favors ionization and increases the rate of the S_N1 reaction of RX and lowers the rate for RX⁺. The changes have little or no effect on the S_N2 reaction; in some instances, they can lower the rate. These effects are the basis of the Winstein-Grunwald linear free energy relation (LFER), $\log k/k_0 = mY$, where k is the rate constant in some solvent, k₀ is the rate constant in the standard solvent, 80% (v/v) ethanol/water, m is a constant characteristic of the substrate, and Y is a constant characteristic of the solvent that is determined using *t*-butyl chloride as the standard substrate with m = 1. There are numerous variations on the original equation.¹

For the S_N2 reaction, increasing the strength of Nu increases the rate (all other things being equal). This is expressed in the Swain-Scott equation, $\log k/k_0 = ns$, where s is a constant characteristic of the substrate and n is characteristic of Nu, measured against MeBr in methanol with n = 1. There are numerous variations on the original equation.¹

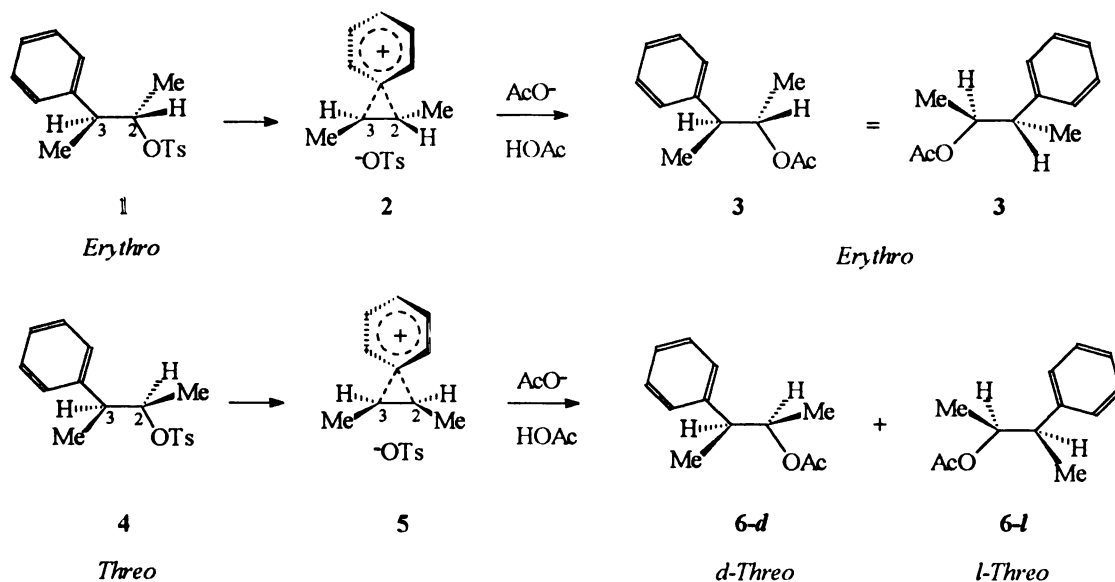
The stereochemical course of the reactions for a substrate that is chiral at the carbon bearing X generally parallels the kinetics: S_N1 ionization to the solvent-equilibrated carbenium ion R⁺ proceeds with complete racemization, while concerted S_N2 reactions undergo inversion of configuration at the reaction center. The stereochemical course is influenced by substitution at the reaction center in two ways. First, with substitution of H with R' (R' = alkyl, allyl, aryl), the stability of R⁺ increases because of inductive, hyperconjugative, or through resonance interactions that in turn aid in the ionization reaction, favoring S_N1. Second, with increasing steric congestion at the reaction center, S_N2 reactions become less likely

UCSF LIBRARY

because of steric inhibition of approach of the nucleophile. Thus, as limits, primary substrates (MeCl) undergo S_N2 reactions and tertiary systems (Ph_3CCl) undergo S_N1 reactions.

These descriptions are reasonable, straightforward, unambiguous, logical; they do not work for many systems, of course. The classical exceptions--allyl, α -carbinyl cyclopropyl, 3-phenyl-2-butyl, norbornyl, neopentyl, etc.--are well and extensively reviewed in the standard texts,¹ and will not be discussed here, with two exceptions, both of which are secondary systems that exhibit stereochemical and kinetic anomalies.

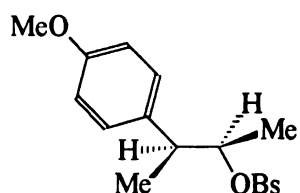
3-Aryl-2-Butyl systems. In 1949, Cram⁴ found that *erythro* (1) and *threo* (4) 3-phenyl-2-butyl tosylate gave exclusively retained (3) and racemic products (6*d,l*), respectively, upon acetolysis in the presence of NaOAc (Scheme 1.1). This product distribution is inconsistent with either an S_N1 or S_N2 reaction, which would be expected to give different product distributions. The results are



Scheme 1.1

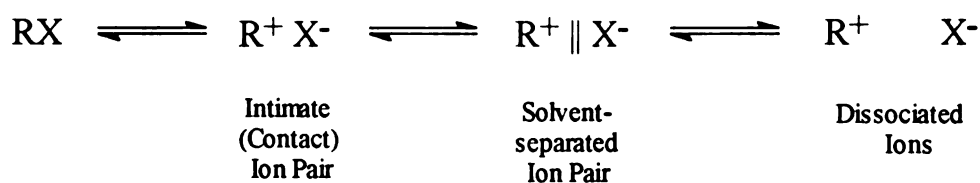
consistent with the bridged phenonium ion intermediates **2** and **5**, in which attack of AcO^- (or AcOH) at either C2 or C3 of the unsymmetrical *erythro* intermediate **2** gives the same product with retention of configuration, while attack of Nu at either C2 or C3 of the *threo* intermediate **5** leads to racemic product.

Winstein Scheme. In 1958, Winstein and Robinson⁵ found anomalous kinetic behavior for the acetolysis of *threo*-3(4-methoxyphenyl)-2-butyl brosylate



7

(7). They measured the rates of racemization (k_α , the polarimetric rate constant) and of disappearance (k_t , the titrametric rate constant) of **7** as a function of the concentration of added LiClO_4 . Two anomalies were found. First, k_α was two-fold greater than k_t . Second, a plot of k_α vs $[\text{LiClO}_4]$ was linear, but a plot of k_t vs $[\text{LiClO}_4]$ showed an initial sharp increase that leveled off to a line essentially parallel to the plot for k_α vs



Scheme 1.2

$[\text{LiClO}_4]$. The latter was called the "special salt effect." The results were interpreted in terms of several intermediate species, the intimate (contact) and solvent-separated ion pairs (Scheme 1.2). Internal return of the intimate ion pair to either C2 or C3 yields racemic starting material and could account for the larger

k_{α} ; in fact, 7 isolated after partial reaction was partially racemized. The special salt effect was the result of interception of the solvent-separated ion pair by ClO_4^- , which prevented the "external" return back to the intimate ion pair. The kinetics governing these processes are complex and have been analyzed in detail by Carpenter.⁶ These and many other examples have established the ion-pair mechanism to the satisfaction of most workers,¹ although not without significant criticism along the way.⁷

One problem with extending this analysis to other systems is that most examples in which there is kinetic and stereochemical evidence for ion pairs were obtained in either pure carboxylic acids (acetic, formic) or pure alcohols (MeOH, EtOH) in which ion pairing would be favored compared to water, where the enthalpy of solvation and the energy gained by stabilizing the ion in a solvent shell would be expected to lead rapidly to dissociated ions. Put another way, on a two-dimensional energy diagram for the reaction, in acids and alcohols the various ion pairs would have essentially equal energies with small barriers of interconversion among them; in water, these energies and barriers would be greatly reduced such that the only significant barriers would be cleavage of the RX bond and the back reaction from the fully dissociated, solvent-equilibrated carbenium ion.

Sneen Scheme. Sneen, who had been a postdoctoral fellow with Winstein, reasoned that diluting an aqueous solution with inert organic solvent should produce conditions under which reactions of contact ion pairs could be observed in aqueous systems. In the event, Weiner and Sneen⁸ and Sneen and Larsen⁹ found evidence for ion pairs in the azide substitution reaction of optically active 2-octyl mesylate in 25 volume % aqueous dioxane. The products ROH and RN_3 were formed with almost complete inversion of configuration, but the kinetics showed "borderline" or intermediate behavior between $\text{S}_{\text{N}}1$ and $\text{S}_{\text{N}}2$: the rate does not double with a doubling of $[\text{NaN}_3]$. The stereochemistry can be rationalized in

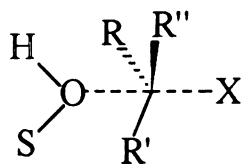
terms of the attack of solvent or azide on the intimate ion pair, leading to inversion, and the kinetics are consistent with a partitioning of the intimate ion pair between water and azide, which gives an expression^{1,6,8,9} (discussed in detail in Chapter 3) in which doubling the azide concentration does not lead to a doubling of k_{obsd} .

The Snee results have been criticized on several grounds. First, no attempt was made to hold the ionic strength of the reaction medium constant, and Schleyer¹⁰ among others argued strongly that the kinetics was the result of an azide salt effect and not of the partitioning of the intimate ion pair between solvent and azide. Second, as Gold¹¹ and Kohnstam¹² had argued, borderline kinetic results are perfectly compatible with a mixed S_N1/S_N2 reaction, for which $k_{\text{obsd}} = k_1 + k_2 [\text{NaN}_3]$, where k_1 = the first order solvolysis rate constant and k_2 is the second-order azide rate constant for a concerted reaction. A plot of k_{obsd} vs. $[\text{NaN}_3]$ would have a slope = k_2 with an intercept = k_1 for the mixed mechanism. Thornton¹³ has made a detailed analysis of both criticisms and points out that Snee's mechanism is perfectly reasonable *i*; it can be shown that no azide product arises from trapping of a solvent-equilibrated carbenium ion intermediate. Neither of these arguments explains the stereochemical results, however. In later work, Snee¹⁴ extended the ion-pair mechanism to substrates such as benzyldimethylsulfoniums. (Thornton's analysis of this system is discussed in detail in Chapters 3 and 4.)

One major failing of the Snee mechanism was his insistence--made, he said,¹⁵ because it was intellectually and aesthetically satisfying--that primary systems also reacted by an ion-pair mechanism, despite the fact that gas-phase and solution data all showed that primary carbenium ions were enormously unstable species, and should remain so within an ion-pair (or, that the back reaction $\text{R}^+ \text{X}^- \rightarrow \text{RX}$ would occur at the diffusion rate, which makes the existence of the primary ion pair moot). This objection has remained unchallenged until quite recently.

Janda, Lerner and their colleagues¹⁶ claim to have evidence for a primary ion pair in the substitution reaction of a substrate on the surface of a catalytic antibody. Part of their rationale for this mechanism is an even more recent paper by Streitwieser and Schleyer¹⁷ in which evidence is presented for a primary ion pair in the reaction $\text{LiX} + \text{MeX}$ ($\text{X} = \text{F}, \text{Cl}$) in the gas phase. An analysis of the computational results show, however, that ΔH^\ddagger for the ion pair reaction is 33.6 kcal/mol higher than ΔH^\ddagger for the normal $\text{S}_{\text{N}}2$ reaction. Computational models suggest that the reaction is merely an $\text{S}_{\text{N}}2$ reaction that occurs under special circumstances.¹⁸

While the Winstein and Snee ion-pair mechanisms are generally accepted for secondary systems, two primary alternatives have been suggested. Schleyer and his colleagues,¹⁹ including Bentley and Harris, Raber, and McManus, have suggested that some of the evidence for ion pairs in secondary systems can be explained by solvent nucleophilic participation in which there is ionization of the substrate "pushed" from the backside by nucleophilic solvent molecules, the



*Schleyer pentacoordinated
solvent-assisted intermediate*

$\text{S}_{\text{N}}2(\text{intermediate})$ mechanism. The substrate may be either an ion pair or a partially ionized species with significant carbocationic character. Much of the evidence for this mechanism comes from solvolysis studies done in perfluorinated alcohol systems, primarily trifluoroethanol (TFE). Jencks has suggested in several papers²⁰ that TFE would form a complex between the carbenium ion and the negative dipolar end of the alcohol ($\text{R}^+ \cdots \text{F}_3\text{CCH}_2\text{OH}$), a structure that has been

found to be a significant intermediate in a recent computational study.²¹ The energy for reaction of this intermediate to form product is consistently two-fold higher than expected from plots of ΔH^\ddagger vs. pK_a of the alcohol, and suggests that selectivity ratios and arguments made about solvent participation in solvolysis reactions should be reconsidered (see Chapter 8).

Jencks Criticism. Jencks has raised serious concerns about the existence of ion pairs in any reaction.²² He has considered the lifetimes of intermediate species and suggested a complex scheme that avoids ion pairs as distinct intermediates.²³ While the formal scheme is formidable and the nomenclature can be cumbersome (a reaction can have an "enforced coupled preassociated concerted" mechanism), the concepts are relatively straightforward.²⁴ If ionization of RX to $R^+ X^-$ occurs in the presence of Nu or ROS, and R^+ is sufficiently stable that it can diffuse out of the initial solvent shell and away from Nu--if R^+ becomes solvent-equilibrated--after which it reacts with Nu or ROS based on nucleophilicity and not molarity, the mechanism is the limiting S_N1 case. As the lifetime of the intermediate becomes less, ionization of RX can take place without assistance (stabilization) of either Nu or ROS and will have first order kinetics, but because the barrier to reaction with Nu or ROS is decreasing as a function of the lifetime of R^+ , no distinct intermediate is formed. R^+ is trapped without complete bond breaking. Nu or ROS react at the diffusion rate with the unstable carbenium ion with a partially broken RX bond. This is the stepwise "uncoupled" mechanism. If ionization occurs as in the ion pair mechanism $RX \rightleftharpoons R^+ X^-$ with a very short lifetime for R^+ , the return reaction always occurs. In the presence of Nu or ROS, however, $Nu \cdots R^+ \cdots X$ will form, with the intermediate complex stabilized by electrostatic interactions with both Nu and X. Jencks speaks of the Nu "tickling" the transition state.²³ Second order kinetics are obtained. This is the "coupled" mechanism. Finally, if R^+ has an extremely short lifetime (such as CH_3^+), the reaction with Nu

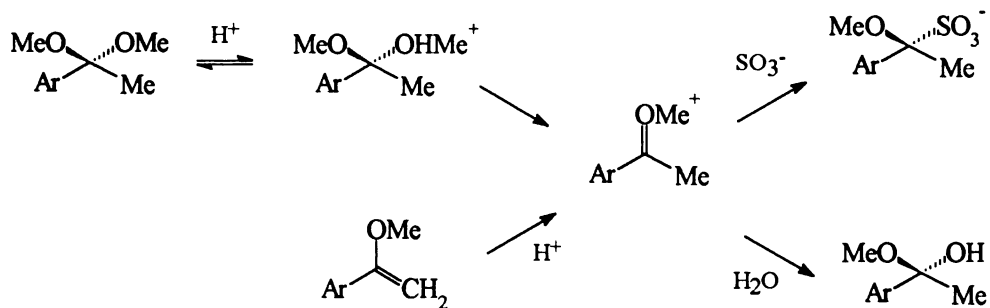
is concerted, the limiting S_N2 mechanism. Because of the instability of the carbenium ions, the mechanisms are said to be "enforced."

Reactions of substrates that have potentially stable carbenium ion intermediates that have second-order kinetics are said to occur through "exploded" activated complexes in which there is significant carbenium ion character in R^+ and a "loose" structure (in Hammond parlance, early for the Nu and late for the leaving group) with stabilization afforded by Nu and the leaving group.²⁵ This structure is reminiscent of Schleyer's S_N2 (intermediate) activated complex.¹⁹ In neither case, however, is the species thought to be an intermediate in the sense that it would exist as a distinct species. Reactions that exhibit these characteristics are the nucleophilic substitution reactions of α -phenylethyl chloride²⁶ and methoxymethyl substrates with either 2,4-dinitrophenolate²⁷ or N,N-dimethylanilinium²⁸ leaving groups. Ironically, Jencks too rejects mixed mechanisms and makes the bold statement²⁸ that "all solvolysis and substitution reactions at saturated carbon that proceed through S_N2 displacement mechanisms do so simply because the intermediate in *the alternative* S_N1 mechanism is too unstable to exist [italics added]." This of course is nonsense.

Stability of Oxocarbenium Ions

It was the bisulfite trapping reaction of oxocarbenium ion intermediates generated from acetophenone dimethylketals that in part led Jencks to his scheme for substitution reactions (Scheme 1.3). Young and Jencks²⁹ measured the ratios of sulfite and water addition products of the oxocarbenium ion generated from either the dimethylketals or enol ethers; both precursors gave the same product ratios, which established that the oxocarbenium ion was a solvent-equilibrated intermediate. With the assumption that sulfite reacts with the oxocarbenium ion at the diffusion rate ($5 \times 10^9 \text{ sec}^{-1}$), a "clock" reaction is established that allows the

UCSF LIBRARY



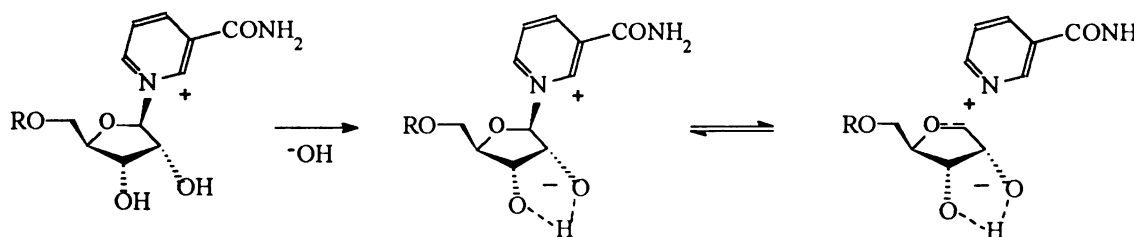
Scheme 1.3

estimate of the lifetimes of the oxocarbenium ions from the various rate constants. Extrapolation of the values for the acetophenone ketals with values for benzaldehyde and formaldehyde acetals yields an estimated lifetime of 10^{-15} sec for the methoxymethyl oxocarbenium ion. Because formaldehyde dimethyl acetal undergoes specific-acid catalyzed hydrolysis ca. 10^4 faster than methylglucoside, Young and Jencks²⁹ argued that the glucose oxocarbenium ion was too unstable to exist as an intermediate. By analogy, ribosyl oxocarbenium ions would be expected to be more unstable still. Indeed, the fact that methyl ribosides undergo specific-acid catalyzed hydrolysis with negative ΔS^\ddagger has been interpreted as evidence for an A-2 mechanism, in which water displaces protonated methanol from the riboside without formation of an intermediate oxocarbenium ion.³⁰

Nicotinamide Adenoside Dinucleotide (NAD⁺) and β -Nicotinamide Riboside and Arabinoside Hydrolysis

Oppenheimer and his students and colleagues³¹⁻³⁵ have been studying the hydrolysis reactions of NAD⁺ and related ribosides and arabinosides. Nicotinamide-ribosyl bond cleavage is important for several classes of enzymes; Handlon³¹ has reviewed these reactions, and they will not be discussed here. With Marschner and Johnson, Oppenheimer³² found that NAD⁺ underwent a pH-independent hydrolysis reaction and a specific-base catalyzed reaction. The latter

was marked by a unity slope for plots of $\log k$ vs. pH that becomes pH-independent above the pK_a of the ribose diol and occurred at much faster rates than the pH-independent reactions. Blocking the 2',3' hydroxyls with an isopropylidene changed this behavior. Thus catalysis is consistent with the involvement of the diol anion, and the rate acceleration is consistent with the stabilization of the oxocarbenium ion by an alkoxide in the



Scheme 1.4

2' position (Scheme 1.4). Shuber and his colleagues³³ had shown that the rate constants for hydrolysis of NAD^+ analogs with different pyridine leaving groups increased as the pK_a of the pyridine decreased. They also found large values of the Brønsted β_{LG} for the hydrolysis (-1.12) and enzyme-catalyzed (-0.9) cleavage. It remained for Handlon^{31,34,35} to show that hydrolysis of a series of β -nicotinamide ribosides and arabinosides bearing different 2' substituents hydrolyzed with rate constants that followed the Taft equation with a high, negative ρ value of -6.9, with little difference in rate between the ara and ribo compounds. He also found relatively high and positive values of ΔS^\ddagger for the hydrolysis.³¹ The rate constant for specific-base catalyzed NAD^+ hydrolysis fell on the Taft line with the substituent constant for alkoxide used.^{34,35}

The diol anion mechanism has important implications for the glycosyl hydrolyase-catalyzed hydrolysis of NAD^+ . Oppenheimer has postulated that a general base in the active site of the enzyme could abstract a proton from the 2' or

3' position, forming the diol anion that would then undergo a dissociative reaction to the oxocarbenium ion that in turn would add water while still bound in the enzyme active site. In recent work, Oppenheimer, Shuber and colleagues³⁵ found that a plot of $\log V_{\max}$ for the enzyme-catalyzed hydrolysis of NAD^+ analogs, synthesized by Tom Xu, bearing the substituents in the 2' position studied by Handlon vs. σ_1 was parallel to the Taft plot obtained by Handlon for the β -nicotinamide ribosides and arabinosides. With Shuber's earlier work on β_{LG} for the enzyme-catalyzed hydrolysis,³³ these results strongly suggest that the enzyme-catalyzed and hydrolysis reaction proceed by the same purely dissociative mechanism, either to the ion-dipole complex or to the solvent-equilibrated oxocarbenium ion, two processes that are forbidden by the Jencks estimate of the lifetime of the glucosyl oxocarbenium ion.²⁹

The work reported here was designed was to resolve this dilemma.

Study Design

Solvolysis of neutral benzyl substrates has been studied extensively.³⁶ It is generally thought that neutral benzyl systems react through ion pairs,³⁷ and Sneed had suggested that 4-methoxybenzyltrimethylsulfonium and benzyltrimethylsulfonium reacted through ion-dipole complexes.¹⁴ Katritzky³⁸ has studied the substitution (with neutral amines in solvent chlorobenzene) and gas-phase dissociation reactions of benzyl systems with highly arylated pyridinium leaving groups, which he claimed reacted through ion-dipole complexes. Surprisingly, however, no work had been done on benzyl pyridiniums in water. If ion-dipole complexes were found to be intermediates in solvolysis of benzyl pyridiniums, it might indicate that they were possible intermediates in the NAD^+ systems. On the other hand, it would be necessary to establish what the relative stabilities of the ribosyl oxocarbenium ion and benzyl carbenium ion were.

Because of solvation effects, this comparison could be made best by having gas-phase data. A compliment to these data would be computational results that could be used to compare relative energies, both in terms of ΔH^\ddagger for bond breaking and of ΔH_R for the over all reaction. These questions were addressed in turn.

Benzyl Pyridiniums. A series of 4-Y-substituted (Y = MeO, Me, H, Cl, NO₂) benzyl pyridiniums were prepared and the azide substitution and solvolysis kinetics were determined using NMR techniques. This was necessary because the high concentrations of nucleophile used precluded the use of UV techniques. No evidence was found for ion-dipole complexes, in contrast to Katritzky's claim³⁸ that benzyl systems with highly arylated pyridine leaving groups reacted through ion-dipole complexes. The kinetic results and an analysis of Katritzky's results and mechanism are given in Chapter 2.

Benzyl Dimethylsulfoniums. Because no evidence for ion-dipole complexes was found for benzyl pyridiniums, the solvolysis and substitution reactions with a large number of nucleophiles of Sneen's signature compound 4-methoxybenzyl dimethylsulfonium¹⁴ were studied in detail, both under conditions of constant ionic strength (to avoid Schleyer's criticism¹⁰ of Sneen's work) and with nucleophile alone at various concentrations (to check Sneen's conditions with nucleophiles other than azide). (Swain and his students³⁹ and later Thornton¹³ had studied other benzyldimethylsulfoniums, and data were available for comparison with 4-methoxybenzyl dimethylsulfonium.) No evidence was found for ion-dipole complexes in either the solvolysis (Chapter 3) or nucleophile substitution reactions (Chapter 4). The results were different than found for the pyridiniums, however.

Gas-phase Dissociation. To obtain data for direct comparison of reactivity in the gas phase, the dissociation of Handlon's series of arabinosides (Chapter 5) and the benzyl pyridiniums and dimethylsulfoniums (Chapter 6) were studied using tandem liquid secondary ion mass spectroscopic (LSIMS) techniques. The

reaction profiles were calculated using semi-empirical techniques. For various reasons, it was more convenient to do these calculations in the Hyperchem software on an IBM clone than to use packages such as MOPAC. To do this, however, required working out the techniques in a software package not explicitly designed to do transition state modeling (Chapter 5).⁴⁰ The solution and gas-phase relative rates all correlated well with the gas-phase computational results. It is possible to show directly that the ribosyl oxocarbenium ion is intrinsically more stable than the 4-methoxybenzyl carbenium ion, a species known from the work of Richard and Amyes³⁶ and the work done here on the dimethylsulfonium, confirmed recently by Kevill and his coworkers,⁴¹ to be a solvent-equilibrated intermediate.

Computational Studies of Related Reactions. With these data in hand, computational studies of the heterolytic cleavage of various substrates with potentially stable oxocarbenium ions were performed with pyridine and dimethylaniline leaving groups (Chapter 7). The results confirm Jencks's contention that the methoxymethyl oxocarbenium ion is not sufficiently stable to exist as an intermediate.^{23,28,29} When the reactions of ROHR' were studied, however, it was found that oxocarbenium ion intermediates for secondary and five- and six-membered ring systems, including ribosyl and glucosyl oxocarbenium ions, were sufficiently stable to exist as intermediates (Chapter 8). Some of these results also offer insight into the conditions under which various proton transfer mechanisms can operate in acetal hydrolysis.

The results and conclusions are summarized in Chapter 9, with an analysis of how glycosyl hydrolases may "catalyze" a dissociative reaction.

References and Notes

(1) These matters are reviewed extensively in the standard texts. Carey, F.A.; Sundberg, R.J. *Advanced Organic Chemistry*; Plenum: New York, 1990; 3rd Ed., Part A, pp. 257-341. Lowrey, T.H.; Richardson, K.S. *Mechanism and Theory in Organic Chemistry*; Harper and Row: New York, 1981; 2nd Ed., pp. 291-463.

(2) A new scheme for designating mechanism has been devised by Guthrie, R.D; Jencks, W.P. *Acc. Chem. Res.* **1989**, *22*, 343-349 at the behest of the IUPAC's Commission on Physical Organic Chemistry. I find the new scheme to be confusing in the extreme and prefer the older, common-sense pneumatic system.

(3) Ingold, C.K. *Structure and Mechanism in Organic Chemistry*; Cornell, Ithica, NY, 1953; pp. 306-419.

(4) Cram, D.J. *J. Am. Chem. Soc.* **1949**, *71*, 3863-3868; *J. Am. Chem. Soc.* **1953**, *74*, 2129-2936.

(5) Winstein, S.; Robinson, G.C. *J. Am. Chem. Soc.* **1958**, *80*, 169-179.

(6) Carpenter, B.K. *Determination of Organic Reaction Mechanisms*; Wiley-Interscience: New York, 1984, pp. 40-51.

(7) Brown (Brown, H.C. *Chem. Soc. (London), Spec. Publ.*, **1962**, *16*, 104-163) argued that the phenonium ion was a transition state structure that occurred between two equilibrating classical structures and not a lower-energy intermediate. After much debate and a series of experiments done in both their laboratories (Brown, H.C.; Kim, C.J.; Lancelot, C.J; Schleyer, P. v. R. *J. Am. Chem. Soc.* **1970**, *92*, 5244-5250), Schleyer convinced Brown that the phenonium ion was a true non-classical intermediate.

(8) Weiner, H.; Sneen, R.A. *J. Am. Chem. Soc.* **1965**, *87*, 287-292; 292-298.

(9) Sneen, R.A.; Larsen, J.W. *J. Am. Chem. Soc.* **1969**, *91*, 362-366.

UCSF LIBRARY

(10) Raber, D.J.; Harris, J.M.; Hall, R.E.; Schleyer, P. v. R. *J. Am. Chem. Soc.* **1971**, *93*, 4821-4832.

(11) Gold, V. *J. Chem. Soc.* **1956**, 4633-4640.

(12) Kohnstam, G.; Queen, A.; Shillaker, B. *Proc. Chem. Soc.* **1959**, 157-160.

(13) Friedberger, M.P.; Thornton, E.R. *J. Am. Chem. Soc.* **1976**, *98*, 2861-2865.

(14) Sneen, R.A.; Felt, G.R.; Dickason, W.C. *J. Am. Chem. Soc.* **1973**, *95*, 638-639.

(15) Sneen, R.A.; Larsen, J.W. *J. Am. Chem. Soc.* **1969**, *91*, 6031-6035;
Sneen, R.A. *Acc. Chem. Res.* **1973**, *6*, 46-53.

(16) Li, T.; Janda, K.D.; Hilton, S.; Lerner, R.A. *J. Am. Chem. Soc.* **1995**, *117*, 2367-2368.

(17) Harder, S.; Streitwieser, A.; Petty, J.T.; Schleyer, P.v.R. *J. Am. Chem. Soc.* **1995**, *117*, 3252-3295.

(18) Buckley, N., two communications submitted to *J. Am. Chem. Soc.*

(19) Bentley, T.W.; Schleyer, P.v.R. *Adv. Phys. Org. Chem.* **1977**, *11*, 1-67.

(20) Richard, J.P.; Jencks, W.P. *J. Am. Chem. Soc.* **1984**, *106*, 1373-1383;
Banait, N.S.; Jencks, W.P. *J. Am. Chem. Soc.* **1991**, *113*, 7951-7958.

(21) Buckley, N., unpublished results. A consistent finding is that the PM3 ΔH^\ddagger for the reaction $R^+ + R'OH, HOH \rightarrow ROHR'^+$ (ROH_2^+) gives an excellent correlation against the experimentally measured $\log k$.

(22) In addition to the references cited below, Jencks made the bold claim to the author and N.J. Oppenheimer (in the middle of the Bay Bridge one dark and stormy night in January, 1990, during a ride from Berkeley to San Francisco) that there was no evidence from any study for the existence of ion pairs.

UCSF LIBRARY

(23) Jencks, W.P. *Acc. Chem. Res.* **1980**, *13*, 161-169; Jencks, W.P. *Chem. Soc. Rev.* **1981**, *10*, 345-375.

(24) Carey and Sundberg (Ref. 1) give a sensible summary of the Jencks scheme, which the discussion given here used as a guide.

(25) Schröder, S.; Buckley, N.; Oppenheimer, N.J.; Kollman, P.A. *J. Am. Chem. Soc.* **1992**, *114*, 8232-8238. This computational study shows that the exploded activated complex for dissociation of NAD^+ is not reproduced in the gas-phase by semi-empirical methods.

(26) Richard, J.P.; Jencks, W.P. *J. Am. Chem. Soc.* **1984**, *106*, 1383-1396.

(27) Craze, G-A.; Kirby, A.J.; Osborne, R. *J. Chem. Soc. Perkin Trans. II*, **1978**, 357-368.

(28) Knier, B.L.; Jencks, W.P. *J. Am. Chem. Soc.* **1980**, *102*, 6789-6796.

(29) Young, P.R.; Jencks, W.P. *J. Am. Chem. Soc.* **1977**, *99*, 8238-8248.

(30) Capon, B. *Chem. Rev.* **1969**, *69*, 407-498. (b) Cordes, E.H.; Bull, H.G. *Chem. Rev.* **1973**, *73*, 581-603.

(31) Handlon, A.L. Ph.D. Dissertation, The University of California, San Francisco, 1991.

(32) Johnson, R.W.; Marschner, T.M.; Oppenheimer, N.J. *J. Am. Chem. Soc.* **1988**, *110*, 2257-2263.

(33) Tarnus, C.; Schuber, F. *Bioorg. Chem.* **1987**, *15*, 31-42; Tarnus, C.; Muller, H.M.; Schuber, F. *ibid.*, **1988**, *16*, 38-51.

(34) Handlon, A.L.; Oppenheimer, N.J. *J. Org. Chem.* **1991**, *56*, 5009-5010.

(35) Handlon, A.L.; Xu, C.; Müller-Steffner, H.-M.; Schuber, F.; Oppenheimer, N.J. *J. Am. Chem. Soc.* **1994**, *116*, 12087-12088.

(36) Amyes, T.L.; Richard, J.P. *J. Am. Chem. Soc.* **1990**, *112*, 9507-9512. These authors provide an extensive review of the literature on benzyl solvolysis.

(37) Reviewed by Shiner, V.J. In *Isotope Effects in Chemical Reactions*, Collins, C.J., Bowman, N.S. Eds.; Van Nostrand Reinhold: New York, 1970; pp 90-159.

(38) Reviewed in Katritzky, A.R.; Brycki, B.E. *Chem. Soc. Rev.* **1990**, *19*, 83-105, and elsewhere. See also Katritzky, A.; Malhotra, N.; Ford, G.P.; Anders, E.; Tropsch, J.G. *J. Org. Chem.* **1991**, *56*, 5039-5044.

(39) Swain, C.G.; Kaiser, L.E. *J. Am. Chem. Soc.* **1958**, *80*, 4089-4092; Swain, C.G.; Kaiser, L.E.; Knee, T.E.C. *J. Am. Chem. Soc.* **1958**, *80*, 4092-4094.; Swain, C.G.; Thornton, E.R. *J. Org. Chem.* **1961**, *26*, 4808-4809. Swain, C.G.; Taylor, L.J. *J. Am. Chem. Soc.* **1962**, *84*, 2456-2457; Swain, C.G.; Rees, T.; Taylor, L.J. *J. Org. Chem.* **1963**, *28*, 2903; Swain, C.G.; Burrows, W.D.; Schowen, B.J. *J. Org. Chem.* **1968**, *33*, 2534-2536.

(40) Buckley, N.; Handlon, A.L.; Maltby, D.; Burlingame, A.L.; Oppenheimer, N.J., *J. Org. Chem.* **1994**, *59*, 3609-3615.

(41) Kevill, D.N.; Ismail, N.H.J.; D'Souza, M.J. *J. Org. Chem.* **1994**, *59*, 6303-6312.

UCSF LIBRARY

Chapter 2
The Solvolysis and Azide Substitution Reactions of
Benzyl Pyridiniums in Water

UCSF LIBRARY

Introduction

Oppenheimer *et al.* have studied the cleavage of the nicotinamide-ribosyl bond in nicotinamide-adenosine dinucleotide (NAD⁺)¹ and in a series of 2'-substituted β -nicotinamide ribosides² and arabinosides,³ and Schuber and his colleagues have studied the solution and enzyme-catalyzed cleavage of NAD⁺ analogs with different pyridine leaving groups.⁴ All the evidence suggests that bond cleavage is either S_N1 or involves an ion-dipole complex (IDC). A purely dissociative mechanism is at odds with a suggestion made by Jencks⁵ that sugar oxocarbenium ions are too unstable to exist as solvent-equilibrated intermediates. In a computational study of the gas-phase dissociation of β -nicotinamide riboside in the presence of several water molecules, Schröder *et al.*⁶ found that the structures of the activated complexes and energies of the transition states for the inversion and retention reactions were different, which led them to question the general validity of the "exploded" transition state invoked by Sinnott and Jencks⁷ to explain the relative reactivities and selectivities of glucosyl pyridiniums.

A recent study of the gas-phase dissociation of Handlon's series² of 2'-substituted β -nicotinamide arabinosides showed that dissociation occurred through an ion-dipole complex (IDC) intermediate.⁸ Correlations among the measured relative rates and the PM3-calculated values of ΔH^\ddagger for the gas-phase reaction and the experimentally determined values of ΔG^\ddagger for the solution reaction strongly suggested that the mechanism of dissociation was the same in both phases, but that the rate-limiting step was different.

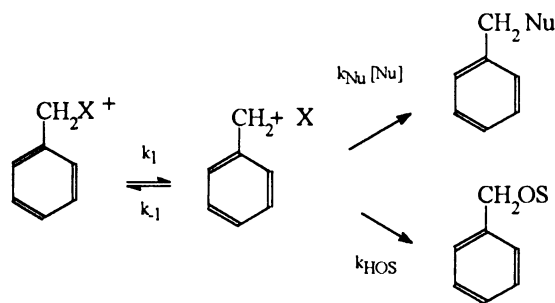
It seemed that some insight into the question of intermediate stability and mechanism might be gained by studying the hydrolysis and nucleophilic substitution reactions of pyridinium substrates with potentially stable carbenium ion intermediates. Benzyl substrates provide a convenient system because the structure of both the putative intermediate and leaving group can be varied easily.

UCSF LIBRARY

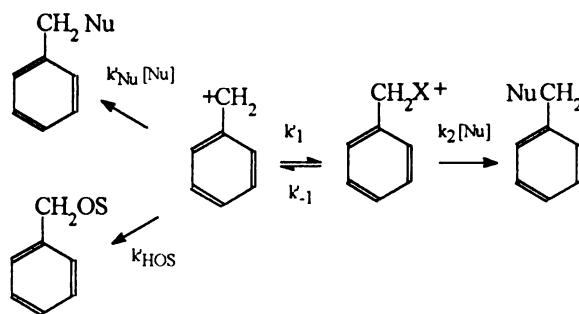
It was established with certainty recently that the 4-methoxybenzyl carbenium ion is an intermediate in the solvolysis and azide substitution reactions of neutral (benzoates and chlorides⁹) and charged (dimethylsulfonium^{10,11}) substrates. Other evidence¹² suggests that benzyl dimethylsulfoniums react with nucleophiles and water by direct displacement.

Katritzky¹³ has published a large amount of data on the substitution reactions of benzyl and other substrates with highly arylated or fused-ring pyridines as the LG in chlorobenzene with neutral amine nucleophiles, primarily piperidine. (4-Methoxybenzyl)-2',4',6'-triphenylpyridinium and several of the fused-ring substrates exhibit borderline kinetics. Benzyl triphenylpyridiniums bearing 4-Y-groups with $\sigma^+ > -0.31$ do not exhibit borderline kinetics, however. The Hammett plot for the second order rate constants of all triphenylpyridinium substrates is linear (see below). Katritzky interpreted these results in terms of an IDC mechanism.

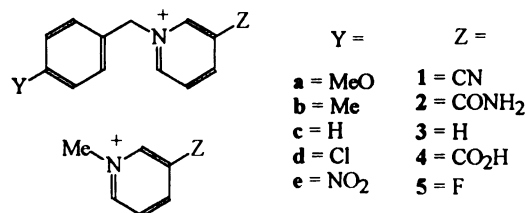
Ion-Dipole Complex Mechanism



Mixed S_N1/S_N2 Mechanism



We have prepared and studied the reaction with azide in deuterium oxide of a series of (4-Y-benzyl)-3'-substituted pyridiniums (Y: MeO = **a**; Me = **b**; H = **c**; Cl = **d**; NO₂ = **e**. Pyridine: 3-CN = **1**; 3-CONH₂ [nicotinamide] = **2**; 3-H = **3**; 3-CO₂H = **4**; 3-F = **5**) and several N-Me pyridiniums (**1-Me** and **2-Me**). Because the



rate constants could be measured conveniently, we have concentrated on **1a-e**. We are limited to the use of azide because of the well-known propensity of anions to add to the 4-position of pyridiniums; thus we can obtain β_{LG} but not β_{Nuc} . Unlike Katritzky's results in chlorobenzene with neutral nucleophiles, we found that all substrates reacted with azide in a strictly second-order manner; reactions in water only appear to involve direct solvent displacement. Because of this discrepancy, we have recalculated some of Katritzky's structures in AM1 and, based on an analysis of these structures and the kinetics of possible mechanisms, suggest that Katritzky's system reacts through a mixed S_N1/S_N2 mechanism, and not through an IDC.

With Maltby and Burlingame, we measured the relative rates for the gas-phase dissociation of these pyridinium substrates and have reported the results elsewhere.¹⁴ Thus we have solution, gas-phase, and computational results, obtained in the same laboratory under essentially identical conditions, for the ribosyl and benzyl pyridiniums that can be compared directly. In brief, the comparison shows that the ribosyl oxocarbenium ions are intrinsically more stable than the benzyl carbenium ions in the gas phase, and that the mechanism of hydrolysis and azide substitution are different, with unimolecular reactions for the

ribosyl compounds and bimolecular reactions for the pyridiniums. (With our work on benzyl dimethylsulfoniums, we have a system with which to compare the effects of the LG.) These results are inconsistent with the supposition that the ribosyl oxocarbenium ions cannot exist as discrete intermediates on the reaction coordinate.

Experimental Section

General. All chemicals were obtained from Aldrich and used without further purification. Proton magnetic spectra were recorded at 300 MHz (TSP = 0 δ) on a General Electric QE-300 FT-NMR fitted with a variable temperature probe rated at $\pm 0.1^\circ\text{C}$. Liquid secondary ion mass spectra (LSIMS) were obtained on a 4-sector Kratos Concept II in the positive ion mode in the UCSF Mass Spectrometry Facility. Plots were made and linear regression was performed on either Sigmaplot or Origin software.

Syntheses. All substrates were prepared by alkylation of the appropriate pyridine with the appropriate benzyl chloride in either acetonitrile or chloroform solution by mixing 1 eq. of the chloride with 1.1 eq. of the pyridine and allowing the mixture to stand at ambient temperature. The progress of the reaction was monitored by TLC (silica, either neat acetonitrile or neat chloroform) until the chloride had disappeared. For reactions in acetonitrile, the solvent was removed by rotary evaporation at reduced pressure, the residue was dissolved in water and extracted several times with chloroform and then with ether to give clear aqueous solutions. For reactions in chloroform, water was added to the organic layer and the aqueous layer was extracted several times with chloroform and then with ether to give a clear aqueous layer. Rotary evaporation of the water at reduced pressure gave glasses that with extensive ethanol flashing yielded waxy solids in essentially quantitative yields; compounds had $>98\%$ purity by NMR. Syntheses in

UCSF LIBRARY

chloroform are much preferred. In some instances, alkylations were performed in the neat pyridines (for liquids) or in melts of solid pyridines. Highly colored solid products were dissolved in water and extracted with chloroform and ether, after which the aqueous solution was heated with Norit A and filtered through a pad of filter aid to give water-white solutions that were evaporated. Nicotinamide and 3-cyanopyridine were alkylated with MeI using the same procedure described for the benzyl substrates. Some products (eg. the nicotinamide derivatives) could be recrystallized from acetonitrile; in general, however, products were used as isolated by the extractive procedure. Appropriate ^1H and ^{13}C NMR and LSIMS spectra¹⁴ were obtained for all compounds, which have been prepared previously as various salts (tosylates, triflates, iodides, etc.) and were not further characterized.

Kinetics. Two methods were used to obtain *pseudo* first-order rate constants (k_{obsd}). For **2a-e** and **3a-e**, ca. 1-2 mM solutions were made up in NMR tubes with the appropriate azide stock solution in D_2O , with NaCl added to control ionic strength, and heated in thermostatted heat blocks (sand bath) at 96°C . Tubes were removed and spectra recorded at approximately 22 hr intervals. For **1a-e**, the appropriate stock solutions of azide in D_2O were heated in the probe of the NMR at various temperatures (40°C - 90°C), the tube was removed, substrate was added to make ca. 5-10 mM solutions, the tube was returned to the probe, shimmed after ca. 1 min. to allow equilibration, and spectra were recorded at various time intervals. For particularly slow reactions--those that were complete within 4-5 hr--tubes were held in thermostatted heat blocks at the appropriate temperature and transferred at various intervals to the heated NMR probe in a round-robin fashion.

Values of k_{obsd} obtained with this method from plots of $\ln(C_t/C_0)$ vs. time were linear ($r > 0.990$ by linear regression). There is, however, an odd--and absolutely reproducible--observation that we should note. Plots for intermediate

and long reaction times obtained in a single day had a slight but noticeable sinusoidal form with a period of oscillation that was shorter on weekdays than on weekends. It finally occurred to us that the periodicity and weekday/weekend dependence could be the result of the location of the magnet within 50 feet of a bank of four heavily used elevators. Frequent, periodic passage of large chunks of iron and steel could perturb the field slightly and produce the aberrant readings; weekend traffic is much lighter than weekday traffic.

For all substrates under these conditions, the 2' and 6' pyridine protons rapidly exchanged. Depending on the substrate, the benzyl methylene protons would also exchange, slowest for the 4-MeO derivatives and fastest for the 4-NO₂ derivatives. Therefore, kinetics were determined by measuring the disappearance of the multiplet for the pyridine 5' proton that did not exchange. The total substrate was taken as the sum of the substrate and product peaks, which provided an internally consistent standard. As a check on the method, in some instances the disappearance of the substrate benzyl aromatic AA'BB' peaks or the 4' pyridine peak; in all instances, the same rate constant was obtained.

Product analysis was performed by extracting reaction mixtures with CDCl₃ and integrating the appropriate aromatic AA'BB' peaks in ¹H-NMR spectra.

Suppression Studies. For studies of the suppression of hydrolysis in the absence of exogenous leaving group, serial dilutions were made of stock solutions of the appropriate pyridinium in D₂O. Aliquots in NMR tubes were heated in thermostatted heat blocks (sand bath) and spectra were recorded at intervals of one to two days. For studies of suppression of hydrolysis with exogenous leaving group for **1a-e**, 5mM solutions of substrate containing 5mM 3-cyanopyridine were heated and analyzed as described above.

Computational Methods. Calculations were performed on a 486/66 (16 MB RAM) using Release 4.0 of the Hyperchem software.⁸ Initial structures were

minimized with MM+ (Hyperchem's version of MM2) using the partial charge option. The Polak-Ribiere block diagonal algorithm was used to an RMS gradient of <0.1 kcal/[Å mol]. Semi-empirical minimizations were unrestricted Hartree-Fock with the wavefunction calculated to a convergence limit of <0.001 .

Results

Azide Kinetics. Values of *pseudo*-first order k_{obsd} were obtained by linear regression as the slopes of plots of $\ln(C_t/C_0)$ vs. time, where C_t was the relative concentration at time t measured from the 5'-pyridine peak and C_0 was the sum of the relative concentrations of C_t and product pyridine. For **1a-e**, plots were linear over 3-4 measured halfives and generally had $r \geq 0.990$; in several instances the r values were in the range 0.980 to 0.990. For **2a-e**, **3a,e**, and **5a,e**, plots were linear over 1-2 measured halfives. Values of k_{obsd} typically varied by 1-10% SE. Second-order rate constants (k_2) were determined by linear regression from plots of k_{obsd} vs. [azide] (Table 2.1). In all but two instances, $r \geq 0.996$. For **1a-e**, plots were based on the averages of 2-8 determinations. For the slower reactions of **2a-e**, **3a,e**, and **5a,e**, plots were based on duplicate determinations.

Activation values for the **1a-e** were determined from 4-5 point Eyring plots (range 50-90°C) by linear regression ($r \geq 0.998$). For **1-Me iodide**, only three points were used ($r = 0.9999$). Values summarized in Table 2.2 are reported \pm S.D.

3-Cyanopyridiniums. These substrates reacted smoothly with azide at convenient rates in the range 50-90°C. Plots of k_{obsd} vs. [azide] were linear over more than half of the concentration of azide, after which a slight curvature could be seen, especially for the plots at 70°, 80°, and 90°C (Figure 2.1). These plots appear to intercept the origin within error; as shown below, however, there is a slow hydrolysis reaction. Second-order rate constants for reaction at 80°C ($\mu = 1.7$, NaCl) determined in the range 0-1.2M azide (all $r > 0.999$), are listed in Table 2.1.

UCSF LIBRARY

Nicotinamides. Rate plots for reaction of azide with **2a-e** were linear over 2-4 half-lives at 96°C (Figure 2.2). Plots of k_{obsd} vs. [azide] are linear between 0

Table 2.1
Second-order rate constants for the reaction of
1a-e (80°C) and 2a-e (96°C) with NaN₃ (k_2) and water (k_w)

Y	k_2 (min ⁻¹ M ⁻¹)	k_w (min ⁻¹ M ⁻¹)	k_{rel}
1a-e			
MeO	$9.6 \pm 0.09 \times 10^{-2}$	23.9×10^{-6}	0.4×10^4
Me	$10.4 \pm 0.4 \times 10^{-2}$	7.8×10^{-6}	1.3×10^4
H	$8.3 \pm 0.3 \times 10^{-2}$	3.1×10^{-6}	2.6×10^4
Cl	$11.2 \pm 0.5 \times 10^{-2}$	1.8×10^{-6}	6.2×10^4
NO ₂	$9.1 \pm 0.3 \times 10^{-2}$	0.3×10^{-6}	36.0×10^4
1-Me	$7.5 \pm 0.2 \times 10^{-2}$	--	--
2a-e			
MeO	$5.3 \pm 0.7 \times 10^{-4}$	2.2×10^{-6}	241
Me	$5.3 \pm 0.8 \times 10^{-4}$	2.3×10^{-6}	230
H	$2.9 \pm 0.1 \times 10^{-4}$	2.0×10^{-6}	145
Cl	$2.4 \pm 0.2 \times 10^{-4}$	2.5×10^{-6}	96
NO ₂	$5.3 \pm 0.8 \times 10^{-4}$	2.0×10^{-6}	265
2-Me	$2.3 \pm 0.7 \times 10^{-4}$	1.6×10^{-6}	144

All rate constants determined at $\mu = 1.7$ (NaCl). Azide range 0-0.85M for **1a**, **2a-e**, **2-Me**; 0-1.7M for **1b-e**, **1-Me**. For **1a-e**, all $r \geq 0.999$; for **2a-e**, all $r \geq 0.980$. $k_w = k_{\text{obsd}}/55.5$. For **1a-e**, k_{obsd} for the water reaction was estimated from the plots in Figure 2.6; for **2a-e** and **2-Me**, k_{obsd} for the water reaction were measured directly (as in Figure 2.2).

Table 2.2.
Eyring activation values for the reaction of 1a-e and 1-Me with NaN₃ at 80°C

Y	ΔH^\ddagger kcal/mol	ΔS^\ddagger gibbs/mol	ΔG^\ddagger_{80} kcal/mol	r
MeO	17.6 ± 0.8	-21.6 ± 2.0	25.2	0.9970
Me	15.7 ± 0.6	-26.9 ± 1.6	25.3	0.9980
H	14.4 ± 0.1	-30.9 ± 0.4	25.3	0.9999
Cl	15.6 ± 0.4	-28.8 ± 1.3	25.2	0.9992
NO ₂	14.8 ± 0.3	-29.7 ± 0.8	25.3	0.9995
1-Me	15.0 ± 0.1	-29.5 ± 0.2	25.8	0.9999

Determined from 4-5 point plots for 1a-e and a 3 point plot for 1-Me.

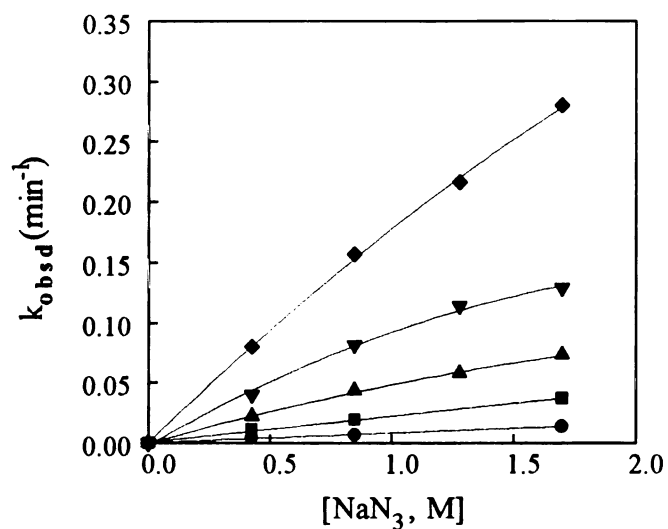


Figure 2.1. Second-order rate plots for the reaction of 1a with NaN₃ ($\mu = 1.7$, NaCl) in D₂O at 50°C (●), 60°C (■), 70°C (▲), 80°C (▼), and 90°C (◆).

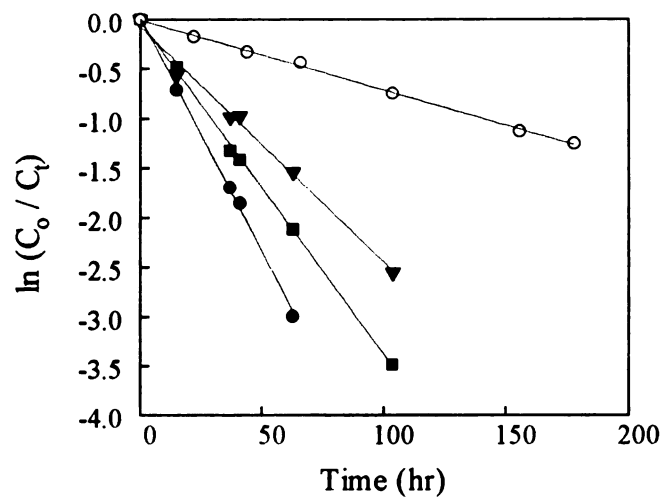


Figure 2.2. Rate plots for the reaction of **2a** with NaN_3 ($\mu = 1.7$, NaCl) in D_2O at 96°C . $[\text{NaN}_3] = 1.7$ (\bullet), 0.85 (\blacksquare), 0.43 (\blacktriangle); $\circ =$ water only. The r values are 0.9994 , 0.9995 , 0.9962 , and 0.9992 , respectively.

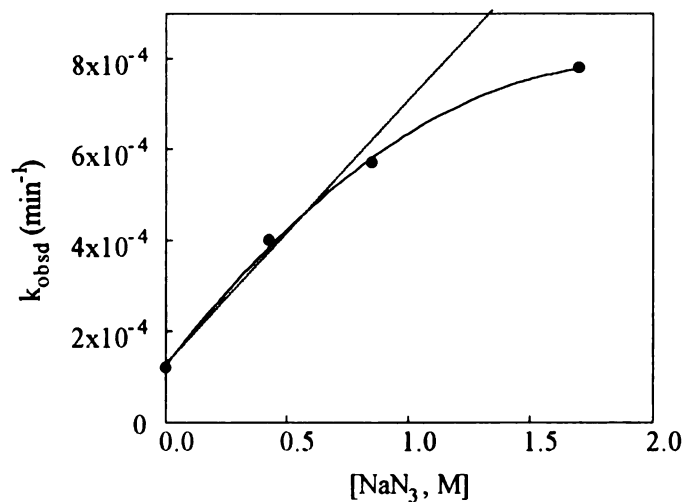


Figure 2.3. Second-order rate plot for the reaction of **2a** with NaN_3 ($\mu = 1.7$, NaCl) in D_2O at 96°C . The straight line is a regression fit ($r = 0.990$) to the point for water alone, 0.43M and 0.85M azide.

and 0.85 M azide, after which curvature appeared in some plots (Figure 2.3). These plots had non-zero intercepts (k_{hyd}), and there was a measurable reaction in water alone; the rate constants were the same within error. Curvature could be the result of some nonspecific salt effect, or it could be the result of azide-catalyzed hydrolysis of the amide; because the pK_a for nicotinic acid is higher than that for nicotinamide, the displacement reactions would be slower and could account for the curvature. Values for the second-order rate constants were taken from the linear portions of the curves; these and the values for k_w , which for comparison with the azide numbers are the second-order rate constants $k_{\text{hyd}}/55.5$, are listed in Table 2.1.

Pyridiniums. **3a** and **3e** reacted very slowly with azide at 96°C. Second-order rate constants are listed in Table 2.1. For **3b-d**, however, *there was no detectable reaction at 96°C in up to 1.7M azide for 6 months!*

D₂O Only Kinetics. *3'-Cyanopyridiniums.* In D₂O alone, the extent of reaction is a function of the concentration of substrate. Shown in Figure 2.4 are plots of $\ln(C_0/C_t)$ vs. time for the hydrolysis of 5-50mM solutions of **1a** and **1b** at 80°C; a similar pattern was found for the slower reactions of **1c-e** at 96°C (5, 20, and 50mM solutions; not shown). This curvature is the same as found for (4-methoxybenzyl)dimethylsulfonium chloride that we have shown¹⁰ is caused by the establishment of the equilibrium $\text{RX}^+ \rightleftharpoons \text{ROH} + \text{H}_3\text{O}^+ + \text{X}^0$ during the course of the reaction. For the sulfonium, data were fitted to a cubic equation derived for the equilibrium that assumed X^0 is not protonated, which is a reasonable assumption for SMe_2 ($\text{pK}_a = -6$). For pyridiniums, however, a significant proportion of the liberated pyridine would be protonated. With the simplifying assumption that $[\text{ROH}] \sim [\text{XH}^+]$, the equation for the equilibrium is $C_0 = K_a K_{\text{eq}} f/(1-f)^2$, where C_0 is the initial concentration of substrate, K_a is the acidity constant for the pyridine,

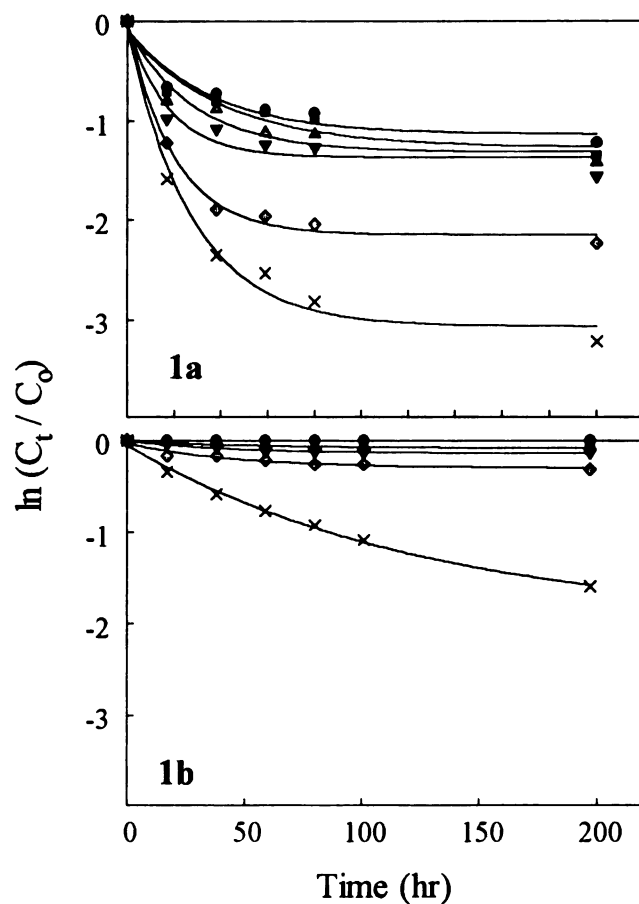


Figure 2.4. Reaction progress for **1a,b** at 80°C in pure D₂O as a function of the initial molar concentration of substrate: 0.005 = x; 0.010 = ◇; 0.020 = ▼; 0.030 = △; 0.040 = ■; 0.050 = ●.

K_{eq} is the equilibrium constant, and f is the fraction remaining ($[\text{RX}^+]/C_0$). The fit of data for **1a** ($C_0 = 0.005$ to 0.05M at $t = 200$ hr) by the Marquand-Leverberger non-linear least squares algorithm in the Origin software is shown in Figure 2.5 ($K_{\text{eq}} = 2.29 \pm 0.06$, $X^2 = 3.84 \times 10^{-6}$).

Studies of exogenous LG were limited for sulfoniums by the solubility of SMe_2 in water.¹⁰ With the pyridiniums, solubility of the LG is not a problem, but it is difficult to analyze and quantitate the aromatic region of spectra containing large amounts of exogenous pyridine; for **1a** and **1b**, however, the methyl signals can be followed conveniently, and the same is true for the methylene signals for **1c** and

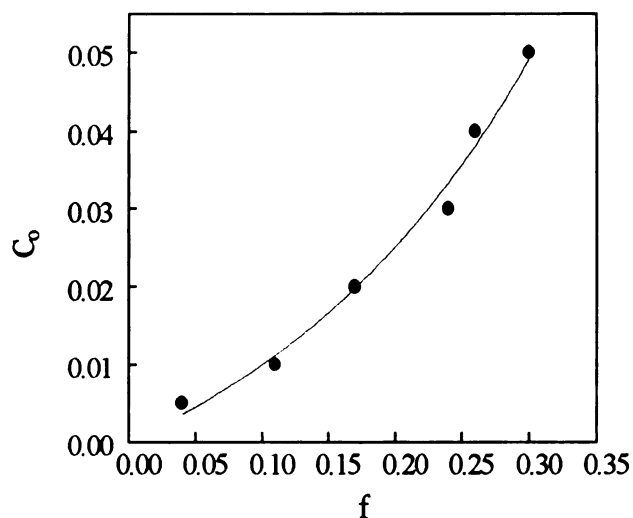


Figure 2.5. Fit of the data for **1a** from Figure 2.4 to the equation for the equilibrium $\text{RPy}^+ \rightleftharpoons \text{ROH} + \text{Py} + \text{H}_3\text{O}^+ \rightleftharpoons \text{PyH}^+$. $K_{\text{eq}} = 2.29 \pm 0.06$, $\chi^2 = 3.8 \times 10^{-6}$.

1d, although for high concentrations of pyridines some exchange of these protons takes place and the readings can be inaccurate. Shown in Figure 2.6 are plots of $\ln(C_0/C_t)$ for the hydrolysis of 5mM solutions of **1a-d** in the presence of 5mM 3-cyanopyridine (closed circles) at 80°C; for comparison, the plots for 5mM substrate alone are included (open circles). The presence of exogenous leaving group further suppresses the reaction.

Because of the severe curvature and the fact that use of the Guggenheim method or inclusion of an infinity value in the rate equation failed to give linear plots, it was difficult to obtain accurate values for the hydrolysis rate constants k_w . Points taken during the first half-life give approximately linear rate plots, however, and the values of k_w can be estimated. These are listed in Table 2.1.

NMR spectra for **1e** are very difficult to analyze because the benzyl methylene protons exchange rapidly under the reaction conditions, and the pyridinium and aromatic protons cannot be resolved well from those for product pyridine or alcohol. Nonetheless, spectra for 5, 30, and 50 mM solutions and 5mM

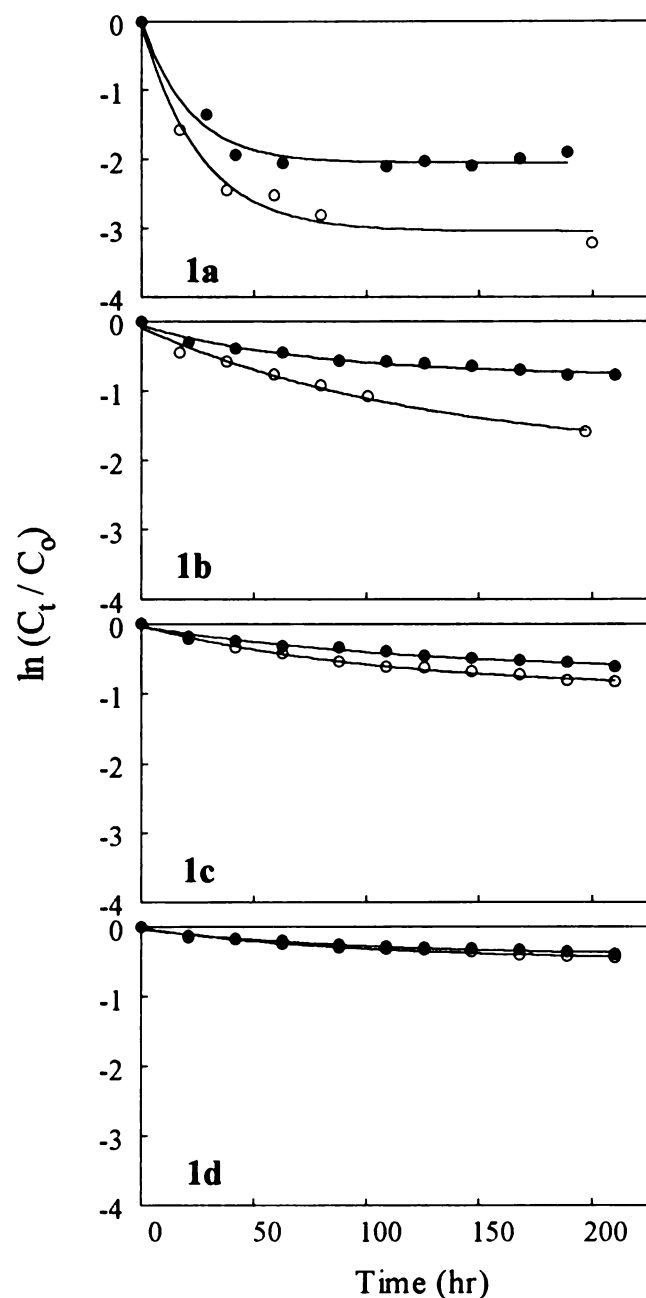


Figure 2.6. Reaction progress for 0.005M **1a-d** at 80°C in pure D₂O (O) and with 0.005M 3-cyanopyridine added (●).

substrate plus 5mM 3-cyanopyridine change only very slowly and to the same extent (measured by noting the change in the relative heights of the substrate and 5 product 5'-proton, which is difficult to quantitate with any accuracy). We did not attempt to characterize this reaction further.

Nicotinamide. The same concentration dependence found for the 3'-cyanopyridinium substrates was seen for the nicotinamide substrates at 96°C; the reaction was slower, and the extent of reaction was less than for the other set. We did not repeat the reaction in the presence of nicotinamide.

In the (4-methoxybenzyl)dimethylsulfonium work, we showed that if SMe_2 were removed as the Hg^{+2} or Zn^{+2} complexes, the reaction went to completion with no suppression.¹⁰ In 5.3M DCl at 96°C, the amide moiety of nicotinamide would be hydrolyzed rapidly to the acid, and any nicotinic acid released by solvolysis would be protonated and the equilibrium with starting material would be suppressed; it is also probable that the *bis* benzyl ether, which would have essentially the same NMR spectrum as the alcohol, would form under these

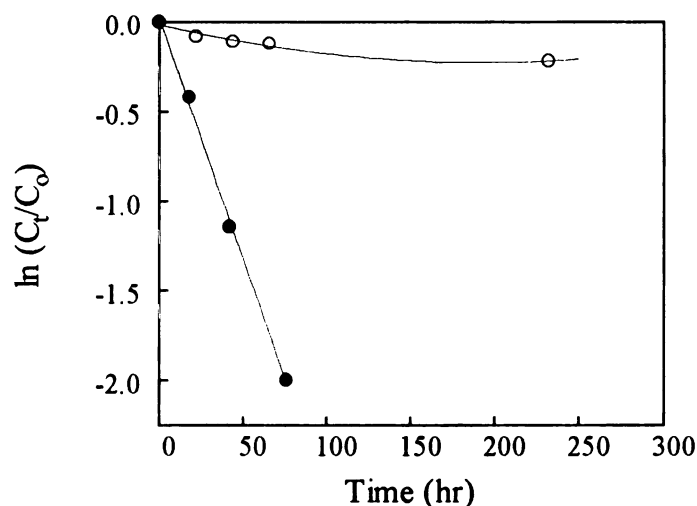


Figure 2.7. Rate plots for hydrolysis of **2a** (almost certainly hydrolyzed to the 3'-carboxy compound **4a**) in 5.3M DCl at 80°C (●), conditions that would prevent the equilibrium among starting material and products. The plot is linear ($r = 0.999$) over > 3 half-lives. For reference, the hydrolysis of 0.005M **4a** at 80°C in pure D_2O is shown (○).

extremely acidic conditions.¹² In the event, solvolysis of **2a** in 5.3M DCl at 96°C proceeded smoothly, and a plot of $\ln(C_t/C_0)$ vs. time was linear over three half-lives (Figure 2.7; $r = 0.999$). Similar plots were obtained for hydrolysis in the

presence of 2M D₂SO₄ (not shown). For comparison, the rate plot for the same concentration of **4a**, which was prepared by saponification of the methyl ester, in D₂O ($\mu = 1.7$, NaCl) is shown in Figure 2.7; the estimated rate constant in DCl is 35-fold higher than in D₂O alone, and the plot for D₂O alone is curved.

Other derivatives. The same concentration-dependent pattern was found for hydrolysis of **5a** and **6a** (plots not shown). Thus the equilibrium among starting material and products is independent of the pK_a of the leaving group and is general for the class.

Linear Free Energy Relations.

Hammett Plots. Hammett plots for the azide reaction of **1a-e** (80°C), **2a-e** (96°C), and **3a,e** (96°C) are shown in Figure 2.8. For **1a-e**, the plot is flat, which

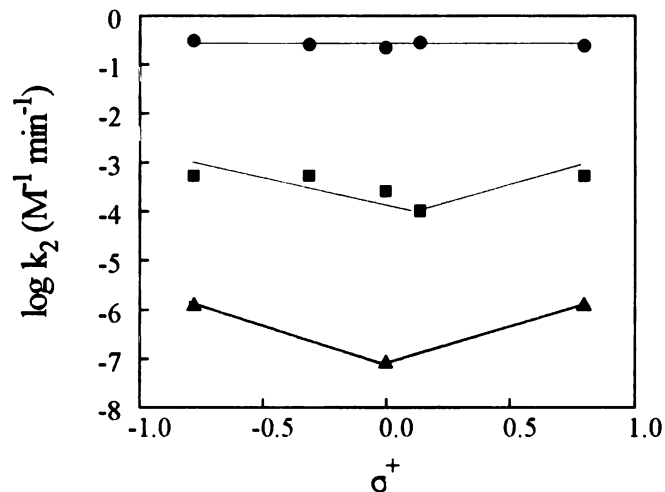


Figure 2.8. Hammett plots for the reaction with azide (k_2) of **1a-e** (●), **2a-e** (■), and **3a,e** (▲) at 96°C ($\mu = 1.7$, NaCl). The point for **3c** ($\sigma^+ = 0$) was estimated as described in the text.

shows little effect of the substituents. (Hammett plots based on k_2 values for lower temperatures show small increases to a V-shaped curve with decreasing temperature. The change is not great, however). For **2a-e**, the plot is V-shaped

with the break at **2c**. As noted above, **3b-d** did not react with azide after six months at 96°C; if it is assumed, however, that 3% reaction--the limit of NMR detection--had occurred for **3c**, the 3-point plot in Figure 2.8 is obtained. This estimated point is the upper limit for k_2 ; it is entirely possible that the 'real' value would be lower, and the break would be deeper. The salient point is that with increasing basicity of the LG, the depth of the break in the Hammett plots increases.

The Hammett plot for the hydrolysis of **1a-e** (Figure 2.9), which is based on estimated rate constants, is linear, which indicates the same mechanism of

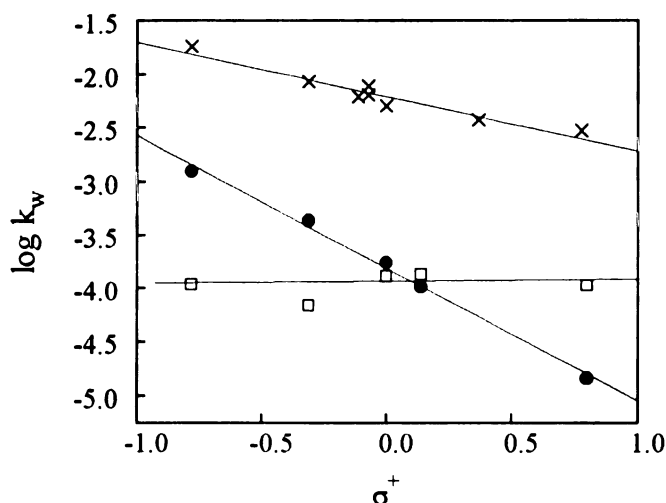


Figure 2.9. Hammett plots for the hydrolysis in D_2O of **1a-e** (●) and **2a-e** (□) at 80°C and 96°C ($\mu = 1.7$, NaCl), respectively. For **1a-e**, $\rho^+ = -1.24$ ($r = 0.997$); for **2a-e**, $\rho^+ = 0.05$ ($r = 0.26$). For reference, the Hammett plot is shown for Katritzky's second-order rate constants³² for the reaction of **6a** with piperidine in chlorobenzene at 100°C (x); $\rho^+ = -0.51$ ($r = 0.960$).

hydrolysis for all substrates. For (4-methoxybenzyl)dimethylsulfonium, the rates of hydrolysis and second-order reaction with azide are within the same range, and we have shown¹⁰ that there is a change in mechanism from S_N1 for the (4-methoxybenzyl)dimethylsulfonium compound to S_N2 for the others, which react

by direct displacement by solvent. Because of the great difference between the hydrolysis and second-order rate constants for **1a-e**, we assume that hydrolysis takes place by direct solvent displacement. The standard test for this, common leaving group suppression, cannot be applied here because of the equilibrium among products and starting materials, so our assignment of mechanism is of necessity circumstantial. The Hammett plot for hydrolysis of **2a-e** (Figure 2.9) is essentially flat.

Brønsted Plots. Values of β_{LG} at 96°C were determined from plots of $\log k_2$ vs. pK_a of the pyridine for **1-3a**, **5a** and for **1-Me** and **2-e**. Values of k_2 used in these plots were based on at least duplicate determinations; the second-order rate constants for the **1a** and **1-Me** were obtained from extrapolation of the Eyring plots. The Brønsted plot for **1a** (Figure 2.10) is linear with $\beta_{LG} = -1.47$. The two-

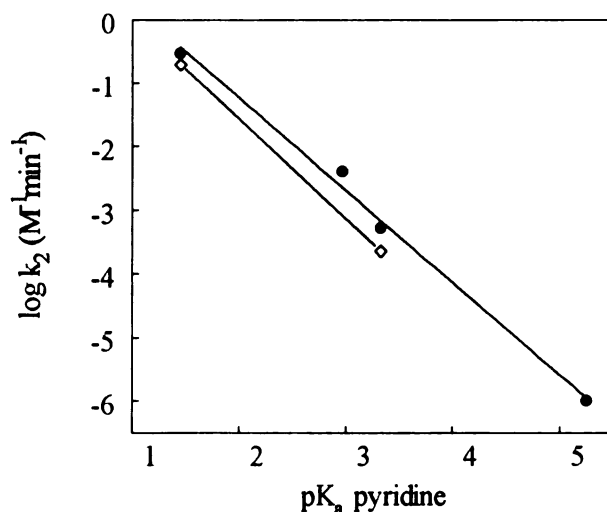


Figure 2.10. Brønsted plot for the azide reaction of (4-methoxybenzyl) pyridiniums at 80°C ($m = 1.7$, NaCl) (●); $\beta_{LG} = -1.45$ ($r = 0.997$). Data for the reactions of N-Me pyridiniums **1-Me** and **2-Me** with azide under identical conditions are shown (◊); $\beta_{LG} = -1.56$.

point "plot" for **1-Me** and **2-Me** (Figure 2.10) has a slope of -1.56; "plots" for **2b-d** and **3b-d** (not shown) are parallel to the 4-point line for **1a**. (The Hammett plot

[vs. σ_m] for the effect of substituents on the pyridine in **1a** is linear [not shown; $r = 0.991$] with $\rho = 8.9$.)

Product Studies. The only product detected in NMR spectra of CDCl_3 extracts of reaction mixtures of **1a-e** was the corresponding benzyl azide. For **2a-e**, ~ 5-10% of the respective alcohol could be detected, which is consistent with the concomitant hydrolysis reaction; the majority of the product was the respective benzyl azide. No alcohol was found for **3a** and **3e**, but because of the slow rate, these reactions were not taken to completion. All of the 4-nitrobenzyl substrates gave bright yellow precipitates upon addition of the substrate to the azide solution, consistent with addition of hydroxide to the 2'-position of the pyridine with subsequent rearrangement to the pyridone for nicotinamide and to other highly-colored products for the other pyridines. Using a measured amount of TSP as an internal standard for the water layer, the samples were extracted with CDCl_3 and the amount of substrate remaining in the D_2O layer was measured. In all instances, the apparently large amount of precipitate amounted to <2% of the substrate; indeed, the bright yellow CDCl_3 solutions has such low concentrations of products that spectra could not be recorded even after long acquisition times.

Discussion

Borderline kinetics in the substitution reactions of benzyldimethylsulfoniums with azide in water¹⁵ and for reactions of benzyl pyridiniums with neutral amines in chlorobenzene¹³ have been interpreted in terms of an IDC mechanism; a mixed $\text{S}_{\text{N}}1/\text{S}_{\text{N}}2$ mechanism was rejected for various reasons. Borderline behavior in the reactions of N-(methoxymethyl)-N,N-dimethylaniliniums with nucleophiles, however, was interpreted by Knier and Jencks¹⁶ as evidence for an "enforced" concerted mechanism because the putative

intermediate in an IDC or stepwise mechanism, $\text{MeO}=\text{CH}_2^+$, was judged to be too unstable to exist as a distinct, solvent-equilibrated species. We have recently examined the gas-phase dissociation of a number of compounds with a variety of oxocarbenium ion intermediates with different LGs (NMe_2Ar , Py, H_2O , MeOH, Me_2O) using semi-empirical methods.¹⁷ We found that neither $\text{MeOCH}_2\text{-NMe}_2\text{Ar}^+$ nor $\text{MeOCH}_2\text{-Py}^+$ had a distinct transition state in either PM3 or AM1, consistent with the arguments of Knier and Jencks.¹⁶ Secondary linear systems such as $\text{MeOCHMe-NMe}_2\text{Ar}^+$, $\text{MeSCH}_2\text{-NMe}_2\text{Ar}^+$, and $\text{MeSCHMe-NMe}_2\text{Ar}^+$ and the respective pyridiniums, protonated hemiacetals, methylacetals, and dimethyloxoniums gave distinct transition states, with the energies of the IDCs much more stable for sulfur than for oxygen stabilization.¹⁷ These results show an LG and substituent dependence that is not consistent with a general view on oxocarbenium ion stability. (Results for cyclic oxocarbenium ions are discussed below.)

An often unstated assumption is that a substitution reaction must occur through a single mechanism; Jencks's reviews on these matters¹⁸ always put the case in terms of *either* a step-wise or concerted mechanism. The last sentence of the Knier-Jencks paper¹⁶ states the consequences of this assumption most boldly: "[A]ll solvolysis and substitution reactions at saturated carbon that proceed through $\text{S}_{\text{N}}2$ displacement mechanisms do so simply because the intermediate in *the alternative* $\text{S}_{\text{N}}1$ mechanism is too unstable to exist [italics added]." It seems reasonable, however, that if the free energies of activation of competing uni- and bimolecular mechanisms are of the same magnitude, there is no reason that mixed mechanisms cannot occur. Neutral⁹ and charged^{10,11} 4-methoxybenzyl substrates are known to dissociate directly to the 4-methoxybenzyl carbenium ion *and* undergo a concerted bimolecular reaction with nucleophiles. Even with an excellent incipient carbenium ion intermediate in a substrate (as in 1-5a), however,

an S_N1 reaction may not occur, which suggests that other, more subtle factors affect the kinetics and mechanism of these seemingly simple substitution reactions.

Our results show that borderline behavior is variable across a series of substrates in which only minor structural changes are made in the LG at some distance from the reaction center. The plots of k_{obsd} vs. [NaN₃] for **1a-e** (Figure 2.1 for **1a**) show that there is no borderline behavior in solvent water for the best LG studied. At long times in the absence of nucleophile, or at elevated temperatures, a slow reaction with water can be measured for **1a-e**, however. The relative rates for the second-order reactions k_2/k_W , where k_W is k_{obsd} for the water reaction/55.5, range from 4×10^3 for **1a** to 3.6×10^5 for **1e** (Table 2.1). For the mixed S_N1/S_N2 azide substitution reactions of benzyl substrates with LGs such as SMe₂ (in water)^{10,11} and Cl (in 20% acetone/water),⁹ the rates for the uni- and bimolecular processes are comparable. While we cannot rule out an S_N1 reaction with absolute certainty because of the equilibrium among products and starting material (see Results), the much slower hydrolysis reaction is consistent with solvent displacement on **1a-e**. Moreover, if an IDC were an intermediate in the pyridinium reactions, it would be expected that an alcohol would be formed by attack of solvent on the intrinsically unstable IDC, but no alcohol products were detected for any 3-cyanopyridinium substrate.

There is borderline behavior for **2a-e**, however: plots of k_{obsd} vs. [NaN₃] have non-zero intercepts and there is a measurable reaction with water alone at 96°C. The rates of the azide and hydrolysis reactions for **2a-e** are comparable, as shown by the rate plots for **2a** in Figure 2.2; the ratios of the second-order rate constants k_2/k_W are between 96 and 265, which is relatively constant and much lower than the range found for **1a-e**. Alcohol products are also found in the azide reaction of the nicotinamide substrates.

The pyridine substrates **3a** and **3e** react at very slow but measurable rates, but **3b-d** do not react in six months with up to 1.7M azide at 96°C.

This pattern of reactivity suggests that the switch from no borderline to borderline behavior for pyridiniums is related to factors other than a change in mechanism. The analysis presented below strongly suggests that borderline kinetics is related to the LG ability and to the different effects of charged or neutral nucleophiles on the structure of the activated complex for a concerted displacement reaction.

Azide Reactions. The Hammett plots for the azide reaction show that the effect of the 4-substituents on the rate constants depends on the LG ability. The plot for **1a-e** is essentially flat, and the plot for **2a-e** is slightly V-shaped; the value of ρ for **2a-d** is ca. -0.7 (Figure 2.8). For the pyridine series, with the point for **3c** based on an estimated upper limit for the rate constant (see Results), the Hammett plot is even more V-shaped. The value of β_{LG} for the 4-methoxybenzyl substrates is -1.45 (Figure 2.10), and the Hammett plot based on σ_m values for the pyridine 3'-substituents is also quite large (+8.9, $r = 0.991$, not shown). Values for the other substituted benzyl substrates, based on more limited rate data, are in the same range. Therefore, the benzyl methylene-LG bond for the azide reaction is very "loose" across the series of substituents.

Westaway and Ali¹⁹ have shown that a change from a better to a worse leaving group (for the reaction of thiophenoxides with substituted benzyl-N,N-dimethyl anilines in DMF) "loosens" the Nu-benzyl methylene bond with little effect on the benzyl methylene-LG bond. Put another way, the better the LG, the more "product-like" the TS. Thus for the azide reaction, the "looseness" of the nucleophile at the TS would decrease as a function of the LG in the order **3** > **2** > **1**, and the extent of substituent effects would be expressed in the same order,

which is the trend seen in the Hammett plots: The more fully formed the nucleophile-carbon bond, the less charge at the reaction center, the less conjugation to the substituents. The same trend is seen at the opposite end of the Hammond effect for the specific-acid catalyzed hydrolysis of substituted aryl acetals, ketals, and orthoesters; the "earliest," most "reactant-like" activated complex occurs for orthoesters, which have the smallest values of ρ .²⁰ We have seen this trend in the computed bond lengths of the activated complexes for the gas-phase dissociation of acetals, ketals, and hemi- and orthoesters in a recent computational study.¹⁷

This qualitative description of the effects of nucleophile, LG, and substituents on the activated complex is in complete accord with the Pross-Shaik²¹ avoided crossing model, which may explain the differences between and among the shapes of the Hammett plots for the three LGs. For the azide reaction, four canonical configurations are important:

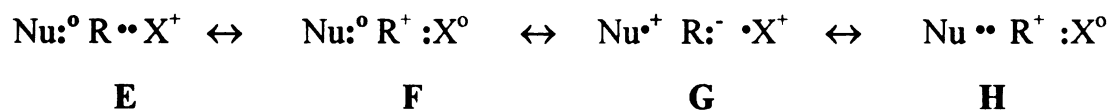


Forms **A** and **D** are the reactant and product configurations, respectively, and **B** and **C** are mixed forms. The TS is a mixture of forms **A-D**; of the intermediate forms, **B** is clearly the more important, and the effects of electron-donating substituents would be expressed in stabilization of R^+ , which is the effect seen. (Note that the relatively higher rate for 4-Cl is also seen in the reaction of negative nucleophiles with neutral substrates, as in the classic study of Hudson and Klopman.²²) Form **C** would be stabilized by an electron-withdrawing group, and accordingly the rate of the 4-NO₂ substrate is increased relative to H. Thus our results conform to Pross's rationale for the shape of Hammett plots for benzyl substrates.²³

Addition of electron-withdrawing substituents to the pyridine LG has two effects: it improves the LG ability by lowering the pK_a and increases the ionization potential of the pyridine, which makes form C less important for TS mixing. With the “tightening” effect of moving to a better LG, benzyl substituent effects should be less important for stabilization of R^+ for better LGs. Both effects lead to a flattening of the Hammett plot for **1a-e** (Figure 2.8).

Hydrolysis Reactions. The Hammett plots for the hydrolysis reaction of **1a-e** and **2a-e** show trends opposite those found for the azide reaction (Figure 2.9). The linearity of the plots for **1a-e** and **2a-e** indicates that there is a single mechanism, and our assumption of reaction through solvent displacement is consistent with the relatively low ρ value of -1.24 for **1a-e**. The Hammett plot for the hydrolysis of **2a-e** is essentially flat, however; the rate constants upon which this plot is based were measured directly and accurately in very dilute solutions (see Figure 2.2), and within error are the same values as the intercepts of plots of k_{obsd} vs. $[\text{NaN}_3]$. Thus while there is no indication of a change in mechanism, it is clear that substituent effects are expressed differently as a function of the LG. While we did not measure the rate constants for the hydrolysis of all benzyl substrates at 96°C, second-order rate constants for **1c,d** (ca. $6\text{-}10 \times 10^{-6} \text{ min}^{-1}\text{M}^{-1}$) are within factors of 3-5 of the second-order rate constants for **2c,d**, which suggests that the value of β_{LG} for the hydrolysis reaction would be quite low.

Differences between the azide and hydrolysis reactions can be rationalized with Pross-Shaik theory. For the reaction of a neutral nucleophile, the TS is a mix of the four forms E-H:



Of the two intermediate forms, **F** is clearly much more stable than **G**. The effects of benzyl substituents would be dominated by electron-donating groups, and it would be expected that the Hammett plot for the displacement reaction by solvent would have a negative slope, which is the trend found (Figure 2.9). While the solvent system and nucleophile are quite different, the second-order rate constants for the reaction of Katritzky's triphenylpyridinium substrates with piperidine in chlorobenzene give a linear Hammett plot with $\rho = -0.51$ (Figure 2.9). The importance of the various configurations favors an LG effect for the reaction with charged but not with neutral nucleophiles, which is the trend seen in the β_{LG} values.

Pross-Shaik theory is not particularly successful explaining why the change from a better to a worse LG for the water reaction leads to a flat Hammett plot for the worse LG. The trend is apparent from other benzyl substrates, however. For the direct displacement reaction by water on benzyl sulfoniums with 4-substituents having $\sigma^+ > -0.31$,¹² in which SMe_2 is a better LG than a pyridine, has $\rho^+ = -1.5$ ($r = 0.96$; not shown); $\rho^+ = -1.24$ for 3-cyanopyridiniums and is essentially 0 for nicotinamides, so the trend is consistent with an LG effect. This suggests that the more basic LG would stabilize R^+ in Form **F** better than a less basic LG, and in a "tight" transition state may lessen or even eliminate the effects of substituents. This argument is consistent with the argument made above for reactions with charged nucleophiles.

In these systems it is reasonable to suppose that changes in reactivity brought about by changing the substituents on the benzyl and LG at large distances from the reaction center should not lead to a change in mechanism. Thus the change from no borderline (**1a-e**) to borderline behavior (**2a-e**), and the change in the shape of the Hammett plots from flat (**1a-e**) to V-shaped (**2a-e** and **3a,e**) are not the result of a change in mechanism, but of the influence of the nucleophile

and LG on the structure of the activated complex despite a *very* "loose" geometry. This also suggests that the mere presence of borderline behavior is not sufficient evidence even to suggest an IDC or ion-pair mechanism. Amyes and Richard have shown that the same rationale is true for neutral benzyl substrates.⁹

Brønsted Coefficients. Brønsted values have been equated with the amount of bond breaking (β_{LG}), bond making (β_{Nuc}), or the development of charge at the transition state. It is generally assumed that they measure the amount of transfer of the substrate to the LG (or nucleophile to the substrate) *relative* to the amount of transfer of a proton to a standard base.²¹ This proposition also assumes that progress along the reaction coordinate, in terms of geometry, and charge development are inextricably linked. Thus a small value of β_{LG} is equated with an "early" ("tight") "reactant-like" activated complex and a large value of β_{LG} is equated with a "late" ("loose") "product-like" activated complex. In the absence of other measures of the transition state structure or energy, however, it is often inadvisable to specify where along the reaction coordinate the transition state occurs. This is particularly true for attempts to use the Hammond postulate²⁴ to describe $\text{S}_{\text{N}}2$ reactions given Hammond's specific warning that *free energies or their relations* may not correlate with the *potential energy surfaces* upon which the postulate is based, and that the postulate should not be applied to systems in which the reactants and activated complexes are separated by large energies.

The link between bond length and energy is reasonable for a strictly unimolecular process. We found that the MNDO-calculated length of the benzyl methylene-SMe₂ bond for gas-phase dissociation of a series of benzyldimethylsulfoniums increased smoothly with an increase in the calculated values of ΔH^\ddagger , in agreement with the Hammond postulate. An excellent correlation between the MNDO ΔH^\ddagger and the experimentally determined relative rates of dissociation

showed that this description of the potential energy surface was not merely a computational artifact.¹⁴ This is not always the case, however, because the computed benzyl methylene-N bond in benzyl pyridiniums remained relatively constant as the AM1 ΔH^\ddagger increased. The relative rates of dissociation and ΔH^\ddagger gave an excellent correlation, however.

Large differences in β_{LG} values for substrates with the same LG may be related to different mechanisms. While we did not measure complete rate profiles for the hydrolysis reactions of **1a-e** at 96°C for comparison with **2a-e**, rate constants measured for **1a,b** are only 2-3-fold greater than for **2a,b**, which suggests that the values of β_{LG} for the hydrolysis reaction would be small. The hydrolysis of **1-Me** and **2-Me** show the same kinetic pattern as the benzyls. The rate constant for hydrolysis of **1-Me** is much less than the rate constant for azidolysis, but the rate constants for hydrolysis and azidolysis of **2-Me** are comparable. At 96°C, however, the rate constants for hydrolysis of **1-Me** and **2-Me** are the same within a factor of 2-3, which suggests that β_{LG} is low for the hydrolysis reaction.

In contrast, large β_{LG} values of -1.11 and -0.91 have been reported for the hydrolysis (100°C) and NAD⁺ glycosylhydrolase [EC 3.2.2.6]-catalyzed cleavage (37°C), respectively, of NAD⁺ analogs with different pyridine LGs.⁴ Sinnott²⁵ reported a β_{LG} value of -1.29 for the hydrolysis of β -D-galactopyranosyl pyridiniums. These values are consistent with a "loose" activated complex for a unimolecular process through a stable oxocarbenium ion intermediate or ion-dipole complex, mechanisms supported both by activation and other values^{2,3} and the results of a recent computational study of the gas-phase dissociation of a large number of charged substrates that contain potentially stable oxocarbenium ions.¹⁷ This picture is supported by the finding of Ta-Shma and Oppenheimer²⁶ that up to 2.3M azide had little effect (ca. 20%) on the rate of disappearance of NAD⁺ in water at 37°C, a kinetic pattern consistent with azide trapping at the solvent-

separated ion pair. The "tight" activated complex for the hydrolysis of the benzyl and methyl pyridinium substrates is consistent with a direct displacement mechanism. This in turn is consistent with our finding that the ribosyl oxocarbenium ion is intrinsically more stable than benzyl carbenium ions.¹⁴

In contrast, the Brønsted coefficients for the azide reaction of **1-3a** and **5a** (Figure 2.10; $\beta_{LG} = -1.47$) and the other benzyl substrates are very large, with a similar value found for the reaction of azide with the N-Me substrates **1-Me** and **2-Me** (open squares, Figure 2.10; $\beta_{LG} = -1.59$). The activation values for **1a-e** and **1-Me** are essentially the same as well (Table 2.2). Thus the activated complex is "loose" for the azide reaction for both benzyl and methyl substrates. While this is consistent with an ion-dipole complex mechanism, the fact that there is no detectable alcohol product and that the rate of hydrolysis is much lower than the rate of reaction with azide suggest that this is merely a very loose concerted displacement reaction. Certainly methyl substrates do not react through ion-dipole complexes.

Arnett and Reich²⁷ measured the forward and reverse rate constants for the Menschutkin reactions of substituted pyridines with MeI. Using their reported rate constants for the reaction of I^- with substituted N-Me-pyridiniums in acetonitrile at 25°C, we calculate a β_{LG} of -1.11 ($r = 0.980$ for 5 points),²⁸ a "loose" activated complex. Metzger,²⁹ however, obtained a β_{LG} value of -0.39 for the reaction of the soft, neutral nucleophile Ph_3P with substituted N-Me-pyridiniums in boiling DMF. The large difference in β_{LG} may reflect the difference between the reaction of a charged or neutral nucleophile with a charged substrate, which would affect the charge distribution in the activated complex, and not the HSAB rank--both I^- and Ph_3P are soft. Westaway and Ali's data¹⁹ for the reaction of benzyl-N,N-dimethyl-4-X-aniliniums with 4-Y-thiophenoxides can be used to obtain β_{LG} values. For $Y = Me, H,$ and Cl in the nucleophile, β_{LG} values for $X = MeO, H,$ and Cl in the

substrate are -0.72, -0.64, and -0.58 ($r = 0.9980, 0.9999, \text{ and } 1.000$, respectively), values that are 1.5- to 2-fold greater than Metzger's series for methyl pyridiniums in the same solvent. (Using pK_a values extrapolated from Bordwell's data³⁰ in DMSO to simulate DMF pK_a 's gives β_{Nuc} 's and β_{LG} 's in the same range, although the DMSO values are slightly lower.). Thus the same general trend is found in both water and DMF.

Pross-Shaik theory has not been able to provide a precise description of methyl transfer reactions, and our results do not improve that situation. Pross has argued that intermediate configurations such as **B**, **C**, **F**, and **G** are not available to unsubstituted methyl, which are limited to mixing of configurations such as **A** and **D** and **E** and **H**. Because of this limitation, β_{LG} will have a different meaning for reactions of methyl and other substrates for which more configurational interaction is possible. He has suggested, however, that for reactions characterized by mixing of three or more configurations, Brønsted values may provide a relative measure of charge development at the TS.

Pross based his analysis for substituted methyl substrates on the results of Knier and Jencks¹⁶ for the reactions of $\text{MeOCH}_2\text{NMe}_2\text{Ar}^+$ with neutral and negative nucleophiles; the LG pK_a s are in the same range (1.5-5.2) as the pyridine LGs used by us and by Arnett and Reich.²⁷ Pross argued that the reported high β_{LG} values are consistent with an important contribution of configuration **B** (through $\text{MeO}=\text{CH}_2^+$) in the substitution reactions with negative nucleophiles.

Unfortunately, the β_{LG} s of -0.89 and -0.70 to which Pross refers his argument for negative nucleophiles were for the reaction of *water and n-propylamine*; however, β_{LG} values of -0.57 and -0.84 can be obtained from 2-point "plots" of data for the reaction of hydroxide and acetate with two anilinium substrates.¹⁶ Thus Pross's analysis is consistent with the limited data for negative nucleophiles, but the small

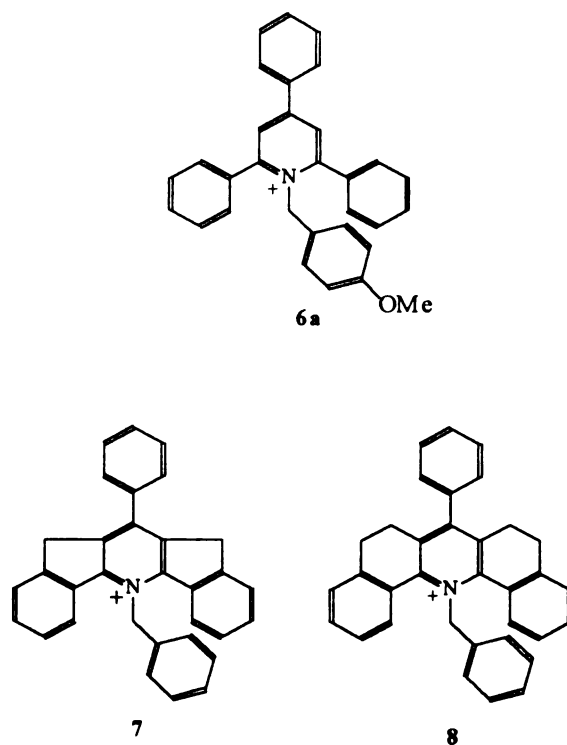
difference of β_{LG} values between neutral and negative nucleophiles shows that the transition state structures are relatively constant.

Our finding that the rates, activation values, response to charged and neutral nucleophiles, and β_{LG} values are essentially the same for N-methyl and benzyl pyridiniums is too compelling to be merely fortuitous, and suggest that the uncoupling of methyl and other substrates is not warranted, at least as Pross-Shaik theory is now understood.

The Effect of Solvent. Our results for the pyridiniums and sulfoniums¹⁰ are in accord with the suggestion of Arnett and Reich²⁷ that the effects of solvation of the LG at the TS are important determinants of reactivity. Based on the pK_a s of the LGs, it would be expected that the dimethylsulfoniums ($pK_a = -6$) would react much faster than the pyridiniums ($pK_a = 1.45-5.25$). In fact, the second-order rate constants at 80°C are the same within a factor of 2. Thus other factors must be important, including the effect of solvent. For instance, the values of ΔG^\ddagger (25.2 kcal/mol) for the reaction of 1a and the corresponding dimethylsulfonium with azide are the same, but the value of $\Delta\Delta S^\ddagger$ is -17 gibbs/mol.¹⁰ For charged substrates, the ground state and activated complexes both bear a full formal positive charge, and only small adjustments in solvation are needed as the transition state is achieved with a subsequent small loss of entropy. The enthalpy and entropy required to desolvate the nucleophile and the entropy loss in bringing the nucleophile and substrate together will be the same for both substrates. Thus the substantial difference in ΔS^\ddagger reflects the large, unfavorable change in solvation entropy of introducing the hydrophilic 3-cyanopyridine ($\Delta S^\ddagger = -21.6$ gibbs/mol) into bulk solvent at the TS and the minor entropic effects of introducing the hydrophobic SMe_2 ($\Delta S^\ddagger = -4$ gibbs/mol) into the cavities or interstitial spaces in bulk solvent. Substantial differences between ΔS^\ddagger for the S_N1 solvolysis of (4-

methoxybenzyl)-dimethylsulfonium in H₂O ($\Delta S^\ddagger = 14.5$ gibbs/mol)¹¹ and in D₂O ($\Delta S^\ddagger = 7$ gibbs/mol)¹⁰ are also consistent with this expression of the hydrophobic effect on kinetics. Values of ΔS° are slightly more negative for the introduction of noble gases and simple hydrocarbons into D₂O than into H₂O,³¹ which is the result of the slightly (5-7%) stronger deuterium bonds in D₂O. Thus it is possible that **1a** does not undergo an S_N1 reaction because of the unfavorable entropy of solvation of the LG, but this is an unproven speculation based on a rather large extrapolation.

Comparison with Katritzky's IDC Mechanism. For all of Katritzky's 4-substituted benzyl 2',4',6'-triphenylpyridinium substrates except (4-methoxybenzyl)-2',4',6'-triphenylpyridinium (**6a**), the reaction with piperidine in



chlorobenzene is strictly S_N2; **6a** exhibits typical borderline behavior. While in the original 1981 papers³¹ on these results the mechanism proposed was mixed

S_N1/S_N2 , in subsequent papers and reviews¹³ Katritzky suggested that this reaction occurs through an IDC mechanism, and has published rate-pressure profiles,³³ computational results,³⁴ and gas-phase dissociation data³⁵ in support of this position. The differences between our results for **1a** and Katritzky's results for **6a** and fused ring systems (**7** and **8**) may be related to several factors, including different mechanisms. There is good reason to believe, however, that the mechanism for the reactions of these highly hindered substrates is mixed S_N1/S_N2 as originally proposed.

Katritzky, Ford, and Anders and colleagues³⁴ have reported the AM1-minimized IDC structure for **8**; we have calculated the MM2 and AM1 structures for the ground states and IDCs for **6a**, **7**, and **8** using their reported values for the benzyl-pyridine bond length. Because we have exactly reproduced the MNDO, AM1, and PM3 energy profiles for gas-phase dissociation of **3c** reported by these authors,⁸ our results are equivalent to the reported structures that were calculated using more sophisticated methods. (Indeed, our calculated structure of **8** matches exactly the structure published by these authors.³⁴) The calculated structures show large differences between the ground and IDC structures for simple benzyl pyridiniums and Katritzky's compounds.

The ground state structures are vastly different. While the torsional angle of the pyridine nitrogen-benzyl methylene bond is 0° in the simple benzyl pyridinium **3c**, there is a progressive distortion of the torsional angle from 9° for **6a** to 18° for **7** to 48° for **8**; there is also "cupping" in the fused ring systems. The calculated ground state structure for **8** is shown in the stereodiagram (cross-eyed) in Figure 2.11. These highly distorted structures suggest that there should be substantial steric acceleration for reactions with nucleophiles, and Katritzky³⁶ reported such an effect on the rates of reaction with piperidine. For instance, the relative rate for **8:6a** is 1568 at 80°C , and ΔH^\ddagger for **8** is ca. 5 kcal/mol lower than that for **6a**.

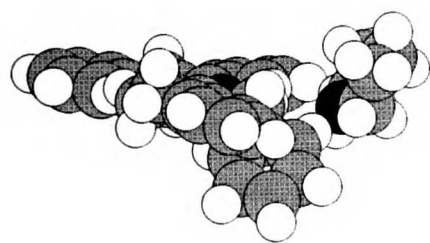


Figure 2.11. Stereodiamgram (cross-eyed) of the AM1-minimized structure for **8**. The severe distortion (48°) of the pyridine-benzyl methylene bond is readily apparent.

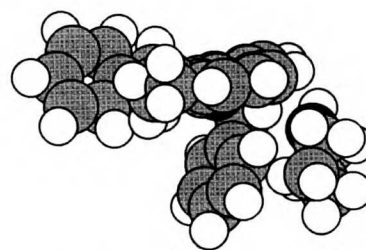
Replacing a pyridine α phenyl with a *tert*-butyl group in **6a** has little effect on the second-order rate constant, but substantially increases the unimolecular rate constant; the minimized structure shows no particular impediment to nucleophile approach for this substitution, but the *tert*-Bu group clearly increases the strain on the benzyl-pyridine bond, which would accelerate the unimolecular reaction.

Because of our supposition that Katritzky's compounds react by a mixed mechanism, we have examined the interactions of the ground state AM1 structures with piperidine. The nucleophile was manually docked at the closest approach without van der Waal interaction in **6a-8**. In all cases, the piperidine nitrogen was within 3\AA of the benzyl methylene (backside), clearly enough distance to begin bond-making. The distortion of the pyridine-benzyl methylene bond angle aided this contact. Shown in Figure 2.12 are CPK renderings of the "flat" unminimized structure for **8** in which the pyridine-benzyl methylene torsional angle is 0° ; the closest approach for piperidine is 3.78\AA . In the AM1-minimized structure with the 48° distortion, the piperidine close approach is 3.11\AA . Thus, as expected, steric impediment to nucleophile approach is less important than relief of strain, which is the dominant factor for the kinetics of reaction for these substrates.

Quite unexpected, however, were the structures of the IDCs. In the AM1 structure for the IDC of **3c** (Figure 2.13, top), the pyridine ring is perpendicular to



8, Unminimized "flat" structure
 Pyridine-benzyl methylene torsional angle = 0°
 Piperidine N-benzyl CH_2 distance = 3.78\AA



8, Minimized structure
 Pyridine-benzyl methylene torsional angle = 48°
 Piperidine N-benzyl CH_2 distance = 3.11\AA

Figure 2.12. Structures obtained by manual docking of piperidine with the unminimized (*left*) and AM1-minimized (*right*) structures for **8**. A bimolecular reaction is possible for the bottom but not the top structure.

the plane of the benzyl carbenium ion, with the nitrogen lone pair in a direct line with the vacant orbital of the carbenium ion. This is a kinetically competent

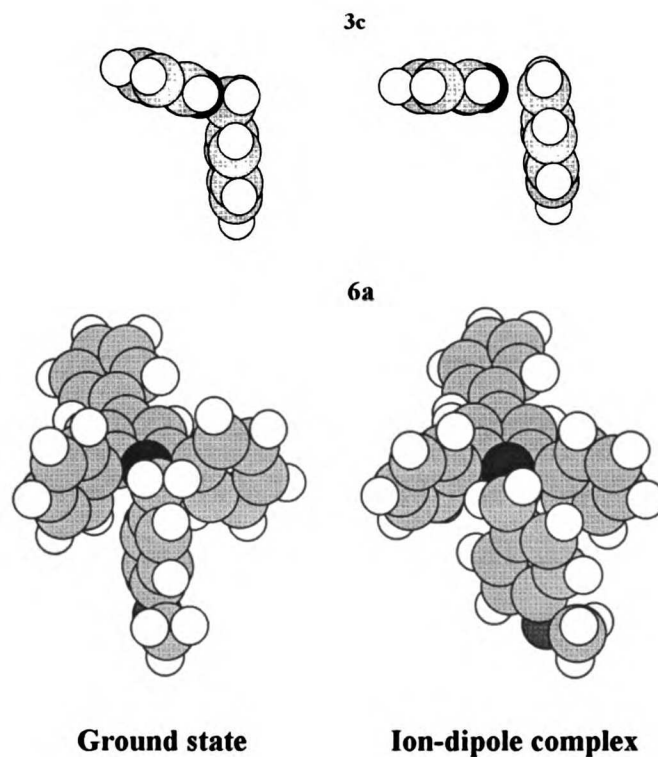


Figure 2.13. Ground states (*left*) and ion-dipole complexes (*right*) for the AM1-minimized structures for **3c** and **6a**.

intermediate in which the return reaction to starting material is unimpeded. The IDC for **6a** has a different structure, however, in which the plane of the fully formed carbenium ion moiety is twisted orthogonal to the pyridine lone pair (Figure 2.13, bottom). This structure is very different than the ground state, in which the benzyl phenyl is nestled between the two pyridine phenyls with the benzyl methylene hydrogens orthogonal to the plane of the benzyl phenyl. Attack of a nucleophile on this structure would not produce a TS in which the phenyl would be conjugated to the reaction center and suggests that substituent effects would not be fully expressed. In fact the ρ value for the reaction with piperidine is -0.5 (see Figure 2.9), which is more consistent with direct attack of nucleophile on the substrate than on the putative IDC. If nucleophile attacked this IDC, in which the carbenium ion is fully formed, the ρ value would be much higher. In the AM1 IDC structure for **7**, the carbenium ion geometry is achieved, with little stacking interaction between the pyridine fused ring system and the benzyl phenyl. In the AM1 structure of the IDC for **8**, however, the pyridine fused-ring system and the fully-developed benzyl carbenium ion are stacked parallel, with the nitrogen lone pair directed 90° to the carbenium ion. The structure appears to represent a π - π stack between the pyridine and benzyl phenyls and a σ - π interaction between the carbenium ion LUMO and the nitrogen p-orbital in the aromatic system.

Differences between the IDC structures for **7** and **8** can be seen clearly in the stereodiagram (crossed) shown in Figure 2.14. It seems probable that the structure for **8** is the result of the strain in the ground state structure, where the highly distorted 48° torsional angle delivers the benzyl carbenium ion moiety into the stacked structure.

These structures help explain an apparent anomaly in the kinetics for the fused ring systems. All the fused-ring substrates undergo a second-order reaction with piperidine, and several, including **7**, undergo a unimolecular reaction.

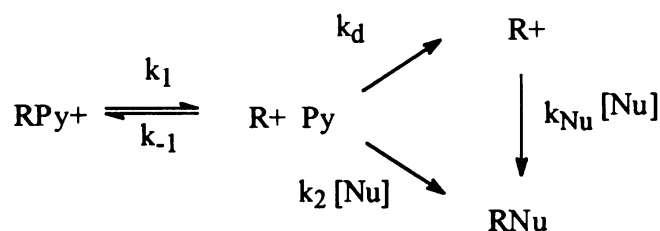


Figure 2.14. Stereodiagram (cross-eyed) showing the AM1-minimized structures for the ion-dipole complexes for **7** (top) and **8** (bottom) . In the structure for **8**, the benzyl carbenium ion is stacked to the pyridine ring.

Because of the enormous strain, **8** would be expected to undergo unimolecular dissociation, but it does not. It is possible that the stacked structure of the IDC is so stable that dissociation of the IDC into the LG and the carbenium ion would be energetically unfavorable. If the pyridine-benzyl bond is broken in the IDCs for **6a** and **7** and the structures are minimized in MM2, the benzyl is forced away from the pyridine, with the nitrogen-methylene bond distance 4.53Å for **6a** and 5.59Å for **7**; there is stacking in the structure for **7**, however. When this operation is performed on **8**, there is no dissociation. Based on this evidence, we believe that of all the structures, **8** forms a stable IDC, but that it is not a *kinetically competent intermediate in terms of the return reaction to the starting structure*, a process that would require overcoming the stabilizing energy of the stacked structure and reintroducing the torsional strain to the pyridine-benzyl bond and the cupping in the ring system. The barrier for the return reaction would be enormous.

In this regard it is interesting to consider the kinetics governing the two possible mechanisms for the solution reactions of the highly strained pyridiniums (Scheme 2.1).³¹ The overall equation for the IDC mechanism (Eq. 2.1, Scheme

Ion-Dipole Complex Mechanism



$$k_{\text{obsd}} = \frac{k_1 (k_d + k_2 [\text{Nu}])}{k_d + k_2 [\text{Nu}] + k_{-1}} \quad (\text{Eq. 1})$$

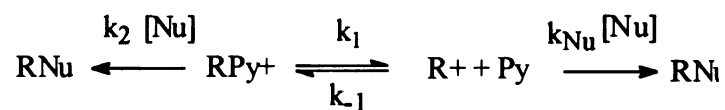
for $k_{-1} \gg k_d + k_2 [\text{Nu}]$,

$$k_{\text{obsd}} = K (k_d + k_2 [\text{Nu}]) = k'_d + k'_2 [\text{Nu}] \quad (\text{Eq. 2})$$

for $k_d + k_2 [\text{Nu}] \gg k_{-1}$,

$$k_{\text{obsd}} = k_1 \quad (\text{Eq. 3})$$

Mixed S_N1/S_N2 Mechanism



$$k_{\text{obsd}} = k_1 + k_2 [\text{Nu}] \text{ for } k_{\text{Nu}} [\text{Nu}] \gg k_{-1} \quad (\text{Eq. 4})$$

Scheme 2.1

2.1) was derived using the steady state approximation and can be simplified. For the case in which the rate of the recombination reaction of the IDC to the ground state is greater than either product-forming rate constant, the equation reduces to the equation for the simple mixed S_N1/S_N2 mechanism (Eq. 2, Scheme 2.1). If, on the other hand, the rate constant for the return reaction is much lower than the

product-forming rate constants, as would be predicted from the analysis of strain effects given above, then the equation reduces to a form (Eq. 3, Scheme 2.1) consistent with simple dissociation with no dependence on nucleophile concentration, which does not match the data. The appropriate match with the data is the equation for the simple mixed S_N1/S_N2 mechanism (Eq. 4, Scheme 2.1).

An important factor in unraveling the mechanism for the benzyldimethylsulfoniums was the use of selectivity data for nucleophile and solvent-derived products that were fit to equations that included various rate constants and product ratios for unambiguous carbenium ion trapping reactions. Katritzky's system, in which solvent chlorobenzene does not react, produces a single product by direct displacement or by trapping of the carbenium ion, and selectivities cannot be used to define the mechanism. (Several products consistent with attack of the benzyl carbenium ion on the benzyl-piperidine products have been identified, however; there is little doubt that a benzyl carbenium ion is formed in the reaction.) In Sneen's treatment of the IDC mechanism (or ion-pair mechanism for neutral substrates), k_1 is treated as part of partitioning ratios for diversion of the IDC to products by solvent and nucleophile.¹⁵ Even with Sneen's more flexible approach, however, the correlations between selectivities and rate data are complicated by salt and solvent effects, as Thornton¹² has pointed out in his perceptive analysis of the Sneen mechanism. Thus even if it were possible to obtain selectivity values, they would be difficult to interpret unambiguously.

Part of Katritzky's rationale for the IDC mechanism is the correspondence between gas-phase and solution results. As discussed above, we have shown recently that the gas-phase and solution dissociation of a series of β -nicotinamide arabinosides occurs through an IDC mechanism in both phases, but with different rate-limiting steps.⁸ We found that the gas-phase dissociation of 4-substituted benzyl pyridiniums and dimethylsulfoniums occurs through an IDC intermediate

(with the exception of the 4-NO₂-benzyl pyridinium substrates, which dissociate directly),¹⁴ but that a dissociative reaction occurs in solution only for the (4-methoxybenzyl)dimethylsulfonium.¹⁰ As found for the benzyl pyridiniums reported here, Friedberger and Thornton¹² have suggested that the other benzyldimethylsulfoniums hydrolyze by direct solvent displacement. Thus in the absence of other data a direct comparison between the gas-phase and solution results is not warranted.

Perhaps the strongest evidence Katritzky has published in support of the IDC mechanism in solution are the effects of pressure on rate.³³ He found that the second-order rate constant for the reaction of 6a with piperidine decreased monotonically with increasing pressure and that the value of ΔV^\ddagger obtained from these data was high and positive. He interpreted this result as evidence for the IDC mechanism because increased pressure would push the starting material-IDC equilibrium to the left (Scheme 2.1). Based on his reasoning, however, the equilibrium depicted for unimolecular dissociation with no IDC in the mixed mechanism scheme would also be affected in the same way. Thus interpretation of the pressure data are of necessity ambiguous. The rate-pressure profile for 8 is biphasic; the second-order rate constant decreases initially and then increases with increased pressure, a profile that was interpreted in terms of an IDC mechanism that switches to a classical S_N2 mechanism after the inflection point. In a recent review, however, Isaacs³⁸ has pointed out that ΔV^\ddagger values for solvolysis and substitution reactions by themselves, both in terms of the sign and magnitude of the effect and the shapes of plots of ln k vs. pressure, cannot be used alone to distinguish among possible mechanisms. He also makes a cogent argument that it is highly unlikely that pressure changes would induce a change in mechanism. Moreover, he points out that measurements may be dominated by solvation effects, especially desolvation of charged reactants. Given these uncertainties, Katritzky's

results are consistent with a number of mechanisms that cannot be distinguished on the basis of kinetics alone.

Thus it seems probable that Katritzky's borderline substrates react with piperidine in chlorobenzene through a mixed S_N1/S_N2 mechanism. The analysis of the AM1 ground and IDC structures presented above are inconsistent with an IDC mechanism, as is the kinetics. The measured activation energies, however, are consistent with a mixed mechanism. While the reactions of charged substrates are not particularly sensitive to solvent polarity or ionic strength,^{11,39} the rates are higher in solvents with low dielectric constants. If ΔG^\ddagger for the uni- and bimolecular reactions of **6a** were of similar magnitude, then in chlorobenzene they may occur simultaneously; as calculated from Katritzky's data, ΔG^\ddagger for both processes is 24.9 kcal/mol at 373° K, which is more favorable than the S_N2 reactions of the benzyl or (4-methylbenzyl)-2',4',6'-triphenylpyridiniums (26.1 and 25.6 kcal/mol, respectively), neither of which has a unimolecular component. In the absence of selectivity data, however, it is not possible to establish either mechanism with certainty.

References and notes

- (1) Johnson, R.W.; Marschner, T.M.; Oppenheimer, N.J. *J. Am. Chem. Soc.* **1988**, *110*, 2257-2263.
- (2) Handlon, A.L.; Oppenheimer, N.J. *J. Org. Chem.* **1991**, *56*, 5009-5010.
- (3) Handlon, A.L.; Xu, C.; Müller-Steffner, H.-M.; Schuber, F.; Oppenheimer, N.J. *J. Am. Chem. Soc.* **1994**, *116*, 12087-12088.
- (4) Tarnus, C.; Schuber, F. *Bioorg. Chem.* **1987**, *15*, 31-42; Tarnus, C.; Muller, H.M.; Schuber, F. *ibid.*, **1988**, *16*, 38-51.

- (5) Young, P.R.; Jencks, W.P. *J. Am. Chem. Soc.* **1977**, *99*, 8238-8248;
Amyes, T.L.; Jencks, W.P. *J. Am. Chem. Soc.* **1989**, *111*, 7888-7900; Banait, N.S.;
Jencks, W.P. *J. Am. Chem. Soc.* **1991**, *113*, 7951-7958.
- (6) Schröder, S.; Buckley, N.; Oppenheimer, N.J.; Kollman, P.A. *J. Am. Chem. Soc.* **1992**, *114*, 8232-8238.
- (7) Sinnott, M.L.; Jencks, W.P. *J. Am. Chem. Soc.* **1980**, *102*, 2026-2032.
- (8) Buckley, N.; Handlon, A.L.; Maltby, D.; Burlingame, A.L.;
Oppenheimer, N.J., *J. Org. Chem.* **1994**, *59*, 3609-3615.
- (9) Amyes, T.L.; Richard, J.P. *J. Am. Chem. Soc.* **1990**, *112*, 9507-9512.
- (10) Buckley, N.; Oppenheimer, N.J. *J. Org. Chem.* **1994**, *59*, 5717-5723
(Chapter 3).
- (11) Kevill, D.N.; Ismail, N.H.J.; D'Souza, M.J. *J. Org. Chem.* **1994**, *59*,
6303-6312.
- (12) Friedberger, M.P.; Thornton, E.R. *J. Am. Chem. Soc.* **1976**, *98*, 2861-
2865.
- (13) Reviewed in Katritzky, A.R.; Brycki, B.E. *Chem. Soc. Rev.* **1990**, *19*,
83-105, and elsewhere.
- (14) Buckley, N.; Maltby, D.; Burlingame, A.L.; Oppenheimer, N.J.,
submitted (Chapter 6).
- (15) Sneen, R.A.; Felt, G.R.; Dickason, W.C. *J. Am. Chem. Soc.* **1973**,
95, 638-639.
- (16) Knier, B.L.; Jencks, W.P. *J. Am. Chem. Soc.* **1980**, *102*, 6789-6796.
- (17) Buckley, N.; Oppenheimer, N.J., submitted (Chapters 7 and 8).
- (18) Jencks, W.P. *Acc. Chem. Res.* **1980**, *13*, 161-169; Jencks, W.P. *Chem. Soc. Rev.* **1981**, *10*, 345-375.
- (19) Westaway, K.C.; Ali, S.F. *Can. J. Chem.* **1979**, *57*, 1354-1367.

(20) Capon, B. *Chem. Rev.* **1969**, *69*, 407-498. (b) Cordes, E.H.; Bull, H.G. *Chem. Rev.* **1973**, *73*, 581-603.

(21) Pross, A. *Adv. Phys. Org. Chem.* **1985**, *21*, 99-196.

(22) Hudson, R.F.; Klopman, G. *J. Chem. Soc.* **1962**, 1062-1067.

(23) Pross, A.; Shaik, S.S. *Acc. Chem. Res.* **1983**, *16*, 363-370.

(24) Hammond, G.S. *J. Am. Chem. Soc.* **1955**, *77*, 334-338.

(25) Hosie, L.; Marshall, P.J.; Sinnott, M.L. *J. Chem. Soc. Perkin Trans. II*, **1984**, 1121-1131.

(26) Ta-Shma, R.; Oppenheimer, N.J., in preparation. Ta-Shma measured kinetics by HPLC; one of us (N.B.) found that the kinetics of hydrolysis of NAD^+ in the pH-independent region measured by NMR was not affected by 2M azide.

(27) Arnett, E.M.; Reich, R. *J. Am. Chem. Soc.* **1980**, *102*, 5892-5902.

(28) Arnett and Reich²⁷ report a value α_{Me} obtained from a plot of ΔG^\ddagger vs. ΔG° for the exchange reactions which they point out "corresponds *operationally* to the Brønsted α for proton transfer [emphasis added]." This is *not* the same value as β_{LG} , however. In his analysis of these Brønsted values, Schuber⁴ uses the α_{LG} value and Metzger's β_{LG} values,²⁹ both of which are low, to argue that the NAD^+ substrates do not undergo displacement by solvent; while his conclusion is correct, his reasoning is in error.

(29) Berg, U.; Gallo, R.; Metzger, J. *J. Org. Chem.* **1976**, *41*, 2621-2624.

(30) Bordwell, F.G.; Zhang, X.-M.; Satish, A.V.; Cheng, J.-P. *J. Am. Chem. Soc.* **1994**, *116*, 6605-6610.

(31) Ben-Naim, A. *Solvation Thermodynamics*; Plenum Press, New York, **1987**, pp. 75-77.

(32) Katritzky, A.R.; Musumarra, G.; Sakizadeh, K.; Misic-Vukovic, M. *J. Org. Chem.* **1981**, *46*, 3820-3823; Katritzky, A.R.; Musumarra, G.; Sakizadeh, K. *J. Org. Chem.* **1981**, *46*, 3831-3835.

(33) Katritzky, A.R.; Sakizadeh, K.; Gabrielsen, B.; le Nobel, W.J. *J. Am. Chem. Soc.* **1984**, *106*, 1879-1884.

(34) Katritzky, A.R.; Malhotra, N.; Ford, G.P.; Anders, E.; Tropsch, J.G. *J. Org. Chem.* **1991**, *56*, 5039-5044.

(35) Katritzky, A.R.; Malhotra, N.; Dega-Szafran, Z.; Savage, G.P.; Eyler, J.R.; Watson, C.H. *Org. Mass Spectrom.* **1992**, *27*, 1317-1321; Katritzky, A.R.; Watson, C.H.; Dega-Szafran, Z.; Eyler, J.R. *J. Am. Chem. Soc.* **1990**, *112*, 2471-2478.

(36) Katritzky, A.R.; El-Mowafy, A.M.; Musumarra, G.; Sakizadeh, K.; Sana-Ullah, C.; El-Shaafie, S.M.M.; Thind, S.S. *J. Org. Chem.* **1981**, *46*, 3823-3830.

(37) In the original papers,³² Katritzky ignored the k_d pathway and published the expression $k_{\text{obsd}} = k_1 k_2 [\text{Nu}] (k_1 + k_2 [\text{Nu}])$, which we assume is a typo because the steady state equation is $k_{\text{obsd}} = k_1 k_2 [\text{Nu}] / (k_1 + k_2 [\text{Nu}])$. The same analysis of the equations given in Scheme 2.1 applies, however: for $k_1 \gg k_2 [\text{Nu}]$, $k_{\text{obsd}} = k_1 k_2 [\text{Nu}] / k_1 = k_2 [\text{Nu}]$, and for $k_2 [\text{Nu}] \gg k_1$, $k_{\text{obsd}} = k_1$.

(38) Isaacs, N.S. *Tetrahedron* **1991**, *47*, 8463-8497.

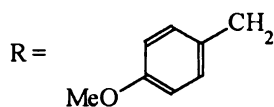
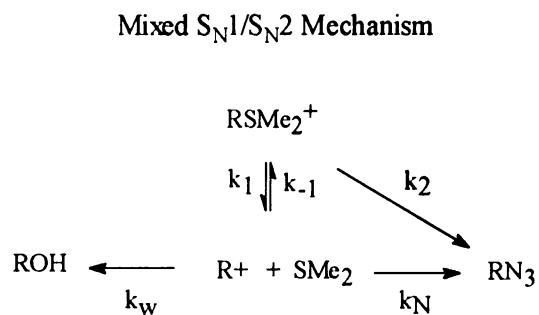
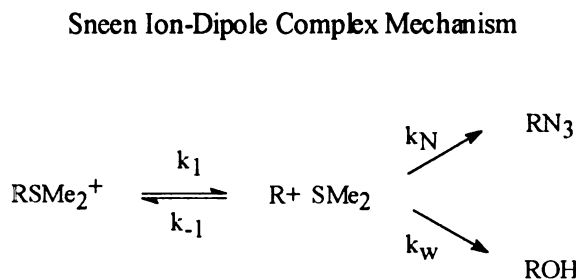
(39) Ingold, C.K. *Structure and Mechanism in Organic Chemistry*; Cornell, Ithica, NY, 1953; pp. 306-419.

Chapter 3
The Hydrolysis of (4-Methoxybenzyl)dimethylsulfonium Chloride

UCSF LIBRARY

Introduction

The hydrolysis¹ and nucleophilic substitution²⁻⁵ reactions of sulfonium derivatives have been studied as prototypes of the Hughes-Ingold Type III-IV nucleophilic substitution reaction for charged substrates.³ As part of the evidence for his general ion-pair mechanism in borderline solvolysis reactions, in 1973 Sneen⁴ published kinetic and selectivity results for the hydrolysis and azide reactions of (4-methoxybenzyl)dimethylsulfonium (1) that he claimed provided evidence for an ion-dipole complex (IDC) intermediate; the alternative to the IDC



Scheme 3.1

mechanism is mixed S_N1/S_N2 (Scheme 3.1). Friedberger and Thornton⁵ studied the sulfur kinetic isotope effects (KIE) for hydrolysis of 1 and other substituted benzyldimethylsulfoniums (BDMS⁺) compounds. They suggested that hydrolysis

occurs with solvent nucleophilic participation, and that an "ion-triplet sandwich" ($\text{N}_3^- \cdot \text{R}^+ \cdot \text{SMe}_2$) was an intermediate in the azide reaction.

We have been studying the nucleophilic substitution reactions of 4-substituted benzyl pyridiniums in water as part of a general program that has examined in some detail the mechanisms of the hydrolysis and substitution reactions of nicotinamide adenosine dinucleotide (NAD^+).⁶ We found that the reaction of all 4-substituted benzyl pyridiniums with azide is an $\text{S}_{\text{N}}2$ process, in contrast to the well-documented results of Katritzky⁷ that reaction of 4-methoxybenzyl pyridiniums with neutral amines in solvent chlorobenzene is a borderline system; Katritzky has suggested that an IDC is an intermediate. Because of this disparity, we examined the reactions of **1** with various nucleophiles in solvent water.

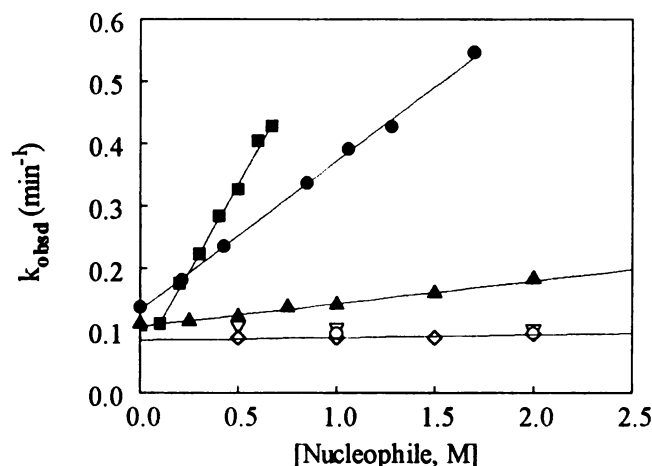


Figure 3.1. Plots of k_{obsd} (min^{-1}) vs. [nucleophile] for the reactions of **1** with Na_2SO_3 (■, $\mu = 2$ with Na_2SO_4), NaN_3 (●, $\mu = 1.7$ with NaCl or NaClO_4), pyridine-d_5 (▲, $\mu = 2$ with NaCl), ND_3 (○, no salt), NaCN (▽, no salt), and NaOD (◇, $\mu = 2$ with NaCl) measured by NMR at 80°C in D_2O .⁹ The reaction with NaSCN and the kinetic technique have been reported.⁸

We found that **1** reacted bimolecularly only with nucleophiles of intermediate hardness (N_3^- , SO_3^- , SCN^- , pyridine-d_5) and not with either hard

(OH⁻, Cl⁻, OCN⁻, ND₃) or soft (CN⁻, I⁻) nucleophiles.^{8,9} While the full details of this study will be published elsewhere,⁹ we include here plots of k_{obsd} vs. [nucleophile] for several of these reactions (Figure 3.1). The ordinate intercepts (k_1) were the same for reaction with N₃⁻, SCN⁻, and pyridine-d₅ either with ($k_1 = 0.110 \text{ min}^{-1}$, $\mu = 2$) or without ($k_1 = 0.150 \text{ min}^{-1}$) added salt to control ionic strength. (The reaction with SO₃⁼ exhibits severe salt effects and the value of k_1 cannot be obtained easily from ordinate intercepts.) The selectivity data for reaction with azide, which will be published with the kinetic results,⁹ rule out an IDC mechanism and are discussed below. In contrast, based on relative abundances in liquid secondary ion mass spectra (LSIMS) and on the results of semi-empirical calculations, we found¹⁰ that the gas-phase dissociation of 4-Y-BDMS⁺ (Y = MeO, Me, H, Cl, and NO₂) is a clear-cut example of a classical Hammond and Hammett system that dissociates through an IDC.

Because of these disparate results, we felt it was imperative to establish the mechanism of hydrolysis for **1**. This task proved to be difficult, however, because of an equilibrium that is set up among starting material and products, which affects the kinetics and attempts to show common leaving group suppression (CLGS) of solvolysis. Despite the experimental difficulties encountered, the results obtained in this study and the results for the nucleophilic substitution reactions^{8,9} show that the hydrolysis of **1** is an S_N1 reaction with no IDC intermediate. Kevill and coworkers¹¹ have recently reached the same conclusion independently.

Experimental Section

General. All chemicals and solvents were obtained from Aldrich and were used without further purification. UV kinetics were measured on a Hewett-Packard 8452A UV-Vis spectrophotometer with a thermostatted cuvette holder. NMR kinetics were measured on a General Electric QE-300 NMR spectrometer with a

variable temperature probe rated at $\pm 0.1^\circ\text{C}$. Tandem LSIMS were recorded under identical conditions in the positive ion mode on a 4-sector Kratos Concept II HH mass spectrometer fitted with an optically coupled 4% diode array detector on MS II.

Synthesis. **1** was routinely synthesized by mixing 1 eq. of 4-methoxybenzyl chloride and 1.1 eq. of SMe_2 in chloroform. The mixture was allowed to stand at ambient temperature, and the reaction was followed by TLC (silica, neat chloroform) until all chloride had disappeared. The chloroform solution was extracted with water, and the water layer was repeatedly extracted with chloroform and then with ether to give a water-white solution that was rotary evaporated to a clear glass under reduced pressure; extensive flashing with ethanol removed the remaining water to give a waxy white solid with $>95\%$ purity. The compound is extremely hygroscopic and was stored in a vacuum dessicator. Even with this precaution, over time the compound would turn milky; it could be purified easily by running through the extraction procedure. ^1H NMR: D_2O ($0 \delta = \text{TSP}$) δ 7.43 (d, $J = 8.6$ Hz, 2H, aromatic AA'), 7.11 (d, $J = 8.6$ Hz, 2H, aromatic BB'), 4.57 (s, 2H, $-\text{CH}_2-$), 3.88 (s, 3H, $-\text{OMe}$), 2.77 (s, 6H, $-\text{SMe}_2$). ^{13}C NMR: $\text{DMSO}-d_6$ δ 160.34, 132.42, 114.94, 66.5, 55.40, 46.33, 23.32. Nontandem positive-ion LSIMS: m/z (%) 121.1 ($\text{M}^+ - \text{SMe}_2$, 100), 183.1 (M^+ , 25); m/z calc. 183.3. (Note that in tandem LSIMS the relative abundances are reversed for collisionally activated dissociation of M^+ in MSII.¹⁰)

UV Kinetics. Rate constants were measured in H_2O and D_2O with (NaCl or NaClO_4) and without exogenous salt added to control ionic strength by following the disappearance of substrate at $\lambda_{\text{max}} = 232$ nm. Solvent was equilibrated in 1-cm cuvettes, 5-10 μL aliquots of **1** in the appropriate solvent were added and mixed, and data collection was begun immediately. The infinity value was obtained after 1 hr.

During initial attempts to measure CLGS in the UV, we heated saturated solutions of SMe_2 in water in the cell holder. Two cuvettes shattered violently (caution! stench!) before we abandoned this attempt.

NMR Kinetics.⁸ Rate constants were measured using the following procedure. Solvent in a standard NMR tube was heated in the probe, withdrawn, and mixed with solid substrate; the tube was returned to the probe and shimmed as rapidly as possible. For runs in D_2O , t_0 was taken as the time of addition of substrate to solvent, and rate constants were measured by following the disappearance of one of the AB doublets in the aromatic region, which gave an internal standard with product alcohol. For suppression runs and for kinetics in 0-1.0M ZnCl_2 , disappearance of the SMe_2 singlet (at 80°C , $\delta = 2.8$ ppm relative to HOD at 4.3 ppm) was followed, with t_0 taken as the time at which constant shims were obtained (usually within 1 min).

Closed Vial Experiments. Stock solutions of **1** were made in D_2O , with or without added salt, and serially diluted into 1.5 mL Teflon-capped, thick-walled reaction vials. Vials were overfilled to give a convex meniscus and then capped with the extrusion of solvent, which assured that there was no void volume. Vials were heated at 80°C in a block for 40 min, chilled in an ice bath, and the extent of reaction was measured by NMR. The fraction of **1** remaining, $f = [\mathbf{1}]/C_0$, was taken as the ratio of the integrated value of **1** divided by the sum of the integrated values for **1** and 4-methoxybenzyl alcohol.

Studies of the Back Reaction. Stock solutions of SMe_2 were made in the following way: a known volume of D_2O was pipetted into a screw-capped vial, which was tared. An aliquot of the volatile SMe_2 was added via syringe to the vial, which was capped and shaken repeatedly to give a cloudy solution. The vial was heated gently with a heat gun until a water-white solution resulted, at which point the vial was capped. After cooling to ambient temperature, the vial was weighed

and the approximate concentration of SMe_2 was calculated. Several dilutions of this stock were made to a constant volume (0.75mL) in D_2O solutions containing a single known concentration of 4-methoxybenzyl alcohol, which served as an internal standard. NMR spectra were recorded and the exact concentration of SMe_2 was determined by comparing the integrated value of the SMe_2 singlet with the MeO- singlet of the alcohol. With the exact $[\text{SMe}_2]$ determined, this stock solution and stock solutions of 4-methoxybenzyl alcohol and DCl in D_2O were serially diluted into test tubes (2 mL total volume) and placed in the capped reaction vials as described above. After heating at 80°C in a block for 40 min, vials were cooled in an ice bath and the extent of the return reaction was measured by NMR.

Isotope Effects. Solvent isotope effects were measured by the UV method. In our NMR study^{8,9} of the nucleophilic substitution reactions of 1, we found that the sulfonium methyl and benzyl methylene protons immediately exchanged for deuterons in the presence of either NaOD or ND_3 . Rate constants could be obtained by measuring the disappearance of one of the AB doublets as described above. Reactions of 1 with NaOD and ND_3 are zero order in nucleophile (Figure 3.1). Therefore, the values of $k_{\text{H}}/k_{\text{D}}$ for the secondary α -deuterium isotope effect could be obtained from these rate constants. This was a fortuitous result.

Results

Kinetics and Activation Values. Rate constants for the hydrolysis of 1 in H_2O and D_2O measured by UV at 80°C were the values of slopes obtained by linear regression from plots of $\ln [A_t - A_\infty]/[A_0 - A_\infty]$ vs. time (Table 3.1)¹²; rate constants calculated with the Guggenheim method gave the same results. Plots were linear over 3-4 half-lives. Values are the averages \pm S.E. for 4-6 determinations. Rate constants were the same in the presence of NaCl or NaClO_4 ,

**Table 3.1. First-Order Rate Constants k_1 (min^{-1}) at 80°C
for the Hydrolysis of 1 in H₂O and D₂O at Various Ionic Strengths**

		D ₂ O			H ₂ O	
	μ	1	1.7	2	0	1.7
UV	0.150 ± 0.003		0.123 ± 0.003 ^{a,b}		0.165 ± 0.006	0.129 ± 0.007 ^a
NMR	0.150 ^c	0.138 ^{a,d}	0.123 ^{a,b,d}	0.110 ^{a,d}		0.135 ± 0.002 ^b
	0.149 ^e	--	--	0.106 ^{a,e}		

^aNaCl.

^bNaClO₄.

^cIntercept of plot in Figure 3.5 for the reaction in ZnCl₂.

^dIntercept from plot of k_{obsd} vs. [NaN₃].

^eIntercept from plot of k_{obsd} vs. [pyridine-d₅].

which rules out a bimolecular reaction with Cl^- . Rate constants (k_1) used to determine the activation values from an Eyring plot¹³ (Figure 3.2) were taken from ordinate intercepts of plots of *pseudo*-first-order rate constants vs. $[\text{NaN}_3]$ in

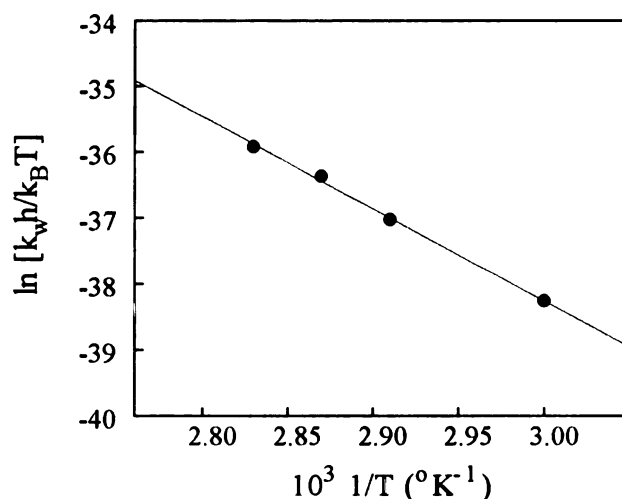


Figure 3.2. Eyring plot for the hydrolysis of **1**. The values of k_1 were taken from the ordinate intercepts for the reaction of **1** with azide (from Ref. 9). The plot is linear ($r = 0.999$) and the activation values are: $\Delta H^\ddagger = 27.7 \pm 1.0$ kcal/mol; $\Delta S^\ddagger = +7.1 \pm 1.0$ gibbs/mol; $\Delta G^\ddagger_{80^\circ\text{C}} = 25.2$ kcal/mol.

the range $60^\circ\text{-}90^\circ\text{C}$.⁹ The values are: $\Delta H^\ddagger = 27.7 \pm 1.0$ kcal/mol; $\Delta S^\ddagger = +7.1 \pm 1.0$ gibbs/mol; $\Delta G^\ddagger_{80^\circ\text{C}} = 25.2$ kcal/mol.

Suppression of Hydrolysis. At concentrations of ca. 10^{-4}M , the reaction goes smoothly to completion; UV samples were routinely analyzed by NMR to assure that a complete reaction had occurred. At "normal" NMR concentrations of ca. 10mM , however, the reaction of **1** in D_2O did not go to completion, and in initial experiments seemed to depend on the concentration of **1**. This pattern was independent of the presence or absence of exogenous salt (NaCl or NaClO_4 , Figure 3.3). When the hydrolysis was run in solvent saturated with SMe_2 --"cured" to relieve pressure by heating at 80°C for 20 min before adding **1** and heating in the

probe of the NMR--the extent of reaction was less than without excess SMe_2 (Figure 3.3). The reaction did not merely slow down, however: it stopped completely.

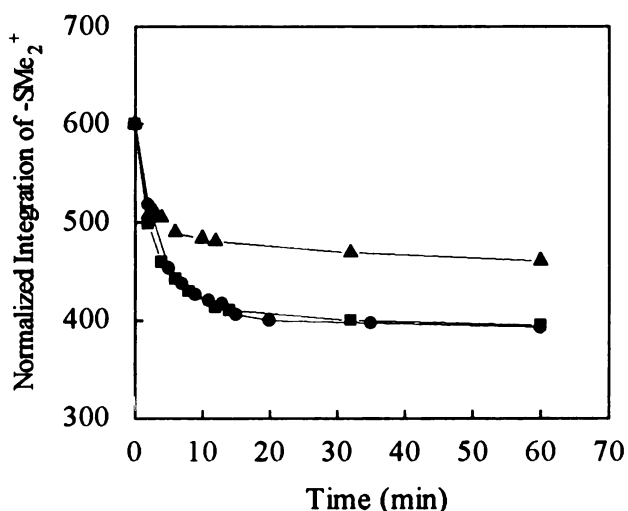


Figure 3.3. Plots of the normalized integrated signal for the SMe_2 signal for 1 at 80°C in pure D_2O (\bullet), $\mu = 1.7$ (NaCl, \blacksquare), and in pure D_2O saturated with SMe_2 and "cured" by heating at 80°C (\blacktriangle). Heating for several more hrs causes no change in the 1 hr value.

Closed-Vial And Zn^{+2} Experiments. Because of different void volumes and leaky caps, it was not possible to measure accurately the extent of reaction for equal concentrations of 1 in NMR tubes. When the reaction was run in sealed vials, however, results were reproducible. Data are the averages of duplicate determinations ($\pm 5\%$ S.E.) made on serial dilutions of two stock solutions with different initial concentrations; as a check, each stock solution was diluted to the same final concentration (ca. 0.033M). The extent of reaction depended on the initial concentration of 1 (Figure 3.4).¹⁴

Hydrolysis in the presence of either HgCl_2 or ZnCl_2 went smoothly to completion. For Zn^{+2} reactions measured in the NMR, plots of $\ln(A_t/A_0)$ vs. time were linear over 4 half-lives and gave the same rate constant at several initial

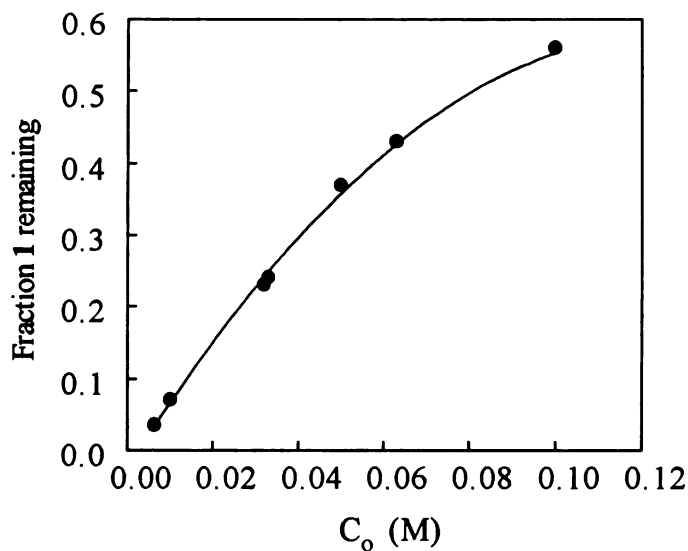


Figure 3.4. Plot of the fraction of 1 remaining vs. the initial concentration of 1 (C_0) after heating various concentrations in sealed vials at 80°C for 40 min. The points are averages of duplicate determinations for serial dilution of two initial concentrations, each of which was diluted to the same concentration (0.033M) as an internal check on the method.

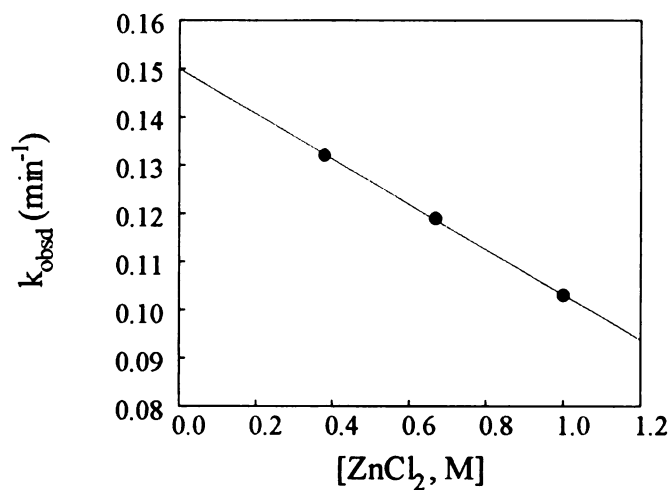


Figure 3.5. Plot of k_{obsd} vs. $[ZnCl_2]$ for the hydrolysis of 1 at 80°C. Points are the averages of three determinations (error bars within symbols). Plots of $\ln(A_t/A_0)$ vs. t used to obtain k_{obsd} were linear over 3-4 half-lives. The plot is linear ($r = 0.9999$) and extrapolates to the value of k_{obsd} (0.150 min⁻¹) found for the hydrolysis of 1 in pure D₂O.

concentrations of **1**. Rate constants were determined at three concentrations of ZnCl_2 (2-3 determinations, S.E. $<\pm 5\%$) and are plotted vs. $[\text{ZnCl}_2]$ in Figure 3.5.

Isotope Effects. The solvent isotope effects were obtained as the ratios of the UV rate constants for reaction in H_2O and D_2O from Table 3.1; they are $k_{\text{H}}/k_{\text{D}} = 1.1$ for water alone and $\mu = 1.7$ (NaCl) at 80°C . The α -deuterium secondary isotope effect $k_{\text{H}}/k_{\text{D}} = 1.26$ per deuterium was obtained from the values for the hydrolysis in pure D_2O (Table 3.1) and the value for the zero-order reaction of ND_3 in D_2O , 0.095 min^{-1} (Figure 3.1), with no exogenous salt added to control ionic strength at 80°C .

Discussion

The plots of k_{obsd} vs. $[\text{nucleophile}]$ (Figure 3.1) for the reaction of **1** with various nucleophiles show borderline behavior for all nucleophiles: the rates do not double with a doubling of nucleophile concentration, and there are non-zero ordinate intercepts. Sneen⁴ found a similar kinetic profile for **1** at 60°C for the reaction of 0-0.12M azide with no control of ionic strength, and interpreted his results in terms of the IDC mechanism. Kinetics alone, however, are not sufficient to differentiate one mechanism from another. In his excellent analysis of the kinetics governing the ion-pair scheme for substitution reactions, Carpenter¹⁵ has pointed out that the presence of CLGS rules out an ion-pair or IDC as an intermediate.

During attempts to measure the rate constant for hydrolysis of **1** by NMR, we found that the reaction stopped completely at the relatively high concentrations of substrate needed for these experiments, and that the extent of reaction was reduced in the presence of an excess of exogenous SMe_2 (Figure 3.3). Results of the closed-vial experiments, which were run in a manner that kept SMe_2 in solution, showed that the extent of reaction was a function of the initial

11005 JDDADV

concentration of **1** (Figure 3.4), and, presumably, of the concentration of SMe_2 released upon hydrolysis. Running the reaction in the presence of either 0.1M Hg^{+2} and 0-1.0M Zn^{+2} at 80°C drives it to completion by removing SMe_2 as the Lewis complex. The plot of k_{obsd} vs. $[\text{ZnCl}_2]$ shown in Figure 3.5 is linear and extrapolates to a value of $k_{\text{obsd}} = 0.150 \text{ min}^{-1}$, the value of the rate constant in the absence of exogenous salt. These results are consistent with CLGS in the hydrolysis of **1**. The dilemma remains, however, that CLGS would be expected to slow but not stop the reaction.

An alternative to CLGS that is consistent with all these results is the establishment of the equilibrium $\text{RSM}_2^+ \rightleftharpoons \text{ROH} + \text{SMe}_2 + \text{H}_3\text{O}^+$ during the course of the reaction. The equation for this equilibrium is $C_o^2 = K_{\text{eq}} f/(1-f)^3$, where C_o is the initial concentration of **1** and f is the fraction remaining at equilibrium. When the data from Figure 3.4 were fitted to this equation with the Marquardt-Levenberg non-linear least-squares algorithm, the plot in Figure 3.6 resulted ($K_{\text{eq}} = 0.00167 \pm 0.00002$, $\chi^2 = 1.4 \times 10^{-8}$). Clearly an equilibrium is established. When equal concentrations (C_p) of the alcohol, SMe_2 , and DCI were mixed and heated in sealed vials for 40 min, the exact amount of **1** predicted by the equation was obtained. For instance, for $C_p = 0.005\text{M}$, $f = 0.05$, and for $C_p = 0.05\text{M}$, $f = 0.38$. Holding the concentration of alcohol and DCI constant and increasing the concentration of SMe_2 incrementally pushed the reaction to the left by the amounts predicted by the equation. Because of this equilibrium, it is not possible to measure CLGS in pure water.

There are literature precedents for both the reverse and forward reactions. Badet, *et al.*,¹⁶ found that treatment of (-)-(R)-2-octanol with a ten- to twenty-fold excess of SMe_2 and methanesulfonic acid in methylene chloride gave the active (2-octyl)dimethyl sulfonium with up to 88% inversion of configuration,

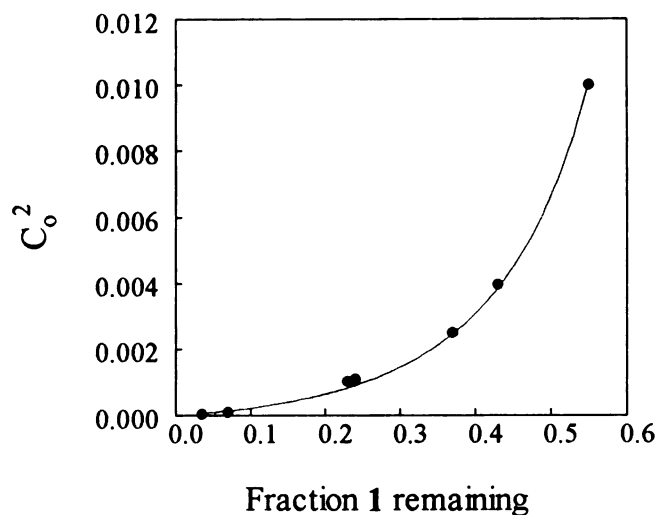


Figure 3.6. Plot of the square of the initial concentration of 1 (from Figure 3.4) vs. the fraction remaining. The line is the fit of the equation $C_0^2 = K_{\text{eq}} f/(1-f)^3$, derived for the equilibrium $\text{RSMe}_2^+ \rightleftharpoons \text{ROH} + \text{SMe}_2 + \text{H}_3\text{O}^+$ to the data by the Marquardt-Levenberg non-linear least-squares algorithm. $K_{\text{eq}} = 0.00167 \pm 0.00002$, $\chi^2 = 1.4 \times 10^{-8}$.

presumably by direct displacement on the protonated alcohol (or a concerted general acid-catalyzed reaction). Because of the vast difference in solvation between methylene chloride and water, the mechanism of our conversion may be different.

The equilibrium had been observed but not fully characterized for other sulfonium salts. Scartazzini and Mislow¹⁷ found that the reaction of *t*-butylethylmethylsulfonium perchlorate in acetic acid stopped after ca. 25% reaction; in the presence of excess sodium acetate, the reaction appeared to behave normally, although it was not followed to completion. Kevill and Anderson¹⁸ found that the acetolysis of 1-adamantylmethylsulfonium stopped after ca. 70% reaction; addition of sodium acetate allowed the reaction to go to completion. Friedberger and Thornton⁵ found that the hydrolysis of 1 stopped after ca. 60% reaction at the relatively high concentrations (0.1M) used to measure sulfur KIEs. They ascribed this effect to some nonspecific interaction of 4-methoxybenzyl alcohol with 1 that

removed the latter from solution. In their recent study of the solvolysis of 1 in various solvent systems, Kevill and coworkers¹¹ found that an equilibrium was established in acetic and formic acids and in various aqueous mixtures of trifluoroethanol and hexafluoro-2-propanol. In the binary solvent systems, the extent of reaction increases with an increase in the water content. The equilibrium in the aqueous binary systems was suppressed by addition of pyridine. We found that pyridine-d₅ reacts with 1 with clean second-order kinetics and that the reaction goes to completion under *pseudo*-first order conditions (see Figure 3.1). In fact, with the exception of the reaction of 1 with thiocyanate that is complicated by extensive equilibria among the products,⁸ 1 reacts cleanly with basic nucleophiles without establishment of the equilibrium under *pseudo*-first order conditions and goes to completion smoothly in the presence of NaOD and ND₃ (zero order in nucleophile; Figure 3.1). Presumably Sneen's⁴ results were unhampered by the equilibrium because the concentration of 1 he used was low (10⁻⁴M; see Figures 3.4 and 3.6). Thus removal of hydronium ion or SMe₂ (Figure 3.6) allows the reaction to go to completion.

The equilibrium may explain apparent anomalies in other studies. Darwish, *et al.*,¹⁹ found that racemization of substituted benzylethylmethylsulfonium salts bearing substituents with σ^+ values > -0.31 occurred though pyramidal inversion of the sulfonium. For (4-methoxybenzyl)ethylmethylsulfonium, however, the kinetics of methanolysis and racemization and the lack of suppression by 0.05M SMeEt suggested that racemization occurred through an IDC mechanism. Our results suggest, however, that racemization may have occurred because of the equilibrium among starting material and products. The relatively low concentration of SMeEt used by Darwish probably had only a slight effect on the rate (see below).

Friedberger and Thornton's sulfur KIE data⁵ for the hydrolysis of **1** formed the basis for a conundrum that they went to great pains to resolve. The issue is plain enough: The Hammett plot (against σ^+ , Figure 3.7A) for the hydrolysis rate

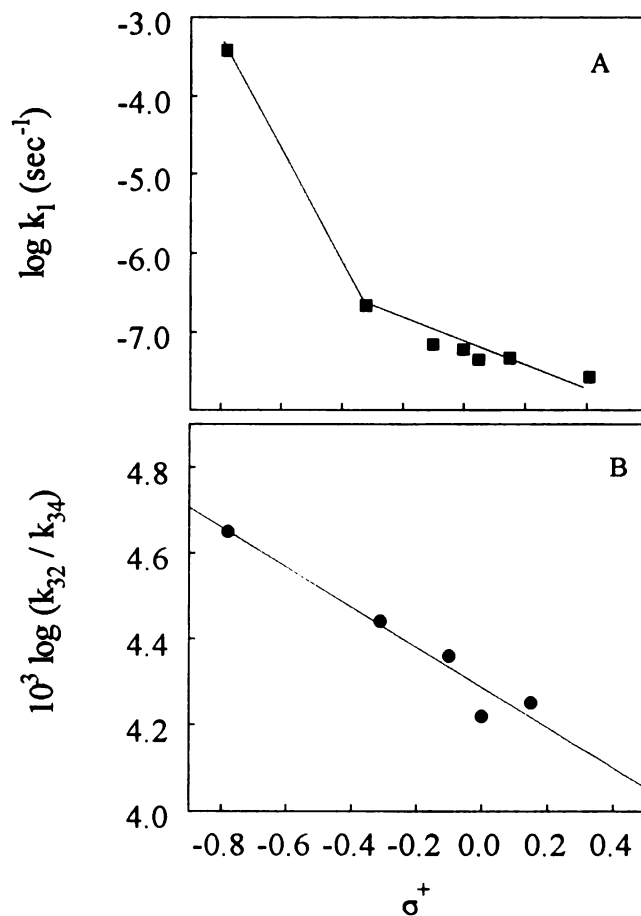


Figure 3.7. Hammett plots for **A.** the hydrolysis (■) and **B.** the sulfur KIE (●) for hydrolysis of 3- and 4-substituted BDMS⁺ at 68°C. Data are from Reference 5.

constants of 3- and 4-Y-BDMS⁺ show a distinct break between **1** and the 4-Me compound, which indicates a change in mechanism, but a plot of $\log k_{32}/k_{34}$ vs. σ^+ is linear (Figure 3.7B), which indicates a common mechanism. Earlier, Hill and Fry²⁰ had found similar anomalous results for the chlorine KIEs for benzyl chlorides. Either there is a single mechanism and the break in the Hammett plot for hydrolysis rate constants reflects other factors; there are two mechanisms with a

fortuitously linear sulfur KIE; sulfur KIEs are an insensitive measure of the difference between S_N1 and S_N2 mechanisms, as suggested by Harris, *et al.*²¹ ; or the value for 1 is in error. The presence of the equilibrium suggests that the last possibility may be the source of the anomaly.

The ratio $k_{32}/k_{34} = (^{34}\text{S}/^{32}\text{S})_{100\%} / (^{34}\text{S}/^{32}\text{S})_{2\%}$ were obtained by mass spectrometry of SMe_2 liberated after 99.99% reaction with hydroxide (conditions that would prevent establishment of the equilibrium) and 2% reaction in water, respectively. Ratios at 2% reaction were used for all substrates except 1, where 25% reaction was used. For data obtained at 25% reaction, where the equilibrium is well-established, the pool of liberated SMe_2 may have mixed back into substrate, and the value of $(^{34}\text{S}/^{32}\text{S})_{100\%} / (^{34}\text{S}/^{32}\text{S})_{25\%}$ may be an inaccurate measure of the KIE. (This assumes that the KIE for capture of R^+ or displacement on ROH_2^+ is much less than that for bond-breaking in 1; because the barriers are low for reactions in the reverse direction compared with the barrier for bond breaking, this seems to be a reasonable assumption.) For the 2% points, however, very low concentrations of SMe_2 are in solution (Figures 3.4 and 3.6) and it is reasonable to expect that little--if any--back mixing would occur. Thus the KIE for 1 is suspect, and the value may be higher as Kevill has suggested.¹¹

The k_{32}/k_{34} values for hydrolysis of 4-Me, 4-H, and 3-Cl BDMS⁺ are almost exactly the same values obtained by Swain and Thornton²² for the reaction of hydroxide with these substrates. These values are substantially lower than the sulfur KIE for hydrolysis of *t*-butyldimethylsulfonium, a compound that may react by an " S_N1 -like" mechanism²³ or with "some nucleophilic solvent participation"^{1,11}; this issue has not been resolved fully. Because of the good match of the hydrolysis KIEs with the hydroxide KIE data, Friedberger and Thornton⁵ argued that hydrolysis of all substrates occurred with solvent nucleophilic participation. We believe that this rationale is appropriate for 4-Y-

BDMS⁺ with $\sigma^+ > -0.31$: the break in the Hammett plots for the rate data indicates a change in mechanism between the 4-MeO- and the other substrates. The intermediate-hardness dependence we found⁹ for nucleophilic substitution reactions of **1** (Figure 3.1) also rules out direct substitution by water, which, even though it is a poor nucleophile, is a hard one. This HSAB sensitivity also tends to rule out the IDC, which should be much less selective than the bare substrate toward nucleophiles.

We note, however, that while we are suspicious of the KIE value for **1**, we have no direct proof against it. It is entirely possible that the value is accurate and that the linear Hammett plot for the KIE data is fortuitous. If the Hill and Fry data²⁰ for benzyl chlorides, which show the same effect, were also judged to be in error, it would require an equilibrium involving Cl⁻. Amyes and Richard²⁴ found a common ion effect (up to 0.2M NaCl) for the hydrolysis of 4-methoxybenzyl chloride in 50% aqueous trifluoroethanol, but they do not report any anomalous behavior over 3 halflives. If their plot of k_{obsd} vs. [Cl⁻] extrapolates to a zero rate constant at high chloride concentrations, the value of the equilibrium constant would of necessity be quite small; their plot very well may reach a plateau value. We also note, however, that the equilibrium is not unique to the sulfoniums. We have established its presence in the hydrolysis of benzylpyridiniums with four pyridine leaving groups.¹⁴ Thus the conundrum remains unanswered.

Even if the Friedberger and Thornton data were not available, we would still face the dilemma of establishing with certainty that the mechanism is S_N1. The new results obtained in the current study--the small solvent isotope effect of $k_{\text{H}}/k_{\text{D}} = 1.1$, the α -deuterium secondary isotope effect $k_{\text{H}}/k_{\text{D}} = 1.26$ per deuterium, which is near the theoretical limit for fully dissociative reactions,²⁵ and the high, positive value of $\Delta S^\ddagger = 7.1$ gibbs/mol--are consistent with either an S_N1 or IDC mechanism. Kevill^{1,11} found that the presence of exogenous SMe₂ in 95% acetone

led to "modest reductions" of the specific rate constant for hydrolysis. With the well known mass-action equation $k_0/k_{\text{expt}} = (1 + \alpha [\text{SMe}_2])$, where k_0 is the first order rate constant in the absence of SMe_2 , k_{expt} is the rate constant in the presence of various $[\text{SMe}_2]$, and α is the mass law constant, Kevill obtains an α value of 4.8 M^{-1} , which is similar to a value of 2.5 M^{-1} for benzhydryl-dimethylsulfonium, a compound that clearly reacts by an $\text{S}_{\text{N}}1$ mechanism.¹ Based on this mass law effect, they argued that **1** does not react through an IDC intermediate.

Thus in order to rule out the IDC mechanism in the hydrolysis of **1**, it is necessary to use other data. The kinetics and selectivities of the reaction of **1** with azide we have measured and will report in detail elsewhere⁹ are consistent with a mixed $\text{S}_{\text{N}}1/\text{S}_{\text{N}}2$ mechanism. Plots of k_{obsd} vs. $[\text{NaN}_3]$ at constant ionic strength are linear over most of the range of nucleophile and have non-zero intercepts (Figure 3.1). The product ratio $[\text{RN}_3]/[\text{ROH}]$ increases smoothly with increasing azide concentration. Sneen⁴ argued that the kinetic and selectivity pattern are consistent with a mechanism in which all RN_3 arises from direct displacement on an IDC. Friedberger and Thornton⁴ pointed out that Sneen's IDC mechanism for the reaction of **1** with azide is reasonable *i*, no azide product arises from trapping of free carbenium ion by nucleophile. If this occurs, the mechanism must be mixed $\text{S}_{\text{N}}1/\text{S}_{\text{N}}2$ (Scheme 3.1).

We found that under conditions of constant ionic strength a plot of the product ratio $[\text{RN}_3]/[\text{ROH}]$ vs. $[\text{NaN}_3]$ (Figure 3.8) is fitted by

$$\frac{[\text{RN}_3]}{[\text{ROH}]} = \left(\frac{k_{\text{N}}}{k_{\text{w}}} \right) [\text{N}_3^-] \left(1 + \frac{k_2}{k_1} [\text{N}_3^-] \right) + \frac{k_2}{k_1} [\text{N}_3^-] \quad (\text{Eq. 3.1})$$

which was derived assuming the mixed $\text{S}_{\text{N}}1/\text{S}_{\text{N}}2$ mechanism,^{26,27} with k_1 (0.123 min^{-1}) and k_2 ($0.238 \text{ M}^{-1}\text{min}^{-1}$) the rate constants for the water-only and azide

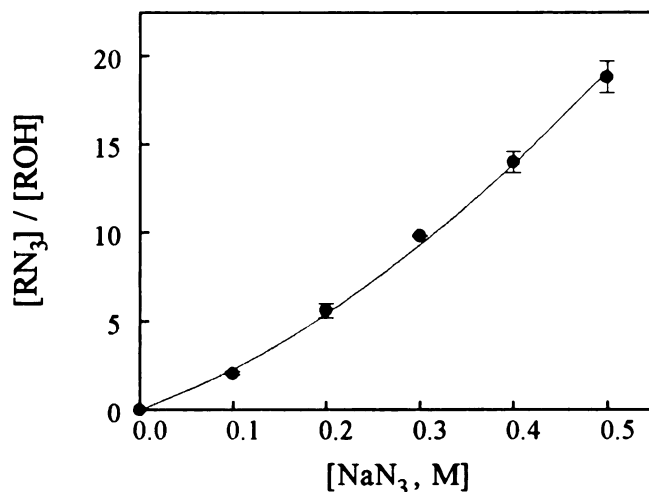


Figure 3.8. Plot of the product ratios vs. $[\text{NaN}_3]$ for the reaction of **1** at 80°C , $\mu = 1$ (NaCl). The points are the experimental data obtained by integration of several peaks in CDCl_3 extracts of reaction mixtures, and the line was fit to points calculated with Equation 3.1 using experimentally determined values for the various ratios (Ref. 9). Error bars are S.E.

reactions at $\mu = 1.7$, respectively, and the value for carbenium ion trapping by azide, $k_N/k_W = 17$, obtained from the product ratios for 4-methoxybenzyl-(4'-sulfo) benzoate,⁹ a water-soluble substrate that is zero order in azide at 80°C . Kevill¹¹ has reanalyzed Sneen's azide data⁴ and concluded that a k_N/k_W ratio of 21.1 M^{-1} is required to fit the 60°C data to an equation derived assuming the mixed mechanism. Our measured value for trapping of the free carbenium ion of **17** at 80°C , in excellent agreement with Kevill's estimate obtained by best fit. We believe that this fit conclusively rules out the IDC mechanism for azidolysis and hydrolysis reactions of **1**.

Ritchie²⁸ has made the bold claim that "all patterns of reactivity and selectivity arise primarily from solvent effects, and not from some inherent property of the solute reactant" and Arnett and Reich²⁹ have suggested that the failure of the Menschutkin reaction to obey the much maligned reactivity-selectivity principle is the result of solvation of the leaving group at the transition state and not the result of substituent effects. Kevill¹¹ has found only modest

effects on the rate of solvolysis of **1** in a variety of solvent systems. Some of our results show dramatic effects in the activation values, however, which tend to support the contentions of Ritchie and Arnett.

For instance, we found that $\Delta\Delta S^\ddagger$ for the azide reactions 4-methoxybenzyl-3'-cyanopyridinium and **1** is -17 gibbs/mol, which we believe reflects the substantial reorganization of solvent about the hydrophilic pyridine and the lack of solvent reorganization about the hydrophobic SMe_2 at the transition state.³⁰ The hydrolysis of **1** shows the hydrophobic effect. In H_2O , Kevill¹¹ found $\Delta S^\ddagger = 13.4 \pm 1.7$ gibbs/mol, but we found that the value in D_2O is 7.1 ± 1.0 gibbs/mol; $\Delta\Delta H^\ddagger$

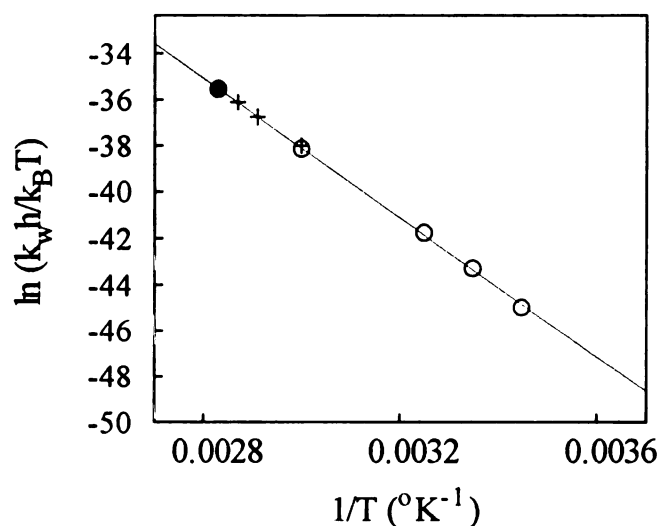


Figure 3.9. Eyring plot of Kevill's titrimetric rate constants¹¹ in H_2O in the range 16-60° (○), our UV value for the rate constant at 80° in H_2O (●), and our UV rate constants in D_2O (+) that are converted to H_2O values using $k_{\text{H}}k_{\text{D}} = 1.1$ and the ratio for reaction at $\mu = 0$ and 1.7. The correlation is excellent ($r = 0.9997$) and shows that there is no error between methods or laboratories.

is much smaller (ca. 2 kcal/mol higher in H_2O). These differences are not the result of error: We measured a UV rate constant in H_2O at 80°C that falls on the line of the Eyring plot made with Kevill's data; converting our D_2O rate constants to H_2O values in the range 60°-80°C using the $k_{\text{H}}/k_{\text{D}}$ value of 1.1 and the conversion from

constant ionic strength to pure water gives points that fall on the line as well (Figure 3.9). Thus this almost two-fold difference is real and, we believe, is the result of the hydrophobic effect. Ben-Naim³¹ found that the ΔS^\ddagger for the transfer of noble gases and methane and ethane from the gas phase into water was slightly more negative for D₂O than for H₂O, presumably because of the slightly stronger (5-7%) deuterium bonds, which is the trend we see in the ΔS^\ddagger values. While solvent effects are often difficult to dissect from other factors, these data may provide a fairly clear example of the importance of solvation and reactivity, at least for charged substrates that do not require extensive solvent reorganization to accommodate the creation of charge at the transition state.

References and Notes

(1) Kevill, D.N.; Anderson, S.W.; Ismail, N.H.; Fujimoto, E.K. In *Physical Organic Chemistry 1986*; Kobayashi, M., Ed.; Elsevier: Amsterdam, 1987; pp. 311-320.

(2) Swain, C.G.; Kaiser, L.E. *J. Am. Chem. Soc.* **1958**, *80*, 4089-4092; Swain, C.G.; Kaiser, L.E.; Knee, T.E.C. *J. Am. Chem. Soc.* **1958**, *80*, 4092-4094.; Swain, C.G.; Taylor, L.J. *J. Am. Chem. Soc.* **1962**, *84*, 2456-2457; Swain, C.G.; Rees, T.; Taylor, L.J. *J. Org. Chem.* **1963**, *28*, 2903; Swain, C.G.; Burrows, W.D.; Schowen, B.J. *J. Org. Chem.* **1968**, *33*, 2534-2536.

(3) Ingold, C.K. *Structure and Mechanism in Organic Chemistry*; Cornell University Press: Ithica, 1953; pp. 306-418.

(4) For reactions of 1: Sneen, R.A.; Felt, G.R.; Dickason, W.C. *J. Am. Chem. Soc.* **1973**, *95*, 638-639. For the ion-pair mechanism for neutral substrates: Sneen, R.A.; Larsen, J.W. *J. Am. Chem. Soc.* **1969**, *91*, 6031-6035; Sneen, R.A. *Acc. Chem. Res.* **1973**, *6*, 46-53.

UNCE IIRBAPV

(5) Friedberger, M.P.; Thornton, E.R. *J. Am. Chem. Soc.* **1976**, *98*, 2861-2865.

(6) Johnson, R.W.; Marschner, T.M.; Oppenheimer, N.J. *J. Am. Chem. Soc.* **1988**, *110*, 2257-2263; Handlon, A.L.; Oppenheimer, N.J. *J. Org. Chem.* **1991**, *56*, 5009-5010.; Schröder, S.; Buckley, N.; Oppenheimer, N.J.; Kollman, P.A. *J. Am. Chem. Soc.* **1992**, *114*, 8232-8238; Buckley, N.; Handlon, A.L.; Maltby, D.; Burlingame, A.L.; Oppenheimer, N.J., *J. Org. Chem.* **1994**, *59*, 3609-3615; Tashma, R.; Oppenheimer, N.J., unpublished results; Buckley, N.; Oppenheimer, N.J., unpublished results.

(7) Reviewed in Katritzky, A.R.; Brycki, B.E. *Chem. Soc. Rev.* **1990**, *19*, 83-105, and elsewhere. See also Katritzky, A.; Malhotra, N.; Ford, G.P.; Anders, E.; Tropsch, J.G. *J. Org. Chem.* **1991**, *56*, 5039-5044.

(8) Buckley, N.; Oppenheimer, N.J. *J. Org. Chem.* **1994**, *59*, 247-249.

(9) Buckley, N.; Oppenheimer, N.J., submitted (Chapter 4).

(10) Buckley, N.; Maltby, D.; Burlingame, A.L.; Oppenheimer, N.J., submitted (Chapter 6).

(11) Kevill, D.N.; Ismail, N.H.J.; D'Souza, M.J. *J. Org. Chem.* **1994**, *59*, 6303-6312.

(12) Our value for 60°C matches the value reported by Sneen⁴ and our 70°C value matches closely Friedberger and Thornton's value⁵ for 69°C. Kevill (Kevill, D.N., personal communication) found a value of $k_{\text{obsd}} = 0.148 \text{ min}^{-1}$ for the 80°C point.

(13) Maskill, H. *The Physical Basis of Organic Chemistry*; Oxford University Press; New York, 1985; pp. 247-249.

(14) Note that benzyl pyridiniums showed the same pattern of suppression, which was most severe for the 4-MeO compound. These data also fit an equation derived assuming the equilibrium among starting material and products. Addition

of exogenous pyridines suppresses the reaction further. When the hydrolysis of several 4-MeO-benzyl pyridiniums was run in 2M DCl or D₂SO₄, conditions that would either protonate most of the liberated pyridine or cause the product alcohol to form the bis ether [Quelet, R.; Allard, J. *Bull. Chem. Soc. Fr.* **1937**, *4*, 1468-1471], good linear plots were obtained over 4-5 half-lives.

(15) Carpenter, B.K. *Determination of Organic Reaction Mechanisms*. John Wiley & Sons: New York, 1984; pp. 40-51.

(16) Badet, B.; Jacob, L.; Julia, M. *Tetrahedron* **1980**, *37*, 887-890.

(17) Scartazzini, R.; Mislow, K. *Tett. Lett.* **1967**, 2719-2722.

(18) Kevill, D.N.; Anderson, S.W. *J. Am. Chem. Soc.* **1986**, *108*, 1579-1585.

(19) Darwish, D.; Hui, S.H.; Tomilson, R. *J. Am. Chem. Soc.*, **1968**, *90*, 5631-5632.

(20) Hill, J.W.; Fry, A. *J. Am. Chem. Soc.* **1962**, *84*, 2763-2768.

(21) Harris, J.M.; Mount, D.L.; Smith, M.R.; Neal, W.C.; Dukes, M.D.; Raber, D.J. *J. Am. Chem. Soc.* **1978**, *100*, 8147-8156.

(22) Swain, C.G.; Thornton, E.R. *J. Org. Chem.* **1961**, *26*, 4808-4809.

(23) Saunders, W.H. Jr.; Asperger, S. *J. Am. Chem. Soc.*, **1957**, *75*, 3443-3447.

(24) Amyes, T.L.; Richard, J.P. *J. Am. Chem. Soc.* **1990**, *112*, 9507-9512.

(25) Shiner, V.J. "Deuterium Isotope Effects in Solvolytic Substitution at Saturated Carbon." In *Isotope Effects in Chemical Reactions*, Collins, C.J., Bowman, N.S. Eds.; Van Nostrand Reinhold: New York, 1970; pp 90-159.

(26) The value of k_{Nu}/k_W depends on the presence or absence of added salt (Ref. 9). In the presence of azide only, the value of k_{Nu}/k_W is ca. 55 over 0-0.5M azide. The azide-only data are fit to a form of Equation 3.1 that includes terms for a preassociated concerted bimolecular reaction with azide.

(27) This equation also gives an excellent fit to the selectivity data for the azide reaction of 4-methoxybenzyl chloride, which occurs through the mixed mechanism in aqueous acetone (Ref. 24).

(28) Ritchie, C.D. In *Solute-Solvent Interactions*; Coetzee, J.F., Ritchie, C.D., Eds.; Marcel Dekker: New York, 1976, Vol. 2; p. 265.

(29) Arnett, E.M.; Reich, R. *J. Am. Chem. Soc.* **1980**, *102*, 5892-5902.

(30) The value of ΔS^\ddagger for the reaction of benzyldimethylsulfonium and trimethyl sulfonium with phenoxide and hydroxide, determined by Swain and Taylor,² are in the same range (-4.4 to -7.9 gibbs/mol) as the values for the azide reaction.

(31) Summarized in Ben-Naim, A. *Solvation Thermodynamics*; Plenum Press, New York, 1987, pp. 75-77.

UCSF LIBRARY

Chapter 4
The Nucleophilic Substitution Reactions of
(4-Methoxybenzyl)dimethylsulfonium Chloride

UCSF LIBRARY

Introduction

Substitution reactions of neutral and charged benzyl derivatives exhibit a range of possible mechanisms.¹ Some reactions are clear-cut. For instance, solvolysis of 4-methoxybenzyl chloride and several benzoates in 50:50 (v/v) trifluoroethanol-water is zero order in azide, while azidolysis of 4-nitrobenzyl derivatives is strictly bimolecular.² Depending on the solvent system, however, reactions of some benzyl derivatives exhibit intermediate kinetic behavior in the "borderline" between S_N1 and S_N2 (kinetic order for nucleophile of between 0 and 1). Hammett plots for either solvolysis³ or substitution reactions⁴ invariably exhibit a break that has been interpreted as a change in mechanism (S_N1 to S_N2)⁵ or as a change in the resonance demand at the reaction center.⁶ (Note that these are *broad* generalizations.) Richard and Yeary⁷ have recently proposed that these breaks are a consequence of effects proposed in the Pross-Shiak VBCM theory.⁸

Reactions of (4-methoxy)benzyl substrates were central to examinations of Sneen's ion pair hypothesis.⁹ Sneen and Larsen¹⁰ proposed that azidolysis of 4-methoxybenzyl chloride occurred through a contact ion pair, while Kohnstam¹¹ argued that the reactions was mixed S_N1/S_N2 . Studies of chlorine isotope effects were interpreted as proof for and against the ion-pair mechanism.¹² Aymes and Richard² recently reported definitive results for the azidolysis of 4-methoxybenzyl chloride in 30% and 25% aqueous organic solvent systems; the reaction is mixed S_N1/S_N2 . The bimolecular reactions (lyoxide, azide) of 4-Me, H, Cl- and 3-Cl-benzyl dialkyl and alkyl/arylsulfonium salts at constant ionic strength is S_N2 .¹³ Richard and Jencks¹⁴ found that azidolysis of (1-[4-methylphenyl]ethyl)dimethylsulfonium is mixed S_N1/S_N2 under conditions of constant ionic strength in trifluoroethanol-water.

Sneen suggested that the reaction of 4-methoxybenzyl- and benzyldimethylsulfonium with nucleophiles occurs through an ion-dipole complex¹⁵ in analogy

with his ion-pair mechanism for neutral substrates, which Katritzky¹⁶ and Darwish¹⁷ have extended to other systems. While Sneen's ion-pair mechanism for neutral substrates has been criticized extensively, Schleyer and Bentley¹⁸ note that the ion-dipole mechanism may be operative for benzyl and allyl substrates. The general rejection of the Sneen mechanism is based on technical and conceptual issues. Sneen's studies were done with added azide only with no control of ionic strength. Schleyer and his colleagues¹⁹ proposed that the kinetics was the result of special azide salt effects and not of ion-pairs, a view that is generally accepted.²⁰

As shown in Chapter 2, reactions of 4-substituted benzyl pyridiniums with azide at constant ionic strength are strictly second order--plots of k_{obsd} vs. [azide] pass through the origin--and show little substituent effects; the activation values are all within a narrow range ($\Delta H^\ddagger \sim 20$ kcal, $\Delta S^\ddagger \sim -25$ gibbs/mol), the shape of the Hammett plots depend on the basicity of the pyridine, and the second-order rate constants and activation values for methyl-3-cyanopyridinium are within the same range as those for the benzyl compounds. Brønsted β_{LG} values for the 4-methoxybenzyl and Me substrates are -1.47, which shows an *enormous* amount of bond breaking in the activated complex for the 4-methoxybenzyl substrate. If there are specific azide salt effects, they are not a major influence on the second-order rate constants for benzyl pyridiniums.

We became intrigued with the possibility that other charged benzyl substrates might have similar behavior, and we needed to explain why our results for the 4-methoxybenzyl pyridinium in water did not match Katritzky's results in chlorobenzene.¹⁶ We decided to repeat Sneen's study of the hydrolysis and substitution reactions of (4-methoxybenzyl)dimethylsulfonium chloride (1) under the original conditions and at constant ionic strength. Our study of the hydrolysis of 1 (Chapter 2)²¹ showed that an ion-dipole complex was not an intermediate, a result confirmed recently by Kevill and his colleagues.^{20,21} We have studied the

substitution reactions of **1** with a wide range of nucleophiles. We find that substitution occurs only for nucleophiles with intermediate hard-soft-acid-base (HSAB) rank through a mixed S_N1/S_N2 mechanism at constant ionic strength or through mixed unimolecular and preassociated concerted mechanisms in the absence of added salt.

Experimental Section

Chemicals and Equipment. All chemicals and solvents were obtained from Aldrich and used without further purification. NMR spectra were recorded on a General Electric QE-300 with a variable temperature probe rated at $\pm 0.1^\circ\text{C}$. Plots and regression analysis were made on Sigmaplot 3.1 or Origin 2.8. Positive- and negative-ion liquid secondary ion mass spectra (LSIMS) were obtained in the UCSF Mass Spectrometry Facility.

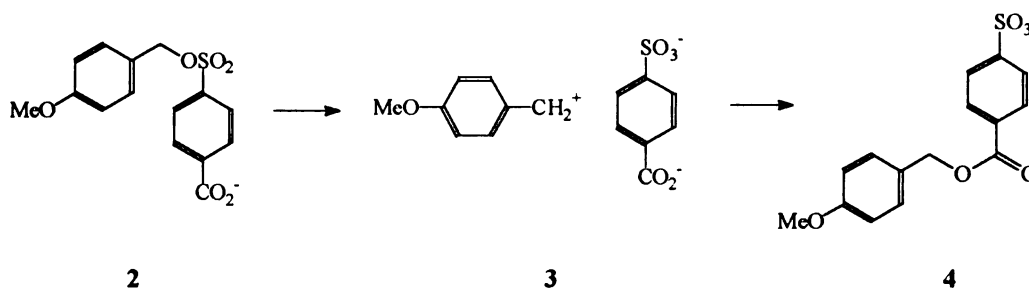
Synthesis.

Trimethylsulfonium iodide. A chloroform solution of 1 eq. of iodomethane and 1 eq. of methyl sulfide was shaken for 5-10 min at ambient temperature; the thin white crystals formed with a slight evolution of heat were collected and washed with chloroform repeatedly. The yield was essentially quantitative.

4-Methoxybenzyl-4'-sulfobenzoate (4). The general method given by Feiser and Feiser²³ was used. An anhydrous pyridine solution with 1 eq. of 4-methoxybenzyl alcohol and 1.1 eq. of 4-carboxybenzenesulfonyl chloride was heated gently, then stored at 0°C overnight. When this solution was poured into ice-cold 0.1M HCl, a white precipitate formed. It was collected and recrystallized by dissolving it in a small amount of boiling water and immediately quenching in iced brine. The solid was collected and dried *in vacuo*. This product, which gave reasonable NMR (>98% purity), FTIR (KBr pellet) and negative-ion LSIMS spectra, was assumed to be the sulfonate ester **2**. Rate constants for solvolysis

were orders of magnitude too low,²⁴ however, but were close to values for 4-methoxybenzyl benzoate esters reported by Aymes and Richard.^{2,25}

The reaction was repeated in an NMR tube at 25°C with pyridine-d₅ as solvent. After 10-15 min, alcohol had fallen to a low, steady level and a complex pattern of peaks appeared, none of which corresponded to the isolated product. If a portion of this solution was evaporated under reduced pressure, added to D₂O, and heated to 80°C for 20 min, the NMR spectrum showed the sulfonic acid and alcohol seen in spectra from solvolysis of the isolated product, and also contained a benzyl AA'BB' pattern that matched the spectrum for 4-methoxybenzyl pyridinium. A portion of the pyridine-d₅ solution was allowed to stand at ambient temperatures for several days and then carefully reduced to an oil; the NMR spectrum of the residue in DMSO-d₆ showed the solid product as the major component, with the only other product the corresponding pyridinium. Apparently in pyridine the sulfonate ester **2** solvolyzes to the ion pair **3** that collapses to the benzoate **4**, which is not soluble in water at ambient temperatures. In pyridine-d₅,



there is concomitant pyridine trapping of the carbenium ion to give the 4-methoxybenzyl pyridinium-d₅. Because of these complications, we did not attempt to isolate **2**. Benzoate: ¹H NMR: pyridine-d₅ (0 δ = TMS) δ 8.42 (d, J = 8 Hz, 2H, benzoate AA'), 8.18 (d, J = 8 Hz, 2H, benzoate BB'), 7.52 (d, J = 8.4 Hz, 2H, benzyl AA'), 7.06 (d, J = 8.4 Hz, 2H, benzyl BB'), 5.42 (s, 2H, -CH₂-), 3.72 (s,

3H, MeO-); DMSO- d_6 ($0 \delta = \text{TMS}$) δ 7.93 (d, $J = 8$ Hz, 2H, benzoate AA'), 7.73 (d, $J = 8$ Hz, 2H, benzoate BB'), 7.43 (d, $J = 8.4$ Hz, 2H, benzyl AA'), 6.97 (d, $J = 8.4$ Hz, 2H, benzyl BB'), 5.27 (s, 2H, $-\text{CH}_2-$), 3.76 (s, 3H, MeO-). ^{13}C NMR: DMSO- d_6 δ 165.30, 159.26, 152.64, 130.09, 129.51, 128.91, 127.93, 125.91, 113.93, 66.15, 55.13. Negative-ion LSIMS: m/z 321.1 M^+ ; calc. 321.2.

NMR Kinetics. All kinetics were measured on a General Electric QE-300 NMR spectrometer with a variable temperature probe rated at $\pm 0.1^\circ\text{C}$. *Pseudo*-first order rate constants for reactions with the nucleophiles and salts listed in Table 4.1 were measured by observing the loss of leaving group in ^1H -NMR spectra in D_2O either at constant ionic strength 1.7 (maintained with either sodium chloride or sodium perchlorate) or without salt added. (For ND_3 and NaOD , however, the AB pattern was followed because the benzyl and sulfonium methyl protons exchanged instantaneously.) The typical concentration of substrate was ca. 0.01M, which allowed spectra with good signal-to-noise ratios to be collected in a single-pulse experiment. Solutions were preheated in the probe (60 - 80°C), removed, added to the substrate, returned to the probe, reshimmed (ca. 1-1.5 min), and the appropriate peak was integrated at various timed intervals. 32K Datum points for a 90° pulse angle were collected in single blocks and processed with a line broadening of 1-1.5 Hz; for fast reactions, 16K datum points were collected at 15 or 30 sec intervals in 8 blocks and processed as described above.

Conversion of RSCN to RNCS Under the Reaction Conditions. Aliquots of stock solutions (ca. 10mM) of 1 in 0.5 and 1.0 M solutions of NaSCN alone or at $m = 5$ (NaCl) in H_2O were heated at 80°C in a heat block and extracted with CDCl_3 at 5 min intervals for up to 1 hr. (No residual product could be detected by *NMR* in D_2O samples treated this way.) Extracts were passed through a short

column of anhydrous sodium sulfate into a dry NMR tube. The isomerization could be monitored in ^1H spectra by observing the change in the intensities of the signals for the methylenes of RNCS ($\delta = 4.64$ ppm) and RSCN ($\delta = 4.15$ ppm).²⁶ Values of k_{obsd} were obtained by linear regression from slopes of plots of $\ln [(C_t - C_\infty)/(C_o - C_\infty)]$ vs. t , where the infinity value was the peak intensity at equilibrium ($r > 0.990$ for 3 plots, $r = 0.976$ for 1 plot). With or without control of ionic strength, doubling the concentration of nucleophile produced a doubling in k_{obsd} .

Selectivities. Reactions were run in NMR tubes; in some instances, tubes from kinetic runs were used and in others fresh solutions were made. At least three batches of substrate were used, and the concentrations of substrate at each $[\text{Nu}]$ were varied. As a check on the method, reactions were run in H_2O and processed as described; this was especially important for reactions in which the benzyl methylene protons exchanged. After heating at 80°C for >10 half-lives, the aqueous layers were extracted with CDCl_3 ; solvent was dried through a short column of anhydrous sodium sulfate, which was washed with a small volume of solvent. Spectra of the remaining clear aqueous layers showed that complete extraction could be achieved with a single volume of CDCl_3 equal to or slightly greater than the reaction volume. Product ratios were obtained by integrating the benzyl methylene peaks of products (4-methoxybenzyl alcohol [$\delta = 4.62$ ppm] or 4-methoxybenzyl azide [$\delta = 4.26$ ppm]). Spectra were obtained under identical conditions at 25°C , with 32K datum points collected in 32-128 acquisitions. In samples with low concentrations of alcohol, both peaks were integrated in pairs 3-5 times, with the slope and curvature of the integration adjusted each time, and the readings averaged. With the exceptions noted above, the product ratios obtained in either D_2O or H_2O were the same, which showed that exchange did not take place on the time scale of the experiments.

Results

Kinetics. Pseudo-first order and second-order rate constants were calculated by linear regression and are reported in min^{-1} or $\text{M}^{-1} \text{min}^{-1}$ as the mean \pm standard error. Because reactions with nucleophiles go to completion, with the exception of the NaSCN reaction (see below),²⁷ no infinity term is included explicitly in the equations. A set of typical rate plots for the reaction of 1 with several

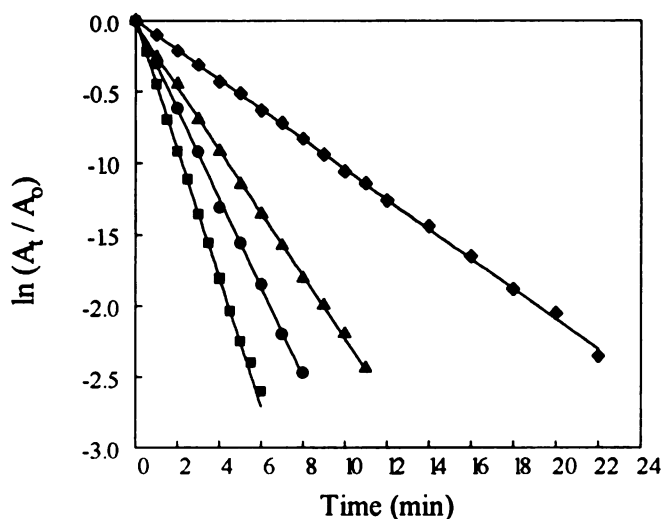


Figure 4.1. Rate plots for the reaction of 1 with 0.1 (\blacklozenge), 0.3 (\blacktriangle), 0.5 (\bullet), and 0.67 (\blacksquare) M Na_2SO_3 in D_2O at 80°C . Plots are linear over 3-4 half-lives; $r = 0.9998, 0.9995, 0.9997,$ and $0.9996,$ respectively.

concentrations of Na_2SO_3 alone (no added salt) is shown in Figure 4.1. Second-order rate plots are shown below with the appropriate nucleophile.

Reaction of 1 with Nucleophiles. A summary of the reactions of 1 with the 14 nucleophiles and salts that cover the HSAB range is given in Table 4.1. 1 shows an order in nucleophile only for nucleophiles of intermediate hardness (N_3^- , SCN^- , SO_3^- , Py) and not with hard or soft nucleophiles. Results for the intermediate nucleophiles will be discussed separately below.

Table 4.1. Reactions of Nucleophiles with 4-Methoxybenzylidimethylsulfonium, 80°C, D₂O

Nucleophile	HSAB	Lone Pair	100% Reaction	Order in Nu	Products	[RNu]/[ROH]*
OH ⁻	H	Yes	Yes	0	ROH	--
ND ₃	H	Yes	Yes	0	ROH, RND ₃	0.43
OCN ⁻	H	Yes	Yes	0	ROH, ROCN, RNCO	--
F ⁻	H	No	Yes	0	ROH	--
SO ₄ ⁻²	H	Yes	Yes	0	ROH	--
Cl ⁻	H	No	No	0	ROH	--
ClO ₄ ⁻	H	Yes	No	0	ROH	--
CN ⁻	S	Yes	Yes	0	ROH, RCN	1.3
I ⁻	S	No	No	0	ROH	--
Br ⁻	I	No	No	0	ROH	--
SCN ⁻	I	Yes	Yes	1	ROH, RSCN, RNCS	7.5
N ₃ ⁻	I	Yes	Yes	1	ROH, RN ₃	55.5
Pyr-d ₅	I	Yes	Yes	1	ROH, R-Py-d ₅ ⁺	1.0
SO ₃ ⁻²	I	Yes	Yes	1	RSO ₃ H, ROH	16

H = hard; S = soft; I = intermediate. R = 4-MeO-benzyl. *Averages of the slopes of plots of [RNu]/[ROH] vs. [Nu] for salt and no salt. ROCN and RNCO hydrolyze and give a complex mixture of products.

The kinetics and products are consistent with the known reactions of **1** and possible products. It would be expected, for instance, that any (4-methoxybenzyl) halide formed by displacement on **1** or by trapping of the carbenium ion would immediately hydrolyze to the alcohol. If displacement occurred, the disappearance of **1** should have a dependence on [halide]; none does. In fact, NaI and NaBr show the same pattern of incomplete hydrolysis documented for **1** with NaCl, NaClO₄, and no added salt (Chapter 3).²¹ In two cases, ND₃ and CN⁻, (4-methoxybenzyl) amine and (4-methoxybenzyl)nitrile are formed, but with no dependence of the rate on the [Nu] (see Figure 4.2 for the CN dependence). Isocyanates and cyanates formed in the reaction of **1** with NaOCN rapidly hydrolyze under the reaction conditions and products were not characterized.

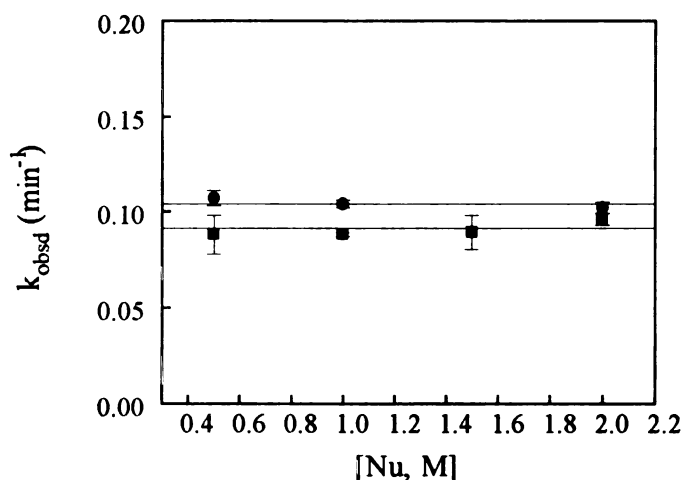


Figure 4.2. Second-order rate plots for the reaction of **1** with NaCN (●) and NaOD (■) at 80°C. Error bars are \pm S.E. The reactions are zero order in nucleophile and independent of the hardness (NaOD) or softness (NaCN) of the nucleophile.

Reactions of NaOD with **1** showed no dependence on [NaOD] with or without NaCl added to control ionic strength, and rate constants at various ionic strengths were in the same range within error (Figure 4.2). While this was at first

surprising, it is the result of an α deuterium secondary isotope effect. For ND_3 and NaOD , benzyl methylene and sulfonium hydrogens exchange rapidly for deuterons. From the water and ND_3 rate constants, it was found that $k_{\text{H}}/k_{\text{D}} = 1.26$ per deuterium for hydrolysis of **1** (1.56 for two deuteriums). Dividing the k_{w} for **1** at $\mu = 0$ and 1.7 by 1.56 gives expected rate constants of 0.096 and 0.079, respectively, which is within a narrow range and within the values, including error, of $0.085\text{-}0.090 \pm 0.003\text{-}0.010$ found for NaOD reaction at the same ionic strengths.

The results for Na_2SO_4 show the effect of anion charge and size on the first-order rate constants. Values of k_{obsd} decrease with increasing concentration of salt; at $[\text{Na}_2\text{SO}_4] = 1\text{M}$, $k_{\text{obsd}} = 0.085 \text{ min}^{-1}$ and at $[\text{Na}_2\text{SO}_4] = 2\text{M}$, $k_{\text{obsd}} = 0.048 \text{ min}^{-1}$, which are about half the values for the corresponding concentrations of NaCl or NaClO_4 , and are consistent with the values obtained as the intercept of plots of k_{obsd} vs. $[\text{Na}_2\text{SO}_3]$ obtained with Na_2SO_4 used to control ionic strength shown in Figure 4.4. This is not surprising because an anion with a higher charge and larger volume will order water differently than a singly charged anion and thus change the activity, which in turn will affect the rate.

Reaction of 1 with Pyridine- d_5 at Constant Ionic Strength and with No Added Salt. For both sets of conditions, plots of $\ln(C_t/C_0)$ vs. time were linear over 2-4 half-lives, and all had $r > 0.996$ (although the great majority had $r > 0.999$); standard errors were 1-9%. Plots of k_{obsd} vs. $[\text{pyridine-}d_5]$ (Figure 4.3), based on the means of 3 or more separate determinations, are linear. With $\mu = 2$ (NaCl), $k_2 = 0.038 \text{ M}^{-1}\text{min}$ and $k_1 = 0.104 \text{ min}^{-1}$ ($r = 0.996$), and with $\mu = 0$, $k_2 = 0.040 \text{ M}^{-1} \text{ min}^{-1}$ and $k_1 = 0.148 \text{ min}^{-1}$ ($r = 0.998$). The values of k_1 are within experimental error of the values obtained with azide as the nucleophile or the values measured in water only (Chapter 3).²¹ The fact that the two lines are essentially parallel shows that there is little or no salt effect on the bimolecular

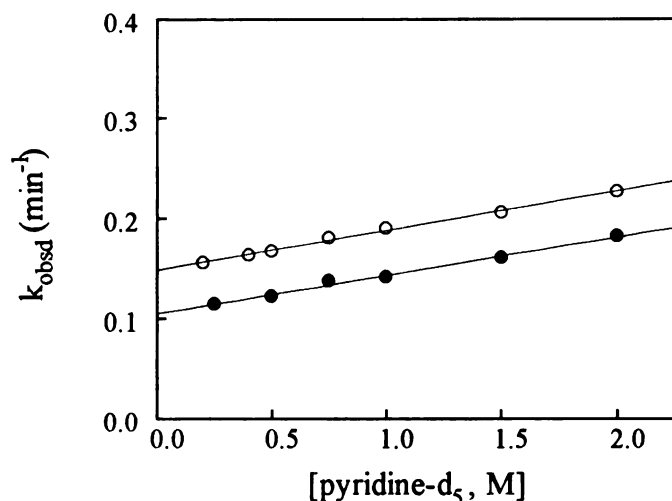


Figure 4.3. Second-order rate plot for the reaction of 1 with pyridine- d_5 with (●) and without (○) NaCl added to control ionic strength. The two lines are parallel.

reactions, and the fact that the no salt line has no curvature suggests that there is no preassociation of the neutral nucleophile with the charged substrate. Thus in this instance preassociation seems to be a nonspecific ionic effect and not an intrinsic property of the substrate.

Reaction of 1 with NaN_3 at Constant Ionic Strength. Values of k_{obsd} were obtained from plots of $\ln(C_t/C_0)$ vs. time that are linear over 2-4 half-lives, and all had $r > 0.996$; standard errors were 1-8%. Plots of k_{obsd} vs. $[\text{NaN}_3]$ for constant ionic strength $\mu = 1.7$ with NaCl or NaClO_4 are shown in Figure 4.4; plots are linear with $r = 0.996$ or greater. Values for the slopes (second-order rate constant k_2 and intercepts (first-order rate constant k_1) are listed in Table 4.2.

Reaction of 1 with NaN_3 with No Added Salt. Plots of $\ln(C_t/C_0)$ vs. time were linear over 2-4 half-lives, and all had $r > 0.996$; standard errors were 1-8%. A plot of k_{obsd} vs. $[\text{NaN}_3]$ at 80°C for 0-1M azide is shown in Figure 4.5. There is a distinct break in the plot at ca. 0.50M azide. The standard errors for 3-10 separate determinations made with at least two separate batches of solvent at 0.42, 0.55,

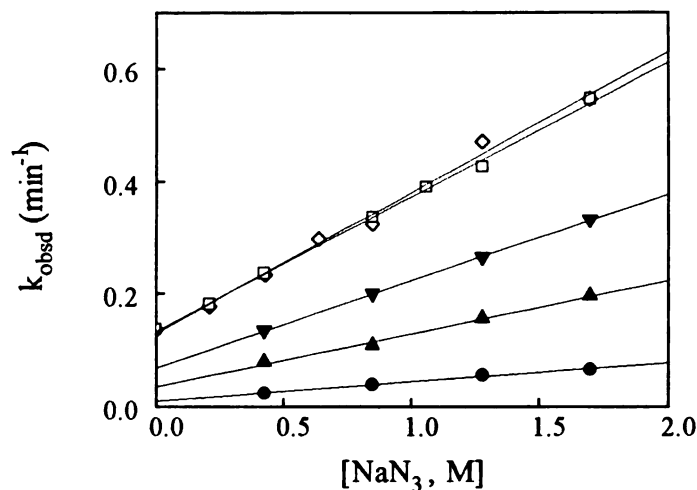


Figure 4.4. Second-order rate plots for the reaction of 1 with NaN_3 at 60°C (\bullet , $r = 0.997$), 70°C (\blacktriangle , $r = 0.997$), 75°C (\blacktriangledown , $r = 0.9999$), and 80°C with NaCl (\circ , $r = 0.999$) or NaClO_4 (\diamond , $r = 0.996$) used to hold the ionic strength constant at $\mu = 1.7$. NaCl was used as the added salt at 60 - 75°C .

Table 4.2. First- and Second-Order Rate Constants for the Reaction of 1 with NaN_3 in D_2O

T ($^\circ\text{C}$)	k_1 (min^{-1})	k_2 ($\text{M}^{-1}\text{min}^{-1}$)	r
$\mu = 0.85$			
80	0.138	0.354	0.999
$\mu = 1.7$			
60	0.010	0.034	0.997
70	0.035	0.094	0.996
75	0.069	0.154	0.9999
80	0.110	0.239	0.999
$\mu = 5$			
80	0.103	0.209	0.999

and 0.64M azide are 1%, 2%, and 1%, respectively; the break is not the result of experimental error in the determinations. Above 0.64M NaN_3 , the points describe a smooth curve that appears to be approaching a limiting value for k_{obsd} . Because

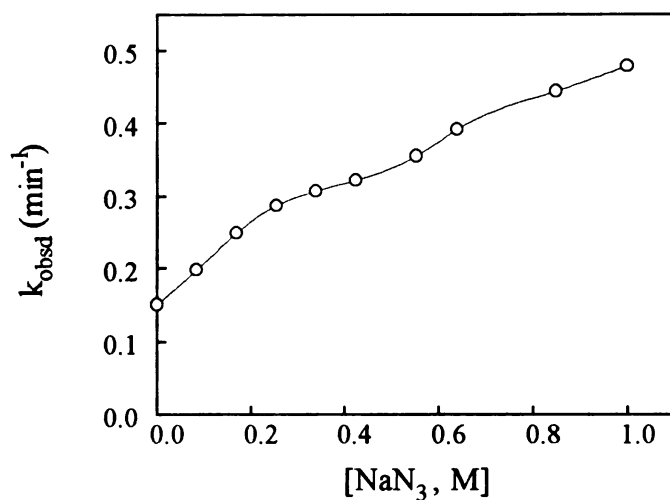


Figure 4.5. Plot of k_{obsd} vs. $[\text{NaN}_3]$ with no salt used to hold the ionic strength constant at 80°C. The full upper portion of the curve (from 0.65 M to 5M) is shown in Figure 4.6.

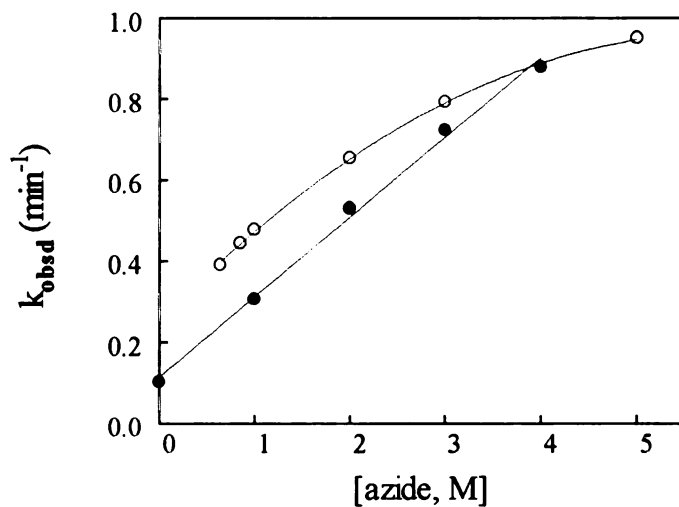
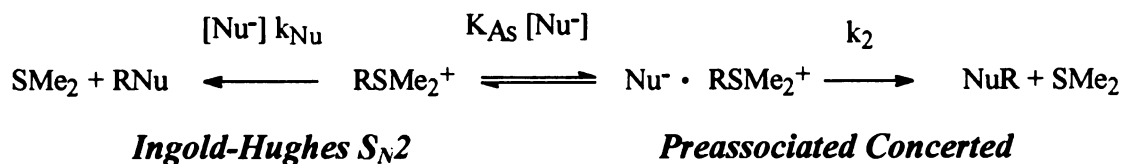


Figure 4.6. Plot of k_{obsd} vs. $[\text{NaN}_3]$ with no salt used to hold the ionic strength constant at 80°C (O). For reference, the values for $\mu = 5$ with NaCl are included (●); the plot is linear ($r = 0.999$) with $k_2 = 0.209 \text{ M}^{-1} \text{ min}^{-1}$.

5.0M NaN_3 is approaching saturation in D_2O and because determination of k_{obsd} was near the technically feasible limit, we could not evaluate k_{obsd} at higher azide concentrations.

The smooth curve above 0.65M NaN₃ is reminiscent of the shape of the curve for a *stepwise preassociated* mechanism



The data from Figure 4.6 were analyzed with a double reciprocal plot of $1/k_{\text{obsd}}$ vs. $1/[\text{NaN}_3]$ that gives the association constant K_{As} as the X-intercept at $1/k_{\text{obsd}} = 0$, with the second-order rate constant k_2 as the 1/Y-intercept. The plot of these values (Figure 4.7) is linear ($r = 0.9965$) and give $k_2 = 1.18 \text{ M}^{-1} \text{ min}^{-1}$ and $K_{\text{As}} =$

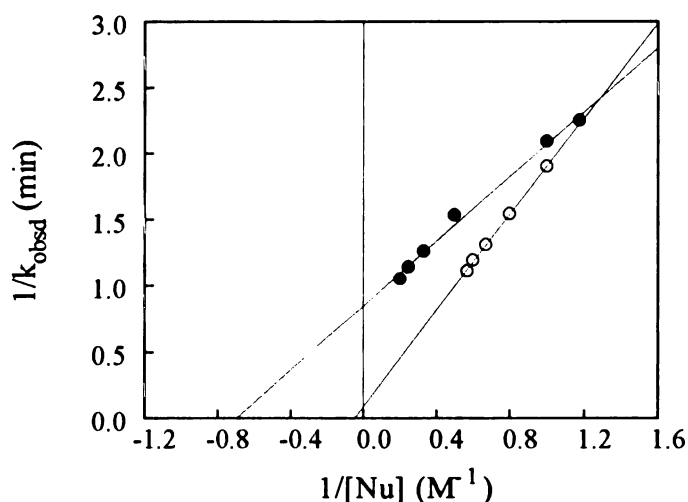


Figure 4.7. Plot of $1/k_{\text{obsd}}$ vs. $1/[\text{NaN}_3]$ (●) and $1/[\text{Na}_2\text{SO}_3]$ (○) for reaction with no salt used to hold the ionic strength constant at 80°C. Data for azide from Figure 4.6, and for sulfite from Figure 4.10.

0.70 M^{-1} . The equation for k_{obsd} for the preassociation concerted mechanism is

$$k_{\text{obsd}} = k_2 K_{\text{As}} [\text{NaN}_3] / (1 + K_{\text{As}} [\text{NaN}_3]) \quad \text{Eq. 4.1}$$

When the experimental points in Figure 4.6 were fit to this equation using the Marquardt-Levenberg nonlinear least-squares algorithm in the Origin software,

with the parameters allowed to float, values of $k_2 = 1.21 \pm 0.04$ and $K_{As} = 0.66 \pm 0.06$ ($\chi^2 = 5.8 \times 10^{-4}$) were obtained, which are in excellent agreement with the values obtained from the double reciprocal plot.

Reaction of 1 with Na_2SO_3 at Constant Ionic Strength. Plots of $\ln(C_t/C_0)$ vs. time were all linear over 3-4 halflives under all conditions studied (Na_2SO_3 alone or with NaCl or Na_2SO_4 as the added salt) with $r > 0.999$ (see Figure 4.1). Values of k_{obsd} had errors of 1-5% SE.

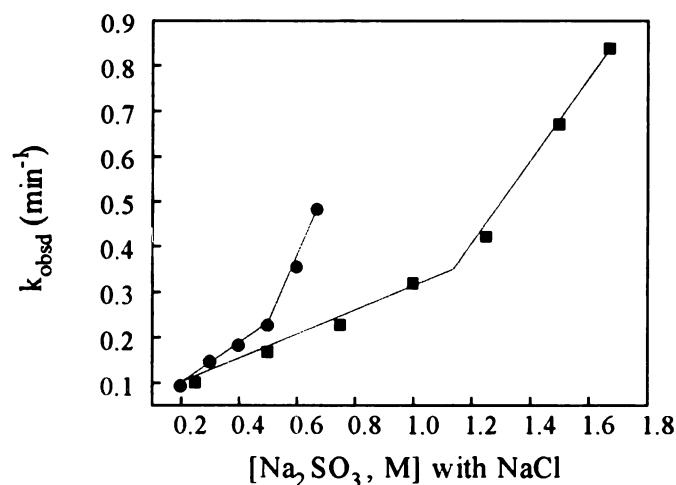


Figure 4.8. Plot of k_{obsd} vs. $[\text{Na}_2\text{SO}_3]$ with NaCl used to hold the ionic strength constant at $\mu = 2$ (●) and $\mu = 5$ (■) at 80°C .

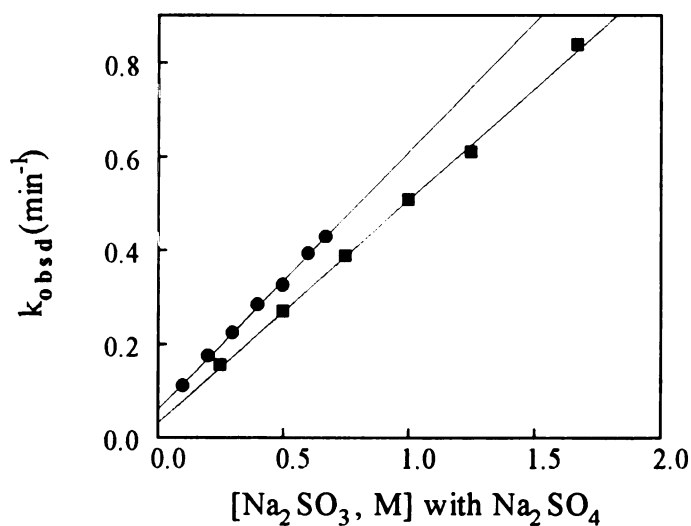


Figure 4.9. Plot of k_{obsd} vs. $[\text{Na}_2\text{SO}_3]$ with Na_2SO_4 used to hold the ionic strength constant at $\mu = 2$ (●) and $\mu = 5$ (■) at 80°C .

The shape of plots of k_{obsd} vs. $[\text{Na}_2\text{SO}_3]$ depended dramatically on the salt used to control ionic strength (Figures 4.8 and 4.9). As expected, the rate constants are lower for the higher ionic strength. For NaCl at $\mu = 2$ and 5, the plots appear to consist of two intersecting straight lines (Figure 4.8). For Na_2SO_4 as the added salt, however, the plots are linear $\mu = 2$ and 5 (Figure 4.9; $r = 0.9991$ and 0.9993 , respectively). The upper portions of the NaCl curves have steep slopes that appear to have the same difference in slope as the two lines for Na_2SO_4 . Values of the various rate constants are summarized in Table 4.3

Table 4.3. First- and Second-Order Rate Constants for the Reaction of Na_2SO_3 with 1 Under Constant Ionic Strength with NaCl and Na_2SO_4

Conditions	k_1 (min^{-1})	k_2 ($\text{M}^{-1}\text{min}^{-1}$)	r
$\mu = 2$, NaCl			
0-0.5 M Na_2SO_3	--	0.438	0.9970
0.5-0.75 M Na_2SO_3	--	1.49	0.9940
$\mu = 5$, NaCl			
0-1.0 M Na_2SO_3	--	0.286	0.9960
1.25-1.67 M Na_2SO_3	--	0.993	1.000
$\mu = 2$, Na_2SO_4	0.059	0.550	0.9990
$\mu = 5$, Na_2SO_4	0.030	0.496	0.9993

Reaction of 1 with Na_2SO_4 with no Control of Ionic Strength. The plot of k_{obsd} vs. $[\text{Na}_2\text{SO}_3]$ shown in Figure 4.10 has the same break found for the reaction of NaN_3 with 1 with no control of ionic strength (Figure 4.5). Unlike the azide results, the upper portion of the curve is linear. A double reciprocal plot of the data for the upper portion, however, yields an excellent straight line (Figure 4.7; $r = 0.9999$) from which values of $k_2 = 7.87 \text{ M}^{-1}\text{min}^{-1}$ and $K_{\text{As}} = 0.070 \text{ M}^{-1}$ can be obtained as described above. When the data of the linear portion were fit to the equation for the preassociated concerted mechanism as described above, values

UCSF LIBRARY

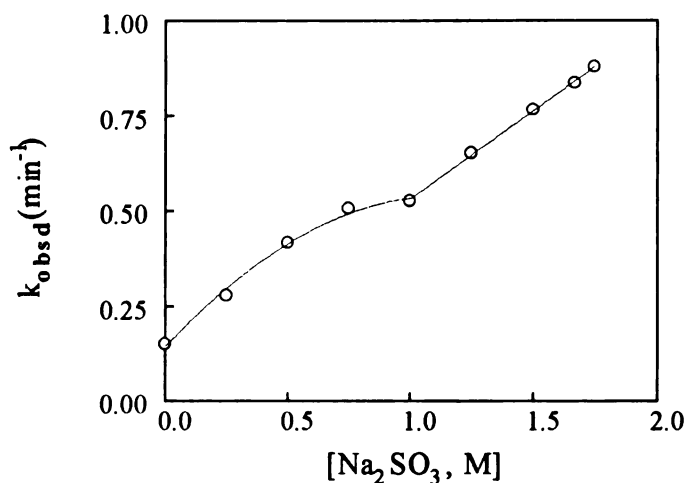


Figure 4.10. Plot of k_{obsd} vs. $[\text{Na}_2\text{SO}_3]$ with no salt used to hold the ionic strength constant at 80°C .

of $k_2 = 7.34 \pm 0.90 \text{ M}^{-1}\text{min}^{-1}$ and $K_{\text{As}} = 0.078 \pm 0.01 \text{ M}^{-1}$ ($\chi^2 = 1.24 \times 10^{-5}$) are obtained by successive fitting, in excellent agreement with the values obtained from the double reciprocal plot. The much later break for Na_2SO_3 (1 M) compared with NaN_3 (0.65M) is consistent both with the lower value of K_{As} and the fact that the ionic strength is changing as the square of the concentration.

*Reaction of 1 with NaSCN.*²⁷ Rate plots for thiocyanate with or without added salt were approximately linear for the first halflife, after which the reaction

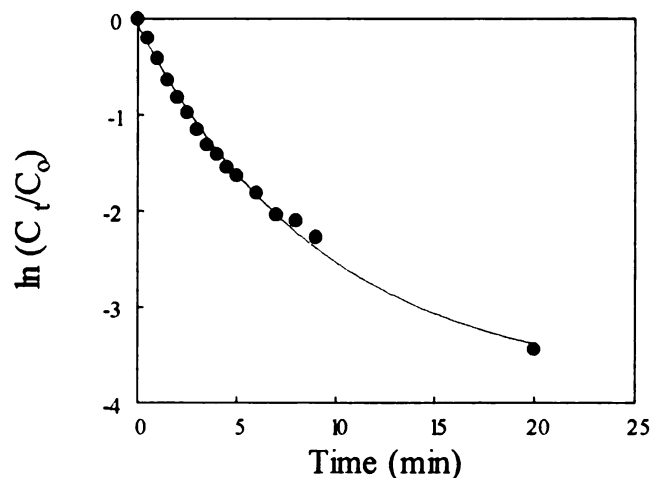


Figure 4.11. Plot of $\ln(C_t/C_0)$ vs. time for the reaction of 1 with 2M NaSCN in D_2O at 80°C .

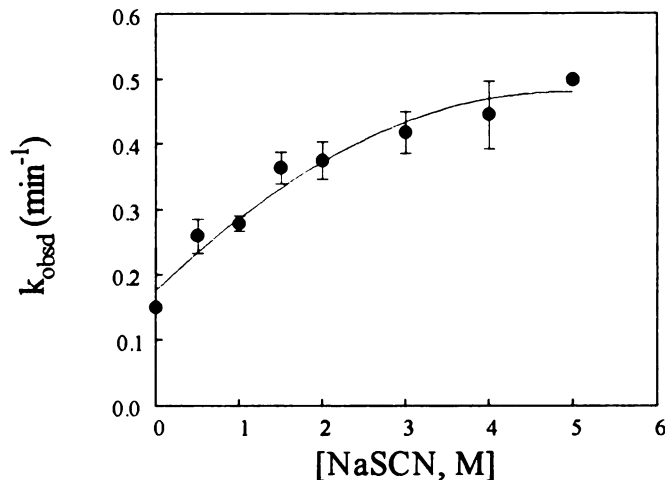


Figure 4.12. Plot of k_{obsd} vs. $[\text{NaSCN}]$ for **1** in D_2O at 80°C with no exogenous salt added to control ionic strength. Values of k_{obsd} are based on first-half-life rate constants and are the averages of 3-5 determinations; bars are S.E.

slowed significantly and the lines curved (Figure 4.11). Use of either an infinity point or the Guggenheim method to analyze the data reduced but did not eliminate the curvature. In addition to the $\text{S}_{\text{N}}1$ component, the reactions of the other nucleophiles with **1** depends on the concentration of nucleophile. Based on first-half-life rates, the reaction of **1** depends on $[\text{NaSCN}]$, although in a plot of k_{obsd} vs. $[\text{NaSCN}]$ data are badly scattered compared with the same plots for the other nucleophiles (Figure 4.12).

One source of the curvature in the rate plots was immediately apparent. The signal for the benzyl methylenes decreased at a faster rate than the corresponding signal for the aromatic protons; exchange of the benzyl protons for deuterons in **1** would lower k_{obsd} because of the secondary α -deuterium isotope effects on the $\text{S}_{\text{N}}1$ reaction.²⁸ (Attempts to measure the rates in H_2O using solvent saturation techniques were unsuccessful.) This alone cannot account for the extent of curvature in Figure 4.11, however. For most reactions of **1** in the presence of most nucleophiles, the signal for $-\text{SMe}_2^+$ disappeared completely (see Table 4.1), but

with thiocyanate a residual signal always remained (ca. 90-95% reaction depending on conditions) even after 1 hr at 80°C. This result was baffling.

Also baffling was the following finding. The signals for the benzyl protons of the products RSCN and RNCS could be seen during the course of the reaction, with $[\text{RSCN}] > [\text{RNCS}]$ at 5-10 min (or 2-4 halfives depending on the $[\text{NaSCN}]$). The amount of ROH produced by solvent trapping of R^+ remained constant. When the selectivities were determined from CDCl_3 extracts of reactions run in various concentrations of NaSCN (in H_2O to avoid exchange) for > 10 halfives, however, $[\text{RNCS}] \gg [\text{RSCN}]$.

These issues were resolved by measuring the kinetics of the conversion of RSCN to RNCS by taking chloroform extracts of the aqueous reaction mixtures; for these studies, H_2O was used to avoid exchange of the benzyl methylene protons. Changes in the intensities of the benzyl methylene peaks²⁶ for the two thiocyanate-derived products were measured in 5-min intervals until equilibrium had been reached. There was a smooth conversion of RSCN to RNCS that leveled off at 13:87. *Pseudo*-first order rate constants calculated from these data, with the inclusion of the equilibrium infinity value in the calculations, showed that under either set of conditions, doubling the $[\text{NaSCN}]$ led to a doubling of the rate of conversion (Table 4.4). Plots of k_{obsd} vs. $[\text{NaSCN}]$ (not shown) pass through the origin, which rules out a unimolecular process and therefore rules out isomerization by ionization. The 2.4-fold difference between the second-order rate constants for $\mu = 5$ and the no salt conditions is consistent with a small effect of ionic strength on second-order reactions of a neutral substrate with an anionic nucleophile.²⁹

Thiocyanates undergo a thermal rearrangement to isothiocyanates.³⁰ While allyl substrates rearrange by several pathways,³¹ including internal cyclization

Table 4.4. Pseudo-first order and second-order rate constants for the conversion of RSCN to RNCS at 80°C in H₂O in the presence of NaSCN

[NaSCN, M]	k_{obsd} (min ⁻¹)	
	No Salt	$\mu = 5$
0.5	0.041	0.020
1.0	0.096	0.040
k_2 (M ⁻¹ min ⁻¹)	0.096	0.040

and dissociation to an ion pair, rearrangements of benzyl substrates are limited to "sluggish" dissociative³² or kinetically bimolecular³³ pathways; an equilibrium mixture is established in the dissociative pathway.

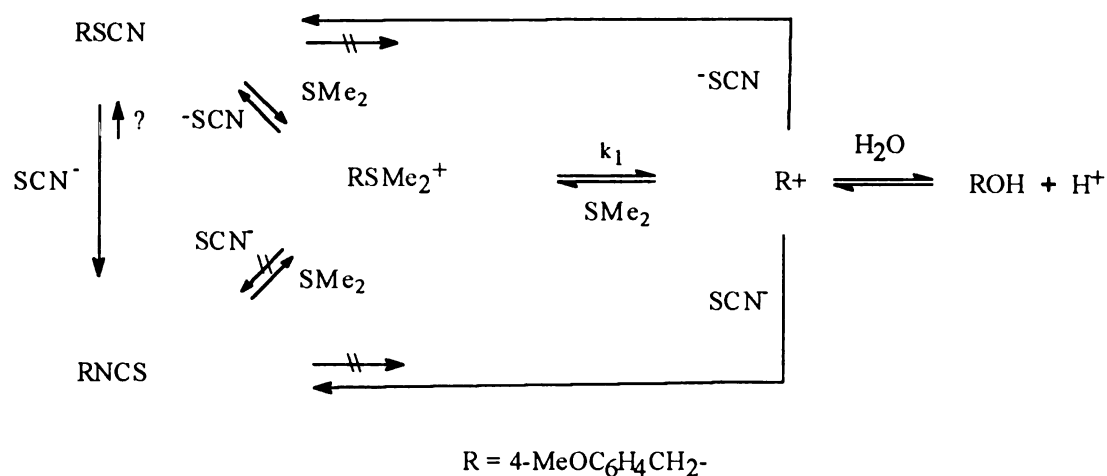
Fava, *et al.*,³³ showed that conversion of benzylthiocyanate to benzylisothiocyanate in the presence of NaSCN in methyl ethyl ketone at 110°C was first order in nucleophile, and that thermal isomerization through the ionization pathway was not important. Spurlock's finding that this conversion in the absence of nucleophile is slow at >100°C is also consistent with our data.³² In contrast, Songstad and coworkers³⁴ have reported that 4-NO₂, -H, and -Me benzyl substrates, which should undergo a second-order reaction much better than the 4-MeO substrate, yielded only the respective thiocyanates in acetonitrile at 25°C. In this instance, it seems probable that the temperature used was too low to allow the bimolecular reaction with SCN⁻ to occur at a measurable rate.

Fava's results³³ do not explain why an apparent equilibrium for all compounds except ROH is reached in our case. (Fava, *et al.*, did not report the extent of reaction for their system.) We found that the hydrolysis of **1** is stopped dead in the water by an equilibrium between starting material and products

UCSF LIBRARY

(Chapter 3).²¹ The sulfur of the ambident ^{-}SCN is 1000-fold more reactive towards benzyl halides than the nitrogen,³⁵ and, because it is the softer of the two nucleophilic sites, would be expected to react preferentially with **1** as well. Because k_{obsd} for bimolecular reactions of **1** and RSCN with NaSCN are of the same magnitude, we suspect that the majority of RNCS must be formed either from RSCN or by trapping of the carbenium ion generated from the unimolecular reaction. In support of this position, the reaction of **1** with sodium cyanate is zero order in nucleophile; thus neither the hard oxygen nor the softer nitrogen can undergo a second-order reaction with **1**. The products with cyanate include ROCN , RNCO , and the respective hydrolysis products. No attempt was made to quantitate the components of this complex mixture.

The predominance of RNCS shows that both the hardness of the nucleophile, the charge on the substrate, and the hardness or softness of the leaving group must be considered. In this regard, we suggest that displacement of ^{-}SCN by SMe_2 occurs under the reaction conditions and leads to an equilibrium mixture of the starting material (5-10% of the total) and the two thiocyanate-derived products (Scheme 4.1). Unfortunately, because of the insolubility of SMe_2



Scheme 4.1

in water, it is not possible to measure directly or accurately either the rate constants for or the extent of substitution. Fava, *et al.*,³³ showed that the exchange of ³⁵SCN for ³²SCN in benzylthiocyanate is much faster than isomerization. The similarity of the Swain-Scott n_{MeI} and n_{Pt} values for SCN and SMe₂ suggests that the exchange of SMe₂ for ⁻SCN can occur, a process that is consistent with soft-soft symbiosis.³⁶ The 95:5 ratio of total thiocyanate-derived product to sulfonium is also consistent with the relative concentrations of the two nucleophiles in the reaction mixtures. Nonetheless, even though the mechanism by which **1** is apparently regenerated in the reaction mixture is a reasonable one, it must remain a conjecture.

Thus the lack of clean *pseudo*-first order kinetics is the result of a combination of complex kinetically and thermodynamically controlled processes. If we had measured the selectivities strictly by the book at long reaction times, we would have been misled concerning the relative nucleophilicities of the sulfur and nitrogen ends of the ambident SCN⁻.

Hydrolysis and Selectivities of 4-Methoxybenzyl-4'-sulfobenzoate (4). In order to calculate the ratio [RN₃]/[ROH] for **1** at constant ionic strength, it was necessary to have the value of $k_{\text{N}}/k_{\text{w}}$ for the 4-methoxybenzyl carbenium ion. We measured k_{obsd} for the benzoate **4** in pure D₂O, brine, and 0.05-1.7M D₂O-NaN₃ solutions in the range 80°-95°C by following the loss of the sulfonate ester AA'BB' pattern in ¹H NMR spectra. Rate constants are zero order in azide at $\mu = 1.7$ with NaCl or NaClO₄, and are ca. 2-fold higher than in D₂O only (Figure 4.13). This pattern is consistent with the ionization of **4** to the solvent-equilibrated carbenium ion with subsequent partitioning between azide and water, such that no RN₃ will arise from a direct displacement on substrate and skew the results for the selectivities.

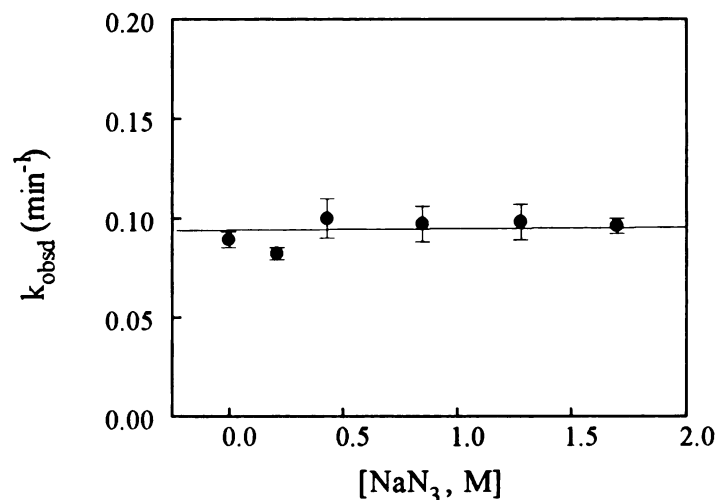


Figure 4.13. Plot of k_{obsd} vs. $[\text{NaN}_3]$ for **4** at 80°C , $\mu = 1.7$ (NaCl). Within error (\pm S.E.), there is no azide dependence.

Selectivities were measured with both NaCl and NaClO₄ as the added salt. Up to 0.5M azide, plots of $[\text{RN}_3]/[\text{ROH}]$ vs. [azide] for both salts are linear (not shown; $r = 0.990$); under both sets of conditions the slope, $k_{\text{N}}/k_{\text{w}}$, is 17.6. The selectivities for Na₂SO₃ were determined in the same way; $k_{\text{N}}/k_{\text{w}}$ is 0.62.

Selectivities for 1 Under Constant Ionic Strength and with No Added Salt.

For constant ionic strength, the plot of $[\text{RN}_3]/[\text{ROH}]$ vs. $[\text{NaN}_3]$ (up to 0.5M NaN₃, which is near the limit of NMR detection) is curved up (Figure 4.18 above, closed circles). These points fit Equation 4.2 derived using the steady-state approximation for the appearance of products through a mixed S_N1/S_N2 mechanism. The ratio $k_{\text{N}}/k_{\text{w}}$ was obtained for partitioning of the pure carbenium ion, and k_2 and k_1 are the appropriate rate constants (Table 4.2). Note that the values for partitioning of the pure carbenium ion, generated solvolytically from the chloride, between azide and water reported by Aymes and Richard² give an excellent fit to our equation (not shown). The equation they use to fit their data is different than Equation 4.2 and was derived based on different assumptions.

For azide only, the plot of $[RN_3]/[ROH]$ is curved; the slope of a line through the first several points (0-0.2M) is linear ($r = 0.999$) with a slope of 46 (Figure 4.18 above, open circles). No alcohol product could be detected at or above 0.75M NaN_3 . The slope reported by Sneen¹⁵ for reaction at 60° is 48. These data are not fit by Equation 4.2 with either the second order rate constants under constant ionic strength or with the rate and association constants for the stepwise preassociated bimolecular reactions; invariably the calculated values are too low to fit the data and lie near the line for constant ionic strength. If rate constants for the S_N2 and preassociated-concerted mechanism are used, however, the data give a good fit to Equation 4.3 (Figure 4.19 above) derived as above assuming a unimolecular and two different bimolecular mechanisms.

Solvolysis of Trimethylsulfonium Iodide. Under conditions used for 1, there was no detectable solvolysis after 24 hr., but almost complete exchange of the methyl protons was observed. Rate constants reported by Swain and colleagues^{13d} for this substrate at 158°C are ca. 3×10^3 lower than rate constants we obtain for 1 at 80°C. Thus, unlike the benzyl and methyl pyridinium substrates that react with azide and water at essentially the same rates (Chapter 2), the methyl dimethyl-sulfonium is very resistant to reaction, despite the fact that the pK_a of the sulfonium is ca. 10 pK units more favorable than the pyridiniums.

Activation Values. The Eyring activation values were determined from four-point plots in the range 60°-90°C ($r > 0.998$ for all plots) and are listed in Table 4.5 for solvolysis and azide substitution reaction of 1 under constant ionic strength and for the bimolecular reaction of 4-methoxybenzyl-3'-cyanopyridinium with azide (Chapter 2).

Table 4.5. Eyring Activation Values for (4-Methoxybenzyl)dimethylsulfonium Chloride and 3'-Cyanopyridinium Chloride Derivatives at Constant Ionic Strength $\mu = 1.7$ (NaCl)

Rate constants	ΔH^\ddagger (kcal/mol)	ΔS^\ddagger (gibbs/mol)	ΔG^\ddagger_{80} (kcal/mol)
Dimethylsulfonium			
k_1	27.7 ± 1.0	7.1 ± 1.0	25.2
k_2	22.2 ± 1.8	-6.7 ± 0.8	24.6
3'-Cyanopyridinium (k_2)	17.6 ± 0.8	-21.6 ± 2.0	25.3

Values determined from 4-point Eyring plots; all lines $r > 0.998$.

Discussion

Both the hydrolysis (Chapter 3)²¹ and nucleophilic substitution reactions of the simple substrate **1** are much more complex than we had anticipated. Several possible mechanisms, including the ion-dipole complex, simple mixed, and mixed preassociated-concerted mechanisms, are discussed below. We believe that the unimolecular component is a constant factor but that the bimolecular component changes depending on the presence of added salt.

HSAB Dependence. It is clear from the data in Table 4.1 that the reactions of **1** depend on the HSAB rank of the nucleophile.³⁶ This seems at first to be an odd result, because Swain and his students had shown that 4-Me, 4-H, and 3-Cl benzyl dimethylsulfoniums react with N_3^- and the hard nucleophiles HO^- , and PhO^-

UCSF LIBRARY

in water,^{13a,b,d} and Sneen had shown that 4-H substrate reacts with the soft nucleophile Γ in water.¹⁵ The rate constants for the oxygen nucleophiles are lower than the azide rate constant. Using Swain's values for the relative rates for N_3^- and HO^- , a plot of $\log k_{rel}$ vs σ for 4-Me, 4-H, and 3-Cl benzyl dimethylsulfoniums is linear (not shown; $r = 0.996$). Extrapolation shows that **1** should react 16-fold faster with N_3^- than with HO^- ; at 80°C, the estimated second-order rate constant for the reaction of **1** with HO^- is $0.028 \text{ M}^{-1}\text{min}^{-1}$. For a mixed mechanism, the estimated k_{obsd} for reaction of the dideutero form of **1** with 2.0M HO^- is 0.147 min^{-1} , almost double the experimentally observed rate constant. Note that these differences are not the result of a large solvent isotope effect, because Schowen^{4b} found a solvent k_H/k_D of 1.08 for the reactions of benzyldimethylsulfoniums with hydroxide, essentially the same value we found for the solvolysis reaction of **1**. Therefore, for hydroxide, at least, normal rate effects cannot account for the dependence.

One consequence of the Klopman-Salem theory³⁷ for frontier-orbital control of substitution reactions is that reactivity should be related in some way to the difference between the energy of LUMO of the electrophile and the HOMO of the nucleophile. This expectation is met by the reactions of **1** with the intermediate nucleophiles. The LUMO energy of **1** and the HOMO energies of SO_3^- , N_3^- , SCN^- , and pyridine were calculated with the PM3 Hamiltonian. A plot of $\log k_2$ vs. $\Delta E = E_{LUMO}$ for **1** - E_{HOMO} for the nucleophiles (in eV) is shown in Figure 4.14. The correlation shows that for the intermediate nucleophiles this energy difference is directly related to the rate. While this correlation is good for the nucleophiles that react, this relation alone cannot be the source of the differential reactivity because ΔE for ND_3 (4.5), HO^- (-4.5), and CN^- (-1.23), which do not react, are within the same range. Thus factors other than the difference in energy between electrophile and nucleophile are probably at work. To understand this apparent dependence on

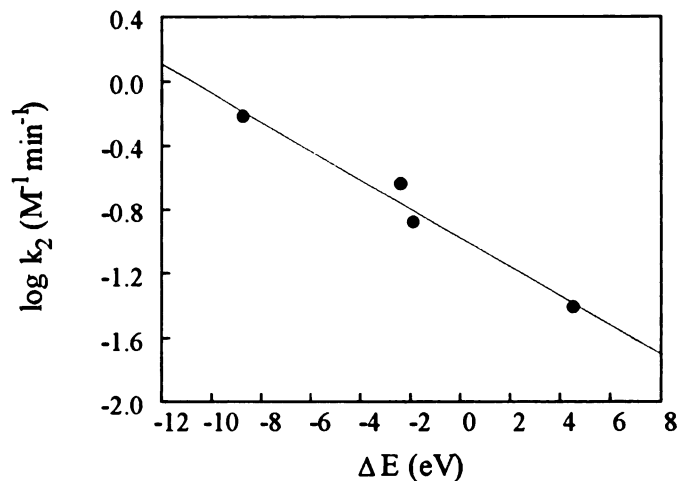


Figure 4.14. Plot of $\log k_2$ vs. the LUMO-HOMO difference ΔE for the reaction of **1** with (left to right) SO_3^- , N_3^- , SCN^- , and pyridine- d_5 at 80°C , $\mu = 1.7$ (NaCl).

the HSAB rank, the potential energy surfaces for the gas-phase reactions would have to be obtained computationally. These studies are in progress.

One difference between hard and intermediate nucleophiles for this system is readily understood. In Chapter 3 we showed that the Hammett plot for the hydrolysis reaction of a series of benzyldimethylsulfoniums had a severe break between the 4-MeO and the 4-Me compounds that was the result of a change in mechanism from $\text{S}_{\text{N}}1$ for the former to $\text{S}_{\text{N}}2$ for the latter. The Hammett plot for the azide reaction, based on our data for **1** and the 4-Me, 4-H, and 3-Cl compounds reported by Swain, Rees, and Taylor^{13c} also has a break (Figure 4.15), but this change is not the result of a change in mechanism. Swain and Thornton^{13a} found that the second order rate constants for the hydroxide reaction of these three substrates gave a curved Hammett plot, with a break between 4-H and 3-Cl. Clearly these changes reflect a change in the structure of the activated complex, but the nature of that change is not readily apparent, despite many historical⁵ and more recent^{6,8} attempts to explain it.

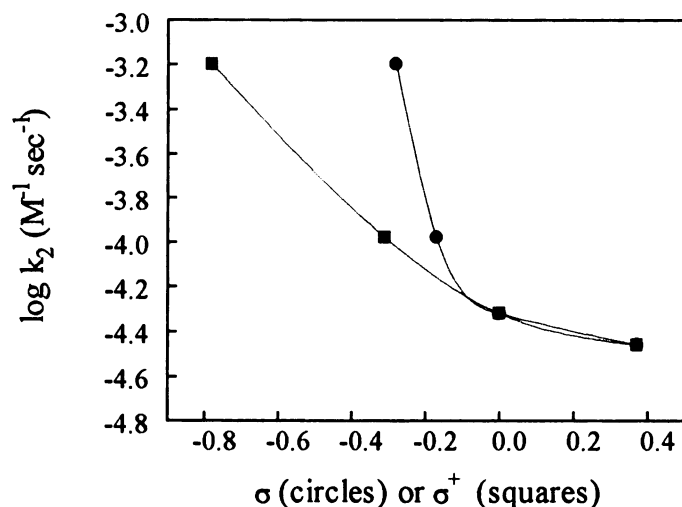


Figure 4.15. Hammett plot for **1** and 4-Me, 4-H, and 3-Cl benzyldimethylsulfoniums in water at 60°C. The point for **1** was corrected to $\sigma = 0.5$, the conditions used by Swain, using the Winstein b value of -0.1 found for **1**.

With the gas-phase and computational results for heterolytic dissociation of a series of 4-substituted benzyldimethylsulfoniums available (Chapter 6), however, it is possible to offer a reasonable speculation about the source of these Hammett effects. Both the LSIMS relative rates and MNDO energy profiles for **1** and 4-Me, 4-H, 4-Cl, and 4-NO₂ benzyldimethylsulfoniums give exquisitely linear Hammett plots against either σ^+ or $\delta\Delta G^\circ$ for the gas-phase equilibrium of a series of 4-X-2-aryl propenes and the corresponding *tert*-cumyl carbenium ions. Thus the intrinsic experimental and computational ΔH^\ddagger show no variation in the structure of the activated complex other than an increase in the methylene-S bond as the electron donating capacity of the substituent decreases. In the hydrolysis reaction, the break is the result of a change in mechanism, which is probably the effect of a more favorable ΔG^\ddagger for the S_N1 process (Chapters 3), but this is apparently not the case for the azide reaction.

The difference between the gas-phase and solution results is of course solvation, but solvation of what? While it is entirely true that solvation of the activated complex or an intermediate carbenium ion is stabilizing, it is not often

remembered that reactions in the gas-phase are much faster than in solution because of the *retarding* effects of solvent (electrostriction), which has many sources. In particular, in the gas-phase there is no retarding effect of the entropy of solvation of the leaving group; only a favorable change in translational entropy is important. We have shown that solvation of the leaving group may account for the difference in hydrolysis mechanisms for **1** and the corresponding 3-cyano-pyridinium (Chapter 2), but for the sulfoniums entropic effects of solvation of SMe_2 should be the same. While it is true that the full positive charge on the sulfur will change with the length of the methylene-S bond that is in turn mediated by the amount of stabilization afforded by the substituent, it is not clear that this difference will be sufficiently large to cause much difference in the solvation about the reaction center, especially given the hydrophobic nature of the leaving group.

Substituents that show the breaks in Hammett correlations invariably are those that can conjugate with the reaction center and in doing so assume a partial positive charge ($MeO^+=C<$, $MeS^+=C<$, $HO^+=C<$, $Me_2N^+=C<$). In addition, resonance affects the charge on 2,4, and 6 positions of the ring. Solvation of the partially charged substituent would stabilize the activated complex, lower the activation barrier, cause the reaction to be "earlier," and the rate to be faster--a clear Hammond effect. Indeed, Westaway and Ali³⁸ and Lee, *et al.*,³⁹ have shown that changing to a better nucleophile for charged benzyl substrates makes the reaction occur earlier in terms of the nucleophile-methylene bond, but has little effect on the methylene-leaving group bond.

Mechanisms. It is clear from the plots of k_{obsd} vs. $[Nu]$ for the reactions of **1** with the intermediate nucleophiles that there is a stark difference between the nucleophile only and nucleophile with control of ionic strength for the anionic nucleophiles. (The rate constants for SCN^- are sufficiently inaccurate that they will

not be used; the general pattern found for NaN_3 and Na_2SO_3 , however, appears to apply to the NaSCN results.) These differences may be the result either of salt effects or of different mechanisms. These possibilities will be discussed in turn.

Salt Effects Under Control of Ionic Strength. The results for the reaction of azide with **1** with either NaCl or NaClO_4 used to control ionic strength (Figure 4.8) show that the added salt does not affect the bimolecular or unimolecular reaction (see Chapter 3 for the unimolecular reaction). The situation is clearly different for the sulfite reaction, where there is a major difference between the plots obtained for reaction with NaCl and Na_2SO_4 used to control ionic strength. The breaks in the NaCl plots show a drastic change in rate constant, while the Na_2SO_4 plot is linear over a large range (out to $\mu = 5$; Figure 4.9). It is known that the charge and volume of a salt anion can change the activity of a second solute anion,⁴⁰ and that the effects are more severe for larger ions. This appears to be the effect seen in Figure 4.8: the activity of sulfite, which will affect the rate constants for the second order reaction, is lowered by the presence of NaCl and increases as NaCl is diluted out. In the presence of Na_2SO_4 , however, which has the same charge and essentially the same ionic volume as the nucleophile, the activity of sulfite is constant over the entire range of nucleophile concentration, and the rate constants increase linearly with an increase in sulfite. Thus these effects are readily understood.

Salt Effects With No Control of Ionic Strength. The fact that the plots of k_{obsd} vs. $[\text{pyridine-d}_5]$ are linear and parallel with and without NaCl added to control ionic strength (Figure 4.3) shows that there is no salt effect for a neutral nucleophile, the activity of which is not affected by the presence of added salt.

For both azide and sulfite, however, the effects are quite different. Both nucleophiles show breaks in plots of k_{obsd} vs. $[\text{Nu}]$ with no added salt that are much more dramatic for sulfite (Figure 4.10) than for azide (Figure 4.5). Assuming

a "normal" salt effect in the region 0-0.3 M NaN_3 gives a Winstein b value of ca. +3.5, the sign and magnitude of which are inconsistent with "normal" salt effects in this region of nucleophile concentration. In their analysis of salt effects in the Snee mechanism, Schleyer and his colleagues¹⁹ assumed a b value of -1 to linearize the Snee-Larsen data for 2-octylmesylate⁴¹ and ascribed this value to a special azide salt effect. The high b value we find, however, is probably the result of the preassociation mechanism and not of a special azide salt effect. Thus if

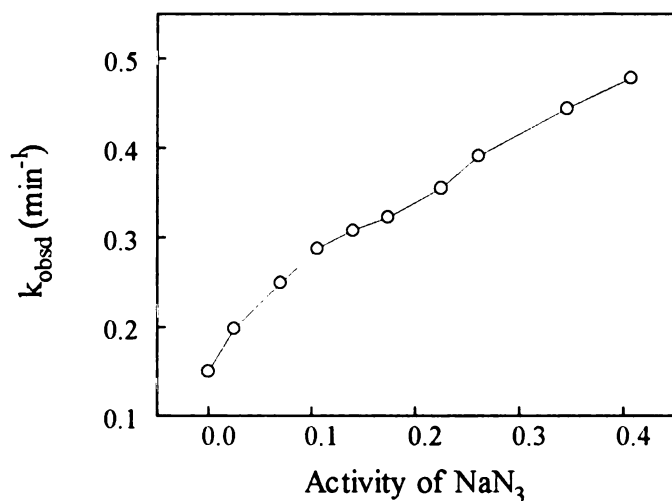


Figure 4.16. Plot of k_{obsd} vs. the activity of NaN_3 for reaction of 1 with no control of ionic strength at 80°C (points from Figure 4.5).

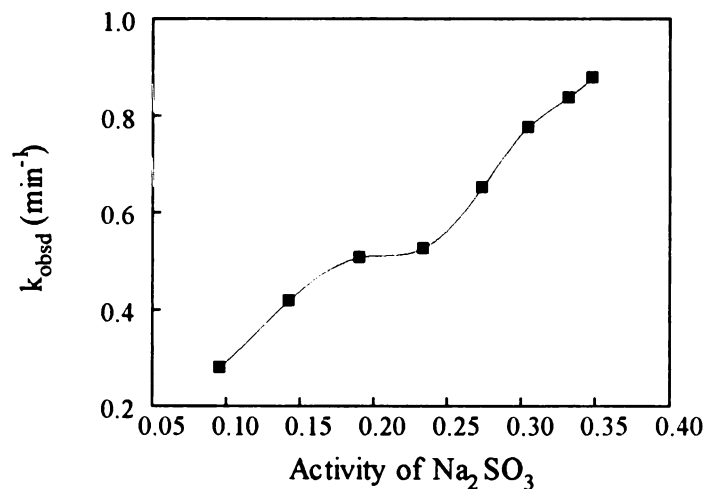
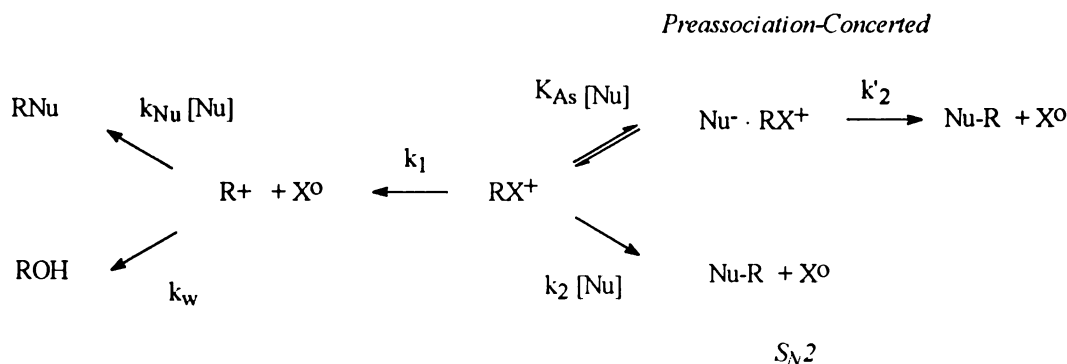


Figure 4.17. Plot of k_{obsd} vs. the activity of Na_2SO_3 for reaction of 1 with no control of ionic strength at 80°C (points from Figure 4.10).

these breaks were the result of a change in activity as a function of concentration, then it would be expected that a plot of k_{obsd} vs. the activity for the two salts would be linear. Measured activity coefficients are available for both azide⁴² and sulfite⁴³ in water. Plots of k_{obsd} vs. activity (Figures 4.16 and 4.17) show the same breaks as the concentration plots, and provide clear evidence that the breaks are not the result of salt effects, but must have their origin in a change in mechanism.

It was shown above that the portions of both azide and sulfite curves above the break point fit the equation for a mechanism involving formation of an ion pair $\text{Nu}^- \cdot \text{RX}^+$ that undergoes a concerted displacement at a faster rate than the encounter complex in the standard Hughes-Ingold $\text{S}_{\text{N}}2$ reaction. Richard and Thayer⁴⁴ point out that in the presence of a preassociation pathway, a concerted bimolecular mechanism is shut down (or severely restricted). This suggests that the break in the curve in the region 0.5-1.0M azide, which is not the result of experimental artifact, may be caused by a switch from the k_2 to the K_{As} pathway for the bimolecular reaction. There is only a small change in k_{w} in the range $\mu = 0-1.0$ (0.150 to 0.138 min^{-1}), while the values of k_2 are dropping rapidly (0.354 $\text{M}^{-1}\text{min}^{-1}$ at $\mu = 1$ to 0.239 $\text{M}^{-1}\text{min}^{-1}$ $\mu = 2$), so it is doubtful that a large change in this rate could account for the break. This mechanism is shown in Scheme 4.2.



Scheme 4.2

While the fits shown in Figures 4.5, 4.10, 4.16, and 4.17 constitute compelling evidence for this mechanism, they do not provide proof of it. It seems probable, however, that the selectivities would be affected, and this proves to be the case. Shown in Figure 4.18 are the selectivities for the reaction of 1 with 0-

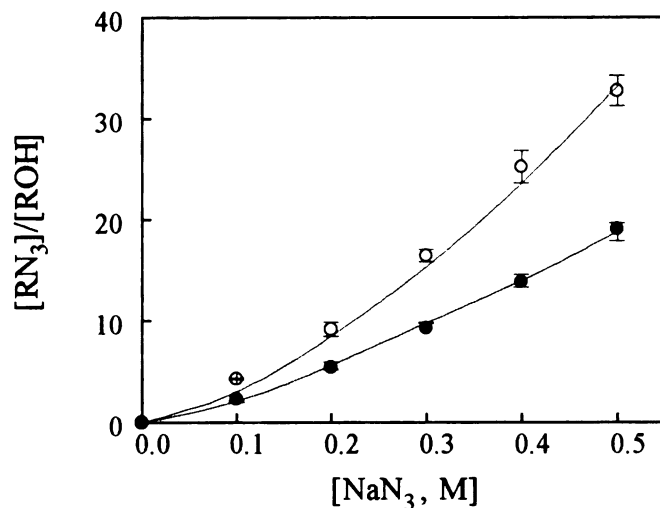


Figure 4.18. Selectivities for the reaction of 1 with NaN₃ at 80°C with (●) and without (O) control of ionic strength. The selectivities are the same if the added salt is NaCl or NaClO₄.

0.5M NaN₃ at 80°C for the nucleophile alone and for reaction with control of ionic strength. The selectivities are clearly different, being much greater for the nucleophile alone. If we assume that under conditions of constant ionic strength the added salt competes with nucleophile for formation of the ion pair, then the preassociated-concerted mechanism should be suppressed relative to the mixed S_N1/S_N2 mechanism. For this situation, using the steady-state approximation for the appearance of products the equation

$$[\text{RN}_3]/[\text{ROH}] = [\text{N}_3^-] (k_N/k_W) \{1 + (k_2/k_1)[\text{N}_3^-]\} + (k_2/k_1)[\text{N}_3^-] \quad \text{Eq.4.2}$$

is obtained. The ratio k_N/k_w is the value obtained for 4 (with either NaCl or NaClO₄ as the added salt; the value for no salt is the same) and represents the selectivity for trapping of the pure solvent-equilibrated carbenium ion. The line through the solid circles in Figure 4.18 is a fit to Equation 4.2 using the rate constants for the reaction at $\mu = 1.7$. The fit is excellent.

For the case with no added salt, all three pathways shown in Scheme 4.2 should operate, and the equation

$$\begin{aligned} [\text{RN}_3]/[\text{ROH}] = & [\text{N}_3^-] (k_N/k_w) \{1 + (k_2/k_1)[\text{N}_3^-] + \\ & (k_2'/k_1) (K_{As}/\{1 + K_{As} [\text{N}_3^-\}) [\text{N}_3^-\})\} + (k_2/k_1)[\text{N}_3^-] + \\ & (k_2'/k_2) (K_{As}/\{1 + K_{As} [\text{N}_3^-\}) [\text{N}_3^-] \end{aligned} \quad \text{Eq. 4.3}$$

is obtained using the steady-state approximation. The line through the open circles in Figure 4.18 is a fit to this equation using the appropriate rate constants for the solvolysis and azide reactions for the ionic strength at the give point, which were estimated using the Winstein b values⁴⁵ for the solvolysis reaction (Chapter 3)²¹ or from plots of k_{obsd} vs. $[\text{Nu}]$ for the no salt conditions. This fit, too, is excellent. These results confirm the supposition that the mechanism for the azide substitution reaction follows the complex pathways shown in Scheme 4.2.

For sulfite, the situation is more complex for several reasons. First, the change in the first-order rate constant is much more severe than for the azide case, as shown by the effect of Na₂SO₄ on the hydrolysis reaction (see Results section). Second, as shown in Figure 4.9, the difference in second-order rate constants between $\mu = 2$ and 5 (Table 4.3) is much less than the azide case (Table 4.2). Third, the odd behavior that is caused by changing from NaCl to Na₂SO₄ as the added salt makes fitting the selectivities for the former much more complex (Figure 4.8). Given all these caveats, however, as shown in Figure 4.19 the

selectivities for no added salt are fit very well by the values calculated using Equation 4.3 for the three pathway mechanism shown in Scheme 4.2. It will be appreciated that because of the low value of both K_{As} (0.07) and k_N/k_w (0.62, determined from reaction of 4 with Na_2SO_3), the fit for the constant ionic strength portion of the curve will be approximately the same as for the no salt case. Thus the sulfite data also confirm that the three-pathway mechanism shown in Scheme 4.2 operates.

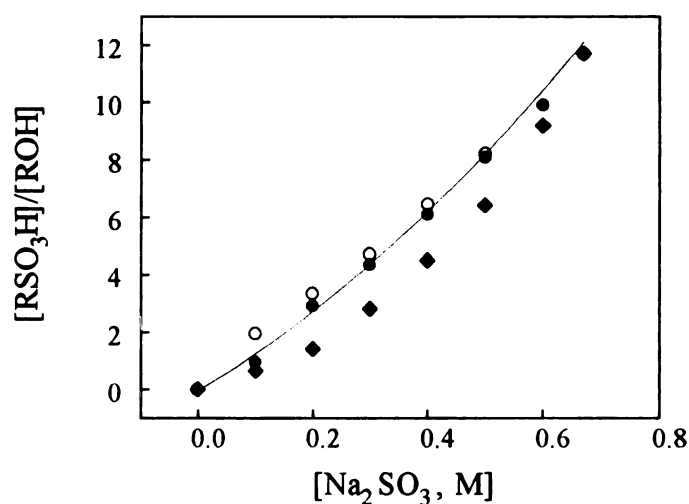


Figure 4.19. Selectivities for the reaction of 1 with Na_2SO_3 at 80°C with (●) and without (○) control of ionic strength with Na_2SO_4 . The selectivities for NaCl as the added salt are included (◆). The line is a fit of the experimental rate constants to Equation 4.3 for the complete mechanism shown in Scheme 4.3.

Sneen Ion-Dipole Complex Mechanism. Sneen¹⁵ suggested that the solvolysis of 1 in the range 0-0.12M azide, with no control of ionic strength, proceeds through an ion-dipole complex intermediate and follows the rate law given in Equation 4.4.

$$k_{\text{obsd}} = k_1 (1 + k_N/k_S [\text{N}_3^-]) / (k_1/k_S + 1 + k_N/k_S [\text{N}_3^-]) \quad \text{Eq. 4.4}$$

This suggestion is inconsistent with our finding (see Chapter 3)²¹ that the solvolysis of **1** in D₂O is an S_N1 reaction, and our selectivity data for the azide reaction also rule out the ion-dipole complex mechanism. Friedberger and Thorton²⁰ point out that Snee's mechanism is reasonable if alkyl azide does not arise from trapping of the solvent-equilibrated carbenium ion. We fit our selectivity data to equations that include $k_N/k_W = 17.6$, determined independently in **4** for the pure 4-methoxybenzyl carbenium ion, to evaluate the unimolecular component; use of the experimental selectivity values ($k_N/k_S = 46$ in the range 0-0.2M azide, no added salt) would have grossly skewed the results. Indeed, the large difference in selectivities between azide only and constant ionic strength mitigate against the ion-dipole complex mechanism. It seems reasonable that at the low azide concentrations used in Snee's study, 0-0.12M, the value of k_1/k_S would appear to be constant and the slope of the plot of $[RN_3]/[ROH]$ would appear to be linear. Extending the range of azide shows that the basic conditions needed for the ion-dipole complex mechanism are not met.

There is ample evidence that ion pairs may exist in nonaqueous organic solvents,¹⁸ and our finding that the sulfonate **2** yields the benzoate **4** as a major product in solvent pyridine-d₅ is consistent with the historical results. There is growing evidence, however, that ion pairs are unlikely to exist in water or highly aqueous mixed solvents.^{18,21,22,46} In the other well-studied solvolysis of a charged substrate, *t*-butyldimethyl-sulfonium,⁴⁷ ion-pair formation is difficult to evaluate because of solvent nucleophilic participation. The high ionic strengths used in our study forces the formation of simple ion aggregates,⁴⁸ but that process is distinctly different than *solvolytic* formation of an ion pair or ion-dipole complex intermediate from a substrate in these media.

Aymes and Richard² argue that the preassociation/enforced mechanism does not operate in the azidolysis of 4-methoxybenzyl chloride at constant ionic

strength ($\mu = 0.5$) in acetone-water mixtures, and Richard and Jencks¹⁴ found that azidolysis of [1-(4-methylphenyl)-ethyl]dimethylsulfonium is mixed S_N1/S_N2 at constant ionic strength ($\mu = 0.5$) in trifluoroethanol-water. Our results are consistent with both results at the concentrations of nucleophile used. In the former instance, no ionic complexation would be expected; in the latter, a shift in mechanism may not occur at the concentrations used or may be so subtle that it is not seen.

We are intrigued by the difference in the second-order rate constants for the preassociation mechanism and the S_N2 mechanism under constant ionic strength; the value for the preassociation mechanism for azide is 4-fold greater than for the nonenforced S_N2 mechanism. Menger⁴⁹ has argued that the rates of intramolecular reactions are accelerated because of the time a nucleophilic group is held at an appropriate distance from a carbon bearing a leaving group. This "spatio-temporal" hypothesis could account for the difference in rate constants we find. In the ionic complex the nucleophile and substrate are held in proximity for times longer than the diffusion rate in solution, which should increase the second order rate constant. Moreover, the energy needed to desolvate nucleophile in the formation of the intermediate complex is included in the equilibrium term, while the desolvation of nucleophile in the nonenforced S_N2 mechanism is a kinetic effect. Thus less energy is required to achieve the transition state for the ionic complex than for the encounter complex, which should increase the rate for the former. Because the observed rate constants for the preassociation mechanism are the result of a combination of kinetic and thermodynamic factors, they are not drastically different than the observed rate constants for the nonenforced S_N2 reaction at constant ionic strength.

Activation Values. For the dimethylsulfonium substrate 1, ΔG^\ddagger for the uni- and bimolecular reactions are very similar (probably within error) despite the large difference in $T\Delta S^\ddagger$, and both reactions can occur simultaneously. (Swain and his colleagues^{13b} found very similar activation values for the bimolecular reactions of several benzyldimethyl-sulfonium substrates with lyoxide and phenoxide.) The pyridinium substrate has a ΔG^\ddagger for the S_N2 reaction in the same range as that for the sulfonium substrate, but is clearly dominated by an unfavorable $T\Delta S^\ddagger$ term (which is larger than the difference in ΔH^\ddagger).

There is a large difference in entropies for the bimolecular reaction between the sulfonium and pyridinium substrates ($\Delta\Delta S^\ddagger = -15$ gibbs/mol) We interpret this difference as the result of solvation of the leaving group at the transition state. Introduction of dimethyl sulfide, which is hydrophobic, into solvent at the transition state would be expected to little effect on the organization of solvent and thus on the entropy, while introduction of very water soluble pyridine would be expected to cause reorganization of solvent at the transition state. These differences are dramatic because water is much less structured in the high temperature range and salt concentration used than at 25°C and low ionic strengths.

Arnett and his colleagues⁴⁷ showed that solvation of the ground state is important for solvolysis of neutral substrates such as *t*-butyl chloride; based on partial molal volumes of activation, Lee and Hyne⁵⁰ argued that positively charged anilinium chloride was not a good transition state model for solvolysis of neutral benzyl derivatives. Because of the general reversal of medium effects between neutral and charged substrates,^{29,46} and because the effect of solvent composition on ΔH^\ddagger are reversed for *t*-butyl chloride and *t*-butyldimethyl sulfonium,⁴⁷ the suggestion that solvation of the activated complex is more important than solvation of the ground state for the benzylsulfoniums seems to be reasonable.

The Jencks Criteria. Jencks⁵¹ has emphasized the importance of the stability of an intermediate and its ability to become solvent equilibrated as determining factors for the particular mechanism a substrate chooses (Chapter 1). In the cases reported here the putative carbenium ion, nucleophile, and solvent are the same, and there are no added cosolvents and therefore no chance of either differential solvation or differential hydrogen bonding of the activated complex or other manifestations of "solvent sorting"; the intrinsic stability of the carbenium ion and the structure of the solvation shell are constant. Hydrolysis of the benzoate 4 produces the carbenium ion as a stable, solvent-equilibrated species that can select between water and azide as expected. Nonetheless, the three substrates exhibit the range of mechanisms from S_N1 to mixed to S_N2 , with no evidence of "borderline behavior" in any instance. The range of mechanism as reflected in the activation values may be combinations of "normal" entropic factors associated with an S_N1 process and of different solvation of the activated complex in S_N2 processes. For the dimethylsulfonium substrate, the difference between formation of the ionic complex and an encounter complex may be merely the result of nonspecific anion complexation that at high concentrations of added salt swamps out formation of the substrate-nucleophile complex. The higher rate constant for the reaction of the ionic complex may be a consequence of an intermolecular form of the Menger hypothesis and not of the stability of the intermediate or even of stabilization of the intermediate by leaving group and nucleophile; if leaving group stabilization were an important process, the values of ΔG^\ddagger for dimethylsulfonium and pyridinium substrates would be expected to be much greater than they are because the ΔpK_a of the leaving groups is ca. 10. *Given these factors, the intrinsic stability of the intermediate in the reactions of these substrates is not a factor that influences the mechanism.*

References and Notes

(1) Aymes and Richard² provide a fairly complete list of references for the solvolysis of various benzyl substrates in mixed solvents; we will not reproduce that list here.

(2) Amyes, T.L.; Richard, J.P. *J. Am. Chem. Soc.* **1990**, *112*, 9507-9512.

(3) Fujio, M.; Goto, M.; Susuki, T.; Akasaka, I.; Mishima, M.; Tsuno, Y. *Bull. Chem. Soc. Jpn.* **1990**, *63*, 1146-1153.

(4) (a) See Hudson, R.F.; Klopman, G. *J. Chem. Soc.* **1962**, 1062-1067. (b) Lyoxide reactions of substituted benzyl dimethyl and phenylmethyl sulfoniums show V-shaped Hammett plots. Schowen, K.B.J. Doctoral Dissertation (MIT, 1964); we thank Dr. Schowen for providing a copy of her dissertation.

(5) Maskill, H. *The Physical Basis of Organic Chemistry*, Oxford: New York, 1985, p. 450.

(6) Young, P.R.; Jencks, W.P. *J. Am. Chem. Soc.* **1979**, *101*, 3288-3294.

(7) Richard, J.P.; Yeary, P.E. "A Simple Explanation for Curved Hammett Plots for Nucleophilic Substitution Reactions at Ring-Substituted Benzyl Derivatives," talk presented at the 206th ACS National Meeting, Chicago, IL, 22-27 August, 1993.

(8) Pross, A. *Adv. Phys. Org. Chem.* **1985**, *21*, 99-196; Pross, A.; Shaik, S.S. *Acc. Chem. Res.* **1983**, *16*, 363-370.

(9) Sneen, R.A. *Acc. Chem. Res.* **1973**, *6*, 46-53.

(10) Sneen, R.A.; Larsen, J.W. *J. Am. Chem. Soc.* **1969**, *91*, 6031-6035.

(11) Kohnstam, G.; Queen, A.; Shillaker, B. *Proc. Chem. Soc.* **1959**, 157-158.

(12) Hill, J.W.; Fry, A.J. *Am. Chem. Soc.*, **1962**, *84*, 2763-2768; Graczyk, D.G.; Taylor, J.W. *J. Am. Chem. Soc.*, **1974**, *96*, 3255-3261.

UCSF LIBRARY

- (13) (a) Swain, C.G.; Thornton, E.R. *J. Org. Chem.* **1961**, *26*, 4808-4809.
(b) Swain, C.G.; Taylor, L.J. *J. Am. Chem. Soc.* **1962**, *84*, 2456-2457. (c) Swain, C.G.; Rees, T.; Taylor, L.J. *J. Org. Chem.* **1963**, *28*, 2903. (d) Swain, C.G.; Burrows, W.D.; Schowen, B.J. *J. Org. Chem.* **1968**, *33*, 2534-2536.
- (14) Richard, J.P.; Jencks, W.P. *J. Am. Chem. Soc.* **1984**, *106*, 1383-1396.
- (15) Sneen, R.A.; Felt, G.R.; Dickason, W.C. *J. Am. Chem. Soc.* **1973**, *95*, 638-639.
- (16) Reviewed in Katritsky, A.R.; Brycki, B.E. *Chem. Soc. Rev.* **1990**, *19*, 83-00, and elsewhere. See also Katritsky, A.; Malhotra, N.; Ford, G.P.; Anders, E.; Tropsch, J.G. *J. Org. Chem.* **1991**, 5039-5044.
- (17) Darwish, D.; Hui, S.H.; Tomilson, R. *J. Am. Chem. Soc.*, **1968**, *90*, 5631-5632.
- (18) Bentley, T.W.; Schleyer, P. v.R. *Adv. Phys. Org. Chem.* **1977**, *14*, 1-67; Raber, D.J.; Harris, J.M.; Schleyer, P.v.R., Ch. 3 in *Ions and Ion Pairs in Organic Reactions*, Vol. 2, Szwarc, M., ed.; Wiley: New York, 1974; Harris, J.M. *Prog. Phys. Org. Chem.* **1974**, *11*, 89-173.
- (19) Raber, D.J.; Harris, J.M.; Hall, R.E.; Schleyer, P. v.R. *J. Am. Chem. Soc.* **1971**, *93*, 4821-4828.
- (20) Friedberger, M.P.; Thornton, E.R. *J. Am. Chem. Soc.*, **1976**, *98*, 2861-2865.
- (21) Buckley, N.; Oppenheimer, N.J. *J. Org. Chem.* **1994**, *59*, 5717-5723 (Chapter 3).
- (22) Kevill, D.N.; Ismail, N.H.J.; D'Sousa, M.J. *J. Org. Chem.* **1994**, *59*, 6303-6312.
- (23) Feiser, L.; Feiser, M.L., *Reagents for Organic Synthesis, Vol 1.*; Wiley: New York, 1961, pp.1180-1181.

(24) Tsuno, *et al.*,³ estimated the rate constant for solvolysis of *p*-methoxybenzyl tosylate at 25°C in 80% aqueous acetone to be 0.83 sec⁻¹; extrapolation to 25°C for the white insoluble solid gives $k = 2.9 \times 10^{-6}$ sec⁻¹.

(25) We thank Dr. John Richard, SUNY Buffalo, for calling this to our attention.

(26) Peak assignments from Parks, T.E.; Spurlock, L. A. *J. Org. Chem.* **1973**, *38*, 3922-3924, corrected to CDCl₃ from CCl₄.

(27) Buckley, N.; Oppenheimer, N.J. *J. Org. Chem.* **1994**, *59*, 247-249.

(28) Shiner, V.J. In *Isotope Effects in Chemical Reactions*; Collins, C.J.; Bowman, N.S., Eds; Van Nostrand Reinhold: New York, 1970; pp. 91-159.

(29) Ingold, C.K., *Structure and Mechanism in Organic Chemistry*, Cornell: Ithica, N.Y., 1953, pp. 306-408.

(30) Spurlock, L.A.; Porter, R.K.; Cox, W.G. *J. Org. Chem.* **1972**, *37*, 1162-1168, provide a list of leading references.

(31) Iliceto, A.; Fava, A.; Mazzucato, U. *Tet. Lett.* **1960** No. **11**, 27-35.
Smith, P.A.S.; Emerson, D.W. *J. Am. Chem. Soc.* **1960**, *82*, 3076-3082.

(32) Spurlock, L.A.; Fayer, R.G. *J. Org. Chem.* **1969**, *34*, 4035-4039.

(33) Fava, A.; Iliceto, A.; Bresadola, S. *J. Am. Chem. Soc.* **1965**, *34*, 4791-4794.

(34) Maartmann-Moe, K.; Sanderud, K.A.; Songstad, J. *Acta Chem. Scand. B* **1982**, *36*, 211-223.

(35) Schiavon, G. *Ric. Sci.* **1962**, *32*, 69-75.

(36) Pearson, R.G. In *Advances in Free Energy Relationships*; Chapman, N.B., Shorter, J., Eds.; Plenum Press: New York, 1972, pp. 281-319.

(37) Klopman, G. *J. Am. Chem. Soc.* **1968**, *90*, 223-234. Salem, L. *J. Am. Chem. Soc.* **1968**, *90*, 543-552.

(38) Westaway, K.C.; Ali, S.F. *Can. J. Chem.* **1979**, *57*, 1354-1367.

(39) Lee, I.; Koh, H.J.; Lee, B.-S.; Sohn, D.S.; Lee, B.C. *J. Chem. Soc. Perkin Trans. II* **1991**, 1741-1746.

(40) Meissner, H.P.; Kusik, C.L. *AIChEJ.* **1972**, *18*, 294-298; Meissner, H.P.; Kusik, C.L. *Ind. Eng. Chem. Process Des. Develop.* **1973**, *12*, 205-208; Harned, H.S.; Robinson, R.A. "Multicomponent Electrolyte Solutions"; Pergamon: New York, 1963.

(41) Sneen, R.A.; Larsen, J.W. *J. Am. Chem. Soc.* **1969**, *91*, 362-366.

(42) Maiorova, T. N.; Karpenko, G. V.; Poltoratskii, G. M.; Goverdovskii, B. A.; Krauklis, I. Deposited Document in the Soviet Archive VINITI 3433-77, 193-7, 1977. This paper was kindly obtained for us by Academician A.S. Zasedatelev, Molecular Biology Institute, Leningrad, at the request of our colleague Richard Shafer.

(43) Morgan, R.S. *J. Chem. Eng. Data* **1961**, *6*, 21-23.

(44) Richard, J.P., personal communication.

(45) Fainberg, A.H.; Winstein, S. *J. Am. Chem. Soc.* **1956**, *78*, 2763-2767.

(46) Kevill, D.N.; Anderson, S.W.; Ismail, N.H.; Fujimoto, E.K.

Physical Organic Chemistry 1986, Elsevier: Amsterdam, 1987, pp. 311-320.

(47) Arnett, E.M.; Bentrude, W.G.; Burke, J.J.; Duggleby, P. McC. *J. Am. Chem. Soc.* **1965**, *87*, 1541-1553.

(48) Loupy, A.; Tchoubar, B.; Astruc, D. *Chem. Rev.* **1992**, *92*, 1141-1165.

(49) Menger, F.M. *Tetrahedron* **1983**, *39*, 1013-1040; Menger, F.M. *Acc. Chem. Res.* **1985**, *18*, 128-134.

(50) Lee, I.; Hyne, J.B. *Can. J. Chem.* **1969**, *47*, 1437-1439.

(51) Jencks, W.P. *Acc. Chem. Res.* **1980**, *13*, 161-169. Jencks, W.P. *Chem. Soc. Rev.* **1981**, *10*, 345-375.

ULSF LIBRARY

Chapter 5
Gas-Phase Dissociation of
2'-Substituted β -Nicotinamide Arabinosides

UCL LIBRARY

Introduction

As part of continuing model studies for the hydrolysis of nicotinamide adenine dinucleotide (NAD⁺),¹ Handlon and Oppenheimer² recently reported rate constants for the pH-independent hydrolysis of a series of 2'-substituted b-nicotinamide arabinosides (**1a-e**) with different oxocarbenium ion intermediates; kinetics and a Taft correlation are consistent with a dissociative mechanism. Studies by Schuber and his colleagues³ of the uncatalyzed and NAD⁺ glycohydrolase [E.C.3.2.2.5]-catalyzed hydrolysis of NAD⁺ analogues with substituted pyridiniums as leaving groups also supports this mechanism. Recent results for the enzyme-catalyzed dissociation of 2'-substituted NAD⁺ analogs reproduce almost exactly the slope of the Taft plot found for non-enzymatic hydrolysis of the arabino and ribo derivatives.⁴

For comparison with these solution results, we have measured the gas-phase dissociation of **1a-e** using tandem positive-ion liquid secondary ion mass spectrometry (LSIMS). With these techniques, it is possible to study directly the gas-phase dissociation of positively charged substrates without the relatively harsh conditions needed to produce the molecular ion in chemical ionization or electron impact methods. Non-tandem spectra give reasonable correlations for these substrates, but the tandem correlations are measurably better because only the molecular ion is collisionally activated and dissociates in MSII. The experimental results and the energies and structures obtained with AM1 suggest that gas-phase dissociation of **1a-e** occurs through an ion-dipole complex (IDC) intermediate.

Experimental Section

Experimental. Syntheses of the substrates have been reported.⁵ Tandem mass spectra were recorded under identical conditions in the positive ion mode on a 4-sector Kratos Concept II HH mass spectrometer fitted with an optically

UCL LIBRARY

coupled 4% diode array detector on MS II. Substrates were sputtered from a glycerol matrix with Cs^+ (18 keV), and the molecular ion was sorted into MSII where fragmentation was induced by collisional activation with helium. Results are the averages of several runs (<5% error); non-tandem LSIMS spectra gives the same trends, although the precision is not as good.

Computational Methods. Calculations were performed on a 486/66 (16 MB RAM) using Release 3.0 of the Hyperchem[®] software. Initial structures were built using the default model building routine. After a single-point calculation to set the Mullikan charge populations was performed, the structure was minimized with MM+ (Hyperchem's version of MM2) using the partial charge option. The Polak-Ribiere block diagonal algorithm was used for all MM+ and semi-empirical minimizations to an RMS gradient of <0.1 kcal/[Å mol]. All semi-empirical calculations⁶ were unrestricted Hartree-Fock with the wavefunction calculated to a convergence limit of <0.001.

To construct the energy profiles, the C_1 '-nicotinamide bond length was increased in steps from the initial length of 1.49-1.52 Å using the restraint function to a final restraint force constant of 10^5 , the value recommended by Hyperchem. Each structure was minimized completely with no restraint other than the reaction coordinate. Values of ΔH_f for each structure were used to construct energy profiles and locate the approximate energy of the transition state; structures were refined until the criterion of a single negative (imaginary) frequency⁷ was obtained for the reaction coordinate using the Vibrational Analysis function. Energies of the oxocarbenium ions were calculated after removal of nicotinamide from the IDC.

Results

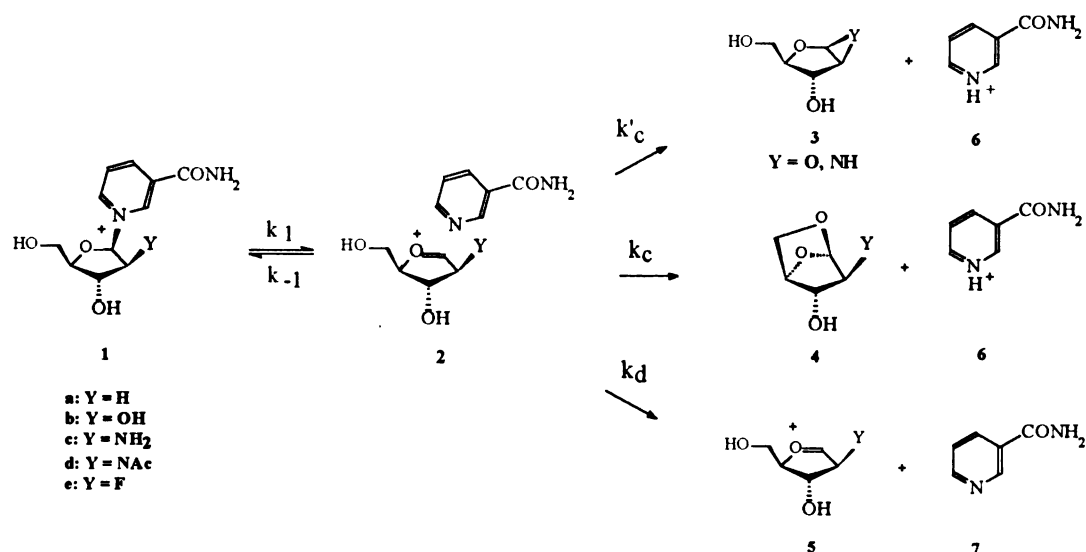
Experimental. In tandem LSIMS spectra of 1a-e, the most abundant peak is the respective molecular ion, followed by peaks for protonated nicotinamide (7, Nic-H⁺) and the respective oxocarbenium ion.⁸ Data are listed in Table 5.1. As

Table 5.1. Relative Abundances for the Gas-Phase Dissociation of 2'-Substituted b-Nicotinamide Arabinosides (M⁺ = 100)

Y	Nic-H ⁺	Oxocarbenium Ions	log (R ⁺ /[R ⁺ +M ⁺]) [*]
H	20	11	-0.62
NH ₂	14	10	-0.71
OH	15	4	-0.80
HNAc	5 (13) [†]	11 (3) [†]	-0.86
F	12	0.8	-0.95

*R⁺ = Nic-H⁺ + oxocarbenium ion.

[†]The numbers in parentheses are the expected values obtained by extrapolation from a plot of log (R⁺/[R⁺+M⁺]) vs the relative abundance of Nic-H⁺ and the oxocarbenium ions.



Scheme 5.1

shown in Scheme 5.1, proton transfer within an IDC and cyclization leads to Nic-H⁺ and neutrals. The alternative is dissociation of the IDC to the free oxocarbenium ions **5a-e** and unprotonated nicotinamide (k_d). If all these processes occur, the total intermediate **2** formed by the two channels (designated R⁺) is the sum of Nic-H⁺ and the respective oxocarbenium ion.

A plot of the log (R⁺/[R⁺ + M⁺]) for **1a-e** vs. σ_F is shown in Figure 5.1; the σ_F value for NAc is not available, but was estimated to be +0.33 by interpolation

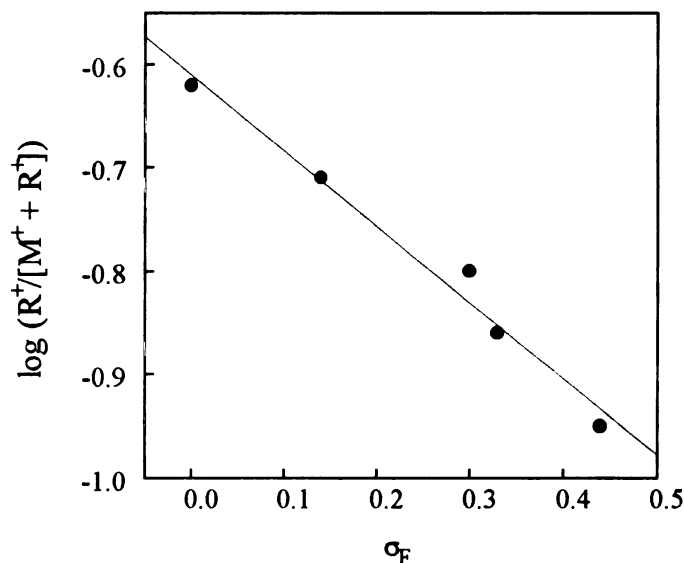


Figure 5.1. Taft plot for the gas-phase dissociation of 2'-substituted β-nicotinamide arabinosides. The σ_F value for NAc is not available, but was estimated as described in the text. The plot is linear (r = 0.990) with ρ_F = -0.75. Left to right the points are for Y = H, NH₂, OH, NAc, and F.

with the σ_I scale.⁹ The plot is linear. With the point for 2'-OH included, r = 0.990, and with the point excluded r = 0.999. In either case, ρ_F = -0.75. The Taft correlation implies a correlation with the solution kinetics (k_w), and a plot (not shown) of log k_w vs. log (R⁺/[R⁺ + M⁺]) is linear (r = 0.988) with a slope of -0.25.

Computational. Methods. Hyperchem Release 3 was not designed to do explicit transition state modeling; nonetheless, all the methods needed to perform

these calculations are in the software, including a modified version of MM2, the full range of semi-empirical methods, and a subroutine for diagonalization of the force constants. Two modifications of the standard approach to transition state modeling should be mentioned.

First, we found that the time needed to do a complete minimization using semi-empirical methods could be cut by one-half to two-thirds if the restraint force constant on the reaction coordinate bond was increased in three equal steps from 10^3 to 10^5 . Values of ΔH_f obtained with the stepped approach were $< \pm 0.1$ kcal/mol of the value obtained by setting the force constant to 10^5 at the outset of the calculation. For instance, increasing the bond in 1c from 2.0 to 2.2 Å gave a ΔH_f of 6.65 kcal/mol for the direct approach and a value of 6.62 kcal/mol for the stepped approach. We do not consider these small differences to be significant for these calculations.

Second, the Vibrational Analysis subroutine was designed to generate IR spectra; complete values for the diagonalized force constants but not the values of the eigenvalues in the Hessian are recorded in the output. The normal mode analysis does provide negative (imaginary) frequencies, however, and the graphic display can localize the frequency to the bond involved. In all cases, the single negative frequency found--the first normal mode--corresponded to the reaction coordinate.¹⁰

Because this approach to transition state modeling has not been documented previously, we generated the energy profiles shown in Figure 5.2 for unsubstituted benzyl pyridinium with the MNDO, AM1, and PM3 methods. Two of the three--AM1 and MNDO--show distinct maxima that meet the criteria of a saddle point on a potential energy surface. As expected, the AM1 and MNDO methods give different energies for the transition state. These plots match exactly those published by Katritzky, Anders, Ford and colleagues (Figure 5 of Ref. 11) who

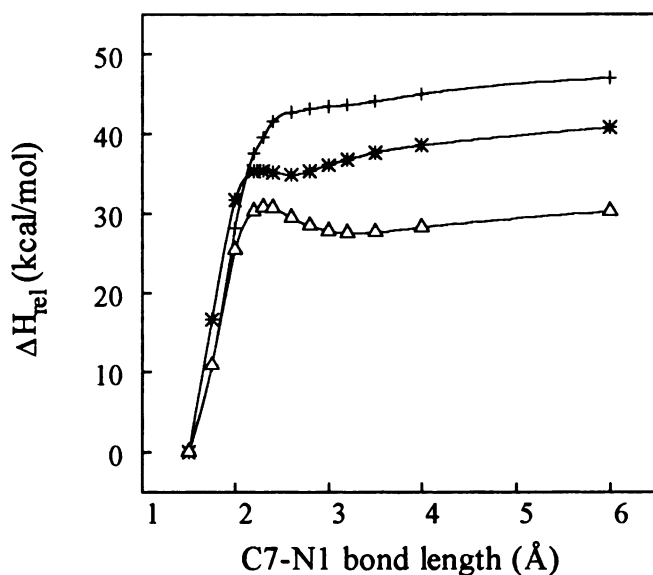


Figure 5.2. PM3 (+), AM1 (*), and MNDO (Δ) energy profiles calculated for benzyl pyridinium using Hyperchem Release 3. The calculated profiles are an exact match for reported profiles (Figure 5 of Ref. 11).

used MOPAC and much more sophisticated stopping criteria for minimization than available in Hyperchem.

Activation Enthalpies. In earlier calculations of the gas-phase dissociation of β -nicotinamide riboside we used the PM3 methodology in preference to AM1.¹² Katritzky, Anders, Ford and colleagues,¹¹ however, found that PM3 failed to provide a distinct transition state for a series of benzyl pyridiniums. For **1a-e**, PM3 gave acceptable energy profiles and met the criterion for transition state saddle points, but a plot of ΔH^\ddagger vs. $\log(R^+/[R^+ + M^+])$ is badly scattered with a correlation coefficient of 0.60, although a general trend correlating the data is evident.

Therefore, the calculations were repeated using the AM1 method. AM1 values for ΔH_f for the starting structures, transition states, IDCs, oxocarbenium ions, and related neutral structures are listed in Table 5.2. Values of ΔH^\ddagger for bond

Table 5.2. Absolute AM1 Enthalpies of Formation (ΔH_f) for the Gas-Phase Dissociation of 2'-Substituted β -Nicotinamide Arabinosides

Substituent	Starting	Transition	Ion-Dipole	Oxocarbenium	Bicyclic	Other
	Structure	State	Complex	Ion	Structure	
H	10.7	31.4	28.2	44.0	-119.3	--
NH ₂	14.0	36.3	33.1 (29.2) [†]	49.6	-117.9	-100.8
OH	-31.2 [*]	-7.90	-12.7	7.3	-160.9	-142.2
NAc	-23.5	0.70	-4.7	15.6	-155.4	-13.3
F	-32.8	-6.80	-9.6	10.9	-163.5	--

All energies in kcal/mol. ΔH_f nicotinamide = -5.8. ΔH_f Nic-N-H[†] = 150.1. ΔH_f Nic-NH₂C=O-H[†] = 154.4.

\S NH₂, β -1',2'-aziridine; OH, β -1',2'-epoxide; NAc, β -1',2'-acylium ion.

^{*}Corrected by adding the energy of formation of a hydrogen bond between the nicotinamide amide carbonyl and the 5'-OH on going to the transition state.

[†]Value in parenthesis is after formation of a hydrogen bond between the nicotinamide amide carbonyl and the 5'-OH between 2.6 and 2.8Å..

Table 5.3. Relative AM1 Enthalpies of Formation (ΔH_f) and Activation (ΔH^\ddagger) for the Gas-Phase Dissociation of 2'-Substituted β -Nicotinamide Arabinosides

Substituent	Ion-Dipole	Oxocarbenium	Bicyclic	Other	ΔH_f^\ddagger	ΔH_f^\ddagger	ΔH_f^\ddagger	Dissociation*	Structures \S	k ₁	k ₋₁	ΔH_f^\ddagger	Dissociation
	Complex	Ion	Structure	Structures \S									
H	17.4	33.3	20.1	--	27.5	20.7	3.3						10.1
NH ₂	15.2(19.1) [†]	35.6	18.2	35.3	29.8	22.3	7.1(3.2)						14.6
OH	18.5	38.5	20.4	39.1	32.7	23.3	4.8						14.2
NAC	18.8	39.1	18.2	4.6	33.3	24.2	5.4						14.5
F	32.2	43.7	19.4	--	37.9	26.0	2.8						14.7

All energies in kcal/mol relative to respective starting structure, except for the ΔH_f^\ddagger for k₋₁ and dissociation, which are relative to the respective ion-dipole complexes.

\S NH₂, β -1',2'-aziridine; OH, β -1',2'-epoxide; NAC, β -1',2'-acylium ion.

* ΔH_f^\ddagger [oxocarbenium ion] + ΔH_f^\ddagger [nicotinamide].

[†]Value in parenthesis is after formation of a hydrogen bond between the nicotinamide amide carbonyl and the 5'-OH between 2.6 and 2.8Å.

cleavage and dissociation and enthalpies of the various structures relative to the starting structure are listed in Table 5.3.

There are two apparent anomalies in the energy profiles shown in Figure 5.3. First, in the profile for the 2'-NH₂ compound 1c there is a drop in energy of 3.9 kcal/mol between 2.6 and 2.8 Å (closed squares, Figure 5.3). Examination of

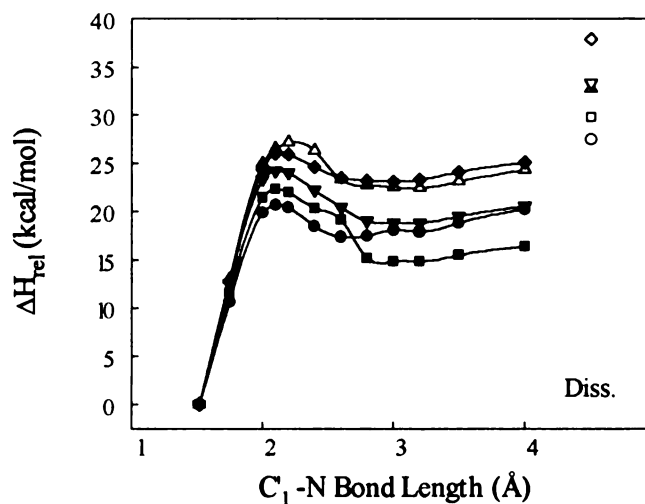


Figure 5.3. AM1 energy profiles for gas-phase dissociation of 1a-e. Y = H (●); OH (△); NH₂ (■); NAc (▼); F (◆). The difference between ΔH_f for the starting structure and the maximum value is ΔH^\ddagger . Energy values obtained from these plots are listed in Tables 5.2 and 5.3.

the structures shows that the nicotinamide ring has rotated about the reaction coordinate and formed a hydrogen bond between the amide carbonyl and the 5'-OH proton, which stabilizes the structure.

Second, the energy profile for the 2'-OH compound 1b gives an energy for the transition state that is higher than the other values (open up triangles, Figure 5.3). In a plot of $\log(R^+/[R^+ + M^+])$ vs. the AM1-calculated ΔH^\ddagger , the points for all substrates except 1b form a straight line (Figure 5.4, $r = 0.9999$); the energy for 1b is too high by 3.9 kcal/mol (open circle, Figure 5.4). This apparent anomaly can be resolved by examining and comparing the calculated structures for all substrates.

WOLF LIDNANI

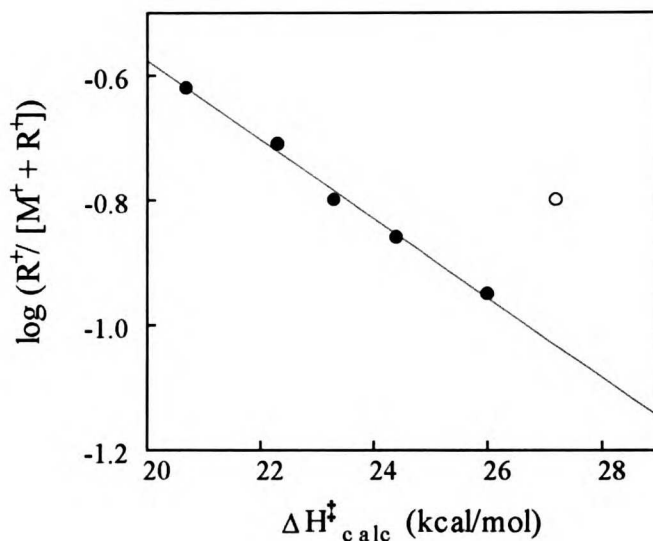


Figure 5.4. Plot of the experimentally determined $\log(R^+/[R^+ + M^+])$ vs. the AM1-calculated values of $\Delta H_{\text{calc}}^{\ddagger}$ for gas-phase dissociation of **1a-e** ($r = 0.998$). The open circle is the value for the 2'-OH compound **1b** before normalization as described in the text. Left to right the points are for $Y = \text{H}, \text{NH}_2, \text{OH}, \text{NAC}, \text{and F}$.

In the ground and transition states and IDCs for **1a** and **1e**, the plane of the nicotinamide ring lies directly along and above the C'1-C'2 bond (Figure 5.5, *left*).

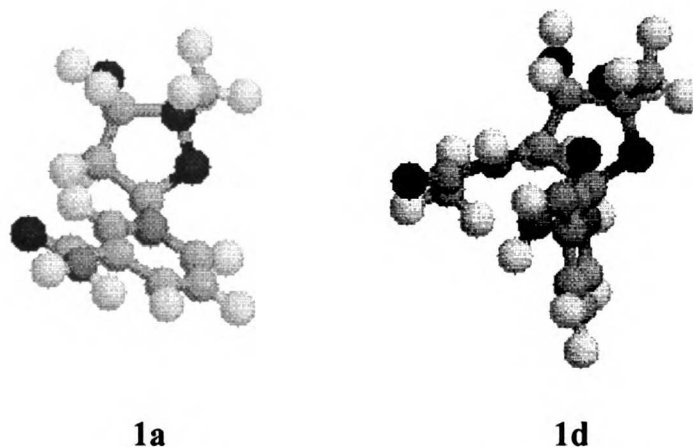


Figure 5.5. Ground states for the 2'-H (**1a**) and 2'-NAC (**1d**) compounds. View is along the plane of the nicotinamide into the plane of the ribose. There is no hydrogen bond between the amide carbonyl and the 5'-OH for **1a** but this bond exists for **1d**.

In the NAc compound, however, the nicotinamide is forced by steric repulsion to rotate away from the substituent, and a hydrogen bond forms between the

carbonyl of the nicotinamide amide and the 5'-OH proton (Figure 5.5, *right*); this conformation is retained from the ground to the transition state, and into the IDC. In the structures for the 2'-OH substrate 1b, the ground state resembles the structure for 1a and 1e (Figure 5.6, *left*). As the bond length in 1b is increased,

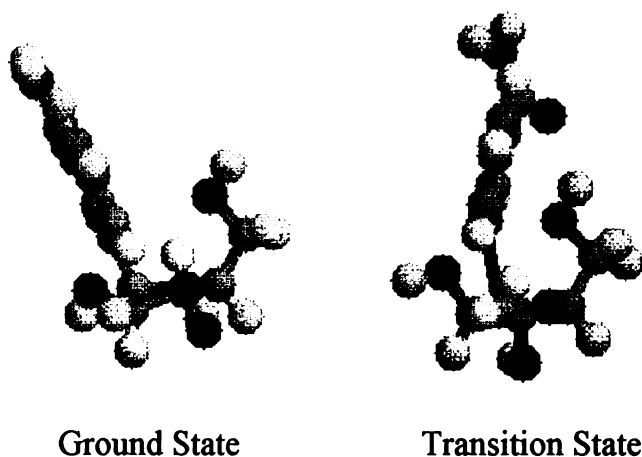


Figure 5.6. Ground state (*left*) and transition state (*right*) for 1b that show formation of a hydrogen bond between the amide carbonyl and the 5'-OH proton during cleavage of the ribosyl-nicotinamide bond.

however, the nicotinamide rotates about the reaction coordinate and a hydrogen bond forms between the carbonyl of the nicotinamide amide and the 5'-OH (Figure 5.6, *right*). Thus there is a difference in energy between the ground and transition states that is not produced by merely breaking the bond. Normalizing the ground state energy by adding the 3.9 kcal/mol for formation of this hydrogen bond gives $\Delta H^\ddagger = 23.3$ kcal/mol, a value that fits nicely on the plot of $\log (R^+/[R^+ + M^+])$ vs. ΔH^\ddagger (Figure 5.4, solid circle).

As the C₁'-nicotinamide bond length is increased, the geometry about the reaction center flattens and the charges on both the ring oxygen and C₁' increase to a plateau value in all substrates. The energies and charge distributions in the activated complexes and IDCs fit the description¹¹ for structures expected to form by heterolytic cleavage of the ribosyl-nicotinamide bond.

For all compounds, the barriers between the IDC and complete dissociation k_d , Scheme 5.1, are lower (10-14.7 kcal/mol) than the barriers for cleavage of the ribosyl-nicotinamide bond (20.7-26 kcal/mol). Moreover, the barriers for the return reaction k_1 , Scheme 5.1 (3.3-5.4 kcal/mol) are lower than those for k_d . Because the barrier to proton transfer is generally lower than the barrier to complete dissociation,¹³ and because the ribosyl zwitterions would be expected to collapse with no barrier,¹² neither of the mechanisms that form neutrals is rate limiting. Therefore, the rate-limiting step is cleavage of the ribosyl-nicotinamide bond.

Structures of Oxocarbenium Ions and the Site of Protonation of Nicotinamide. In Schemes 5.1 and 5.2, we have drawn the structures of the oxocarbenium ions as ring structures and Nic-H⁺ as the ring N-protonated species, when in fact we know with certainty only the value of m/z. It is possible that the ring structures could open to give O=CH-CHY-CH(OH)-CH(+)CH₂OH that by nicotinamide-catalyzed β -elimination could give one (or both) of two enols, O=CH-CHY-CH(OH)=CHCH₂OH or O=CH-CHY-CHOH-CH=CHOH.¹⁴ When the cyclic form of the oxocarbenium ions are opened and minimized in MM+, linear carbenium ions result. When these structures are minimized in AM1, however, they return through rather convoluted pathways back to the cyclic oxocarbenium ion structures (in the [C=O-C]⁺ canonical form). Computationally, at least, the cyclic oxocarbenium structures are more stable than the open-chain forms of the cations. This is not surprising because oxygens α to cationic centers confer an enormous amount of stabilization energy, even in ring structures.¹²

There are two sites of protonation on the nicotinamide, the ring nitrogen and the amide carbonyl. The AM1 ΔH_f for the two protonated species show that the ring N-protonated species is 4.3 kcal/mol more stable than the O-protonated form (150.1 vs. 154.4 kcal/mol, respectively). As discussed above, in several of

the IDCs there is a hydrogen bond between the amide carbonyl and the 5'OH proton, which could lead to concerted removal of a proton during dissociation (for **1b,d**) or favor O-protonation within the IDC (**1b,c,d**). We argue below that concerted proton abstraction in **1d** is inconsistent with the experimental results. Because of the regular, monotonic change in Nic-H^+ along the series, which includes two structures in which there is no apparent hydrogen bond between the amide carbonyl and the 5'-OH proton (**1a,e**), we suspect that the site of protonation in Nic-H^+ is relatively unimportant; the important point is that proton transfer occurs at all. It is also highly probable that *all* of the hydrogen bonds structures are an artifact of the AM1 method; no hydrogen-bonded structures were seen in the PM3 structures.

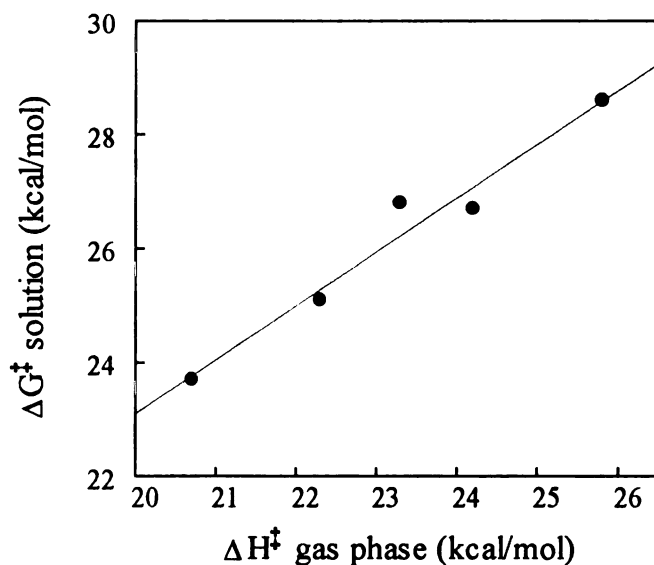


Figure 5.7. Plot of ΔG^\ddagger for the hydrolysis of **1a-e** (Ref. 19) vs. the AM1-calculated values of ΔH^\ddagger ($r = 0.980$). Left to right the points are for $Y = \text{H}, \text{NH}_2, \text{OH}, \text{NAc}, \text{and F}$.

Correlation with Solution Activation Values. There is a crude correlation ($r = 0.919$, not shown) between ΔH^\ddagger for the solution and gas-phase dissociations;

Handlon¹⁵ found a similar crude correlation between the rates and enthalpies for the solution reaction. Assuming that $-T\Delta S^\ddagger$ is constant for this series in the gas phase, a plot of the solution ΔG^\ddagger vs. the gas phase ΔH^\ddagger should represent a direct linear free energy relation (LFER); this plot (Figure 5.7) is linear ($r = 0.994$, slope = 0.94) and shows that the relative effects of substituents on the dissociation reaction are independent of the phase. The absolute correlation, of course, would depend on the entropies for the gas phase, which are not available.

Discussion

In comprehensive reviews, Morton^{16,17} has presented compelling evidence that radical cations and some even-electron ions such as protonated ethers¹⁸ dissociate in the gas phase through IDCs, which are equivalent to a contact ion pair in the Winstein scheme.¹⁹ Heterolysis ($RX^+ \rightarrow R^+ + X^0$) is favored over homolysis ($RX^+ \rightarrow R\cdot + \cdot X^+$) if the charge remains on the fragment that did not contain it initially. If R^+ is a stable carbenium ion, and X is an electronegative, polarizable group, as is the case with our substrates, heterolysis should be favored. Recently McAdoo and Morton¹⁷ pointed out that heterolytic cleavage favors formation of an IDC rather than simple dissociation of the fragments. Depending on the chemistry, proton transfers tend to take place more efficiently within IDCs than between members of a dissociative fragment pair.

In some ribosyl systems, concerted proton transfer during dissociation is possible. McCloskey and coworkers²⁰ have reported correlations between the solution and gas-phase dissociation of 7- and 9- β -D-ribofuranosyl-purines in chemical ionization mass spectra (CIMS). The relative abundances of these species (BH_2^+/M^+) correlate with the rate constants for hydrolysis (plot not shown; $r = 0.89$).²¹ Based on isotopic labeling experiments, these workers suggested that a prominent rearrangement of protonated purine nucleosides in CIMS occurs by

INCIDENT

heterolysis with concerted abstraction of a proton from an available sugar hydroxyl by a second heteroatom on the purine. The ribosyl zwitterion collapses to a neutral, bicyclic product. We performed transition state modeling (PM3) on deoxy adenosine and found that there is a hydrogen bond between the purine N3 and the 5'-OH proton during the entire course of glycosyl bond cleavage, which is consistent with a concerted mechanism of proton abstraction. No IDC would be formed during this bond cleavage.

Katritzky, *et al.*, have studied the gas-phase dissociation of pyridinium substrates²² and have reported the results of semi-empirical calculations (MNDO, AM1, and PM3) for dissociation of pyridinium substrates in which the structures of both the putative carbenium ions and pyridine leaving groups were varied.¹¹ Their results are consistent with dissociation to IDCs in the gas phase.

We have obtained tandem LSIMS spectra for a series of 4-substituted benzyl substrates with different pyridine leaving groups and of the corresponding substituted benzyl dimethylsulfoniums.²³ While results for the dimethylsulfonium compounds give an excellent Hammett plot [vs. σ^+], Hammett plots for benzyl substrates with nicotinamide, pyridine, 3-chloro, and 3-cyanopyridine leaving groups show a drastic downward break between 4-chloro and 4-nitro benzyl compounds. The MNDO-calculated energy profiles for the sulfonium series are well-behaved, reaction coordinate bond lengths at the transition state follow the Hammond Postulate, energies are consistent with an IDC intermediate, and the calculated values of ΔH^\ddagger correlate well with the gas-phase experimental results. We will discuss these results in Chapter 6.

Thus there are gas-phase results for precursors that give ribosyl oxocarbenium ions and for pyridinium and other charged substrates that are consistent with formation of an IDC as an intermediate in gas-phase dissociation. Despite the precedents, however, we are not sanguine about assigning a

mechanism for the dissociation of our compounds. We believe that a close analysis of our data for the NAc derivative **1d** shows the intermediacy of an IDC, and that the existence of a series of LFERs that correlate all the data strongly suggests that the entire series of compounds dissociates by the same mechanism. The computational results are consistent with our proposed mechanism.

Mechanism of Gas-Phase Dissociation. The most straightforward gas-phase mechanism is direct dissociation to the oxocarbenium ion and neutral nicotinamide. The presence of Nic-H⁺ rules out this mechanism, unless there is concerted proton transfer during dissociation. Based on the AM1 structures, this could occur only for the NAc compound **1d** because of the constant presence of a hydrogen bond between the amide carbonyl and the 5'-OH. If this occurred, however, the amount of Nic-H⁺ would be *greater than expected* relative to the correlation with the other compounds; the finding that the relative abundance of Nic-H⁺ is *much less than expected* rules out concerted dissociation and proton removal in the best case. As discussed above, however, the PM3 structures did not contain similar hydrogen bonds in either the starting, transition state, or IDC structures; the hydrogen-bonded structures may be an artifact of the AM1 method.

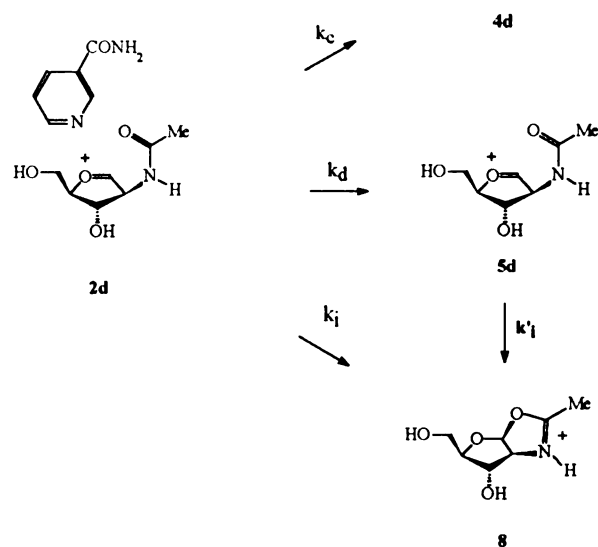
The relative abundance of Nic-H⁺ down the series 2'-H (most stable oxocarbenium ion) to 2'-F (least stable oxocarbenium ion) changes by only a factor of 1.75, while the relative abundance of the oxocarbenium ions changes by a factor of 17 (Table 5.1). Thus, according to the mechanism in Scheme 5.1, k_{-1} increases and k_1 and k_d decrease down the series, while k_c and/or k_c' remain essentially constant as expected for the relative stabilities of the IDCs and the oxocarbenium ions. These trends, while crude, are seen in the calculated enthalpies (Table 5.3).

The presence of Nic-H⁺ suggests that proton transfer occurs after the rate-limiting step. Partitioning of an IDC **2** between neutral and charged species can

occur by three processes (Scheme 5.1). Within the IDC, which should be a series of local minima of similar energy, nicotinamide can abstract a proton from the 5'-OH in **1a-e** and/or from the 2'-OH or 2'-NH₂ in **1b** and **1c** to give zwitterions that can collapse to neutrals. In all substrates when the 5'-OH proton is removed from the respective cation or IDC and minimized in AM1, the zwitterion collapses to the bicyclic structure **4**. The calculated ΔH_f for all bicyclic structures are within a narrow range (18.2-20.4 kcal/mol relative to the starting structure, Table 5.3).

For the 2'-OH and 2'-NH₂ substituents in **1b,c**, there are two possible mechanisms of collapse for the k'_c pathway: either initial abstraction of the proton with collapse of the respective zwitterion to a neutral, or direct cyclization to give the protonated aziridine **3c** or epoxide **3b**, from which the proton could be removed. The respective zwitterionic structures immediately collapse to the aziridine or epoxide on AM1 minimization. In contrast, AM1 minimization of the protonated aziridine or epoxide leads directly back to the cation, which eliminates this mechanism. In fact, collapse to either the aziridine or epoxide may not be energetically favorable. The values for the respective species listed in Table 5.3 show that the bicyclic structures **4b,c** are much more stable than either the aziridine **3c** ($\Delta H_f = 35.3$ kcal/mol) or the epoxide **3b** ($\Delta H_f = 39.1$ kcal/mol). The stability of ca. 15 kcal/mol of the bicyclic structures is the result of relief of ring strain relative to the cation. Formation of the neutral bicyclic structure relieves the strain about the reaction center, while formation of either the aziridine or epoxide retains the essentially flat geometry about the reaction center and introduces the additional strain of a three-membered ring. Thus the computational results suggest that proton abstraction and cyclization to **4a-e** should be an energetically favored processes, which is borne out by the relative abundances for Nic-H⁺ and oxocarbenium ions (Table 5.1). In general, separation of the IDC into a cation and a neutral species is a higher energy process than proton abstraction.¹³

While the total relative abundance of cationic species for the NAc derivative **1d** is within the expected range, the relative abundances of Nic-H⁺ and **5d**, **5** and **11**, respectively, are significantly different than the expected values of 13 and 3 obtained by extrapolation of the relative abundances of the respective species with the totals (not shown). While these data are consistent with an anchimeric assistance mechanism, this process cannot occur in the β -arabino configuration in which the NAc and the leaving group are *cis*. Solvolysis of α -nicotinamide 2'-NAc arabinoside and β -nicotinamide NAc riboside, in which the NAc group is *trans* to the leaving group, is anchimerically assisted. In solution this intermediate is sufficiently stable that both the *trans* ara and ribo configurations of **8** have been observed by ¹H-NMR during hydrolysis.^{2,15} The two substrates with the NAc group *cis* to the leaving group hydrolyze with rate constants that correlate with σ_I .



Scheme 5.2

Of the several possible cyclization pathways (Scheme 5.2), only one decreases Nic-H⁺ and increases the abundance of cations with *m/z* 174 (**5d** and **8**). A reasonable assumption would be that nicotinamide is forced to depart because of

ACCEPTED MANUSCRIPT

steric repulsion by the NAc group, although the bulk of substituents did not affect the kinetics of hydrolysis.^{2,15} The NAc group in **1d** is polarized, and in the IDC can swing into a position to collapse to **8**. When this structure is formed manually and minimized in AM1, the acylium ion **8** forms (Figure 5.8). In fact, the energies

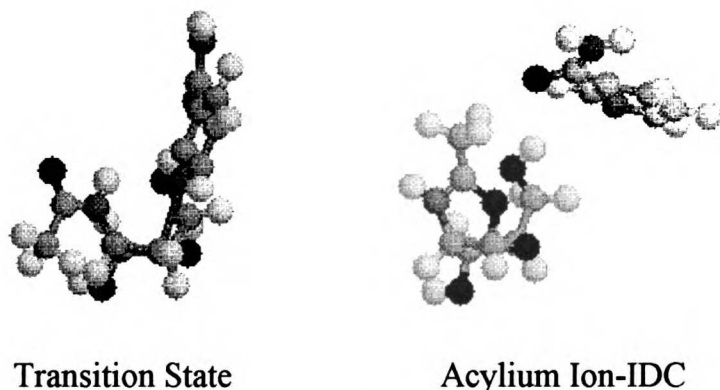


Figure 5.8. Change in structure between the transition state and cyclization to the acylium ion within the IDC for **1d** (Scheme 5.2). The nicotinamide ring has been forced up and away from the transition state position.

listed in Table 5.3 show that the acylium ion is more stable than the bicyclic structure (ΔH_f of 4.6 and 18.2 kcal/mol, respectively, relative to the starting structure). Thus, competition of NAc collapse with proton removal and cyclization within the IDC (k_i) would lower Nic-H^+ and give **8**, which is the effect observed (Table 5.1). We believe this interpretation is consistent with an IDC in the gas phase.

Substituent Effects/LFERs. Bagno and Scorrano²⁴ have suggested recently that substituent effects are better differentiated in solution than in the gas phase despite the well-known solvent attenuation (substantially lower values of ΔG° in solution) and that ρ values for gas-phase reactions should be clustered about unity, provided the LFERs are constructed with data for substituent effects determined in

the same system in the two phases. Both sets of substituent constants used to analyze our data were determined directly from either gas-phase⁹ (σ_F) or solution²⁵ (σ_I , 50% v/v EtOH/water) ionization of 4-substituted bicyclo[2.2.2]octane-1-carboxylic acids. Despite the different phases, the values of σ are essentially the same in both scales. (Bagno and Scorrano did not define a new σ scale in their work, but based their correlations on $\delta_X \Delta G$ values for ionization of aromatic systems such as phenols and anilines.)

The Taft plot of $\log (R^+/[R^+ + M^+])$ vs. σ_F is shown in Figure 5.1. The value of ρ_F of -0.75 is substantially less than the ρ_I of -6.7 for the solution reaction.² In solution, the k_{rel} for **1a** and **1e**, the extremes of the series, is 3500; in the gas phase, k_{rel} is 2.5. Thus the difference we find in the kinetic ρ values is similar to that found by Bagno and Scorrano for proton transfer equilibrium ρ values; the difference is related to the relative dissociation of the substrates and not to the substituent scales used. To our knowledge, this is the first kinetic correlation that shows this effect.

The correlation with substituent constants in each phase implies a correlation between gas-phase and solution dissociation, and a plot of $\log (R^+/[R^+ + M^+])$ vs. $\log k_w$ for hydrolysis of the substrates² (not shown) is linear ($r = 0.988$). A more direct free energy correlation is shown in 5.7, which is a plot of ΔH^\ddagger for the solution hydrolysis vs. ΔH^\ddagger calculated for gas-phase dissociation. This correlation assumes that for a group of substrates with very similar structures, the value of $-T\Delta S^\ddagger$ in the gas phase is relatively constant and is dominated by the entropy for dissociation and translation; vibrational and rotational entropies should be small and of comparable magnitude across the series.

Mechanisms in the Two Phases. The existence of a good correlation does *not* mean that we can infer the *mechanisms* in solution and the gas phase are the

same. For direct dissociation, the mechanisms in the two phases would be the same. The IDC mechanisms would not be precisely the same in the two phases because there can be no intermediate equivalent to a solvent-separated IDC in the gas phase. Substituents would affect the stabilities of both free oxocarbenium ions and IDCs in the same way, but to different extents. Linearity of LFERs over the entire range of substituents implies a constant mechanism, but this is not diagnostic of what the mechanism is. While the sign of ρ values is diagnostic of the charge that develops in the transition state relative to the ground state, the absolute values of ρ can span large ranges for a single mechanism that occurs in substrates of greatly different structure. Thus other evidence is needed to choose among alternative mechanisms.

Handlon¹⁵ found that the presence of up to 2M nicotinamide did not greatly affect the value of k_{obsd} for hydrolysis of 1a. The hallmark of an $S_{\text{N}}1$ mechanism is common leaving group suppression; the lack of this effect is indicative of an IDC mechanism, but cannot be used to distinguish between a contact or a solvent-separated pair as kinetically competent intermediates.¹⁹ Ta-Shma and Oppenheimer²⁶ have evidence from selectivity data in aqueous trifluoroethanol mixtures that the solvolysis of NAD^+ occurs through an IDC mechanism, with the IDC trapped at the solvent-separated stage.

Thus both the solution and gas-phase reactions occur through a mechanism that has an IDC intermediate. It is probable, however, that the rate-limiting step is different in the two phases. In solution it is interception of the solvent-separated IDC by solvent or nucleophile. As discussed above, the barrier to separation of the components of the IDC in the gas phase is low. In all substrates, the barrier to complete dissociation relative to the energy of the IDC is less than ΔH^\ddagger for bond cleavage. Thus in the gas phase the rate-limiting step is formation of the intermediate and not its dissociation. The existence of LFERs that correlate the

solution and gas-phase energies must then reflect the *relative* effect of the substituents on the kinetics in the two phases, but the existence of an LFER clearly does not indicate that the mechanisms are strictly the same.

References and Notes

- (1) Johnson, R.W.; Marshner, T.M.; Oppenheimer, N.J. *J. Am. Chem. Soc.* **1988**, *110*, 2257-2263.
- (2) Handlon, A.L.; Oppenheimer, N.J. *J. Org. Chem.* **1991**, *56*, 5009-5010.
- (3) Tarnus, C.; Schuber, F. *Bioorg. Chem.* **1987**, *15*, 31-42; Tarnus, C.; Muller, H.M.; Schuber, F. *ibid.*, **1988**, *16*, 38-51.
- (4) Handlon, A.L.; Xu, C.; Müller-Steffner, H.-M.; Schuber, F.; Oppenheimer, N.J. *J. Am. Chem. Soc.* **1994**, *116*, 12087-12088.
- (5) Sleath, P.R.; Handlon, A.L.; Oppenheimer, N.J. *J. Org. Chem.* **1991**, *56*, 3608-3613.
- (6) AM1:Dewar, M.J.S.; Zoebisch, E.G.; Healy, E.F.; Stewart, J.J.P. *J. Am. Chem. Soc.* **1985**, *107*, 3902-3909. PM3:Stewart, J.J.P. *J. Comp. Chem.* **1989**, *10*, 209-220.
- (7) McIver, J.W., Jr.; Komornicki, A. *Chem. Phys. Lett.* **1971**, *10*, 303-306.
- (8) The 2'-azido substrate reported in Ref. 2 did not give a peak corresponding to the oxocarbenium ion and was not included in this analysis.
- (9) Taft, R.W.; Topsom, R.D. *Prog. Phys. Org. Chem.* **1987**, *16*, 2-83.
- (10) Thomas Slee of Hypercube confirms that this use of the Vibrational Analysis subroutine is valid for these calculations.
- (11) Katritzky, A.R.; Malhotra, N.; Ford, G.P.; Anders, E.; Tropisch, J.G. *J. Org. Chem.* **1991**, *56*, 5039-5044.
- (12) Schröder, S.; Buckley, N.; Oppenheimer, N.J.; Kollman, P.A., *J. Am. Chem. Soc.* **1992**, *114*, 8231-8238.

(13) Bowen, R.D. *Acc. Chem. Res.* **1991**, *24*, 364-371.

(14) We thank John Bartmess for pointing out this possibility.

(15) Handlon, A.L.; Oppenheimer, N.J., in preparation.

(16) Morton, T.H. *Tetrahedron* **1982**, *38*, 3195-3243.

(17) McAdoo, D.J.; Morton, T.H. *Acc. Chem. Res.* **1993**, *26*, 295-302.

(18) Kondrat, R.W.; Morton, T.H. *J. Org. Chem.* **1991**, *56*, 952-957.

(19) Carpenter, B.K. *Determination of Organic Reaction Mechanisms*, Wiley-Interscience: New York, 1984, pp. 40-49, gives an excellent brief review of the Winstein ion-pair scheme.

(20) (a) McCloskey, J.A.; Futrell, J.H.; Elwood, T.A.; Schram, K.H.; Panzica, R.P.; Townsend, L.B. *J. Am. Chem. Soc.* **1973**, *95*, 5762-5764. (b) Wilson, M.S.; McCloskey, J.A. *J. Am. Chem. Soc.* **1975**, *97*, 3436-3444. (c) McCloskey, J.A. *Acc. Chem. Res.* **1991**, *24*, 81-87.

(21) We determined these r values from plots of $\log k_{\text{hydrolysis}}$ vs. $\log [\text{BH}_2^+/\text{M}^+]$ reported in Ref. 20a. If nebularine is included in the analysis for the 7-substituted compounds, $r = 0.69$.

(22) Katritzky, A.R.; Watson, C.H.; Dega-Szafran, Z.; Eyler, J.R. *J. Am. Chem. Soc.* **1990**, *112*, 2471-2478.

(23) Buckley, N.; Maltby, D.; Burlingame, A.L.; Oppenheimer, N.J., submitted (Chapter 6).

(24) Bagno, A; Scorrano, G. *J. Chem. Soc. Perkin Trans. 2* **1991**, 1601-1606.

(25) Charton, M. *J. Org. Chem.* **1964**, *29*, 1222-1227.

(26) Ta-Shma, R.; Oppenheimer, N.J., in preparation.

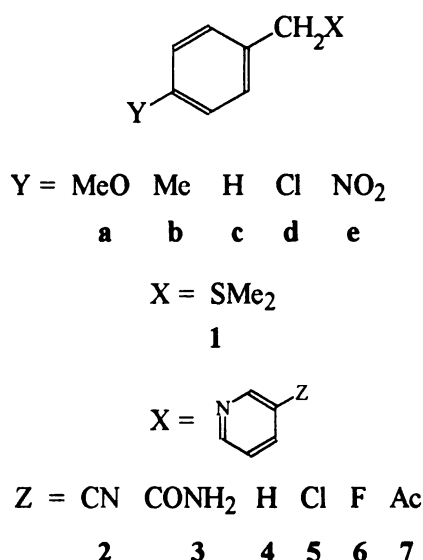
Chapter 6
Gas-Phase Dissociation of
(4-Substituted Benzyl) Dimethylsulfoniums and Pyridiniums

157

Introduction

As part of continuing studies on the cleavage of the nicotinamide-ribose bond in β -nicotinamide adenosine dinucleotide (NAD⁺),¹ we recently reported the results of a study of the gas-phase dissociation of a series of 2'-substituted β -nicotinamide arabinosides.² The relative rates of dissociation, measured by tandem positive-ion liquid secondary ion mass spectrometry (LSIMS), follow the Taft equation and correlate with the relative rates for the dissociation in water.³ An analysis of the product ratios and the AM1 energy profiles for dissociation of the nicotinamide-ribose bond show that an ion-dipole complex (IDC) intermediate is involved. Rearrangements within the IDC that occur after the rate-limiting step are readily explained by the relative energies of the possible products. The system is complex, but easily understood.

The hydrolysis and nucleophilic substitution reactions of benzyl dimethylsulfoniums (**1**) have been interpreted in terms of an IDC mechanism.⁴ The



kinetics of the nucleophilic substitution reactions of the (4-MeO-benzyl) dimethylsulfonium (**1a**) with a large number of nucleophiles and added salts have been measured.⁵ **1a** reacted only with nucleophiles of intermediate hardness and

not with hard or soft nucleophiles. The hydrolysis reaction is complicated by the establishment of an equilibrium among starting material and products.⁶

Nonetheless, it is clear from the kinetics and the selectivities that the reaction is mixed S_N1/S_N2 under constant ionic strength. Kevill and his colleagues⁷ have reached the same conclusion independently. Hammett plots for the azide reaction and hydrolysis show distinct breaks, but are not V-shaped.

The kinetics of the reaction between azide and **2-4a-e** in water have been measured.⁸ The reactions are strictly S_N2 with no borderline behavior and no evidence for an IDC intermediate, despite the fact that there is an enormous amount of bond breaking in the activated complex ($\beta_{LG} = 1.4-1.6$). The rates for the hydrolysis reactions of **2a-e** are quite slow compared with the rates for the azide reaction, but the rates of the two reactions are comparable for **3a-e**. The Hammett plots for hydrolysis of **2-3a-e** are linear but have different slopes. While **4a,e** react very slowly with azide, **4b-d** did not react with either water or 2M azide after 6 months at 96°C.

In contrast, Katritzky and his colleagues⁹ found that the reactions between 4-substituted benzyl substrates with highly arylated pyridine LGs and neutral amine nucleophiles in solvent chlorobenzene exhibited borderline kinetic behavior for the 4-MeO-benzyl compounds but not for substrates with less electron donating substituents. These results were interpreted in terms of an IDC mechanism, which was supported by the results of ion cyclotron resonance (ICR) experiments^{10,11} and a computational study.¹²

These wildly different results prompted us to examine the gas-phase dissociation of **1a-e** and four series of benzyl pyridiniums (**2-5a-e**) with tandem LSIMS. Energy profiles for the dissociation of **1a-e** and **4a-e** were calculated using MNDO and AM1, respectively. Hammett plots based on relative rates for gas-phase and solution dissociation of **1a-e** and **2-5a-e** show differences among and

between the two series in both phases. The results are supported by thermodynamic stabilities calculated for model systems.

Experimental Section

General. All chemicals and solvents were obtained from Aldrich and used without further purification. NMR spectra were recorded in D₂O at 300 MHz.

Synthesis. All substrates were prepared by mixing 1 eq. of the appropriate benzyl chloride with 1.1 eq. of either SMe₂ or the appropriate pyridine in chloroform at ambient temperature. Reactions were followed by TLC (silica, neat chloroform) until all chloride had disappeared. The chloroform layer was extracted with water, and the aqueous layer was back extracted extensively with chloroform and then with ether to give water-white solutions. Rotary evaporation at reduced pressure with repeated flashing with ethanol to remove traces of water gave products that were >95% pure by proton NMR. For several of the 3-CN-pyridine substrates, the alkylation was performed by adding the chloride to a melt of the pyridine, which was held in a drying oven at ca. 110°C for 10-20 min. After cooling, the (usually dark brown) solid was dissolved in water and carried through the extraction procedure. Heating the water layer with Norit A and filtering through a pad of Filtre-Aid, followed by evaporation, gave pure compound. All compounds are known with various counterions and were characterized only by proton NMR and LSIMS.

LSIMS Spectra. Tandem mass spectra were recorded under identical conditions in the positive ion mode on a 4-sector Kratos Concept II HH mass spectrometer fitted with an optically coupled 4% diode array detector on MS II. Substrates were sputtered from a glycerol matrix with Cs⁺ (18 keV), and the

molecular ion was sorted into MSII where fragmentation was induced by collisional activation with helium (13eV). Seven to 10 determinations were collected and averaged in the computer (<5% error).

Computational Methods. MNDO, AMI, and PM3¹³ calculations were performed as described in Chapter 6. Initial structures were built using the default model builder and minimized with MM+ (Hyperchem's version of MM2) using the partial charge option. The Polak-Ribiere block diagonal algorithm was used for all minimizations to an RMS gradient of <0.1 kcal/[Å mol]. Semi-empirical calculations were unrestricted Hartree-Fock with the wavefunction calculated to a convergence limit of <0.001. To construct the energy profiles, the benzyl-C7-LG bond length was increased in steps from the initial length (1.80-1.83Å for sulfoniums, 1.49-1.52 Å for pyridiniums) using the restraint function to a final restraint force constant of 10⁵. Each structure was minimized completely with no restraint other than the reaction coordinate. Transition state structures were refined until a single negative (imaginary) frequency¹⁴ was obtained using the Vibrational Analysis subroutine. Energies of the carbenium ions were calculated after manual removal of the LG from the IDC.

For the norcaradienyl carbenium ions (9), structures were formed from the corresponding benzyl carbenium ions (8) and minimized in MM+ before being fully minimized in AM1.

Results

Experimental

LSIMS Results. LSIMS spectra obtained in MSII had two peaks that corresponded to the parent molecular ion M⁺ and the respective benzyl carbenium ion R⁺. The relative rates for dissociation were obtained as the ratio of the relative

UNIVERSITY OF TORONTO

abundances $[R^+ / (R^+ + M^+)]$, with $M^+ \equiv 100$. These values are summarized in Table 6.1. Because the average error in the measurements is $<5\%$, in plots of these data the error bars are within the symbols.

Table 6.1. $\log [R^+ / (R^+ + M^+)]$ for the Gas-Phase Dissociation of (4-Y-benzyl) Dimethylsulfoniums and 3-Z-Pyridiniums

LG/Y	MeO	Me	H	Cl	NO ₂
SMe ₂	-0.78	-1.06	-1.23	-1.14	-1.71
3-CN-Py	-0.95	-1.05	-1.14	-1.16	-1.83
3-Cl-Py	-0.95	-1.07	-1.15	-1.21	-1.89
Nicotinamide	-1.00	-1.11	-1.21	-1.20	-2.05
3-H-Py	-0.99	-1.25	-1.29	-1.31	-2.30

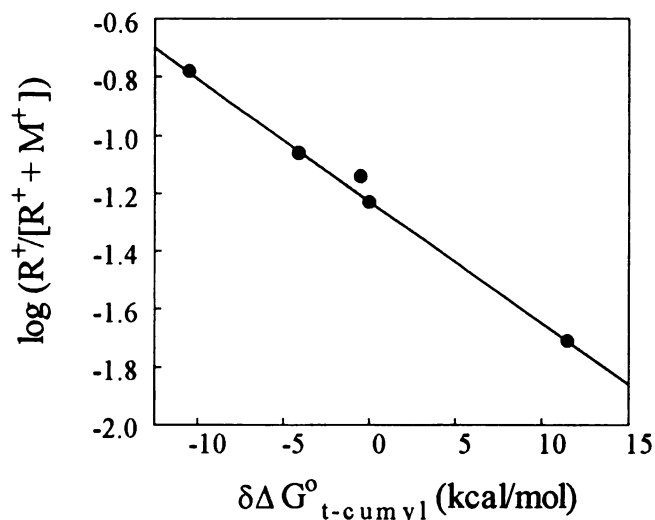


Figure 6.1. Plot of the LSIMS data for **1a-e** vs. the relative free energy for gas-phase formation of *t*-cumyl carbenium ions. The point off the line is for **1d**; the regression line is for the other points with a slope of $\gamma^{+} = -0.042$ ($r = 0.9999$). With the point for **1d** included, $r = 0.996$. Left to right the points are for **1a**, **1b**, **1d**, **1c**, and **1e**.

ACCEPTED MANUSCRIPT

Linear Free Energy Relations (LFERs). Because it is advisable to use a scale derived from gas-phase data, Hammett plots of $\log [R^+ / (R^+ + M^+)]$ for **1a-e** (Figure 6.1) and **2-5a-e** (Figure 6.2) were constructed vs. $\delta\Delta G^\circ_{t\text{-cumyl}}$ for the gas-phase reaction $4\text{-Y-C}_6\text{H}_4\text{-C}(\text{Me})=\text{CH}_2 + \text{H}^+ \rightleftharpoons 4\text{-Y-C}_6\text{H}_4\text{-CMe}_2^+$; values have been summarized by Taft and Topsom.¹⁵ (The $\delta\Delta G^\circ_{t\text{-cumyl}}$ and σ^+ scales correlate well; for substituents **1a-c,e**, $r = 0.9999$ with a slope of 14.) The plots are clearly different, with good linearity for the sulfoniums and a distinct break for the pyridiniums. The slopes " γ^+ " are -0.042 ($r = 0.99999$ with the point for **1d**

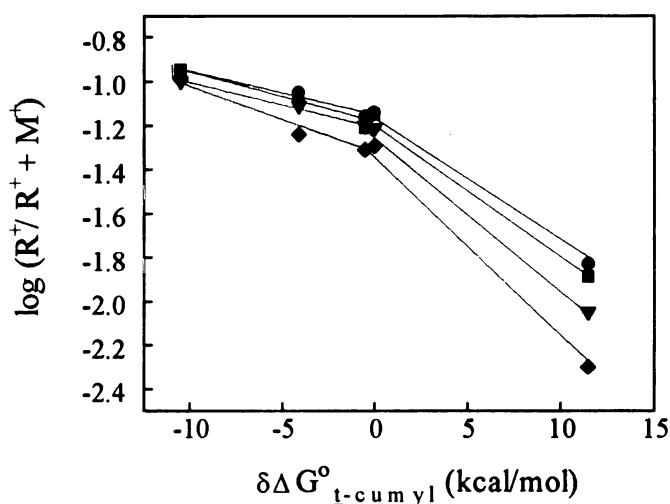


Figure 6.2. Plots of the LSIMS data for **2a-e** (●), **3a-e** (■), **4a-e** (▼), and **5a-e** (◆) vs. the relative free energy for gas-phase formation of *t*-cumyl carbenium ions. Left to right the points are for **a-e**. The slopes of " γ^+ " are: **2 a-d** = 0.020 ($r = 0.98$), **3 a-d** = 0.022 ($r = 0.96$), **4 a-d** = 0.020 ($r = 0.996$), and **5 a-d** = 0.030 ($r = 0.97$).

excluded, $r = 0.9964$ with the point for **1d** included) for **1a-e**, and -0.020 ($r = 0.983$), -0.022 ($r = 0.960$), -0.020 ($r = 0.996$), and -0.030 ($r = 0.970$) for **2a-d**, **3a-d**, **4a-d**, and **5a-d**, respectively. (Hammett plots for **1a-e** and **2a-d** against σ^+ are shown in Figures 6.8 and 6.10 with the data for hydrolysis.)

For Brønsted plots of the experimental data for the four complete series of pyridiniums, with additional points for **6a,e** and **7a,e**, $\log [R^+ / (R^+ + M^+)]$ was

UNIVERSITY OF TORONTO

plotted vs. values of $\delta\Delta G_{\text{Py}}^{\circ}$ for the gas-phase protonation of pyridines¹⁵ (Figure 6.3). The value for nicotinamide is not available, but was estimated by

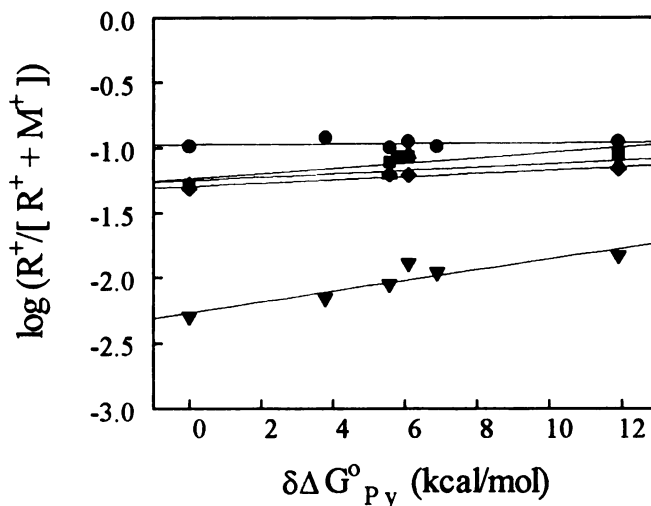


Figure 6.3. Plots of the LSIMS data for 2-7a (●), 2-5b (■), 2-5c (▲), 2-5d (◆), and 2-7e (▼) vs. the relative free energy for gas-phase protonation of the respective pyridine LGs. Slopes for the a-d compounds are 0.01-0.04, and for the e compounds is 0.12.

interpolation against solution pK_{a} values, which assumes that the effects are constant between the gas phase and solution. (Brønsted plots for some of the calculated values were constructed using water pK_{a} values.) For 2-7a and 2-5b-d, plots are grouped together and have small slopes; for 2-7e, however, there is a definite slope, which corresponds to the pattern seen for the spread of points for 2-5e in Figure 6.2.

Computational

Sulfoniums. The general energy profile for gas-phase dissociation is shown in Scheme 6.1. The PM3 and AM1 energy profiles had no distinct transition states (not shown). MNDO profiles, however, showed distinct transition states and IDCs for 1a-e (Figure 6.4). Values for the various energies are listed in Table 6.2; the activation values obtained from these energies are summarized in Table 6.3. With

UNIVERSITY OF TORONTO

Table 6.2. Enthalpies of Formation for the Gas-Phase Dissociation of (4-Y-Benzyl) Dimethylsulfoniums (MNDO) and Pyridiniums (AM1) (kcal/mol)

	Starting Structure	Transition State	Ion-Dipole Complex	Carbenium Ion	
SMe₂/MNDO					
	MeO	143.3	151.9	147.0	168.0
	Me	176.5	189.4	168.8	208.4
	H	184.6	198.3	209.8	217.9
	Cl	180.4	195.4	193.5	215.4
	NO ₂	209.1	228.2	228.1	250.8
Pyridine/AM1					
	MeO	170.3	201.0	197.6	173.0
	Me	201.0	234.8	233.4	209.6
	H	209.8	245.1	244.6	221.9
	Cl	204.5	239.9	239.1	216.1
	NO ₂	221.8	--	--	243.9

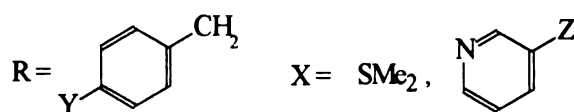
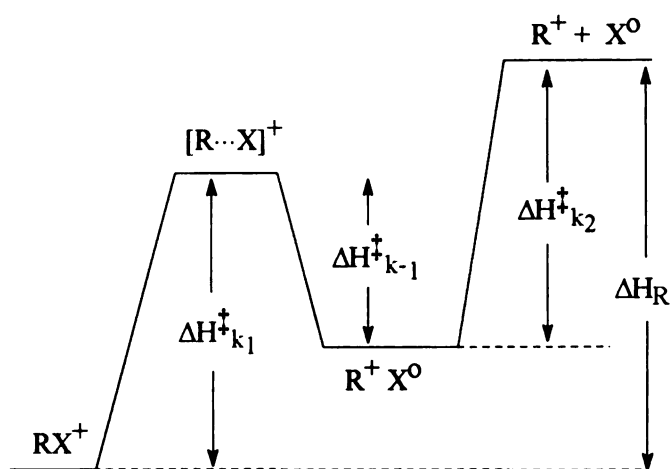
ΔH_f SMe₂ = -17.1 kcal/mol (MNDO); ΔH_f pyridine (AM1) = 31.9 kcal/mol.
Designations refer to Scheme 6.1.

Table 6.3. Activation Enthalpies and Enthalpies of Reaction for the Gas-Phase Dissociation of (4-Y-Benzyl) Dimethylsulfoniums (MNDO) and Pyridiniums (AM1) (kcal/mol)

	ΔH^\ddagger k ₁	ΔH^\ddagger k ₋₁	ΔH^\ddagger k ₂	ΔH_R	
SMe₂/MNDO					
	MeO	8.5	4.5	3.9	7.6
	Me	12.9	2.6	4.5	14.8
	H	13.7	2.2	4.7	16.2
	Cl	15	1.9	4.8	17.9
	NO ₂	19.7	0.7	5.6	24.6
Pyridine/AM1					
	MeO	30.7	3.4	7.3	34.6
	Me	33.8	1.4	8.2	40.5
	H	35.5	0.8	9.2	44.0
	Cl	35.4	0.5	8.9	43.5
	NO ₂	--	--	--	54

Designations refer to Scheme 6.1.

UNIVERSITY OF TORONTO



$$\Delta H_{k_1}^\ddagger = \Delta H_f [\text{transition state}] - \Delta H_f [\text{starting structure}]$$

$$\Delta H_{k-1}^\ddagger = \Delta H_f [\text{transition state}] - \Delta H_f [\text{IDC}]$$

$$\Delta H_{k_2}^\ddagger = (\Delta H_f [\text{cation}] + \Delta H_f [\text{LG}]) - \Delta H_f [\text{IDC}]$$

$$\Delta H_R = (\Delta H_f [\text{cation}] + \Delta H_f [\text{LG}]) - \Delta H_f [\text{starting structure}]$$

Scheme 6.1

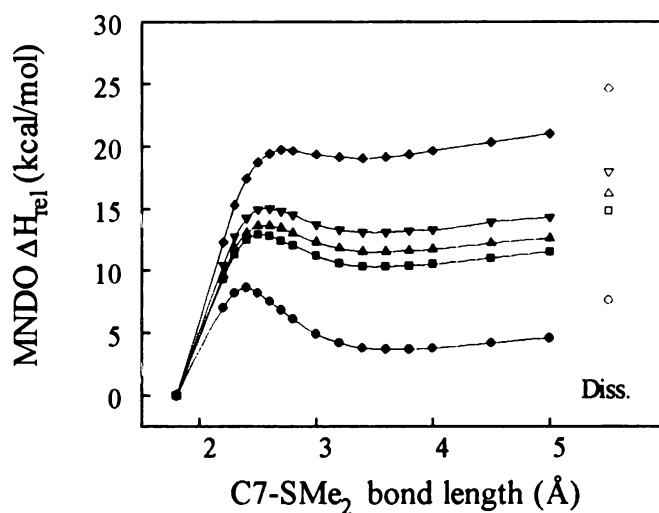


Figure 6.4. MNDO energy profiles for the gas-phase dissociation of **1a** (●), **1b** (■), **1c** (▲), **1d** (▼), and **1e** (◆). The open symbols are values for ΔH_R for complete dissociation of the carbenium ion and LG. Note the steady increase of the bond length at the transition state along the series.

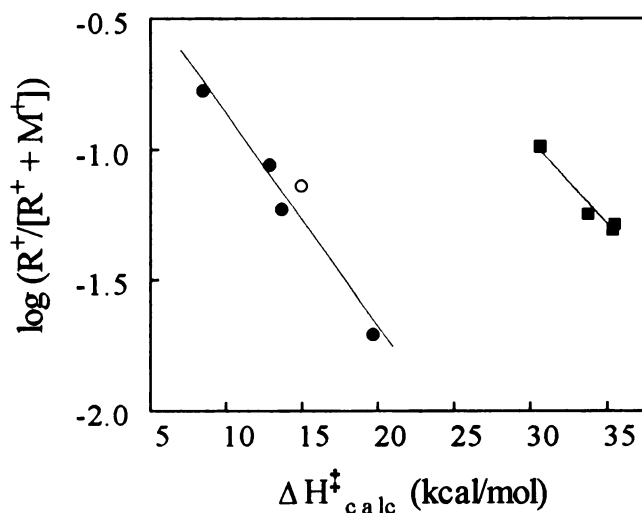


Figure 6.5. Plots of the LSIMS data vs. the MNDO ΔH^\ddagger for **1a-e** (●) and the AM1 ΔH^\ddagger for **2a-d** (■). The regression line through ● (**1a,b,c,e**) has $r = 0.993$; with the point for **1d** ○ included, $r = 0.970$. The regression line for **2a-d** has $r = 0.980$.

the exception of the point for the 4-Cl compound **1d**, there is a good correlation between the experimental data and the calculated values of ΔH^\ddagger (Figure 6.5).

Pyridiniums. Because there is little effect of the LG on the experimental data, complete energy profiles were calculated only for **4a-e**, which is the simplest pyridinium computational system. To illustrate various points, profiles were calculated for several other 4-MeO-benzyl substrates with different pyridine leaving groups (LGs).

Our results agree with those reported by Katritzky, et al.,¹² that the PM3 energy profiles for pyridiniums have no distinct transition states (not shown; the profile for **4c** has been reported²). In AM1, profiles for **4a-d** had distinct transition states, but the profile for **4e** was consistent with dissociation without an IDC (Figure 6.6). We calculated several profiles for various pyridiniums in MNDO and found that the energies were several kcal/mol lower than found for AM1; the MNDO profile for **4c** has been reported.² Values for the various energies are listed in Table 6.2; the activation values obtained from these energies are summarized in Table 6.3. There is a good correlation between the data for **4a-d** and the calculated

values of ΔH^\ddagger (Figure 6.5); because no transition state was found, **4e** is not included.

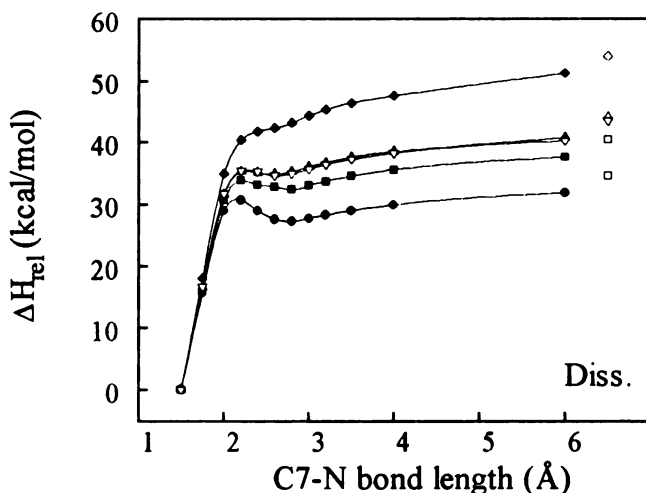


Figure 6.6. AM1 energy profiles for the gas-phase dissociation of **5a** (●), **5b** (■), **5c** (▲), **5d** (▽, shown open for clarity), and **5e** (◆). The open symbols are values for ΔH_R for complete dissociation of the carbenium ion and LG. The bond length at the transition state is relatively constant at ca. 2.2 Å.

There is an excellent correlation between ΔH^\ddagger and ΔH_R for the sulfoniums and pyridiniums (Figure 6.7), in accord with the Hammond postulate.¹⁶

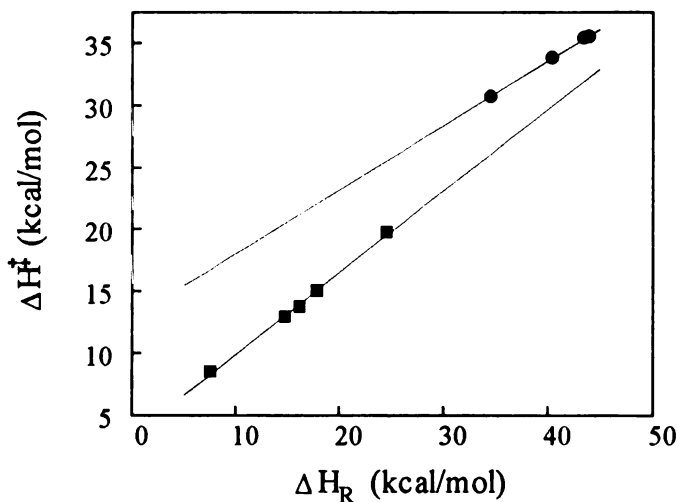


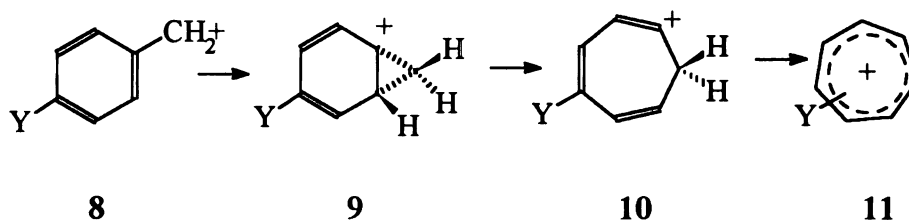
Figure 6.7. Plots of the calculated ΔH^\ddagger vs. ΔH_R for **5a-d** (AM1 values, ●) and **1a-e** (MNDO values, ■). Slopes are 0.54 for **5a-d** and 0.66 for **1a-e**; $r = 0.999$ for both lines.

UNIVERSITY OF TORONTO

Discussion

The lowest energy path for dissociation of a charged species that contain a potentially stable carbenium ion and a polarizable, electronegative LG is formation of an IDC.¹⁷ Katritzky has presented evidence from ICR measurements that simple¹⁰ and sterically crowded¹¹ benzyl pyridiniums dissociate in the gas phase through an IDC mechanism. In our work on the gas-phase dissociation of β -nicotinamide arabinosides,² we found that proton transfer reactions and cyclizations that led to neutrals and protonated nicotinamide, or direct cyclization to low-energy charged species, occur within an IDC. Thus there is ample evidence that gas-phase dissociation of charged substrates occurs through an IDC mechanism. Our results for benzyl sulfoniums and pyridiniums are consistent with this general mechanism, although there are differences between and among the series. There are also differences between the unimolecular reactions in the gas phase and the hydrolyses that emphasize the importance of solvation as it affects mechanism.

Before we discuss these results, however, it is necessary to address the question of the fate of the benzyl carbenium ions (8), which may rearrange to tropylium carbenium ions (11) in the gas phase [Scheme 6.2].¹⁸ Values of ΔH^\ddagger



Scheme 6.2

calculated for heterolytic cleavage of the benzyl methylene-pyridine bond would not be affected by rearrangements that take place in the IDC after bond cleavage. Our experimental results, however, depend on the relative abundances of the

parent molecular ions and carbenium ions, and the stabilities of the carbenium ions is therefore of some importance.

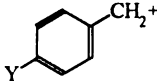
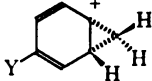

Katritzky^{10,11} measured the appearance potentials (APs) for carbenium ions formed by collisional activation of laser-desorbed 4-Y-substituted benzyl pyridiniums. Because of a correlation between the APs and AM1 values of ΔH_R for benzyl, but not for tropylium, carbenium ions formed from simple, unhindered pyridiniums, Katritzky¹⁰ argued that no benzyl-to-tropylium rearrangement took place within the IDC (although the 4-Br and 4-Cl compounds may have undergone this rearrangement; but see Ref. 21). For highly hindered 4-Y-substituted benzyl substrates (Y = MeO, Me, H, F, Cl, NO₂) with 2,4,6-triphenylpyridinium LGs, however, he¹¹ argued that the measured APs and the calculated AM1 ΔH_R were consistent with benzyl-to-tropylium rearrangements within the IDC. While the correlations between AP and the AM1 ΔH_R for dissociation to either tropylium or benzyl carbenium ions are not good (Figure 1 of Ref. 11), using the published values for the APs ΔH_R , we found that the correlation is measurably better for the benzyl energies ($r = 0.90$) than for the tropylium energies ($r = 0.82$) in plots of AP vs. ΔH_R (not shown). If the points for 4-NO₂ and 4-H are ignored, the correlation coefficients are 0.94 and 0.95 for benzyls and tropyliums, respectively, which reflects the effects of the substituents on the stabilities of the carbenium ions, not on the ability of the benzyls to rearrange. By themselves, these fits of data and computed energies show that the benzyl carbenium ions are stable within the IDC for both groups of pyridine LGs.

Dewar and his colleagues have calculated the barriers to isomerization of benzyl¹⁹ and substituted benzyl²⁰ carbenium ions into the corresponding tropylium carbenium ions through the sequence shown in Scheme 6.2. In MINDO/3, the barrier for **8** \rightarrow **11** is ca. 33 kcal/mol. While we did not determine the activation barriers, we calculated ΔH_R in AM1 (Table 6.4) for the conversion **8** \rightarrow **9**. The 4-

UNIVERSITY OF TORONTO

MeO-norcaradienyl carbenium ion **9** reverts to the 4-MeO-benzyl carbenium ion upon minimization; the other compounds have values of ΔH_R 4 to 6 fold greater than ΔH^\ddagger for dissociation of the IDC into the carbenium ion and the LG. The sequence **9** \rightarrow **10** \rightarrow **11** would require more energy; ΔH_f for the tropyliums in PM3 are 10-20 kcal greater than the corresponding MINDO/3 values,^{20a} which suggests that the total energy of conversion would be 40-50 kcal/mol, assuming--crudely--simple additivity between the methods. This energy profile suggests that diffusion apart of the LG and carbenium ion is the lower energy pathway. Moreover, if benzyl carbenium ions other than the 4-MeO- isomerized to tropylium ions

Table 6.4. AM1 ΔH_f and ΔH_R , from the Pyridiniums, of (4-Y-Substituted) Benzyl, Norcaradienyl, and Tropylium Carbenium Ions (kcal/mol)

Y			
	8	9	11
ΔH_f			
MeO	173.0	173.0	167.7
Me	209.6	262.4	200.7
H	221.9	271.3	210.3
Cl	216.1	269.2	207.9
NO ₂	243.9	291.3	233.3
ΔH_R			
MeO	34.6	34.6 ^a	29.3
Me	40.5	93.3	31.6
H	44.0	93.4	23.4
Cl	43.5	96.6	35.3
NO ₂	54.0	101.4	43.9

^aReverts to the benzyl carbenium ion upon minimization.

in our systems, a break between the energies for **1-5a** and the other compounds would be expected; there is none. Note that the break at the 4-NO₂ compound for the pyridiniums **2-5** is not the result of an isomerization. First, if this were the case

the line in Figure 6.2 should break up, not down. Second, it has been estimated that the energies for the isomerization of the 4-MeO and 4-NO₂ benzyl carbenium ions are the same.^{18a} Thus we are confident that the benzyl carbenium ions do not rearrange in the sulfonium and pyridinium IDCs under our experimental conditions.

Sulfoniums

Gas-Phase Dissociation. The Hammett plot of $\log [R^+ / (R^+ + M^+)]$ against $\delta\Delta G^\circ_{t\text{-cumyl}}$ (or σ^+ , see Figure 6.8; $\rho^+ = -0.57$) is linear and indicates a single mechanism for dissociation (Figure 6.1). The MNDO energy profiles (Figure 6.4) are consistent with the formation of an IDC after rate-limiting cleavage of the benzyl methylene-sulfur bond. Moreover, the length of the benzyl methylene-sulfur bond at the transition state increases smoothly from 2.3Å for **1a** to 2.7Å for **1e** in excellent agreement with the Hammond Postulate.¹⁶ The MNDO values for the ΔH^\ddagger of bond cleavage correlate with the experimental data for dissociation (Figure 6.5). The calculated ΔH_f for the IDC and cations, ΔH_R for all substrates, and the ΔH^\ddagger for the various processes shown in Scheme 6.1 all correlate with $\delta\Delta G^\circ_{t\text{-cumyl}}$ and σ^+ (none shown).²¹ In the mass spectrometer and the computer, this is a very well-behaved system in which heterolytic cleavage occurs with full resonance participation by the electron-donating substituents, including Cl.

Dissociation in Water. The Hammett plot (vs. σ^+) for the hydrolysis in pure water (no added salt) of a series of 3- and 4-substituted benzyl dimethylsulfonium substrates²² shown in Figure 6.8 has the break between **1a** and **2a** typically found for the solvolysis and substitution reactions of neutral benzyl substrates.²³ It was reported recently⁶ that this break does in fact indicate a change in mechanism from S_N1 for the 4-MeO compound to S_N2 for compounds with 4-substituents with

UNIVERSITY OF TORONTO

$\sigma^+ > -0.31$. Kevill and his colleagues⁷ have reached the same conclusion independently.

On the basis of a study of the substitution reactions of a large series of substituted benzyl halides, Richard and Yeary²⁴ have suggested recently that "virtually all" Hammett plots for benzyl substrates that show breaks are the result

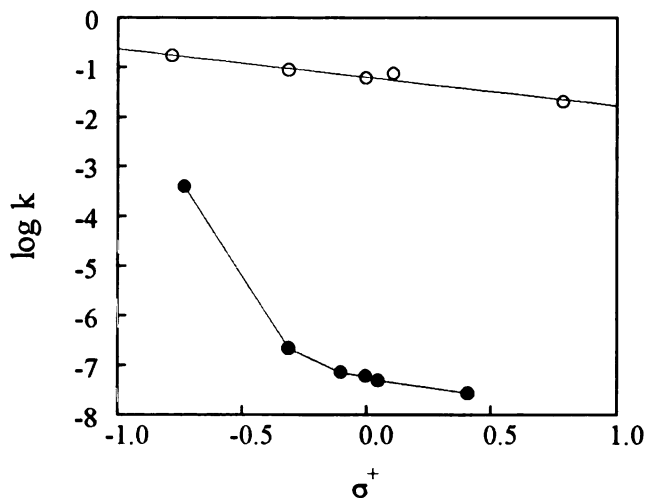


Figure 6.8. Plots of the gas-phase relative rates ($k = R^+/[R^+ + M^+]$, O) for **1a-e** and the hydrolysis rate constants at 70°C for **1a,b,c** and the (3-Me-benzyl)- and (3-Br-benzyl)dimethylsulfonium compounds from Ref. 22 (●) vs. σ^+ . For the gas-phase data, $\rho^+ = -0.57$ ($r = 0.9999$ with the point for Cl excluded). For the hydrolysis data, $\rho^+ = -7.7$ for the regression line between **1a** and **1b**, and $\rho^+ = -0.82$ ($r = 0.993$) for the compound with $\sigma^+ < -0.06$.

of a change in the resonance stabilization of the activated complex with different substituents and not of a change in mechanism from a unimolecular to a bimolecular process. The results presented above are not consistent with this suggestion, nor are the results for the pyridiniums presented below. In addition, Richard, et al.,²⁵ have recently reported the kinetics for the specific-acid catalyzed conversion of 3- and 4-substituted *t*-cumyl alcohols into equilibrium mixtures of the alcohols, 2,2,2-trifluoroethyl ethers, and styrenes in water/TFE mixtures. Plots of the $\log k_H$ vs. either σ^+ or the PM3-calculated ΔH_R (not shown) are linear from the 4-MeO to the 3-F compounds. These results are consistent with the modeling

studies discussed below. It is clear from these results that there is no general rule to cover the substitution reactions of benzyl substrates.

Pyridiniums

Gas-Phase Dissociation. The break in the Hammett plot (Figure 6.2) for the four series of benzyl pyridiniums is the result of a change in mechanism from dissociation to the IDC for **2-5,a-d** to direct dissociation without formation of an IDC for **2-5e** as shown by the energy profile in Figure 6.6. In contrast to the results for the sulfonium series, the C7-N bond length in the activated complex remains relatively constant at ca. 2.2Å, although our computational method would not resolve relatively small differences in bond length. The value of ρ^+ for **2a-d** is -0.27 (from Figure 6.10), one-half the value for **1a-e**. The bond length in the activated complexes for **1a-e** increase steadily with the increasing electron withdrawing ability of the substituent, while bond lengths for **2a-d** remain essentially constant. This difference in progress along the reaction coordinate accounts nicely for the ρ^+ values.

Energy profiles for **2-4a** calculated in AM1 show that while the value of ΔH^\ddagger for k_1 decreases slightly as the pK_a of the pyridine decreases, a result that is expected, ΔH^\ddagger for k_{-1} , the barrier for the return reaction from the IDC, remained constant at 4.9 kcal/mol (Figure 6.9), a result that is consistent with Ritchie's N_+ scale.²⁶

Dissociation in Water. Comparison with the solution reactions is more difficult than for the sulfoniums, which hydrolyze at measurable rates at 80°C and give clear ordinate intercepts in plots of k_{obsd} vs. [Nu] for the substitution reactions.⁶ For **2a-e**, however, hydrolysis is much slower than the azide S_N2 reaction, and plots of k_{obsd} vs. $[\text{NaN}_3]$ pass through the origin.⁸ At long times, however, the substrates hydrolyze ($t_{1/2}$ s of 9 to 480 hr). The rate constants

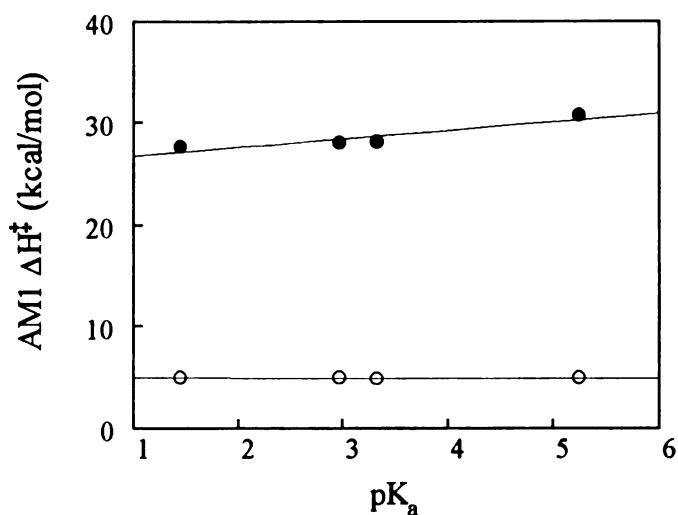


Figure 6.9. Plots of AM1 ΔH^\ddagger for bond cleavage (k_1 , ●) and return to the transition state from the IDC (k_{-1} , ○) for (left to right) **2a**, **5a**, **3a**, and **4a**. There is an increase in ΔH^\ddagger as the LG becomes more basic for k_1 , but the ΔH^\ddagger is constant for the return reaction.

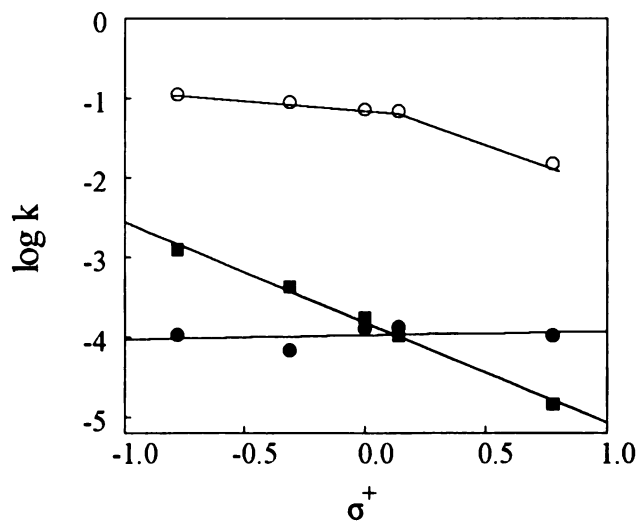


Figure 6.10. Plots of the gas-phase relative rates ($k = R^+/[R^+ + M^+]$, ○) for **2a-e** and the hydrolysis rate constants at 70°C for **2a-e** (■) and **3a-e** (●) vs. σ^+ . For the gas-phase data for **2a-d**, $\rho^+ = -0.24$ ($r = 0.998$), which is one-half the value for **1a-e** (Figure 6.8). For the hydrolysis data, $\rho^+ = -1.25$ ($r = 0.997$) for **2a-e** and 0 for **3a-e**.

UNIVERSITY OF TORONTO

obtained at 80°C are inaccurate because, as found for the sulfoniums,⁶ there is an equilibrium $\text{RPy}^+ \rightleftharpoons \text{ROH} + \text{Py} + \text{H}_3\text{O}^+$ established during the reaction that causes the reaction to slow and eventually to stop. Complete profiles for **2a-d** show the same dependence on initial concentration of substrate as found for hydrolysis of **1a**, and addition of exogenous 3-CN-pyridine slows the reaction in a concentration-dependent manner. The initial portions of plots of $\ln(C_t/C_0)$ vs. t are linear (ca. 40% reaction) and the slopes may be assumed to be approximate measures of the hydrolysis rate constant. A Hammett plot based on these estimated rate constants is linear (Figure 6.10). Rates for the hydrolysis and azide substitution reactions of the nicotinamide substrates **3a-e** are comparable, and rate constants for the water-only reaction could be measured accurately, either directly or as intercepts of plots of k_{obsd} vs. $[\text{N}_3]$. The Hammett plot is linear and essentially flat (Figure 6.10). Thus the break in the Hammett plot for the gas-phase reaction is consistent with a change in mechanism, but Hammett plots for the hydrolysis of **2a-e** and **3a-e** are consistent with a single mechanism, direct displacement by solvent. (Reasons for the difference in slopes are discussed elsewhere⁸ in terms of Pross-Shiak theory.²⁷) These results, which show a change in mechanism between the gas phase and solution that is opposite the change found for **1a-e**, are not consistent with the suggest of Richard and Yeary.²⁴ The change of mechanism in the gas phase is related to intrinsic energetics; the change (or lack of it) in water must be the result of solvation.

The Effect of Solvent on Mechanism. Ritchie²⁸ has written that "all patterns of reactivity and selectivity arise primarily from solvent and not from some inherent property of the solute reactants." Arnett and Reich²⁹ have argued that the failure of the Menschutkin reaction to follow the reactivity-selectivity principle (RSP) is the result of solvation of the LG at the transition state. Very recently,

Brauman³⁰ concluded that solvation and not substituent effects are important for S_N2 reactions. Our results support these positions.

In addition to the general effects of solvent electrostriction, two factors seem to be important. The first is the driving force to stabilization of the 4-MeO-benzyl carbenium ion from **1a**. Because ΔH^\ddagger for formation of this cation is 4.4 kcal/mol lower and the cation is 7.2 kcal/mol more stable than the 4-Me-benzyl carbenium ion in MNDO (Table 6.3), and because $-T\Delta S^\ddagger$ for solvation of the LG is constant, the enthalpy gained by solvation of the carbenium ion must lower ΔG^\ddagger for dissociation sufficiently that reaction by direct displacement is not favorable. In fact, ΔG^\ddagger for the S_N1 reaction of **1a** is 25.2 kcal/mol, which is 4.7 kcal/mol lower than ΔG^\ddagger for the solvent displacement reaction estimated by extrapolation of the points for Thornton's compounds²² shown in Figure 6.8.

The second factor is solvation of the leaving group. Large differences in ΔS^\ddagger for the azide reaction between the **2a** and **1a** ($\Delta\Delta S^\ddagger = -17.6$ gibbs/mol in favor of **1a**) and between H₂O and D₂O for the hydrolysis of the **1a** ($\Delta\Delta S^\ddagger = 7.0$ gibbs/mol) have been interpreted in terms of differential solvation of the LGs or the hydrophobic effect, respectively.⁶ The effect of the highly negative $-T\Delta S^\ddagger$ for the hydrolysis of **2a** must increase ΔG^\ddagger for direct dissociation sufficiently to favor the displacement reaction; this effect would be much smaller for **1a**, however, and may be the source of the differences in reactivity and mechanism in solution for **1a** and **2a**. In the gas phase, only a change in translational entropy is important, and both substrates dissociate to the IDC. Clearly the presence or absence of solvent can determine the mechanism of dissociation.

Relative Stabilities of the Ribosyl Oxocarbenium Ion and Benzyl Carbenium Ions in the Gas Phase. Using extrapolated results obtained from a clock reaction for sulfite trapping, Young and Jencks³¹ suggested that the methoxymethyl

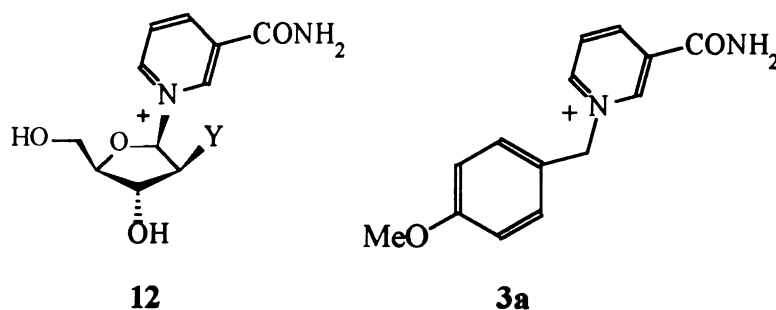
oxocarbenium ion ($\text{MeO}=\text{CH}_2^+$) generated by specific-acid-catalyzed hydrolysis of formaldehyde dimethyl acetal was too unstable to exist as an intermediate on the reaction coordinate. Because k_{rel} between methyl β -D-glucopyranoside and formaldehyde dimethyl acetal is 6.4×10^{-4} at 25°C , they claimed that the glycosyl oxocarbenium ion was too unstable to exist. While the initial estimate of the lifetime of the glycosyl oxocarbenium ion, 10^{-15} sec,³¹ has been revised downward over the years to near the diffusion limit of 10^{-12} sec,³² Jencks has maintained his contention that glycosyl oxocarbenium ions are not distinct intermediates in either solvolysis,³³ acid-catalyzed hydrolysis,^{31,32} or nucleophilic substitution reactions.³⁴

Despite Jencks's contention, there is a large body of evidence, including high, positive values of ΔS^\ddagger and fits to Bunnett's ω scale,^{35,36} that suggests the mechanism of acid-catalyzed hydrolysis of glucosides,³⁷ and acetals and ketals formed from "normal" aldehydes, ketones, and aliphatic alcohols,³⁸ is A-1. As shown in Chapters 7 and 8,³⁹ however, the energy profiles for dissociation of methoxymethyl derivatives depend on the leaving group and either has ($\text{LG} = \text{MeOH}, \text{H}_2\text{O}$) or does not have ($\text{LG} = \text{NMe}_2\text{Ar}, \text{Py}$) a distinct transition state for bond cleavage. The secondary linear and cyclic systems MeOCHMe- , tetrahydrofuranyl, tetrahydropyranyl, ribosyl, xylopyranosyl, and glucopyranosyl substrates with any of the four LGs dissociated readily to stable IDCs, however. The computational results are consistent with the experimental evidence reported by Knier and Jencks⁴⁰ for $\text{MeOCH}_2\text{-NMe}_2\text{Ar}^+$ substrates in support of the suggestion by Young and Jencks,³¹ but are not consistent with the proposition that all substrates containing potential oxocarbenium ions react in the same way.

There is also extensive evidence that specific acid-catalyzed hydrolysis of methyl and other alkyl furanosides³⁷ and the acid-catalyzed and "spontaneous" hydrolyses of 2-aryloxytetrahydrofurans⁴¹ occur through an A-2 mechanism.

Because of these results and the assumption that the ribosyl oxocarbenium ion should be intrinsically less stable than the glycosyl oxocarbenium ion, we have faced a dilemma. All evidence, including high values of the Taft ρ_T ,^{1,3} high, negative Brønsted β_{LG} values,⁴² and positive ΔS^\ddagger values,⁴³ points to a well-behaved dissociative reaction for NAD^+ and 2'-substituted β -nicotinamide arabinosides and ribosides that may occur through an IDC both in water^{3,44} and in the gas-phase.² Moreover, there is similar evidence that glucosyl pyridiniums react through an $\text{S}_{\text{N}}1$ mechanism.⁴⁵ There is no controversy regarding the stability of the 4-MeO-benzyl carbenium ion, which has been shown to be a solvent-equilibrated intermediate in the solvolysis of neutral (chloride and benzoates) substrates⁴⁶ and **1a**.^{6,7}

The relative *intrinsic* gas-phase stabilities of the carbenium ions derived from ribosyl compounds and 4-MeO-benzylnicotinamide **3a** can be



compared directly from our data, which were obtained under identical conditions for all compounds, and from the computational results. For instance, the value of $R^+/[R^+ + M^+]$ for the 2-deoxyribose- β -nicotinamide (**12**), which forms the most stable carbenium ion in the arabinosyl series, is 0.24, while that for **3a** is 0.10. The AM1-calculated ΔH^\ddagger for the carbon-nicotinamide cleavage is 20.1 kcal/mol for **12** and 30.1 kcal/mol for **3a**. The corresponding values for the 2'-F-arabinoside, which forms the least-stable oxocarbenium ion in the series, are 0.11 and 26.0 kcal/mol, respectively. The same trend is found in ΔH_{R} ; for **3a** the value is 34.6 kcal/mol,

while the values for 2'-H, 2'-NH₂, 2'-OH, 2'-NAc, and 2'-F arabinosyl β-nicotinamide compounds, listed in the order of decreasing stability of the oxocarbenium ions, are 27.5, 29.8, 32.7, 33.3, and 37.9 kcal/mol, respectively. Thus with nicotinamide as the LG, in the gas phase the ribosyl IDCs and oxocarbenium ions form at much faster rates and to greater extents than the quite stable 4-MeO-benzyl IDCs and carbenium ions. By this measure, the intrinsic stabilities of the ribosyl oxocarbenium ions within the IDC, and the bare species that remain after diffusion away of the LG, are greater than the 4-MeO-benzyl carbenium ion.

Even by Jencks's rate comparison criterion,³¹ the same trend is found in solution: the k_{rel} for hydrolysis of **12** and **3a** is 6.4×10^4 at 96°C. This comparison is invalid, however, because in solution **12** appears to solvolyze through an IDC,^{21,44} while **3a** solvolyses by direct displacement by solvent.⁸

Model Gas-Phase Systems. Schröder, et al.,⁴⁷ found that addition of an oxygen (or nitrogen) α to a cationic center in simple aliphatic systems can increase the PM3-calculated gas-phase stabilization energies by significant amounts. For instance, replacement of a methyl group in Me₃O⁺ with MeOCH₂- led to spontaneous cleavage of a carbon-oxygen bond to liberate Me₂O. Bond cleavage in the (methoxymethyl)dimethyl-oxonium is 46.5 kcal/mol more exothermic than cleavage of the trimethyloxonium, and [MeO=CH₂]⁺ is 91.4 kcal/mole more stable than the methyl cation.

To check this result in a cyclic aliphatic system, we modeled the gas phase dissociative reactions of protonated cyclopentanol (**13**) and the protonated α -oxygen homolog (**14**, the cyclic acetal of 4-hydroxybutanal). Using PM3 values for ΔH_{R} , we calculated the stabilities of the two cations relative to the protonated

arabinosides gas-phase dissociations.² The expected trend of an increase in ΔH_R with decreasing stability of the oxocarbenium ions **18** was found (Figure 6.11).

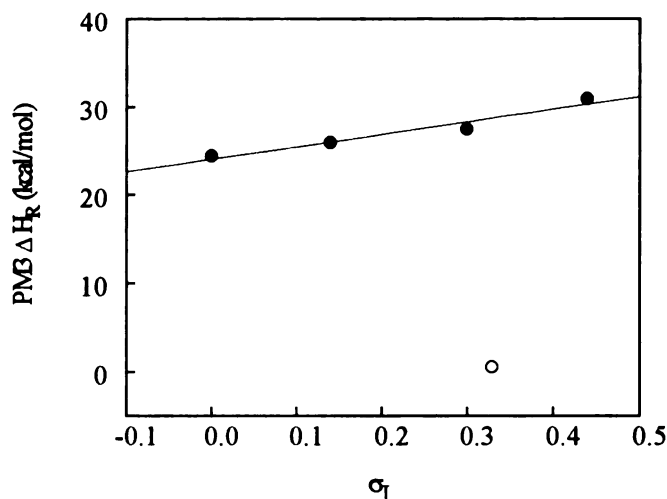


Figure 6.11. Plot of PM3 ΔH_R vs. the inductive substituent constant σ_I for the gas-phase dissociation of *cis*-3-*X*-substituted-2-dimethyl-sulfonium-tetrahydrofurans (left to right, *X* = H, NH₂, OH, NAc, F). The open point is for **19**, which cyclizes to the more stable **20**.

Note that the point that is substantially off the line (open circle) is for the NAc substrate; the cation **19** collapses with no barrier to the acylium ion **20**, which has a much lower energy than the uncyclized cation.² (In solution, it was found that hydrolysis of β -nicotinamide arabinosides and ribosides in which the nicotinamide and N-Ac groups were *trans* occurred with anchimeric assistance.⁴³) The slope of the line for a plot of ΔH_R for the 2'-substituted β -nicotinamide arabinosides is essentially the same as that for the model system.

We calculated the PM3 values of ΔH_R for the reaction series 4-Y-C₆H₄-CH₂X⁺ \rightarrow 4-Y-C₆H₄-CH₂⁺ + X⁰ where Y = Me₂N, MeO, Me, H, and NO₂ and X = H₂O, MeOH, Me₂O, SH₂, HSMe, and 3-H-, 3-CN-, and 3-F-pyridine. ΔH_R is a measure of the effect of substituents on the overall energy of the reaction; these are thermodynamic and not kinetic measures of stability, although the calculated

values of ΔH^\ddagger for k_1 and ΔH_R correlate for the sulfoniums and pyridiniums (Figure 6.7). In the oxygen LG series, PM3 minimization of the MM2-minimized ground state structures for the Me_2N - and MeO - substrates (and the H_2N -, HO -, and O - substrates as well; not shown) lead to complete dissociation of the methylene-oxygen bond; oxygen LG compounds with less efficient electron donating groups were stable. PM3 minimization of a series of protonated 3- and 4-substituted *t*-cumyl alcohols reported by Richard, et al.,²⁵ caused spontaneous cleavage of the methylene-oxygen bond in all compounds; these results will be discussed in detail elsewhere.⁴⁸ PM3 minimization of the sulfur or pyridine compounds did not lead to spontaneous dissociation of the benzyl-LG bond.

As shown by the plots of ΔH_R vs. $\delta\Delta G^\circ_{t\text{-cumyl}}$ in Figure 6.12, dissociation of substrates in the oxygen LG series is much more exothermic than in the sulfonium or pyridinium series. The fact that the slopes of all plots are approximately the same, however, shows that the effect of substituents on a series with the same

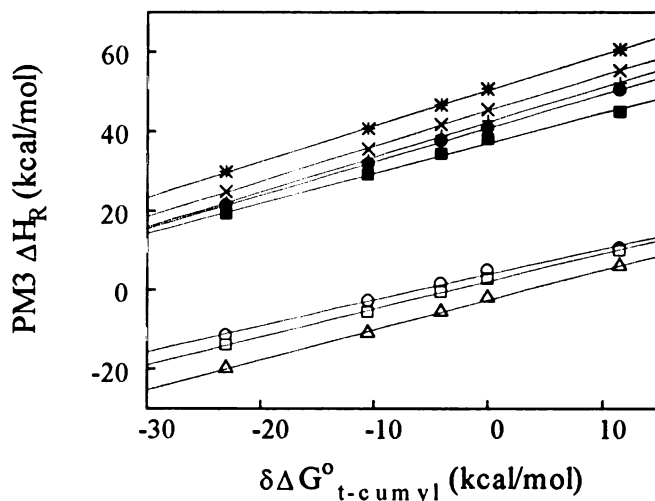


Figure 6.12. Plots of the PM3 ΔH_R vs. the relative free energy for gas-phase formation of *t*-cumyl carbenium ions for 4-Y-substituted benzyl compounds (left to right, Y = NMe_2 , MeO , Me , H , NO_2) with oxygen (Δ = Me_2O , \square = MeOH , \circ = H_2O), pyridine (\blacksquare = 3-CN, \bullet = H), and sulfur ($+$ = SMe_2 , \times = SMeH , $*$ = SH_2) LGs. Exothermicity follows the HSAB rank of the LG, not the pK_a (see text).

UNIVERSITY OF CALIFORNIA

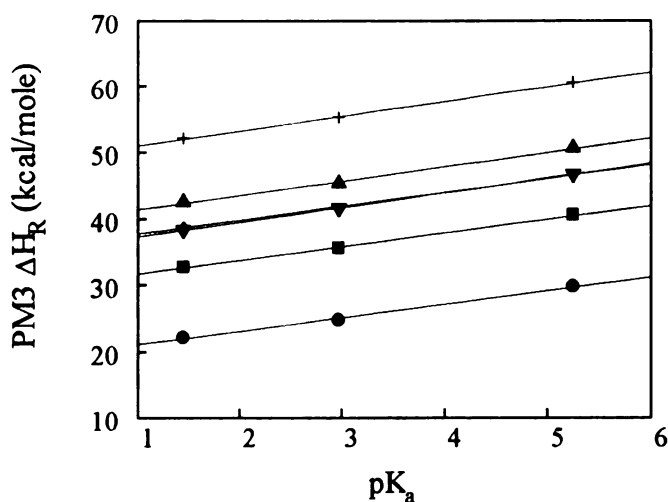


Figure 6.13. Bronsted-like plot for the PM3 ΔH_R vs. the pK_a of the pyridine LG (left to right, 3-CN, 3-F, 3-H) for 4-Y-substituted benzyl compounds (\bullet = NMe₂, \blacksquare = MeO, \blacktriangle = Me, \blacktriangledown = H, \blacklozenge = Cl, + = NO₂). The slopes range from 2.09-2.22, with all $r \geq 0.999$.

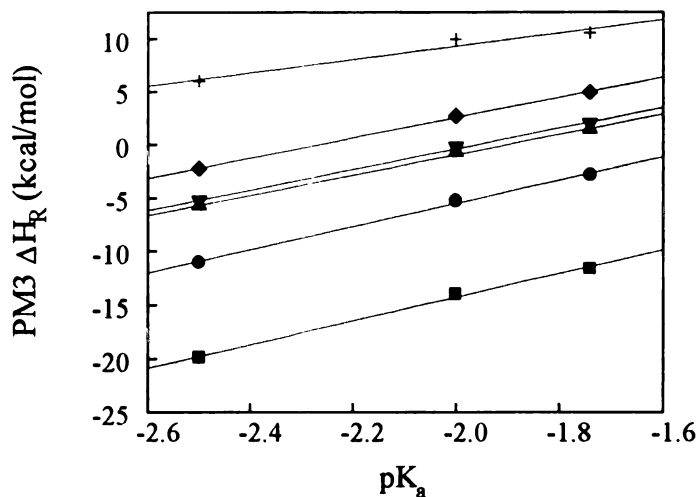


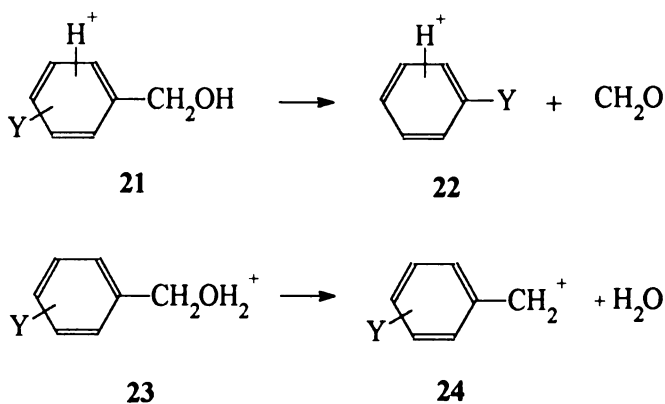
Figure 6.14. Bronsted-like plot for the PM3 ΔH_R vs. the pK_a of the oxygen LG (left to right, Me₂O, MeOH, H₂O) for 4-Y-substituted benzyl compounds (\bullet = NMe₂, \blacksquare = MeO, \blacktriangle = Me, \blacktriangledown = H, \blacklozenge = Cl, + = NO₂). The slopes range from 11.1 for NMe₂ to 6.3 for NO₂, with $r \geq 0.999$ except for NO₂, $r = 0.980$.

class of LG is the same. Essentially the same pattern is shown in Figures 6.13 and 6.14, which are plots of ΔH_R vs. the solution pK_a of the LG for the pyridinium and oxygen series, respectively. Within each series, the slopes of the plots are the

same, and the relative energies increase with the decrease in electron-donating ability of the substituent. There is no correlation between the series, however, because the slopes are different.

It is significant that the exothermicity does not correlate with the pK_a of the LG. ΔH_R for sulfur (pK_a 's of -5 to -6) and the pyridine (pK_a 's of 1.45 to 5.25) LGs have essentially the same energy, while the oxygen LGs, with pK_a 's of intermediate values (ca. -2.0) are the most exothermic. These results do parallel the HSAB rank of the LGs, however. The oxygen LGs are hard, while the sulfur and pyridine LGs are soft to intermediate (and SMe_2 and pyridine have the same n_{MeI} value of 5.3). The carbenium ions are soft to soft-intermediate, depending on the extent of delocalization of charge into the ring or substituents. Thus the enthalpies of bond cleavage reflect the relative energies of the starting structures considered as Lewis complexes.

Data obtained from CI mass spectra (H_2 and CH_4 reagent gases) of substituted benzyl alcohols confirm the patterns shown by the computational results. With one exception, the most prominent peak in spectra of 10 benzyl



$Y = \text{H}$ and 2-, 3-, 4- Me, OH, NH_2

alcohols corresponds to $[\text{MH}^+ - \text{H}_2\text{O}]$. Because of the differences in internal energies of the substrates, the data for the alcohols cannot be compared directly

1954

1955

1
2
3
4
5
6
7
8
9
10
11
12
13
14
15
16
17
18
19
20
21
22
23
24
25
26
27
28
29
30
31
32
33
34
35
36
37
38
39
40
41
42
43
44
45
46
47
48
49
50
51
52
53
54
55
56
57
58
59
60
61
62
63
64
65
66
67
68
69
70
71
72
73
74
75
76
77
78
79
80
81
82
83
84
85
86
87
88
89
90
91
92
93
94
95
96
97
98
99
100

1
2
3
4
5
6
7
8
9
10
11
12
13
14
15
16
17
18
19
20
21
22
23
24
25
26
27
28
29
30
31
32
33
34
35
36
37
38
39
40
41
42
43
44
45
46
47
48
49
50
51
52
53
54
55
56
57
58
59
60
61
62
63
64
65
66
67
68
69
70
71
72
73
74
75
76
77
78
79
80
81
82
83
84
85
86
87
88
89
90
91
92
93
94
95
96
97
98
99
100

A comparison of the relative abundances for β -nicotinamide arabinosides and benzyl pyridiniums shows that the arabinosyl oxocarbenium ions are intrinsically more stable than the benzyl carbenium ions in the gas phase. Computational results on model systems show that addition of an oxygen α to the developing cationic center markedly lowers the enthalpies of activation and the overall reaction. For water as an LG, this substitution leads to spontaneous cleavage of the oxygen-carbon bond with no barrier for cyclopentyl systems; protonated 4-Me₂N- and 4-MeO-benzyl alcohols collapse to the IDC with no barrier, while benzyl alcohols with less efficient electron donating groups are stable.

References and Notes

- (1) Johnson, R.W.; Marshner, T.M.; Oppenheimer, N.J. *J. Am. Chem. Soc.* **1988**, *110*, 2257-2263. Handlon, A.L.; Xu, C.; Muller-Steffnar, H.; Shubert, F.; Oppenheimer, N.J. *J. Am. Chem. Soc.*, in press.
- (2) Buckley, N.; Handlon, A.L.; Maltby, D.; Burlingame, A.L.; Oppenheimer, N.J. *J. Org. Chem.* **1994**, *59*, 3609-3615.
- (3) Handlon, A.L.; Oppenheimer, N.J. *J. Org. Chem.* **1991**, *56*, 5009-5010.
- (4) For reactions of **1a,c**: Sneen, R.A.; Felt, G.R.; Dickason, W.C. *J. Am. Chem. Soc.* **1973**, *95*, 638-639. For the ion-pair mechanism for neutral substrates: Sneen, R.A. *Acc. Chem. Res.* **1973**, *6*, 46-53.
- (5) Buckley, N.; Oppenheimer, N.J., submitted (Chapter 4).
- (6) Buckley, N.; Oppenheimer, N.J. *J. Org. Chem.* **1994**, *59*, 5717-5723.
- (7) Kevill, D.N.; Ismail, N.H.J.; D'Souza, M.J. *J. Org. Chem.* **1994**, *59*, 6303-6312.
- (8) Buckley, N.; Oppenheimer, N.J., submitted (Chapter 2).
- (9) Reviewed in Katritzky, A.R.; Brycki, B.E. *Chem. Soc. Rev.* **1990**, *19*, 83-105, and elsewhere

1
2
3
4
5
6
7
8
9
10
11
12
13
14
15
16
17
18
19
20
21
22
23
24
25
26
27
28
29
30
31
32
33
34
35
36
37
38
39
40
41
42
43
44
45
46
47
48
49
50
51
52
53
54
55
56
57
58
59
60
61
62
63
64
65
66
67
68
69
70
71
72
73
74
75
76
77
78
79
80
81
82
83
84
85
86
87
88
89
90
91
92
93
94
95
96
97
98
99
100

1
2
3
4
5
6
7
8
9
10
11
12
13
14
15
16
17
18
19
20
21
22
23
24
25
26
27
28
29
30
31
32
33
34
35
36
37
38
39
40
41
42
43
44
45
46
47
48
49
50
51
52
53
54
55
56
57
58
59
60
61
62
63
64
65
66
67
68
69
70
71
72
73
74
75
76
77
78
79
80
81
82
83
84
85
86
87
88
89
90
91
92
93
94
95
96
97
98
99
100

- (10) Katritzky, A.R.; Watson, C.H.; Dega-Szafran, Z.; Eyley, J.R. *J. Am. Chem. Soc.* **1990**, *112*, 2471-2478.
- (11) Katritzky, A.R.; Malhotra, N.; Dega-Szafran, Z.; Savage, G.P.; Eyley, J.R.; Watson, C.H. *Org. Mass Spectrom.* **1992**, *27*, 1317-1321.
- (12) Katritzky, A.R.; Malhotra, N.; Ford, G.P.; Anders, E.; Tropsch, J.G. *J. Org. Chem.* **1991**, *56*, 5039-5044.
- (13) MNDO: Dewar, M.J.S.; Thiel, W. *J. Am. Chem. Soc.* **1977**, *99*, 4899-4907; 4907-4917. AM1:Dewar, M.J.S.; Zoebisch, E.G.; Healy, E.F.; Stewart, J.J.P. *J. Am. Chem. Soc.* **1985**, *107*, 3902-3909. PM3:Stewart, J.J.P. *J. Comp. Chem.* **1989**, *10*, 209-220; 221-264.
- (14) McIver, J.W., Jr.; Komornicki, A.. *Chem. Phys. Lett.* **1971**, *10*, 303-306.
- (15) Taft, R.W.; Topsom, R.D. *Prog. Phys. Org. Chem.* **1987**, *16*, 2-83.
- (16) Hammond, G.S. *J. Am. Chem. Soc.* **1955**, *77*, 334-338.
- (17) Morton, T.H. *Tetrahedron* **1982**, *38*, 3195-3243. McAdoo, D.J.; Morton, T.H. *Acc. Chem. Res.* **1993**, *26*, 295-302. Kondrat, R.W.; Morton, T.H. *J. Org. Chem.* **1991**, *56*, 952-957.
- (18) (a) Kuck, D. *Mass Spectrom. Rev.* **1990**, *9*, 187-233. (b) For an extensive review of earlier work, see Bursey, J.T.; Bursey, M.M.; Kingston, D.G.I. *Chem. Rev.* **1973**, *73*, 191-234.
- (19) Cone, C.; Dewar, M.S.J.; Landman, D. *J. Am. Chem. Soc.* **1977**, *99*, 372-376.
- (20) (a) Dewar, M.J.S.; Landman, D. *J. Am. Chem. Soc.* **1977**, *99*, 4633-4639. (b) Dewar, M.J.S.; Landman, D. *J. Am. Chem. Soc.* **1977**, *99*, 7439-7445.
- (21) In this and other work on the dissociation of benzyl diazonium ions (Buckley, N., unpublished results) a consistent finding is that energies calculated for aromatic chlorines, in either the 3 or 4 positions of the benzene ring, do not fit

1951

1952

correlations for experimental or other computed values for other substituted benzyl derivatives.

(22) Friedberger, M.P.; Thornton, E.R. *J. Am. Chem. Soc.* **1976**, *98*, 2861-2865.

(23) See for example Fujio, M.; Goto, M.; Susuki, T.; Akasaka, I.; Mishima, M.; Tsuno, Y. *Bull. Chem. Soc. Jpn.* **1990**, *63*, 1146-1153. Ref. 46 has an extensive review of studies on the substitution reactions of benzyl derivatives.

(24) Richard, J.P.; Yeary, P.E. "A Simple Explanation for Curved Hammett Plots for Nucleophilic Substitution Reactions at Ring-Substituted Benzyl Derivatives," talk presented at the 206th ACS National Meeting, Chicago, IL, 22-27 August, 1993.

(25) Richard, J.P.; Jagannadham, V.; Amyes, T.L.; Mishima, M.; Tsuno, Y. *J. Am. Chem. Soc.* **1994**, *116*, 6706-6712.

(26) Ritchie, C.D. *Acc. Chem. Res.* **1972**, *5*, 348-354.

(27) Pross, A. *Adv. Phys. Org. Chem.* **1985**, *21*, 99-195.

(28) Ritchie, C.D. In *Solute-Solvent Interactions*; Coetzee, J.F., Ritchie, C.D., Eds.; Marcel Dekker: New York, 1976, Vol. 2; p. 265.

(29) Arnett, E.M.; Reich, R. *J. Am. Chem. Soc.* **1980**, *102*, 5892-5902

(30) Wladkowski, B.D.; Wilbur, J.L.; Brauman, J.I. *J. Am. Chem. Soc.* **1994**, *116*, 2471-2480.

(31) Young, P.R.; Jencks, W.P. *J. Am. Chem. Soc.* **1977**, *99*, 8238-8248.

(32) Amyes, T.L.; Jencks, W.P. *J. Am. Chem. Soc.* **1989**, *111*, 7888-7900.

(33) Sinnott, M.L.; Jencks, W.P. *J. Am. Chem. Soc.* **1980**, *102*, 2026-2032.

(34) Banait, N.S.; Jencks, W.P. *J. Am. Chem. Soc.* **1991**, *113*, 7951-7958.

(35) Schaleger, L.L.; Long, F.A. *Adv. Phys. Org. Chem.* **1963**, *1*, 1-34.

(36) Bunnett, J.F. *J. Am. Chem. Soc.* **1961**, *83*, 4956-4968; 4968-4973; 4973-4978; 4978-4983.

(37) Capon, B. *Chem. Rev.* **1969**, *69*, 407-498.

(38) Cordes, E.H.; Bull, H.G. *Chem. Rev.* **1974**, *74*, 581-603.

- (39) Buckley, N.; Oppenheimer, N.J., submitted (Chapters 7 and 8).
- (40) Knier, B.L.; Jencks, W.P. *J. Am. Chem. Soc.* **1980**, *102*, 6789-6798.
- (41) Craze, G-A.; Kirby, A.J. *J. Chem. Soc. Perkin Trans. II*, **1978**, 354-356;
Craze, G-A.; Kirby, A.J.; Osborne, R. *J. Chem. Soc. Perkin Trans. II*, **1978**, 357-368.
- (42) Tarnus, C.; Schuber, F. *Bioorg. Chem.* **1987**, *15*, 31-42; Tarnus, C.;
Muller, H.M.; Schuber, F. *ibid.*, **1988**, *16*, 38-51.
- (43) Handlon, A.L. Ph.D. Dissertation, The University of California, San
Francisco, 1991.
- (44) Ta-Shma, R.; Oppenheimer, N.J., in preparation.
- (45) Hosie, L.; Marshall, P.J.; Sinnott, M.L. *J. Chem. Soc. Perkin Trans. II*,
1984, 1121-1131.
- (46) Amyes, T.L.; Richard, J.P. *J. Am. Chem. Soc.* **1990**, *112*, 9507-9512.
- (47) Schröder, S.; Buckley, N.; Oppenheimer, N.J.; Kollman, P.A., *J. Am.*
Chem. Soc. **1992**, *114*, 8231-8238.
- (48) Buckley, N., in preparation.

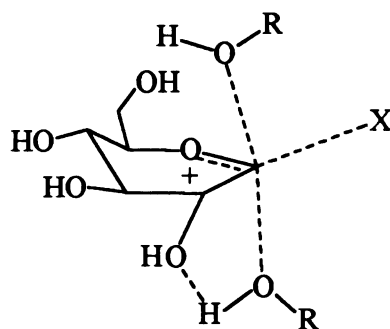
Chapter 7
A Semi-empirical Study of the Kinetic and Thermodynamic
Stabilities of Linear and Cyclic Oxo- and Thiocarbenium Ions
Generated from Pyridiniums and Dimethylaniliniums



Introduction

On the basis of an extrapolation of the results of a sulfite "clock" trapping reaction during the hydrolysis of ketals and acetals, in 1977 Young and Jencks¹ suggested that the methoxymethyl carbenium ion ($\text{MeO}=\text{CH}_2^+$) was too unstable to exist as a solvent-equilibrated intermediate on the reaction coordinate for simple dissociative reactions. The fact that the rate constants for acid-catalyzed cleavage of formaldehyde acetals were much greater than those for cleavage of methyl glucosides led Young and Jencks to propose that the glucosyl oxocarbenium ion could not exist as an intermediate. Knier and Jencks² studied the reactions of neutral and negative nucleophiles with $\text{MeOCH}_2\text{NMe}_2\text{Ar}^+$. The borderline kinetic behavior found and the use of various linear free energy relations (LFERs) led Knier and Jencks to conclude that the original estimate of the lifetime of $\text{MeO}=\text{CH}_2^+$ was valid. They also made the bold suggestion that substrates will undergo an $\text{S}_{\text{N}}2$ reaction "simply because" the incipient carbenium ion is too unstable to exist as a solvent-equilibrated intermediate; inherent in this statement is the assumption that substitution reactions must occur through a single mechanism. Because of these rationales, the mechanism of the hydrolysis reactions of $\text{MeOCH}_2\text{NMe}_2\text{Ar}^+$ was attributed to direct solvent displacement. Using these and other results, Jencks has formulated a scheme for substitution reactions that rejects the ion-pair and mixed mechanisms in favor of preassociated stepwise or enforced concerted mechanisms.³ This scheme has important implications for an understanding of the mechanisms used by enzymes such as lysozyme and the glycosyl hydrolases. In particular, Sinnott and Jencks⁴ have suggested that the "exploded" transition state is important for enzymatic cleavage of bonds at the anomeric carbon of glycosyl substrates.

The original estimate of the lifetimes in solution of both $\text{MeO}=\text{CH}_2^+$ (10^{-15} sec) and the glucosyl oxocarbenium ion (10^{-11} to 10^{-15} sec *or less*) have been



The "Exploded" Transition State

revised upward over the years and now stand near the diffusion limit at 10^{-12} sec.⁵ Despite these estimates, there are extensive experimental data, including Taft and Brønsted coefficients and activation values for solution and enzyme-catalyzed reactions, that are consistent with unimolecular dissociative reactions of pyranosyl and ribosyl pyridinium substrates. Schröder et al.⁶ have challenged the view that ribosyl pyridiniums such as nicotinamide-adenosine dinucleotide (NAD^+) react via the "exploded" transition state, and Shuber, et al.,⁷ Johnson, et al.,⁸ Handlon and Oppenheimer⁹ and Buckley, et al.¹⁰ have published experimental and computational results that strongly suggest NAD^+ analogs dissociate to ion-dipole complexes in solution and the gas phase. The excellent correlation of experimental and computational results found for the gas-phase dissociation of β -nicotinamide arabinosides¹⁰ prompted us to perform the computational study reported here.

We calculated the energy profiles in AM1 for a series of pyridinium substrates that can undergo heterolytic cleavage to give oxocarbenium ions. The relative stabilities of the oxocarbenium ions formed were evaluated in terms of ΔH^\ddagger and ΔH_R and compared with experimental data from the literature and from our own work. The systems studied have the advantage of defining reaction characteristics in two standard states, the gas phase and pure water (or deuterium oxide); complicating factors such as solvent sorting present in mixed solvent systems are avoided. In brief, our results confirm the original suggestion that $\text{MeO}=\text{CH}_2^+$ is too unstable to exist as an intermediate *for the model reaction of a*

charged pyridinium or dimethylanilinium substrate, but they also suggest that use of the lifetime of this species to estimate the lifetime of cyclic oxocarbenium ions such as ribosyl or glucosyl carbocations is not justified.

Computational Methods

Calculations in AM1¹¹ and PM3¹² were performed as describe in Chapter 5 using Release 4.0 of the Hyperchem software. ΔH_R was calculated as $[\Delta H_f \text{ cation} + \Delta H_f \text{ leaving group}] - \Delta H_f \text{ starting structure}$.

Results

Values of ΔH^\ddagger were determined from energy profiles such as those shown in Figure 7.1 for 1-3 and in Figure 7.2 for 4 and 5. Results of the AM1 calculations for the model compounds studied are listed in Table 7.1. Katritzky et al.¹⁴ have show, and we¹⁰ have confirmed, that benzyl pyridiniums do not give a

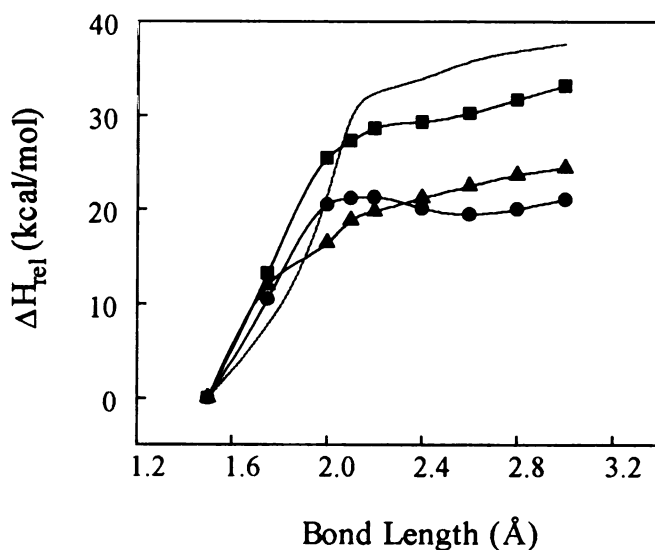


Figure 7.1. AM1 energy profiles for the dissociation of $\text{MeOCH}_2\text{Py}^+$ (1, ■), MeOCHMePy^+ (3, ●), and $\text{MeOCH}_2\text{NMe}_2\text{Ph}^+$ (2, ▲). The dashed line is the PM3 energy profile for 1.

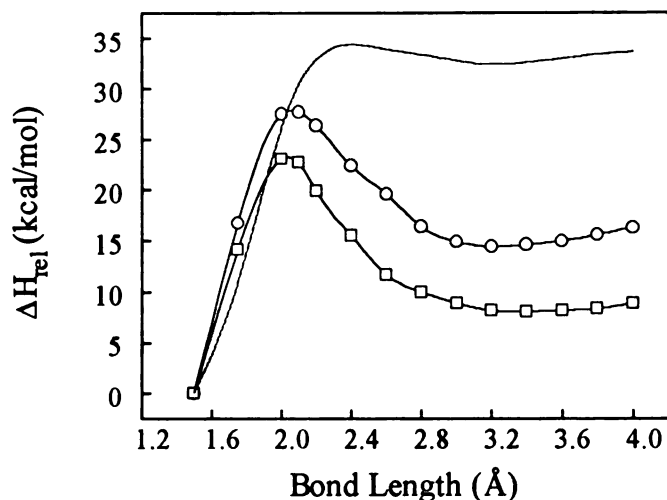
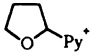
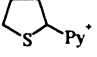
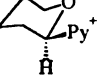
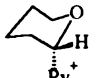
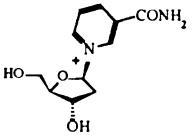
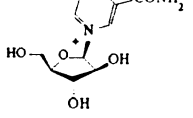
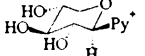
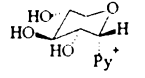
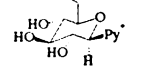
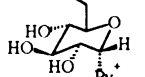
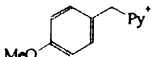


Figure 7.2. AM1 energy profiles for the dissociation of MeSCH₂Py⁺ (4, O), and MeSCHMePy⁺ (5, □). The dashed line is the PM3 energy profile for 4.

transition state in PM3 but they do in AM1. Because of this and some aberrant results, we calculated ΔH^\ddagger for the β -nicotinamide arabinosides in AM1.¹⁰ As a check on the method, we generated energy profiles for 1 and 3 in PM3, AM1, and MNDO; the PM3 and AM1 results are shown in Figures 7.1 and 7.2. 1 did not give a transition state in any method, but 3 gave a transition state in all methods.

Apeloig and Karni¹⁵ have published the results of *ab initio* calculations on the relative stabilities of the α -oxy and α -thio carbenium ions. They found that the energies depended on the basis set used, with the "best" energies obtained at the MP3/6-31G* level. As a check on our methods, many of the reactions studied by Apeloig and Karni were calculated in AM1 and PM3; the results are listed in Table 7.2 with the available gas-phase experimental values. In most instances, the *ab initio* and semi-empirical energies are in good agreement and show the same trends in stability; in only one instance did AM1 fail to reproduce the sign and magnitude of the energies calculated with the other methods. The difference in the AM1 ΔH_R between the α -oxy and α -thio compounds is consistent at 13 kcal/mol (Table 7.1), but the results in Table 2 suggest that this number is too high by a factor of 2-3.

Table 7.1. AM1 Enthalpies of Activation (ΔH^\ddagger) and Reaction (ΔH_R) for the Dissociation of Methoxymethyl and 1-Oxa-cyclic Pyridinium Substrates

Entry	Substrate	ΔH^\ddagger	ΔH_R
1	MeOCH ₂ Py ⁺	No transition state	46.7
2	MeOCH ₂ NMe ₂ Ph ⁺	No transition state	38.3
3	MeOCHMePy ⁺	21.3	33.3
4	MeSCH ₂ Py ⁺	27.7	29.1
5	MeSCHMePy ⁺	23.1	20.3
6		22.7	34.1
7		24.1	21.6
8		19.0	26.7
9		19.3	28.6
10		20.7	27.5
11		23.3	32.7
12		22.5	29.8
13		25.7	33.0
14		23.6	31.0
15		26.3	30.6
16		30.7	34.6

All energies in kcal/mol. Py = pyridine. Entries 10 and 11 are from Ref. 10, Entry 16 from Ref. 18.

Table 7.2. Comparison of the 6-31G*, MP3/6-31G*, AM1, and PM3 $\Delta H'_R$ and the Experimental Values for Hydride and Chloride Exchange for α -Oxo and α -Thio Methyl Carbenium Ions in the Gas Phase

Reaction	MP3/				Expt ^c
	6-31G*	6-31G** ^a	AM1 ^b	PM3 ^b	
$\text{CH}_3^+ + \text{MeOH} \rightarrow \text{CH}_4 + ^+\text{CH}_2\text{OH}$	-51.7	-62.1	-42.7	-51.4	-65.6
$\text{CH}_3^+ + \text{MeSH} \rightarrow \text{CH}_4 + ^+\text{CH}_2\text{SH}$	-45.0	-59.7	-56.5	-50.8	-64.0
$\text{CH}_3^+ + \text{MeOMe} \rightarrow \text{CH}_4 + ^+\text{CH}_2\text{OMe}$	-64.6	-72.7	-56.2	-49.9	-71.0
$\text{CH}_3^+ + \text{MeSMe} \rightarrow \text{CH}_4 + ^+\text{CH}_2\text{SMe}$	-57.8	-73.4	-67.1	-57.4	-74.0
$\text{HOCH}_2^+ + \text{MeSH} \rightarrow \text{HOMe} + ^+\text{CH}_2\text{SH}$	8.4	2.4	-13.8	0.6	1.5
$\text{MeOCH}_2^+ + \text{MeSH} \rightarrow \text{MeOMe} + ^+\text{CH}_2\text{SH}$	7.4	-0.7	-17.2	-1.5	
$\text{MeSCH}_2\text{Cl} + ^+\text{CH}_2\text{OMe} \rightarrow$					
$\text{MeSCH}_2^+ + \text{ClCH}_2\text{OMe}$	2.3	-3.9 ^d	-17.8	-7.2	

Energies in kcal/mol. $\Delta H'_R = \Sigma \Delta H_f \text{ products} - \Sigma \Delta H_f \text{ reactants}$.

^a*Ab initio* values from Ref. 15.

^bSemi-empirical values from this study.

^cExperimental values from Taft, R.W.; Martin, R.H.; Lampe, F.W. *J. Am. Chem. Soc.* **1965**, **87**, 2490-2497 (cited in Ref. 15).

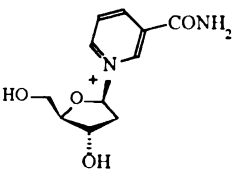
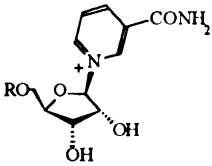
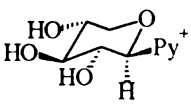
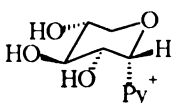
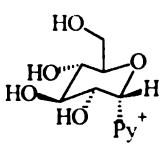
^dAt the MP2/6-31G* level.

Discussion

Values of ΔH^\ddagger and ΔH_R obtained from the AM1 energy profiles (Figure 7.1 for 1-3, Figure 7.2 for 4 and 5) are listed in Table 7.1. There are Taft ρ values, ΔS^\ddagger values (Table 7.3), and Brønsted β_{LG} values available for the solution reactions of many of the substrates studied. In the sections that follow, we will discuss the computational results in light of these solution values. There is a

consistent match of the computational stabilities and reactivities with the solution values.

Table 7.3. Values of ΔS^\ddagger for the Hydrolysis of Pyridinium Substrates

Entry	Compound	ΔS^\ddagger (gibbs/mol)	Ref.
2	$\text{MeOCH}_2\text{NMe}_2\text{Ar}^+$	-1.2 (-9.2 for $k_{\text{obsd}}/55.5$)	2
16	MeOCH_2OAr $(\text{MeOCH}_2\text{OAr} + \text{I}^-)$	-6.7 -8.5	29
10		9.5 ± 2.5	31
17		6.2 ± 2.5	32
12		31 ± 3	26
13		24 ± 6	26
15		15.2 ± 3.3	26

Linear Oxygen Compounds. Of the 15 compounds studied, only MeOCH₂Py⁺ (1) and MeOCH₂NMe₂Ph⁺ (2) failed to give a distinct transition state (Figure 7.1). As we have argued elsewhere,¹⁰ the fact that a mechanism occurs in the gas phase is not proof that the same mechanism will occur in solution. For heterolytic cleavage of charged substrates in the gas phase, dissociation can occur directly (generally for substrates such as Me-Py⁺ containing a *very* unstable incipient carbenium ion,¹⁴ although there are exceptions in which proton abstraction can occur simultaneously with bond cleavage for species with excellent oxocarbenium ions¹⁶) or, the most common occurrence, with bond cleavage and formation of an ion-dipole complex.¹⁷ In all systems we have studied, ΔH^\ddagger for the return reaction from the ion-dipole complex to the starting material or for diffusion apart of the elements of the ion-dipole complexes are lower than ΔH^\ddagger for bond cleavage.^{10,18}

If a simple heterolytic cleavage occurs by direct dissociation in the gas phase without the formation of an ion-dipole complex, there is good reason to suppose that dissociation will not occur in solution under more energetically demanding conditions. The two main restraints to reaction in solution are electrostriction¹⁹ and the loss of entropy of solvation of either or both the transition state or the leaving group²⁰; we have shown²¹ for benzyl substrates that solvation of pyridines and SMe₂ has a striking effect on ΔS^\ddagger . While time is said to be the quantity that keeps everything from happening at once, solvent keeps things from falling apart all at once (or nearly so) or at all.²² Thus the computational results for 1 and 2 suggest that MeO=CH₂⁺ is too unstable to exist as an intermediate *for the model reaction of a charged substrate*, in accord with the estimate of Young and Jencks¹ and the data of Knier and Jencks.²

Replacing a methylene proton by a methyl, however, produces a substrate (3) that gives a distinct transition state. This is not the result of relief of strain; the

compound obtained by replacing a methylene proton in **1** with CF_3 , a group that will destabilize the activated complex by withdrawal of electron density, does not give a distinct transition state. Thus the oxocarbenium ion derived from a secondary alkyl system, presumably because of inductive or hyperconjugative effects, or both, is sufficiently stable to achieve a distinct transition state. What is at issue, of course, is the stability of the ion-dipole complex that may form upon dissociation, which is determined by the intrinsic stability of the carbenium ion within the ion-dipole complex. Indeed, the stability of the ion-dipole complexes formed from arabinosyl nicotinamides is directly related to the intrinsic stability of the carbenium ion.¹⁰

Linear Sulfur Compounds. This requirement is illustrated for the sulfur analogs **4** and **5**. Using pulsed ICR techniques, Caserio²³ has shown that $\text{MeS}=\text{CH}_2^+$ is more thermodynamically stable than $\text{MeO}=\text{CH}_2^+$ in the gas phase both in terms of chloride affinity ($\text{MeO}=\text{CH}_2^+ + \text{MeSCH}_2\text{Cl} \rightarrow \text{MeOCH}_2\text{Cl} + \text{MeS}=\text{CH}_2^+$) and hydride transfer reactions ($\text{MeO}=\text{CH}_2^+ + \text{MeSMe} \rightarrow \text{MeOMe} + \text{MeS}=\text{CH}_2^+$). Accordingly $\text{MeSCH}_2\text{Py}^+$ (**4**) and MeSCHMePy^+ (**5**) give distinct transition states (Figure 7.2) because the ion-dipole complexes are stable. In the AM1-minimized ion-dipole complexes for both compounds, the pyridine has moved away from a direct line with the positive carbon center and is interacting with the sulfur in a bridged structure very much like phenonium ions; the same structure forms for **7** (Figure 7.3). The extra stability afforded by this structure can be seen clearly in the energy profiles shown in Figure 7.2. Because AM1 appears to overestimate the energies of sulfur compounds, however, this difference may be an artifact of the parameterization of AM1; the ion-dipole complex for the PM3-calculated energy profile is not nearly as stable (Figure 7.2). The differences in AM1 energies between **4** and **5** suggests that changing from a primary to a



Figure 7.3. Stereodiagram (cross-eyed) of structures of the ion-dipole complexes for 4 (left) and 7 (right) showing a bridged structure between the carbon and sulfur. The energy before bridging begins is much lower than energy of the ion-dipole complexes for the oxo compounds; bridging alone is not responsible for the stability.

secondary system is worth 4.2 kcal/mol in ΔH^\ddagger and 8.7 kcal/mol in ΔH_R ; the difference in ΔH_R between 4 and 5 in PM3 is 7.4 kcal/mol.

Because Caserio's hydride transfer results²³ showed that thio analogs are favored kinetically over oxo analogs, she argued that the hydrolysis of the chlorides, for which the oxo compound reacts faster than the thio compound, is the result of solvation effects. Apeloig and Karni¹⁵ have shown that the predominance of the sulfur carbenium ion in the chloride exchange reaction with the oxocarbenium ion is the result of substantial ground-state stabilization of the oxo compound, which agrees with the semi-empirical results reported here (Table 7.2). They also showed that, relative to the hydrocarbons, $\text{HO}=\text{CH}_2^+$ is 2.4 kcal/mol more stable than $\text{HS}=\text{CH}_2^+$ at the MP3/6-31G* level of theory (and by 1.5 kcal/mol in the gas phase, Table 7.2), and we found it to be 0.6 kcal/mol more stable in PM3. Nonetheless, relative to the hydrocarbons, $\text{MeS}=\text{CH}_2^+$ is more stable than $\text{MeO}=\text{CH}_2^+$ by 0.7 kcal/mol at the MP3/6-31G* level of theory and 1.5 kcal/mol in PM3 (Table 7.2), which must reflect the inductive effect of the Me. It is doubtful that there is a substantial hyperconjugative effect, given Bordwell's finding²⁴ that there is no resonance interaction between ring substituents and the sulfur atom in the solvolysis of chloromethyl aryl sulfides.

In the model pyridinium dissociative reaction, the sulfur compounds are more stable thermodynamically (by 12.6-13 kcal/mol in AM1 ΔH_R and 7.4

kcal/mol in PM3 ΔH_R), but the oxygen compounds have lower values of ΔH^\ddagger (by 1.6-1.8 kcal/mol), which matches the relative rates for solution dissociation of alkyl chloroethers and thioethers.²⁴ Recently Richard²⁵ found that the rate constants for hydrolysis of α -MeO-benzyl azides are greater than those for α -MeS-benzyl azides, despite the greater thermodynamic stability of the sulfur compound as measured by the product ratios in a "clock" reaction. While we are great champions of the effects of solvation, it is clear that in this case intrinsic factors control rates and thermodynamic factors differently, and the usual supposition that reactivity follows thermodynamic stability is not true.

Unsubstituted Cyclic Compounds. The simple unsubstituted tetrahydrofuran (6), tetrahydrothiophene (7), and tetrahydropyran (8, 9) substrates have distinct transition states in AM1 (Table 7.1). The six-membered systems 8 and 9 are more stable than 6 and have lower values of ΔH^\ddagger , which reflects the greater flexibility--and therefore the smaller number of non-bonded interactions upon reaching the activated complex--of the six-membered system. Dissociation of the equatorial pyridine (8) is slightly favored over the axial (9), in contrast to the solution reactions for the corresponding xylopyranosylpyridiniums 12 and 13 in which the rate for the axial is favored by a modest amount.²⁶ The oxygen and sulfur compounds 6 and 7 show the same trends in AM1 ΔH^\ddagger and ΔH_R as found for the linear analogs.

Arabinosyl-, Xylopyranosyl-, and Glucopyranosylpyridiniums. These compounds have secondary structures at the reaction center and give distinct transition states in AM1 (Table 7.1). The 2'-deoxy arabinosyl compound 10 has a lower ΔH^\ddagger than the THF compound 6, which is the result of the stability afforded by the 5'-hydroxymethyl group.⁶ The xylopyranosyl (12 and 13) and

glucopyranosyl (14 and 15) compounds have lower values of ΔH^\ddagger than the arabinosyl compounds bearing the same 2' substituent (compare 11 and 12). As found for the THP compounds 8 and 9, the equatorial pyridine is favored over the axial pyridine by 3.2 kcal/mol in ΔH^\ddagger , which is the reverse of the relative rates in solution.²⁶ We assume that this difference reflects differential solvation of the ground and transition states for the anomers⁶ and that the gas-phase values more accurately reflect the *intrinsic* reactivity, including a stereoelectronic preference for expulsion of the axial pyridine,²⁷ but we have no proof for this assumption. While of interest, this difference is inconsequential to our main concern, which is that *both* classes of compounds give distinct transition states and react faster than the arabinosyl compounds. They are well-behaved systems that undergo unambiguous heterolytic cleavage of the carbon-pyridine bond.

The Estimation of the Stability of Glucosyl and Ribosyl Oxocarbenium Ions. Because of vast differences in solvation of the ground and transition states of formaldehyde acetals and methyl glucosides, we believe that the kinetic comparison used by Jencks^{1,5} to estimate the lifetime of the glucosyl oxocarbenium ion is unwarranted *a priori*. Without making assumptions, we can compare directly the relative gas-phase stabilities of the oxocarbenium ions generated from our substrates. The extent of gas-phase dissociation is far greater for β -nicotinamide arabinosides¹⁰ (e.g. 10 and 11) than for benzyl sulfoniums or pyridiniums¹⁸ (e.g. 16) under identical conditions; the computed values favor 10 over 16 by 10 kcal/mol in ΔH^\ddagger and by 7.1 kcal/mol in ΔH_R . Thus for the standard reaction, the ribosyl oxocarbenium ion is kinetically and thermodynamically more stable than the 4-methoxybenzyl carbenium ion. As noted above, β -nicotinamide arabinosides dissociate through the same mechanism in the gas phase and in solution,¹⁰ which with the results for the other compounds reported here supports

our contention that a cyclic oxocarbenium ion can exist in solution either as a distinct solvent-equilibrate intermediate or as an element of a contact or solvent-separated ion-dipole complex.

The mere presence of a favorable carbenium ion in a favorable substrate that dissociates in the gas phase is not sufficient, however, to assure that a dissociative reaction will occur in solution. Of the 20 benzyl dimethylsulfoniums and pyridiniums that we have found to dissociate to an ion-dipole complex intermediate in the gas phase,¹⁸ only one, (4-methoxybenzyl)dimethylsulfonium, dissociates in solution by an S_N1 mechanism.^{21,28}

Activation Values and Linear Free Energy Relations (LFERs) For the Model Reactions. Because it reflects a large change in translational entropy, ΔS^\ddagger is the activation value most often used to differentiate between uni- and bimolecular mechanisms.²⁰ In systems containing the same (or very similar) leaving groups that would be solvated in the same way, this seems to be an appropriate measure. Among the various LFERs used in attempts to define the structure of activated complexes are Hammett, Taft, and Brønsted correlations. Secondary deuterium isotope effects have been measured for many of the reactions studied here, but Kirby²⁹ has argued cogently that use of apparently disparate values from many different studies to define structures of the activated complex for either solution or enzyme-catalyzed reactions is fraught with difficulty; therefore, we will not discuss the extensive and contradictory data here.

Activation Entropy. Values of ΔS^\ddagger (Table 7.2) are available for the hydrolysis reactions of some of the compounds studied computationally. The ΔS^\ddagger for **2** is -1.2 gibbs/mol for k_{obsd} or -9.2 for the second-order rate constant ($k_{\text{obsd}}/55.5$), and the value for the reaction of **2** with *n*-propyl amine is -2.1 gibbs/mol. The equivalent 2,5-dinitrophenol derivative **16** has values of -6.7

gibbs/mol for the pH-independent hydrolysis and -8.5 gibbs/mol for the reaction with iodine.³⁰ The negative entropies, and especially the correspondence of the values for reactions with neutral and negative nucleophiles, are consistent with reaction by direct solvent displacement. Unlike the cyclic compounds, however, the linear substrates may lose rotational entropy ($\text{MeO-CH}_2\text{-Py}^+ \rightarrow \text{MeO=CH}_2\text{---Py}^+$) between the ground state and activated complex. While this loss of entropy may be important in these systems, it is difficult to assess its relative contribution to the total entropy of activation. It should be noted, however, that in minimized ground-state structures, the methoxy group has assumed the position expected for conjugation and loss of rotational entropy, and there will be little or no change in entropy between the ground and transition states.

The high, positive ΔS^\ddagger values for the pyridine arabinosyl, xylopyranosyl, and glucopyranosyl compounds, which are in the range for tertiary and aryl compounds known to undergo unimolecular solvolysis,²⁰ are clearly consistent with an $S_{\text{N}}1$ reaction, especially the extremely high values²⁶ for the xylopyranosyl compounds 11 and 12. The value for pH-independent hydrolysis of β -nicotinamide deoxyribose³¹ (10) is 9.5 ± 2.5 gibbs/mol, and for NAD^+ (17) is 6.2 ± 2.4 gibbs/mol.³² These values are consistent with the energy profiles calculated for this class of compounds.¹⁰

There are correlations ($r = 0.90\text{-}0.92$) between the AM1 values of ΔH^\ddagger and the experimental ΔH^\ddagger and ΔS^\ddagger for the hydrolysis of 2'-substituted β -nicotinamide arabinosides³¹ and the xylopyranosyl- and glucopyranosylpyridiniums²⁶ (Figure 7.4). The rate constants for hydrolysis of the three six-membered compounds also correlate with the AM1-calculated ΔH^\ddagger (not shown; $r = 0.90$); the correlation for the arabinosyl compounds, which is measurably better, has been reported.¹⁰ As expected from the relative stabilities and computed ΔH^\ddagger , the five and six-membered compounds fall on two distinct lines.

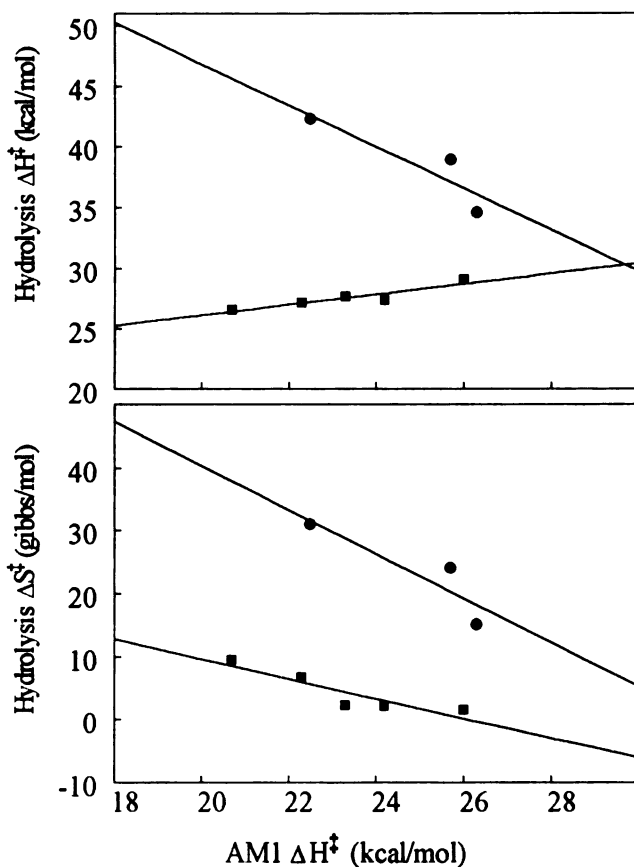


Figure 7.4. Correlations between the AM1-calculated ΔH^\ddagger and the experimental values of ΔH^\ddagger (top) and ΔS^\ddagger (bottom) for the hydrolysis of xylopyranosyl- and glucopyranosylpyridiniums (circles, Ref. 26) and 2'-substituted β -nicotinamide arabinosides (squares, Ref. 10 for AM1, Ref. 31 for experimental values).

Taft Correlations. The effects of 2'-substituents on the acid-catalyzed dissociation of glucosides³³ and purine nucleosides³⁴ are consistent with a dissociative mechanism. To our knowledge, the only systematic study of the effect of substituents on the rates for the uncatalyzed hydrolysis of compounds studied here is Handlon's study⁹ of the hydrolysis of 2'-substituted β -nicotinamide arabinosides and ribosides, both of which give $\rho_1 = -6.7$, a value consistent with an S_N1 mechanism. Relative rates for the gas-phase dissociation of the arabino series follow the Taft equation ($\rho_F = -0.75$) and the computed values of ΔH^\ddagger correlate well with the relative rates.¹⁰

Brønsted Correlations. The Brønsted coefficient β_{LG} is often taken as a measure of the extent of bond-breaking in the activated complex. Values are available for some of the model reactions studied here. The β_{LG} for the reaction of $\text{MeOCH}_2\text{NMe}_2\text{Ar}^+$ with water is -0.89 and is -0.70 for *n*-propyl amine²; values for hydroxide and acetate estimated from data for two substrates are in the same range. For hydrolysis of **12**, **13**, and **15** the values are -1.20, -1.28, and -1.06, respectively.²⁶ Schuber and his colleagues⁷ report a value of -1.12 for the hydrolysis of NAD^+ analogs and a value of -0.98 for enzyme-catalyzed bond cleavage. All of these values are consistent with a "late," "loose" transition state structure for bond cleavage.

Brønsted values must be used with caution to describe transition state structures, however. For instance, it is generally assumed that large negative β_{LG} values for nucleophilic substitution reactions of compounds containing incipient, stable carbenium ions indicate a large amount of "carbenium ion character" in the activated complex. Recently we³⁵ found, however, that β_{LG} for the azide reaction of 4-substituted benzyl *and* methyl pyridiniums were of essentially the same large, negative values of -1.4 to -1.6. Other data for the reactions of methylpyridiniums with iodide³⁶ ($\beta_{LG} = -1.13$) or triphenylphosphine³⁷ ($\beta_{LG} = -0.4$), both of which are soft nucleophiles, suggests that the charge on the nucleophile and not its hard-soft-acid-base rank are important.

Nucleophile and leaving group bond lengths obtained from AM1-minimized activated complexes for $\text{S}_{\text{N}}2$ reactions of MeOCH_2X^+ , 4-MeO-benzyl X^+ , and MeX^+ suggests that the activated complexes for reaction with neutral nucleophiles such as water are "tight" ("early" for the leaving group and "late" for the nucleophile) and for negative nucleophiles such as azide are "loose" ("late" for the leaving group and "early" for the nucleophile) regardless of the incipient carbenium ion in the substrate.³⁸ The AM1 pyridine bond lengths for the $\text{S}_{\text{N}}2$

reaction of water with **1** and **2** are 2.58 Å and the nucleophile-carbon-leaving group torsional angle is bent from colinearity, which is consistent with the suggestion of Dougherty and Dewar³⁹ that reactions of MeOCH₂X substrates with nucleophiles would be hampered by unfavorable orbital repulsions between the nucleophile and the methoxy oxygen orbitals. For comparison, the pyridine bond length for the S_N2 reaction of water with Me-Py⁺ and the benzyl substrate **16** are 1.62 Å and 1.78 Å, respectively; for the reaction with azide, the bond lengths are 2.89 Å and 3.05 Å, respectively.³⁸ Thus it is not appropriate to compare the β_{LG} values of the Knier-Jencks substrates with any of the ribosyl or pyranosyl substrates.

The AM1 computed bond lengths to the nicotinamide leaving group¹⁰ for Handlon's arabinoside series⁹ are relatively constant at ca. 2.1Å, despite Shuber's finding of a large β_{LG} for dissociation of analogs of **17** with different pyridine leaving groups in solution.⁷ The AM1 bond lengths to the pyridine leaving group for the xylopyranosyl and glucopyranosyl substrates are in the range 2.1-2.2 Å. The AM1 bond lengths for dissociation of benzyl pyridiniums in the gas-phase¹⁸ are relatively constant at 2.1 Å, but all substrates appear to hydrolyze by direct solvent displacement.³⁵ On the other hand, the MNDO bond lengths for dissociation of 4-Y-substituted benzyl dimethylsulfoniums¹⁸ increase with the decreasing stability of the carbenium ion, in total accord with the Hammond postulate.⁴⁰ The computed ΔH[‡] and the experimental relative rates for gas-phase dissociation correlate very well.^{10,18} In solution, however, only the 4-methoxy substrate undergoes an S_N1 reaction^{21,28}; the others react by direct solvent displacement.^{35,41}

Thus the lack of any pattern that is predictive of the structure of the activated complex between the gas phase and solution emphasizes the importance of solvation of both the ground and transition states. Solvation effects can be very

1951

1952

subtle. We found, for instance, that ΔS^\ddagger for solvolysis of (4-methoxybenzyl) dimethylsulfonium is 7 gibbs/mol in D_2O ²¹ but is 13.7 gibbs/mol in H_2O ,²⁸ an astonishing difference that may be related to the hydrophobic effect for solvation of SMe_2 at the transition state. The much shorter computed bond lengths found for the arabinosyl, xylopyranosyl, and glucopyranosyl substrates compared with the relatively large β_{LG} values for dissociation in water may reflect stabilizing effects of solvent. It is also possible that β_{LG} values have entirely different physical meanings that depend on the mechanism. Both of these suggestions are of course the rawest kind of speculation. Nonetheless, all of these factors suggest that β_{LG} values as measures of bond length in the activated complex must be used with caution, and that solvation may be the most important factor that determines a particular value. Thornton⁴² and Pross⁴³ have pointed out that there is no particular reason to suppose that charge development and geometry are explicitly linked.

Conclusions. The computational results reported here are consistent with the idea first suggested by Young and Jencks¹ that $MeO=CH_2^+$ is too unstable to exist as an intermediate on the reaction coordinate, despite the direct conjugation that is possible. Our finding that linear and cyclic secondary systems give distinct transition states by dissociating to stable ion-dipole complexes suggests that there is no *intrinsic* limit to the stability of glucosyl and ribosyl oxocarbenium ions. In fact, arabinosyl, xylopyranosyl, and glucopyranosyl compounds dissociate with lower values of ΔH^\ddagger than benzyl compounds (Table 7.1), and the oxocarbenium ions are more stable than substituted benzyl carbenium ions in the gas phase. There are also sufficient data for solution reactions to suggest that reactions of $MeOCH_2X^+$ substrates, including hydrolysis, are bimolecular, but that hydrolysis reactions for ribosyl-, xylopyranosyl-, and glucopyranosylpyridiniums are S_N1 , which is consistent with the computational results.

References and Notes

- (1) Young, P.R.; Jencks, W.P. *J. Am. Chem. Soc.* **1977**, *99*, 8238-8248.
- (2) Knier, B.L.; Jencks, W.P. *J. Am. Chem. Soc.* **1980**, *102*, 6789-6798.
- (3) Jencks, W.P. *Acc. Chem. Res.* **1980**, *13*, 161-169. Jencks, W.P. *Chem. Soc. Rev.* **1981**, *10*, 345-375.
- (4) Sinnott, M.L.; Jencks, W.P. *J. Am. Chem. Soc.* **1980**, *102*, 2026-2032.
- (5) Amyes, T.L.; Jencks, W.P. *J. Am. Chem. Soc.* **1989**, *111*, 7888-7900.
- Banait, N.S.; Jencks, W.P. *J. Am. Chem. Soc.* **1991**, *113*, 7951-7958, 7958-7963.
- (6) Schröder, S.; Buckley, N.; Oppenheimer, N.J.; Kollman, P.A., *J. Am. Chem. Soc.* **1992**, *114*, 8231-8238.
- (7) Tarnus, C.; Schuber, F. *Bioorg. Chem.* **1987**, *15*, 31-42; Tarnus, C.; Muller, H.M.; Schuber, F. *ibid.*, **1988**, *16*, 38-51.
- (8) Johnson, R.W.; Marshner, T.M.; Oppenheimer, N.J. *J. Am. Chem. Soc.* **1988**, *110*, 2257-2263.
- (9) Handlon, A.L.; Oppenheimer, N.J. *J. Org. Chem.* **1991**, *56*, 5009-5010.
- (10) Buckley, N.; Handlon, A.L.; Maltby, D.; Burlingame, A.L.; Oppenheimer, N.J. *J. Org. Chem.* **1994**, *59*, 3609-3615.
- (11) Dewar, M.J.S.; Zoebisch, E.G.; Healy, E.F.; Stewart, J.J.P. *J. Am. Chem. Soc.* **1985**, *107*, 3902-3909.
- (12) Stewart, J.J.P. *J. Comp. Chem.* **1989**, *10*, 209-220.
- (13) McIver, J.W., Jr.; Komornicki, A.. *Chem. Phys. Lett.* **1971**, *10*, 303-306.
- (14) Katritzky, A.R.; Malhotra, N.; Ford, G.P.; Anders, E.; Tropsch, J.G. *J. Org. Chem.* **1991**, *56*, 5039-5044.
- (15) Apeloig, Y.; Karni, M. *J. Chem. Soc. Perkin Trans. II* **1988**, 625-636.

These authors provide an excellent summary of the gas-phase and solution data for these compounds.

(16) McCloskey, J.A.; Futrell, J.H.; Elwood, T.A.; Schram, K.H.; Panzica, R.P.; Townsend, L.B. *J. Am. Chem. Soc.* **1973**, *95*, 5762-5764. Wilson, M.S.; McCloskey, J.A. *J. Am. Chem. Soc.* **1975**, *97*, 3436-3444. McCloskey, J.A. *Acc. Chem. Res.* **1991**, *24*, 81-87.

(17) Morton, T.H. *Tetrahedron* **1982**, *38*, 3195-3243. McAdoo, D.J.; Morton, T.H. *Acc. Chem. Res.* **1993**, *26*, 295-302. Kondrat, R.W.; Morton, T.H. *J. Org. Chem.* **1991**, *56*, 952-957.

(18) Buckley, N.; Maltby, D.; Burlingame, A.L.; Oppenheimer, N.J., submitted (Chapter 6).

(19) Reichard, C. *Solvent Effects in Organic Chemistry*. Verlag Chemie: New York, 1979. Ch. 5.

(20) Schaleger, L.L.; Long, F.A. *Adv. Phys. Org. Chem.*, **1963**, *1*, 1-34.

(21) Buckley, N.; Oppenheimer, N.J. *J. Org. Chem.* **1994**, *59*, 5717-5723.

(22) For instance, we found that 4-Me, 4-H, and 4-Cl benzyl pyridinium dissociate readily in the gas phase (Ref. 18), but that they failed to react with either water or 1.7M azide *after six months at 96°C* (Ref. 35).

(23) Pau, J.K.; Ruggera, M.B.; Kim, J.K.; Caserio, M.C. *J. Am. Chem. Soc.* **1978**, *100*, 4242-4248.

(24) See Bordwell, F.G.; Cooper, G.D.; Morita, H. *J. Am. Chem. Soc.* **1957**, *79*, 376-378. Also see Jones, T.C.; Thornton, E.R. *J. Am. Chem. Soc.* **1967**, *89*, 4863-4867, for a very detailed study of the hydrolysis of methyl chloromethyl ether.

(25) Jagannadham, V.; Amyes, T.L.; Richard, J.P. *J. Am. Chem. Soc.* **1993**, *115*, 8465-8466.

(26) Hosie, L.; Marshall, P.J.; Sinnott, M.L. *J. Chem. Soc. Perkin Trans. II*, **1984**, 1121-1131.

(27) Kirby, A.J. *Acc. Chem. Res.* **1984**, *17*, 305-311. This author champions the stereoelectronic argument, while Sinnott (Ref. 26) opposes it.

(28) Kevill, D.N.; Ismail, N.H.J.; D'Souza, M.J., submitted to *J. Org. Chem.*

(29) Craze, G-A.; Kirby, A.J.; Osborne, R. *J. Chem. Soc. Perkin Trans. II*, **1978**, 357-368.

(30) Craze, G-A.; Kirby, A.J. *J. Chem. Soc. Perkin Trans. II*, **1978**, 354-356.

(31) Handlon, A.L. Ph.D. Dissertation, University of California, San Francisco, 1991.

(32) Note that the value reported in Ref. 8 is erroneous. Using the rate constants in the range 37-95°C, an Eyring plot of $\ln [k_{\text{obsd}} h/Tk_B]$, where h is Planck's constant and k_B is the Boltzmann constant, vs. $1/T$ gives $\Delta S^\ddagger = 6.2 \pm 2.4$ gibbs/mol and $\Delta H^\ddagger = 26.5$ kcal/mol ($r = 0.998$).

(33) Marshall, R.D. *Nature* **1963**, *199*, 998-999. Withers, S.G.; Pervival, M.D.; Street, I.P. *Carbohydrate Res.* **1989**, *187*, 43-66.

(34) York, J.L. *J. Org. Chem.* **1981**, *46*, 2171-2173. Zielonacka-Lis, E. *Nucleosides Nucleotides* **1989**, *8*, 383-405.

(35) Buckley, N.; Oppenheimer, N.J., submitted (Chapters 2 and 3).

(36) Arnett, E.M.; Reich, R. *J. Am. Chem. Soc.* **1980**, *102*, 5892-5902.

(37) Berg, U.; Gallo, R.; Metzger, J. *J. Org. Chem.* **1976**, *41*, 2621-2624.

(38) Buckley, N., unpublished results. All structures of the activated complexes were fully minimized in AM1 using the methods described above; the only final constraint restricted the nucleophile-carbon-leaving group bond to colinearity. All activated complexes gave single negative eigenvalues upon diagonalization of the force constant matrix, and the first normal (negative) mode corresponded to the reaction coordinate.

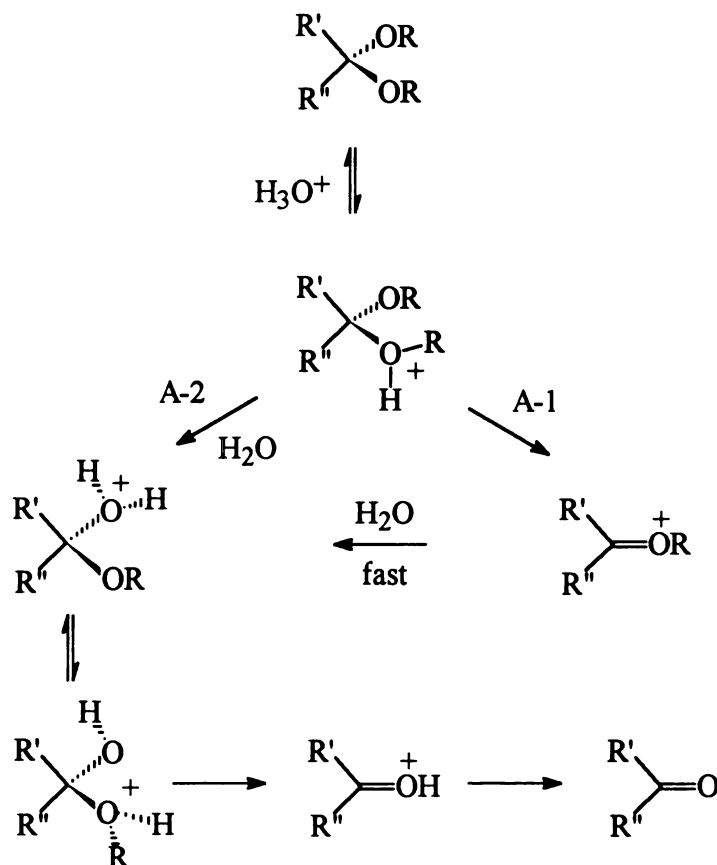
- (39) Dewar, M.J.S.; Dougherty, R.J. *PMO Theory of Organic Chemistry*. New York: Plenum, 1975, pp. 262-263.
- (40) Hammond, G.S. *J. Am. Chem. Soc.* **1955**, *77*, 334-338.
- (41) Friedberger, M.P.; Thornton, E.R. *J. Am. Chem. Soc.* **1976**, *98*, 2861-2865.
- (42) Thornton, E.R. *J. Am. Chem. Soc.* **1967**, *89*, 2915-2927. "There is no reason why geometry and charge separation should parallel one another precisely" (p. 2922).
- (43) Pross, A. *Adv. Phys. Org. Chem.* **1985**, *21*, 99-196. "[T]he Brønsted parameter does not constitute a measure of transition state charge development, and it is unlikely to represent a meaningful measure of transition state geometry" (p. 151).

Chapter 8

A Semi-empirical Study of the Kinetic and Thermodynamic Stabilities of Linear and Cyclic Oxo- and Thiocarbenium Ions Generated from Aldehyde Hydrates, Hemiacetals, Acetals, and Methyl Ribosides and Glucosides

Introduction

There is substantial evidence that the specific-acid catalyzed hydrolysis of acetals, ketals, and orthoesters occurs by an A-1 mechanism (Scheme 8.1).^{1a-c}



Scheme 8.1

General acid catalysis is observed only for substrates with good leaving groups and potentially stable oxocarbenium ions (1-aryloxytetrahydrofurans [THF-OAr]² and tetrahydropyrans [THP-OAr]³) or exceedingly stable carbenium ions (tropone diethylketal,⁴ dioxolane hemi⁵ and ortho esters⁶). Acetals and ketals formed from "ordinary" carbonyl compounds and weakly basic aliphatic alcohols do not undergo general acid catalysis.¹ THF- and THP-OAr substrates with electron-withdrawing groups on the phenol undergo pH-independent "spontaneous" bond cleavage,^{2,3} and methoxymethylaryloxy substrates undergo nucleophilic

substitution reactions.^{7,8} Methyl glucopyranosides do not undergo general acid catalysis, which has caused somewhat of a dilemma because the glycosyl bond in polysaccharides is cleaved readily by lysozyme, which must act through general-acid catalysis.^{1a}

As part of our computational study of the gas-phase dissociation of charged benzyl substrates,⁸ we attempted to minimize (in AM1 and PM3) the ground states for protonated benzyl alcohols bearing 4-substituents (O-, OH, MeO, NH₂, NMeH, NMe₂, SH, SMe, Me, H, Cl, NO₂). The methylene-oxygen bond underwent spontaneous cleavage upon minimization in all substrates except the 4-nitro compound. There is a precedent for this reaction in the literature. Ichikawa and Harrison⁹ found that there is essentially complete dissociation of the methylene-oxygen bond in the chemical ionization spectra (methane or ammonia reagent gases) of substituted benzyl alcohols. (There is a second reaction in which ring-protonated substrate expels formaldehyde.) A similar computational result has been reported by Schröder, et al.,¹⁰ who found that addition of an oxygen (or nitrogen) to a cationic center in simple aliphatic systems can increase the PM3-calculated gas-phase stabilization energies by significant amounts and can lead to spontaneous bond cleavage. Replacement of a methyl group in Me₃O⁺ with MeOCH₂- led to spontaneous cleavage of a carbon-oxygen bond to liberate Me₂O. Bond cleavage in the (methoxymethyl)-dimethyloxonium is 46.5 kcal/mol more exothermic than cleavage of the trimethyloxonium, and [MeO=CH₂]⁺ is 91.4 kcal/mole more stable than the methyl cation. Caserio found that cyclic ortho esters with oxonium leaving groups dissociate rapidly and completely in the gas phase.¹¹ Thus the driving force is the stability of the products, and the reaction occurs with a small or no barrier. In initial studies on cyclic systems, we found that minimization of protonated cyclopentanol in AM1 or PM3 did not lead to bond cleavage. Upon minimization of the protonated α -oxygen homolog (the

cyclic hemiacetal of 4-hydroxybutanal [13a]), however, the bond length of the reaction coordinate increased spontaneously from 1.58Å to 2.78Å; to obtain ΔH_f for the ground state, it was necessary to constrain the C-O bond. The cyclic oxocarbenium ion is 5.5 kcal/mol more stable than the cyclic aliphatic carbenium ion.

This suggested that a relatively simple "yes-no" computational test for relative stabilities might be obtained merely by attempting to minimize protonated forms of various substrates. In the event, the situation is much more complex: cleavage of the C-O bond depends on the leaving group, leaving group conformations, anomeric effects, substituent effects, and the stability of the resulting carbenium ions. Results for the protonated oxygen substrates reported here generally parallel those found for the corresponding pyridinium substrates reported in the preceeding paper,¹² with a few notable exceptions.

Methods

Computations. The semi-empirical methods reported in Chapter 5 were used here.¹² For the THF, THP, and sugar substrates, the various conformations were set manually and minimized. Succeeding conformations were set by rotating the protonated leaving group 60°. The same relative orientation of the proton and lone pairs, designated as *i-vi* for the six principal conformations, were used consistently for the structures shown in the figures and drawings. For the studies of general-acid catalysis, the O---H---O bond between substrate LG and acid was constrained to 180°.

Controls. For several of the systems studied here, *ab initio* values are available that can be compared with the semi-empirical energies. They are discussed at the appropriate place. In general, there is good agreement among the

results obtained by the two methods; certainly the trends in *relative* energies and *relative* stabilities obtained with semi-empirical and *ab initio* methods agree.

As a further check on the internal consistency of the semi-empirical method, we calculated the starting, intermediate, and final structures in a six-step mechanism for the specific-acid catalyzed hydrolysis of formaldehyde dimethylacetal and compared the overall ΔH° obtained for each step with the value obtained by considering only the initial and final products (Figure 8.1). The value

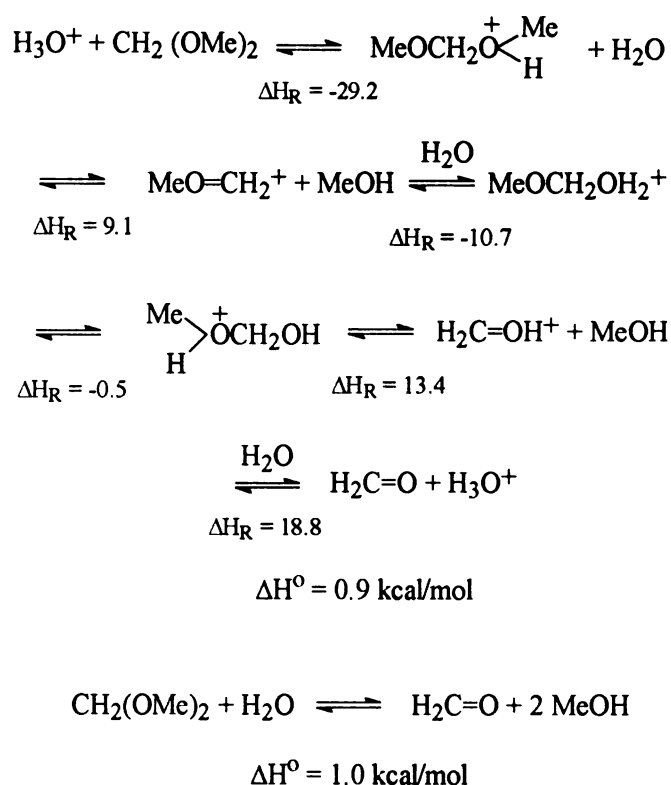


Figure 8.1. Step-wise mechanism for the specific-acid catalyzed hydrolysis of formaldehyde methyl acetal. ΔH_{R} for each step is $\Sigma \Delta H_{\text{f}}$ [products] - $\Sigma \Delta H_{\text{f}}$ [reactants]; ΔH° is the sum of ΔH_{R} for each step. The value of ΔH° for the step-wise mechanism (ten catalysts, products and/or reactants) is within 0.1 kcal/mol of ΔH° obtained considering only reactants and products.

of ΔH° obtained by summing the values of ΔH_{R} for each reaction in the step-wise mechanism is 0.1 kcal/mol lower than the value obtained considering the initial and final products, which is excellent agreement considering the possible error for

each step and the fact that the absolute energies were rounded off to the nearest 0.1 kcal/mol. This agreement shows that the method is internally consistent and that numbers may be compared between and among series.

Results and Discussion

Linear Compounds.

Formaldehyde Hydrate. The simplest member of the series of linear compounds studied is formaldehyde hydrate, $\text{CH}_2(\text{OH})_2$ (1). Wipff¹³ has reported low-level *ab initio* energies (at the 4-31G level) for ground-state and protonated forms of several conformations of 1. The PM3 energies for the ground-state rotomers 1A-D show the same trend in relative energies reported by Wipff, although the PM3 energies are lower by a factor of 2 (Figure 8.2); the structures and energies mirror the trends found for $\text{CH}_2(\text{OMe})_2$ by Andrews, et al.,¹⁴ that are discussed below (see Figure 8.9). The PM3 energies for the protonated forms 1AH⁺-1DH⁺, with torsional angles constrained to reproduce Wipff's structures, show the same trends in relative energies he reported, but PM3 minimization of the unrestricted forms 1BH⁺-1DH⁺ lead to more stable forms 1BH⁺r-1DH⁺r (Figure 8.2) that reflect the stabilizing $n\sigma^*$ interactions within the structures emphasized by Andrews, et al.,¹⁴ for the dimethoxy series.

The complexity of this relatively simple system can be appreciated from the various local minima that can be obtained from 1CH⁺ (Figure 8.3). The initial structure has a staggered conformation (viewed along the O₂-C bond) obtained by constraining the H₃-C-O₁-H₁ bond angle α and the H₃-C-O₂-H₂ bond angle β to 60° and restraining the C-O₂ bond--the reaction coordinate--to 1.61Å, the reaction coordinate distance in PM3 structures for 1AH⁺-1DH⁺; after full minimization, $\Delta H_f = 105.3$ kcal/mol. Removal of all restraints, or of the torsional angle α ,

followed by minimization gives 1CH^+ra , in which the O_1 hydroxyl has rotated by 60°C to introduce two stabilizing $n\sigma^*$ interactions; this minor change in structure is worth 4.5 kcal/mol in energy of stabilization. If only the restraint on the reaction

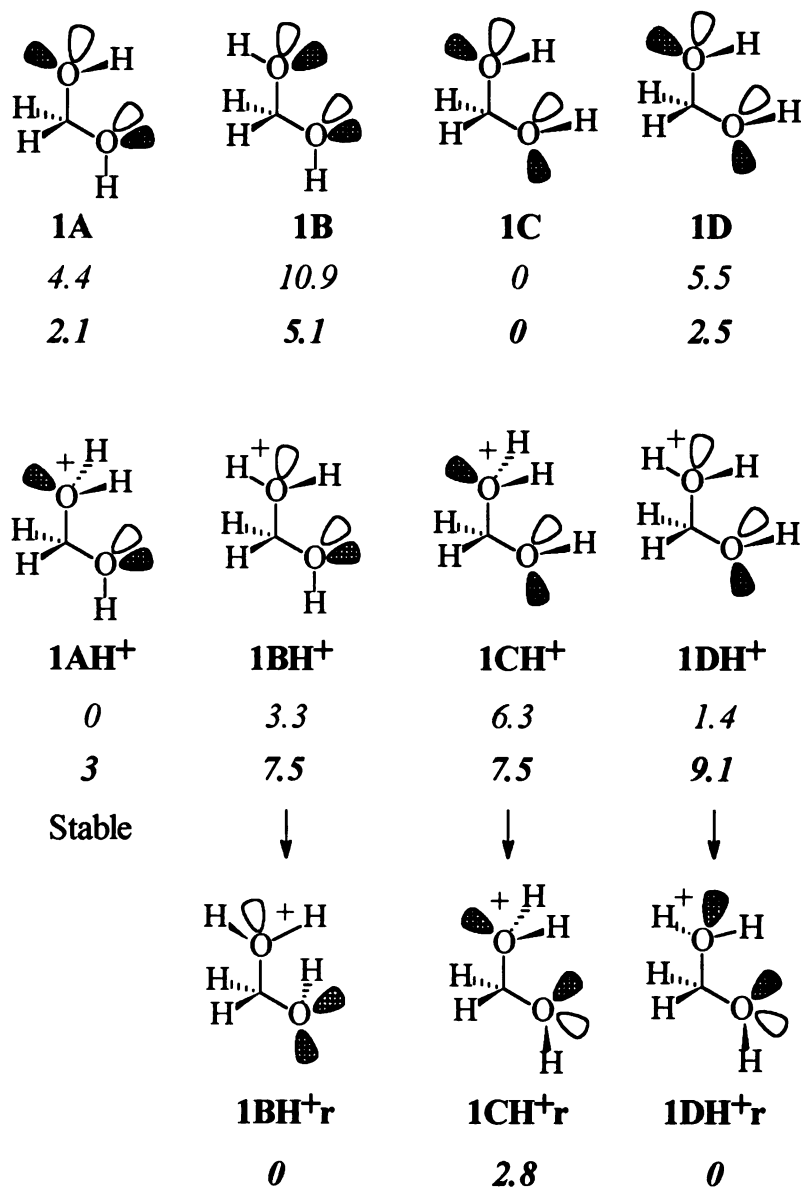


Figure 8.2. Structures and energies for formaldehyde hydrate (1). The unprotonated structures **1A-1D** are those considered by Wipfl¹³ and calculated at the 4-31G level of theory with *ab initio* methods (relative energies in italics); the PM3 values obtained in this study are given in bold face italic. Upon full PM3 minimization with no constraints, three of the protonated forms, **1BH⁺-1DH⁺** revert to much more stable rotomers **1BH⁺r-1DH⁺r**. **1AH⁺** is stable.

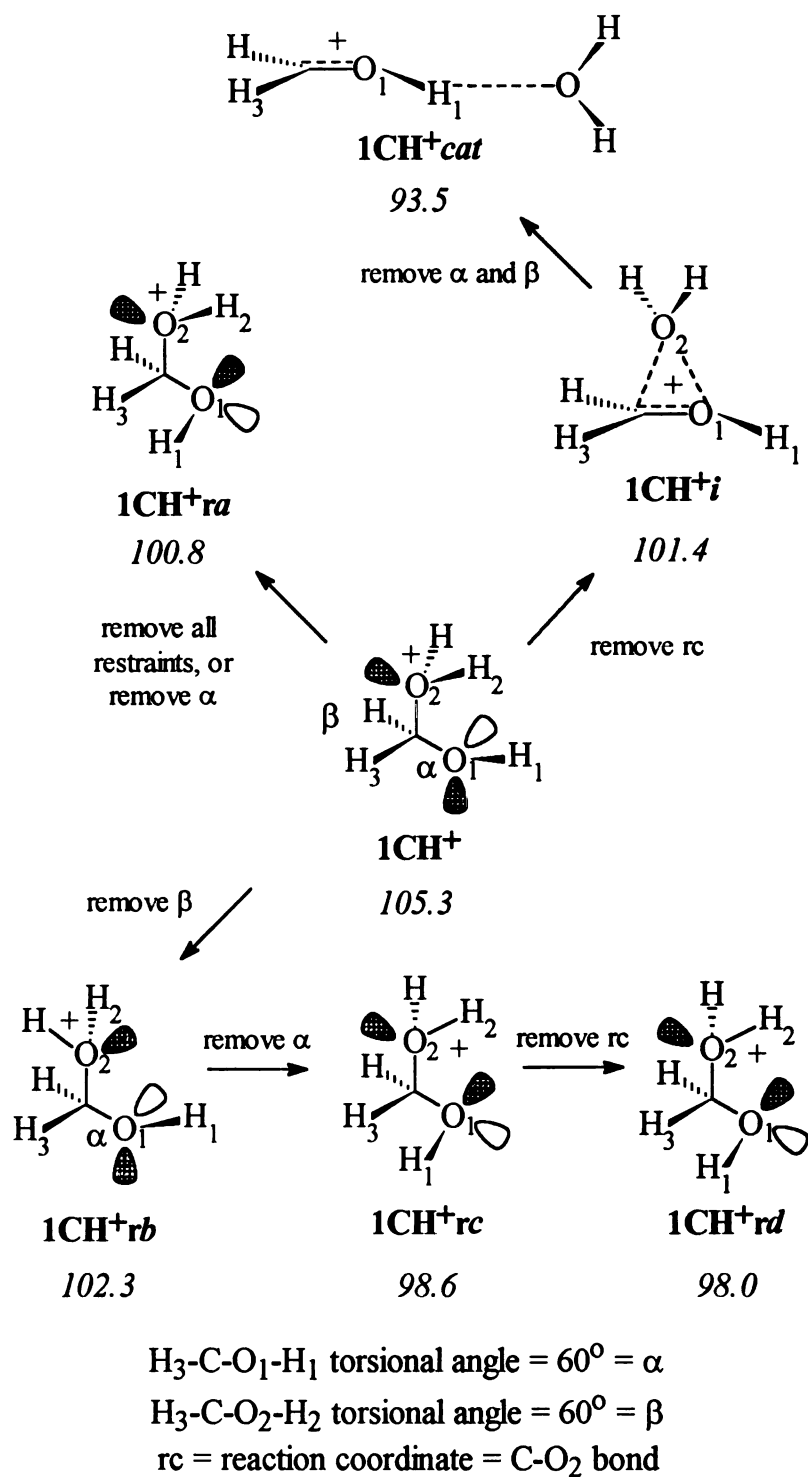


Figure 8.3. Various structures obtained upon full PM3 minimization of 1CH^+ by step-wise removal of the torsional angle restraints α and β and the reaction coordinate. Each restraint was held at a force constant of 10^3 . The numbers in italics are the absolute PM3 ΔH_f for each structure.

coordinate is removed for 1CH^+ , spontaneous bond cleavage occurs to 1CH^+i because of the antiperiplanar orbitals in 1CH^+ . (Note that in the first case, rotation removes the antiperiplanar interaction and prevents bond cleavage.) It is interesting that the stable ion-dipole complex 1CH^+i has a symmetrical bridged structure--C-O₂ and O₁-O₂ bond length = 2.72Å and O₁-C-O₂ and C-O₁-O₂ bond angles = 76°--not unlike phenonium ions, which is very similar to ion-dipole complexes obtained for several pyridinium compounds reported in Chapter 7.¹² While the ion-dipole complex is 3.9 kcal/mol more stable than the structure from which it was generated, it is 3.4 kcal/mole less stable than the most stable rotomer 1CH^+rd . 1CH^+i , however, is an intermediate; removal of the α and β torsional angle restraints followed by minimization leads to the planar oxocarbenium ion 1CH^+cat in which the departed water is hydrogen bonded to the O₁ hydroxyl. This is the most stable structure found in this series ($\Delta H_f = 93.5$ kcal/mol).

These structures are reproduced if the rc bond length is increased in 0.1Å steps from the initial structure in which the torsional angle restraints have been removed; the complete energy profile is shown in Figure 8.4. A small change in the rc (0.04Å) leads to a large stabilization in energy to point A; increasing the bond length leads to B. The transition from B to C in Figure 8.4 represents inversion of the departing water hydrogens from syn to O₁ to anti. Further increases in the bond length lead to point D, which is the bridged structure 1CH^+i (Figure 8.3). A 0.1Å change in reaction coordinate bond length leads to a precipitous drop in energy caused by the formation of a hydrogen bond between the departing water and the O₁-hydroxyl (H₁) to give a structure that eventually minimizes to 1CH^+cat . Thus an initial structure in which there are antiperiplanar orbitals can collapse to the oxocarbenium ion with which the LG is still associated, although not in a position to return easily to either the intermediate or the ground-state structure.

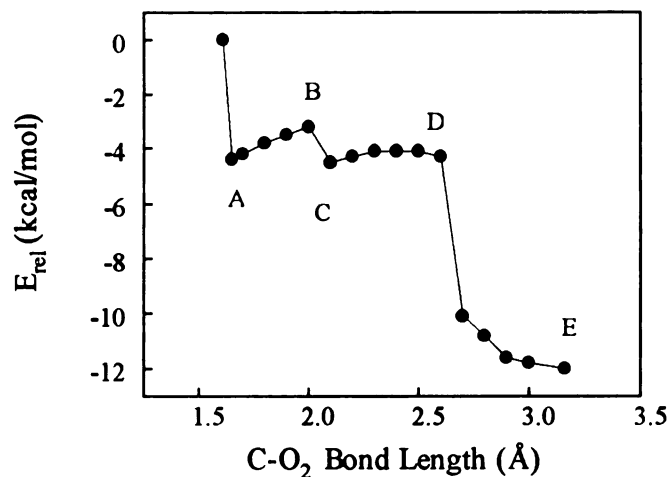


Figure 8.4. Full PM3 energy profile for minimization of 1CH^+ after removal of the restraint on the reaction coordinate. The reaction coordinate bond length was increased in 0.1Å steps and each structure was fully minimized. The transition $A \rightarrow B$ represents the energy associated with an increase in the reaction coordinate bond length; $B \rightarrow C$ represents a simple umbrella inversion of the protons on the leaving group oxygen; $C \rightarrow D$ represents a change from a structure in which the C-O_2 bond is perpendicular to the plane of the insipient oxocarbenium ion to the symmetrical bridged structure 1CH^+i (Figure 8.3); $D \rightarrow E$ represents the "folding over" of the departing water with formation of an hydrogen bond, eventually yielding the structure 1CH^+cat .

Collapse need not occur, however. If the antiperiplanar orbital interaction is eliminated by removal of the constraint on the torsional angle β , full minimization yields structure 1CH^+rb in which the O_2 protonated hydroxyl has rotated to form a second staggered rotamer that adds two $n\sigma^*$ interactions and removes the antiperiplanar interaction, worth 3.1 kcal/mol (Figure 8.3). (Note that removal of the restraint on the reaction coordinate in this structure followed by minimization increases the reaction coordinate bond length to 1.74Å without catastrophic bond cleavage and increases the stability by 0.2 kcal/mol , presumably because a repulsion between orthogonal lone pairs on O_1 and O_2 is reduced.) Removal of the α torsional angle from 1CH^+rb followed by full minimization causes both O_1 and O_2 hydroxyls to rotate to give 1CH^+rc , a maneuver that produces three $n\sigma^*$ interactions and removes the orthogonal repulsion, worth 3.7 kcal/mol relative to

1CH⁺rb and 6.7 kcal/mol relative to the starting structure **1CH⁺**. Finally, removing the rc restrain from this structure and minimizing gives **1CH⁺rd**, in which the rc bond length decreases to 1.57Å and the energy is lowered by 0.6 kcal/mol, presumably by increasing the O₂-C-H nσ* interaction.

The wide range of structures with different energies that can be obtained by relatively minor step-wise alterations in geometry of this simple molecule shows the complexity inherent in the general system. As we show below, changes in the LG (from OH₂ to MeOH, say) or the heteroatom (from O to S) can affect the reactivity and the reaction profiles drastically.

Formaldehyde Methyl Hemiacetal (2). Jefferies, et al.,¹⁵ have reported the *ab initio* (HF/4-31G) ground state energies for various conformers of this compound in which the torsional angles of the MeO and OH groups are restrained to be 60° out of the O-C-O plane (Figure 8.5). In all but one instance (**2D**), the PM3 relative energies show the same trends, although they are lower than the HF/4-31G values as found above for **1**. If the restraints are released from the various conformers which are then fully minimized, the same relative energies are obtained; the differences are related to the change in torsional angle, by up to as much as 22°--from 60° to 38° for the MeO in **2A,C,D**, for example. We also found that **2C** minimizes to **2A** and **2E** minimizes to **2B** with the restraints released, which limits the stable PM3 structure to the three, similar to structures identified by Andrews, et al.,¹⁴ for formaldehyde dimethyl acetal (see Figure 8.9); these workers also found a similar trend in relative energies (see below).

There are two potential leaving groups for this compound. MeOCH₂OH₂⁺ (**3**) is 0.5 kcal/mol less stable than ⁺MeOHCH₂OH (**4**) in accord with the expected proton affinities. (Both structures were generated by restricting the respective C-O bond length to 1.56Å and minimizing fully in PM3 to the most stable rotomer.)

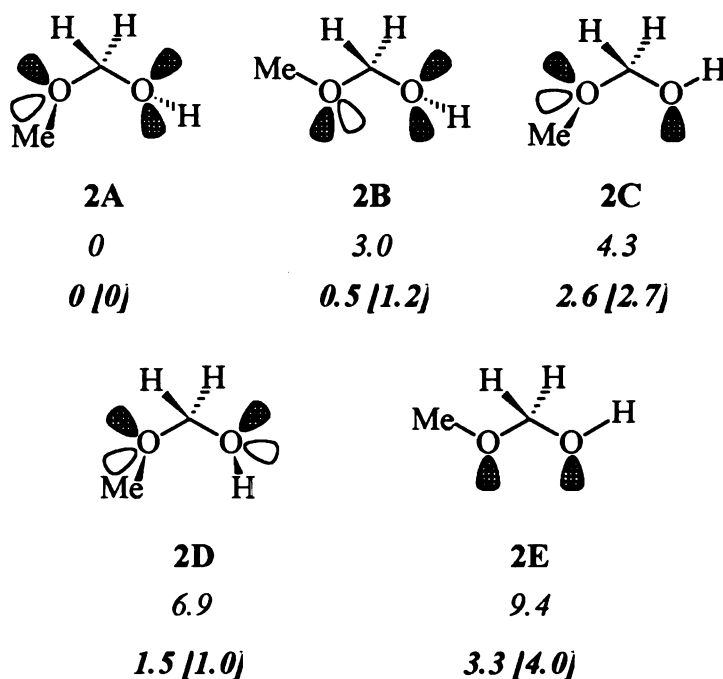


Figure 8.5. Structures and energies for formaldehyde methyl hemiacetal (**2**). The numbers in italics are the relative energies (in kcal/mol) calculated by Jeffery, et al.,¹⁵ at the HF/4-31G level of theory, with the torsional angles of the methoxy and hydroxyl restrained at 60° from the O-C-O plane. The numbers in boldface italic are PM3 relative energies calculated in this study, with the same restraints used by Jeffery, et al. The numbers in brackets are PM3 energies obtained from full minimization after removal of the restraints; the basic conformations are retained, although the torsional angles change by as much as 22°.

Protonation of either lone pair on the methoxy O produces the *R*- or *S*- form of **4**, both of which were examined.

Unlike the energy profiles for the pyridinium analogs reported in Chapter 7,¹² the calculated stability of these compounds depends on the semi-empirical method used. PM3-minimization of **3** leads to cleavage of the C-O bond for three rotomers (**3iv-3vi**), all of which are subject to orbital repulsion (Figure 8.6). The other rotomers are stable. AM1-minimization of **3** does not lead to bond cleavage for any rotomer, however. This difference is also reflected in the energy profiles (Figure 8.7). In PM3, **3i** has a small but distinct ΔH^\ddagger and forms an

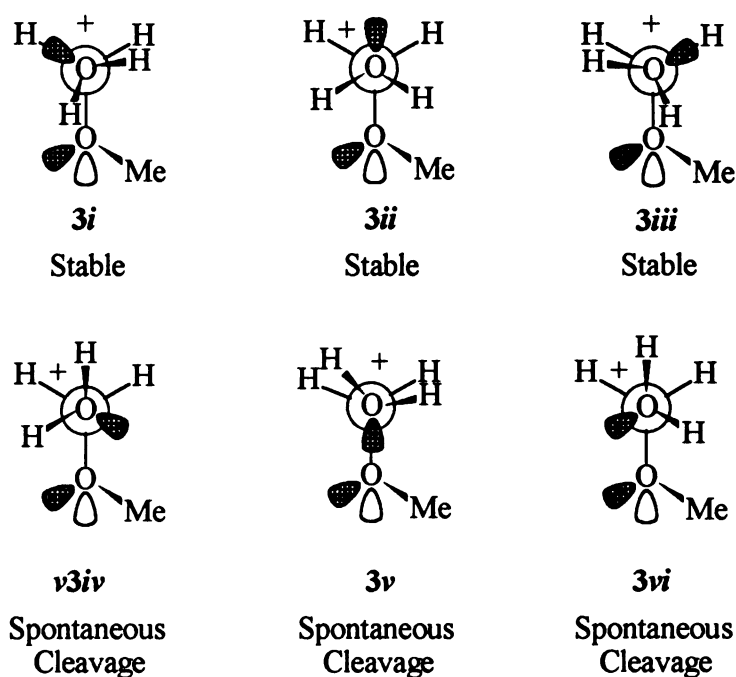


Figure 8.6. PM3 structures of 60° rotomers for protonation on the hydroxyl of 2. *4i-iii* are stable, *4iv-vi* undergo spontaneous cleavage upon minimization.

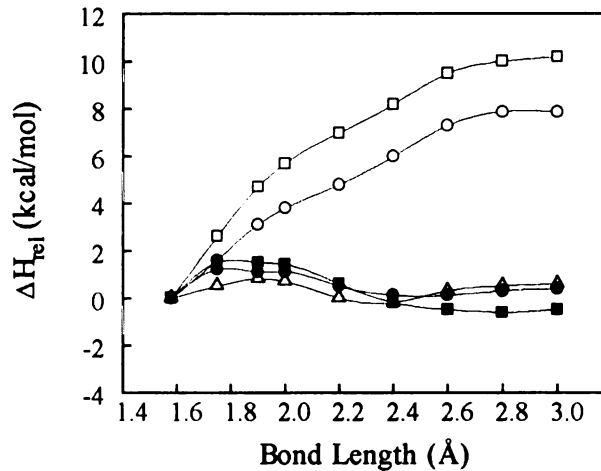


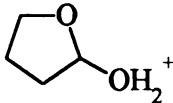
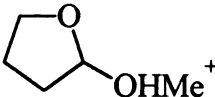
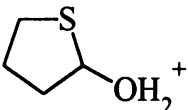
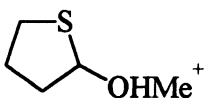
Figure 8.7. Energy profiles for dissociation of the C-O bond the most stable ground-state structures for 3 (○ = AM1; ● = PM3), 4 (□ = AM1; ■ = PM3), and 7 (△, AM1).

ion-dipole complex, while in AM1 there is no distinct transition state, and the values of ΔH_R are high and positive (Table 8.1).

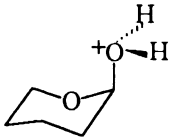
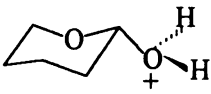
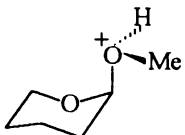
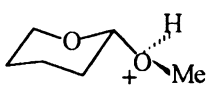
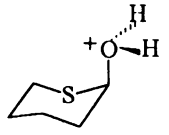
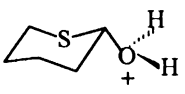
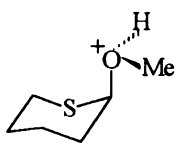
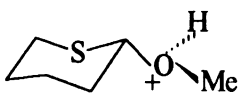
1941

1942

Table 8.1. Semi-empirical Enthalpies of Reaction (kcal/mol)

Compound	ΔH_R	
	AM1	PM3
$\text{MeOCH}_2\text{OH}_2^+$	21.1	10.0
$\text{MeOCH}_2\text{OHMe}^+$	22.8	8.5
MeOCHMeOH_2^+	12.5	2.6
MeOCHMeOHMe^+	11.5	0.4
$\text{MeSCH}_2\text{OH}_2^+$	-6.7	-7.8
$\text{MeSCH}_2\text{OHMe}^+$	-4.9	-7.5
MeSCHMeOH_2^+	-12.9	-10.5
MeSCHMeOHMe^+	-12.5	-12.7
	12.7	3.6
	12.6	0.6
	-14.4	-10.2
	-12.2	-15.6

(Table 8.1, con't)

Compound	ΔH_R	
	AM1	PM3
	9.5	0.8
	4.7	-0.1
	6.9	-5.0
	7.9	-4.6
	-13.8	-12.0
	-15.7	-14.2
	-17.0	-16.5
	-18.4	-17.4

Protonation of either methoxy lone pair in **2** gives either the (*R*)- or (*S*)-form of **4** (Figure 8.8). The reactivity or stability of these conformers were

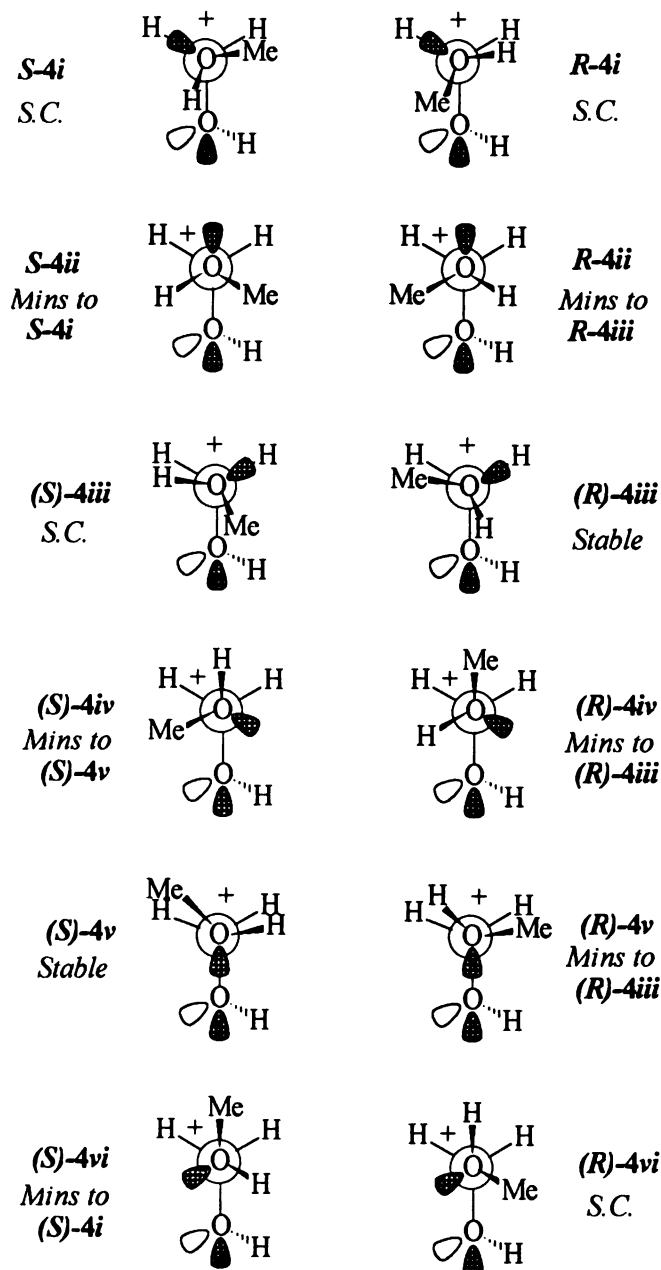
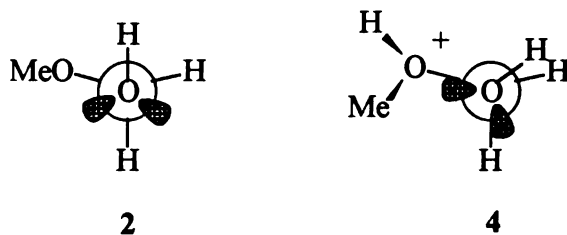


Figure 8.8. The 12 60° chiral rotomers obtained by protonating the methoxy oxygen (0.5 kcal/mol more stable than the protonated hydroxyl form) of the most stable rotomer of **2**. The reactions are discussed in the text. S.C. = spontaneous cleavage; *Mins to* refers to the structure obtained on full PM3 minimization with no constraints.

analyzed by full PM3 minimization. Unlike the unprotonated conformers, in which the hydroxyl and methylene groups exist in a staggered conformation, in the protonated form the hydroxyl and methylene groups are eclipsed, a conformation that remains stable in all 12 rotomers considered. This conformation prevents an



antiperiplanar alignment between the hydroxyl and methoxy orbitals in the protonated forms. The forms that undergo spontaneous cleavage upon minimization do so because of steric repulsion between the methoxy methyl and the hydroxyl in eclipsed conformers such as (*R*)-4*i* and (*S*)-4*iii* or by orbital repulsion as in (*R*)-4*vi* and (*S*)-4*iii*. It is interesting to compare (*R*)-4*vi* and (*S*)-4*vi* (Figure 8.8). Both have the extreme orbital repulsion caused by a gauche-gauche interaction between the methoxy orbital and the two orbitals on the hydroxyl. The gauche methoxy methyl-hydroxyl conformation in (*R*)-4*vi* causes spontaneous cleavage, but in (*S*)-4*vi*, in which the methoxy methyl and hydroxy are *trans*, minimization to the stable form (*S*)-4*i* occurs with relief of the orbital repulsion and no spontaneous cleavage. (The same situation occurs in the dimethoxy compound, as in (*R*)-6*aiv* [see Figures 8.10 and 8.11].) In (*S*)-4*iii*, there is only steric repulsion between the methoxy methyl and the hydroxyl held in the eclipsed conformation. While a simple 60° rotation of the hydroxyl (to a staggered conformer) would produce an antiperiplanar alignment with the orbital of the methoxy oxygen that would satisfy the Deslongchamp criteria for bond scission,¹⁶ spontaneous cleavage occurs without a change in the geometry of the hydroxyl, which suggests in turn that steric repulsion is sufficient to cause cleavage. It

should be noted, however, that the eclipsed conformation between the methylene and the hydroxyl may be the most stable form because it allows conjugation with the methylene carbon in the cation ($\text{H}_2\text{C}=\text{OH}^+$) without major geometric reorganization; it is also probably true that there is partial conjugation in the eclipsed ground-state conformers.

Formaldehyde Dimethyl Acetal (5). Andrews, et al.,¹⁴ have performed *ab initio* computations on the neutral and protonated forms of this compound at a high level of theory (6-31G*). The most stable of the neutral forms have the geometries shown in Figure 8.9. The PM3 ΔH_f values parallel those of Andrews, et al.,¹⁴ and roughly match those for 4.

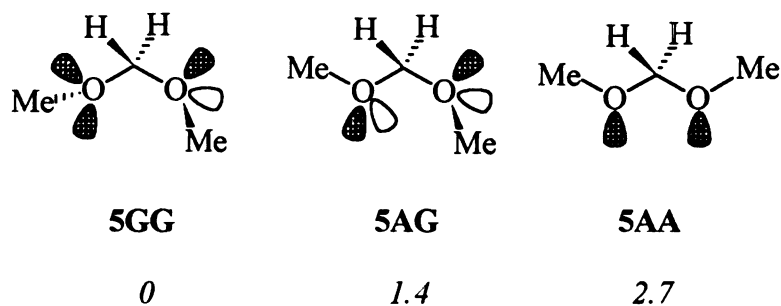


Figure 8.9. The three stable rotomers of 5. The designations GG, AG, and AA are those used by Andrews, et al.¹⁴ The numbers in italics are the relative PM3 ΔH_f in kcal/mol for the unconstrained structures.

Protonation of the most stable conformer **5GG** on either lone pair leads to either (*S*)-**6siv** or (*R*)-**6sii** (Figure 8.10). The ΔH_f values obtained by full minimization of the constrained rotomers show that (*S*)-**6siv** is 0.8 kcal/mol less stable than (*R*)-**6sii**, presumably because of the orbital repulsion in (*S*)-**6siv**. When constraints are removed from (*S*)-**6siv** and (*R*)-**6sii** and both are fully minimized, (*S*)-**6siv** undergoes spontaneous cleavage, presumably because of an antiperiplanar alignment, while (*R*)-**6sii** minimizes to (*R*)-**6siii**, which is 4.2 kcal/mol more stable than (*R*)-**6sii**.

10
11
12
13
14
15
16
17
18
19
20
21
22
23
24
25
26
27
28
29
30
31
32
33
34
35
36
37
38
39
40
41
42
43
44
45
46
47
48
49
50
51
52
53
54
55
56
57
58
59
60
61
62
63
64
65
66
67
68
69
70
71
72
73
74
75
76
77
78
79
80
81
82
83
84
85
86
87
88
89
90
91
92
93
94
95
96
97
98
99
100

101
102
103
104
105
106
107
108
109
110
111
112
113
114
115
116
117
118
119
120
121
122
123
124
125
126
127
128
129
130
131
132
133
134
135
136
137
138
139
140
141
142
143
144
145
146
147
148
149
150
151
152
153
154
155
156
157
158
159
160
161
162
163
164
165
166
167
168
169
170
171
172
173
174
175
176
177
178
179
180
181
182
183
184
185
186
187
188
189
190
191
192
193
194
195
196
197
198
199
200

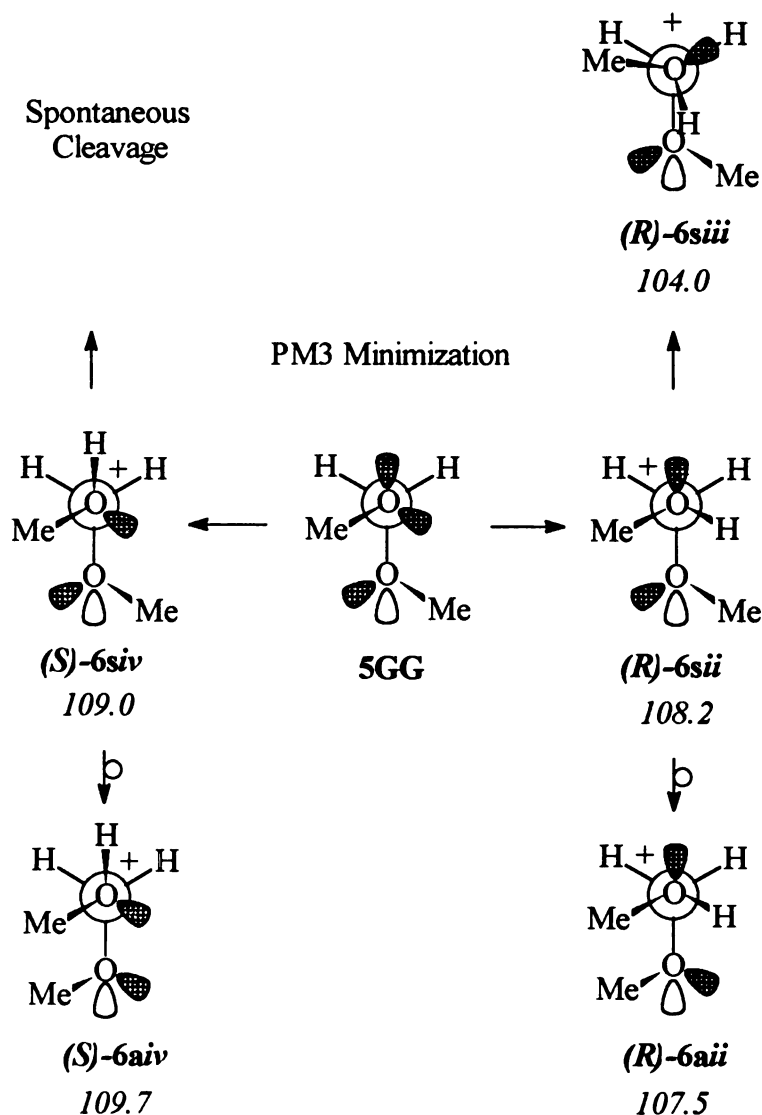


Figure 8.10. Two chiral forms obtained by protonation of either lone pair on the oxygen of 5GG. In the numbering system for the forms, *s* refers to the methyl on the unprotonated methoxy being "syn" to the lone pair on the protonated methoxy, *a* as the methyl "anti" to the lone pair; italicized lower case Roman numerals refer to the rotomer in Figure 8.11. The italicized numbers are the absolute PM3 ΔH_f . See text for a description of the manipulations involved.

Rotation of the unprotonated methoxy into a gauche methyl-methyl interaction increases the energy of *(S)*-6aiv by 0.7 kcal/mol but decreases the energy of *(R)*-6aii by 0.7 kcal/mol. In the former case, methyl-methyl and lone pair-lone pair interactions are introduced, and a methyl-lone pair interaction is

1950

1951

eliminated in the latter case, which suggests that the methyl-lone pair interaction is more important than the purely steric methyl-methyl gauche interaction.

The reactivity of all 12 60° rotomers of (*S*)-**6a** and (*R*)-**6a** are shown in Figure 8.11; the relative energies of each rotomer are included. More rotomers in this series undergo spontaneous cleavage than do the protonated rotomers of the hemiacetal, which reflects the greater number of steric interactions present in the acetal rotomers. The basic pattern of reactivity is the same for the two series, however.

The energy profile for the acetal shows the same method dependence found for the hemiacetal. A distinct transition state is found only in PM3 (Figure 8.7). Thus in the simple linear system, these effects are independent of the leaving group.

Replacing a proton on the aldehyde carbon with a methyl to give a secondary system affects the reactivity. Spontaneous bond cleavage occurred for all rotomers in MeOCHMeOH_2^+ (**7**) and MeOCMeCHOMeH^+ (**8**) in either AM1 or PM3. In PM3, **7** had a small but distinct transition state (Figure 8.7). The values of ΔH_R are 7.4 and 8.1 kcal/mol lower for **7** and **8** than for the corresponding primary systems (Table 8.1). With the exception of the conformation dependence, these result parallel those found for dissociation of the corresponding pyridinium compounds.¹²

The effects of replacing an oxygen with a sulfur in the hemiacetal and acetal are dramatic. Minimization of $\text{MeSCH}_2\text{OH}_2^+$ (**9**) and $\text{MeSCH}_2\text{OHMe}^+$ (**10**) in AM1 and PM3 leads to cleavage of all rotomers, and the reactions are more exothermic by ca. 27 kcal/mol and ca. 17 kcal/mol in PM3 than for corresponding oxo compounds, respectively, which parallels the values for the pyridinium analogs reported in Chapter 7.¹² In the PM3 energy profile for **9** (not shown),

1950

1951

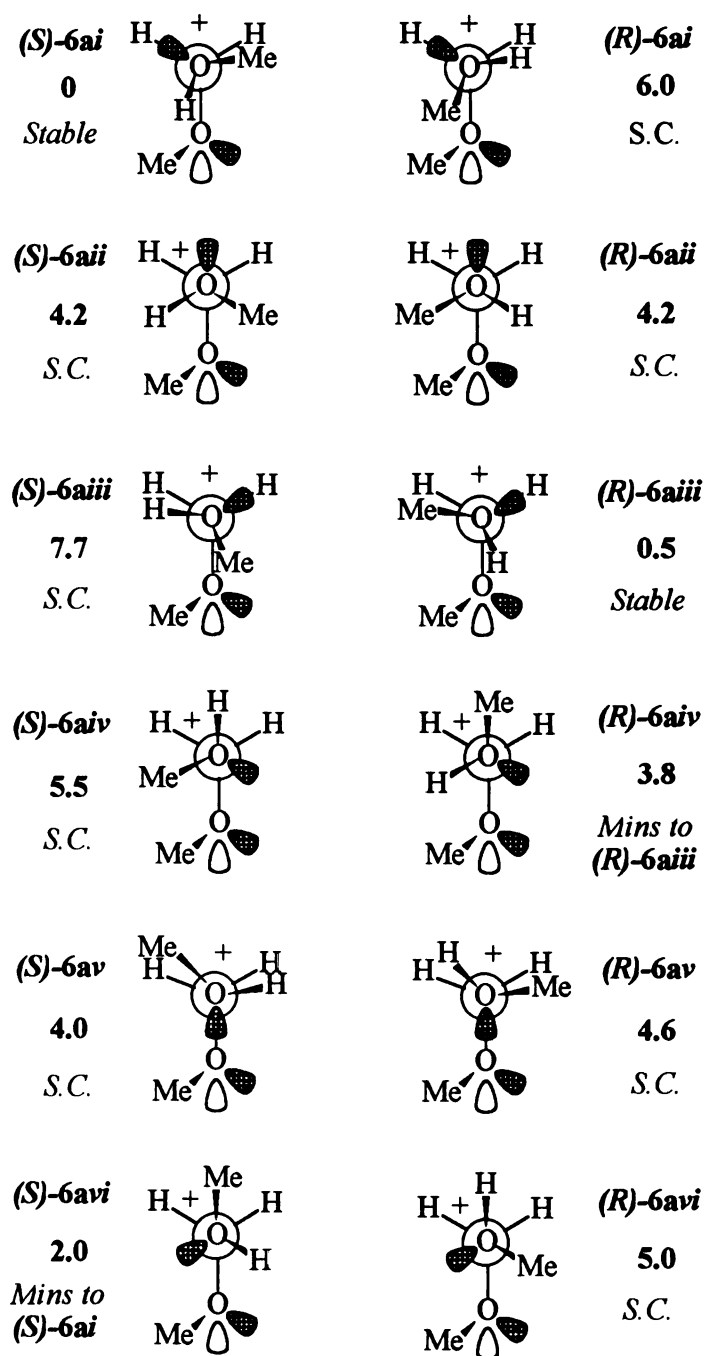
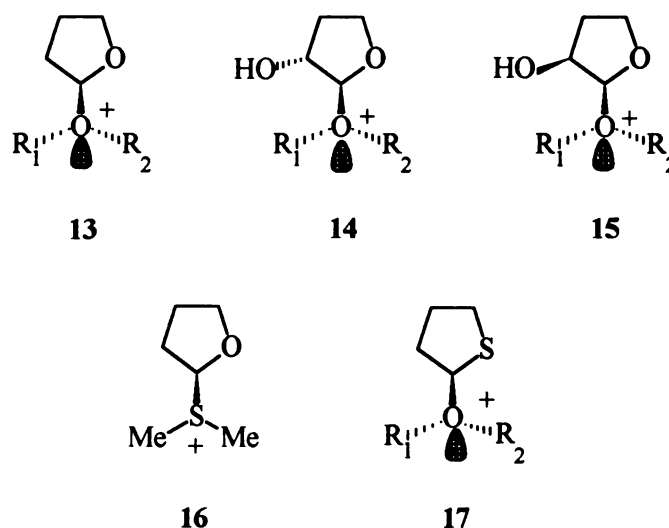


Figure 8.11. The 12 60° chiral rotomers obtained by protonating the methoxy oxygen of the anti form of **6** (see legend to Figure 8.10 for explanation). The reactions are discussed in the text. The numbers in bold face are the relative PM3 ΔH_f with torsional angle and reaction coordinate constraints used to hold the conformation. Note that the stability is a direct function of ΔH_R , which reflects either steric or orbital interactions. *S.C.* = spontaneous cleavage; *Mins to* refers to the structure obtained on full PM3 minimization with no constraints.

the ion-dipole complex has a relative energy of -16.3 kcal/mol and a C-OH₂ bond length of 3.2Å. The change from a primary to a secondary system by the methyl-for-proton replacement in this series lowers ΔH_R by 2.7 kcal/mol for MeSCHMeOH₂⁺ (11) and by 5.2 kcal/mol for MeSCHMeOHMe⁺ (12) relative to the primary compounds. (A more general analysis of the effect of the sulfur for oxygen substitution is given below.)

Cyclic Compounds.

Five-Membered Rings. A number of THF and thio-THF systems were studied (Chart 2). Spontaneous bond cleavage depends on the conformation of the leaving group relative to the ring oxygen and on the leaving group.



a: R₁ = R₂ = H; b: R₁ = H, R₂ = Me; c: R₁ = R₂ = Me

Six conformations of 13a were studied. All three staggered conformations (13a_{ii}, 13a_{iv}, and 13a_{vi}, Figure 8.12) and one eclipsed (13a_v) cleaved spontaneously to an ion-dipole complex that is *ca.* 7 kcal/mol more stable than the ground state structures (Table 8.1). Two of the eclipsed conformations (13a_i and

1950
1951
1952
1953
1954
1955
1956
1957
1958
1959
1960

1961
1962
1963
1964
1965
1966
1967
1968
1969
1970

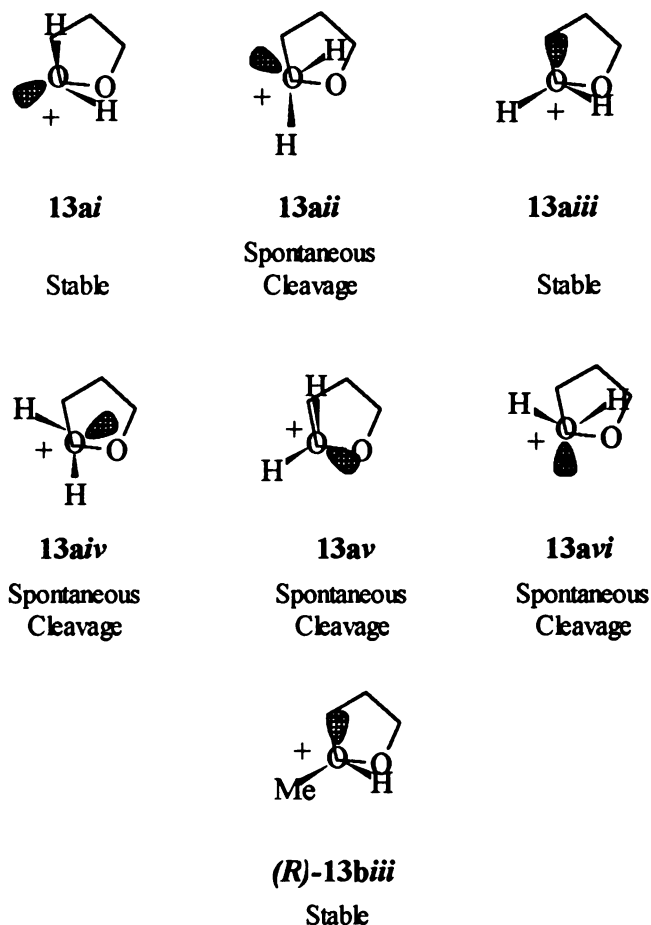
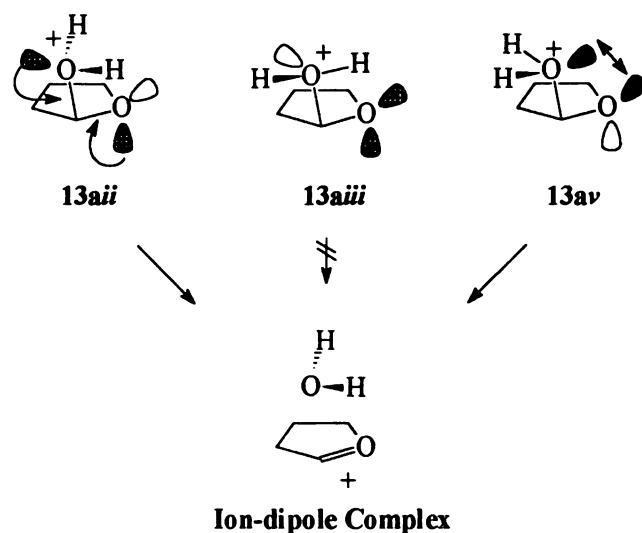


Figure 8.12. The six conformers for the protonated form of the cyclic hemiacetal of 4-hydroxybutanal, which show the same reactivity pattern found for **4** (see Figure 8.6), with the exception of **13aii**, which cleaves upon minimization. All conformers of the *R*- and *S*- forms of **13b** cleave except **13bii**, and all conformers of **13c**, the dimethyloxonium salt, cleave.

13aiii) were stable. Note that with the exception of **13aii**, this is the same pattern as seen for **6** and **16Eai-vi** in PM3. If the reaction coordinate bond is restrained, rotomers that cleave minimize to stable structures: **13aii** → **13ai**, **13av** → **13avi**, etc. Only one eclipsed conformation (**13biii**) was stable in **13b** (LG = MeOH) and no conformation was stable in **13c** (LG = Me₂O). Cleavage is apparently the result either of an appropriate anti-periplanar arrangement in the Deslongchamps scheme¹⁶ (**13aii**) or orbital repulsion (**13aiv**, **13av**, and **13avi**), neither of which is present in the stable structures. Differences between AM1 and PM3 are limited to

1950

1951



cleavage of rotomers in conformation *ii*, which are stable in AM1 but cleave in PM3.

The energy profile for **13a** was generated by restraining the reaction coordinate bond to 1.57 Å (the length of the bond in stable structures) and minimizing the initial structure; **13a_i** was obtained. In PM3, a distinct transition state ($\Delta H^\ddagger = 2$ kcal/mol) with a stable ion-dipole complex was obtained (Figure 8.13). Energy profiles for **13b** have no barrier to collapse with formation of a

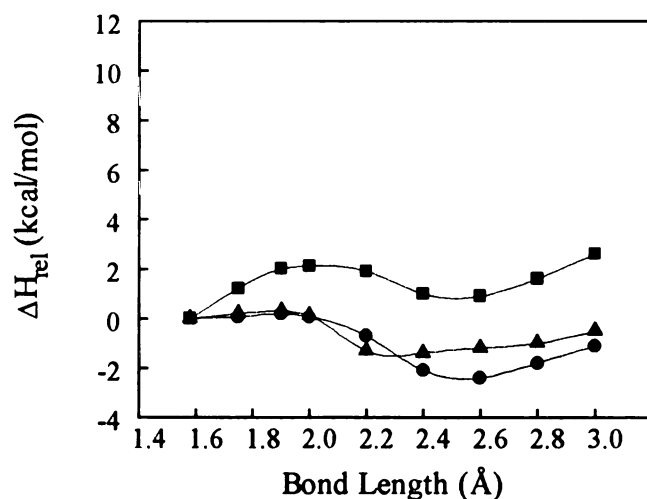


Figure 8.13. PM3 energy profiles for cleavage of **13a_i** (■), **16Aa** (▲), and **16Ea** (●).

1950

1951

stable ion-dipole complex (not shown), which parallels the pattern for the deoxy methylribofuranoside discussed below.

As found for the corresponding pyridinium substrates,¹² the THF substrate has a higher ΔH^\ddagger (2.1 kcal/mol) than the THP substrates, in which the axial compound had a slightly higher (0.2 kcal/mol) ΔH^\ddagger than the equatorial compound (0.1 kcal/mol). Thus the arguments give in Chapter 7 in terms of activation values for the stabilities of the pyridinium compounds apply equally to the hydroxy compounds.

The *trans*-3-hydroxy compound **14** shows essentially the same pattern as found for **13**, despite the fact that the oxocarbenium ion would be destabilized by the inductive effect of the 3-hydroxy, which is analogous to the effect in β -nicotinamide ribosides.¹⁷ The *cis*-3-hydroxy compound **15**, however, shows a different pattern in which formation of a hydrogen bond between the protons on the 2-hydroxy and the oxygen of the 3-hydroxy stabilizes the structure and

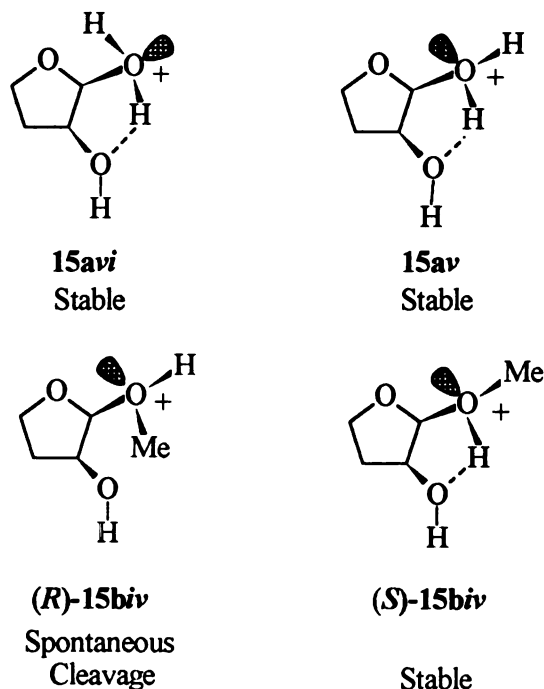


Figure 8.14. The effect of hydrogen bond formation on the stability of several conformers of **15**.

1951
1952
1953
1954
1955

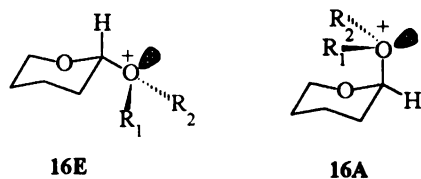
prevents spontaneous cleavage upon minimization. For instance, both **14avi** and **14av** (Figure 8.14) are stable structures, while the corresponding rotomers **14av** and **14avi** (Figure 8.12) undergo spontaneous cleavage upon PM3 minimization. The same pattern is seen in **15bvi**; the (*R*)-form, which will not form a hydrogen bond, undergoes spontaneous cleavage, while the (*S*)-form, which can form a hydrogen bond, is stable (although we cannot rule out steric repulsion in the former case).

Neither pyridine¹² nor dimethylsulfide (**16**) is expelled upon minimization of the respective 2-THF derivatives. Water, methanol, and dimethyl ether are expelled spontaneously upon PM3 minimization of the MM2-minimized forms of thio-THF compounds **17a-c**, however. This suggests that the stability of the insipient carbenium ion or ion-dipole complex and not stereoelectronic or repulsive interactions is responsible for cleavage. Thus the results for the five-membered systems parallel those found for the corresponding pyridinium compounds reported in Chapter 7.

Six-Membered Rings. Several six-membered compounds were studied. The equatorial hemiacetal **16E** showed essentially the same conformational dependence seen for **2** (Figure 8.6) and **15** (Figure 8.12). Some forms minimized to stable forms by simple rotation of the leaving group (Figure 8.15). Simultaneously, the geometry around the anomeric carbon was flattening; if the minimization was stopped and the original rotomer reestablished manually, bond cleavage occurred through **16Eavii**. The energy difference is ca. 0.2 kcal/mol. The same pattern was found for both (*R*)- and (*S*)- forms of **16Eb**, with the exception that **16Ebii** minimized to a stable form or cleaves via **15Ebvi** (Figure 8.16). In the axial compound **16Aa**, the only stable structure was **16Aai**. For the corresponding rotomer in the methoxy compound, the (*R*)- form was stable while the (*S*)- form

MEMPHIS

1951



a: $R_1 = R_2 = H$; **b:** $R_1 = H, R_2 = Me$; **c:** $R_1 = R_2 = Me$

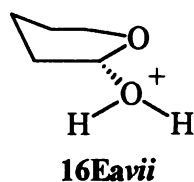
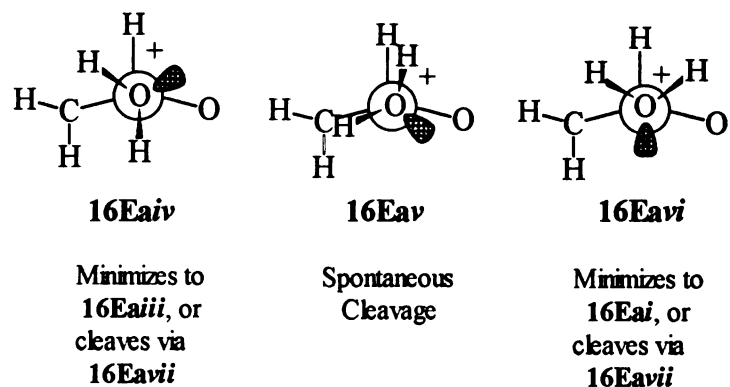
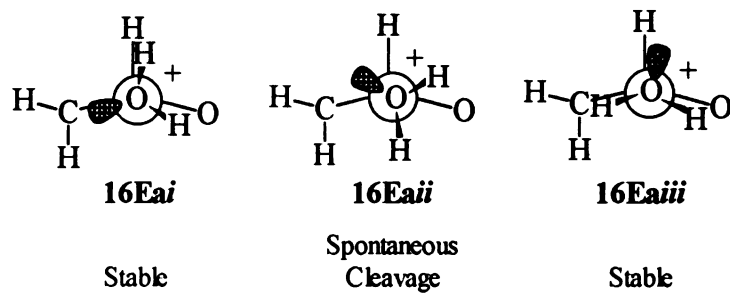
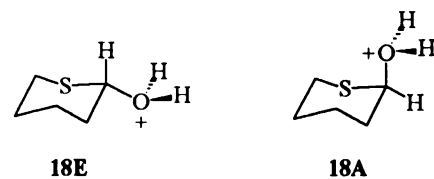
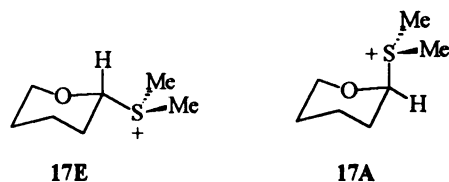


Figure 8.15. The six 60° rotomers for the protonated forms of equatorial 2-hydroxy-THP. **16Eavii** is an intermediate form produced by minimization of several rotomers (see text).

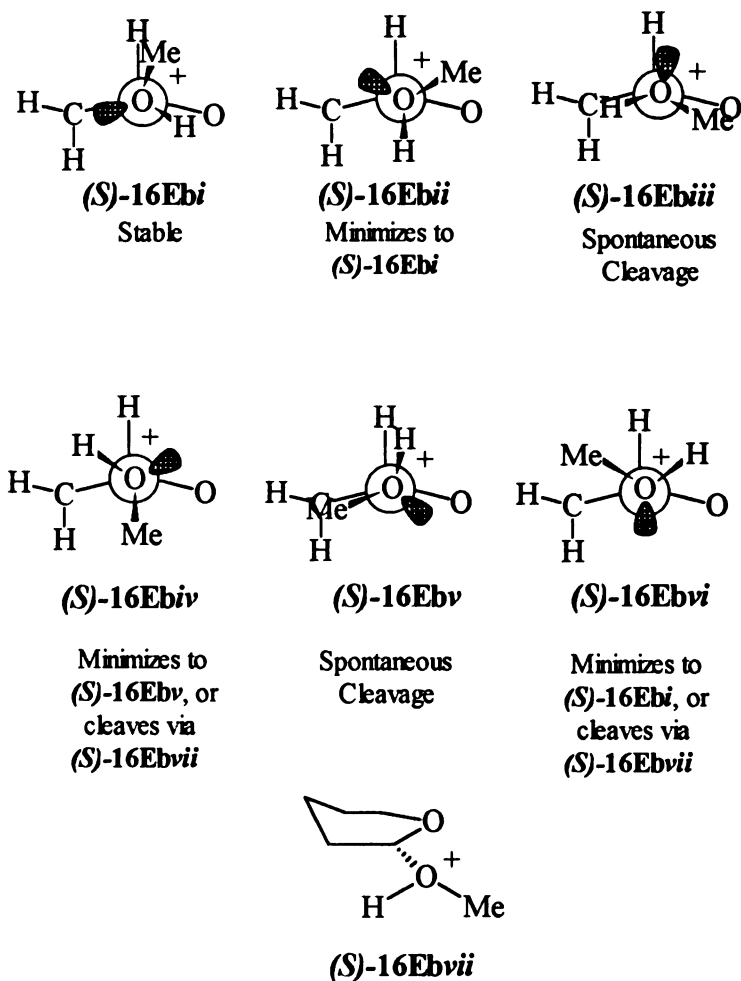
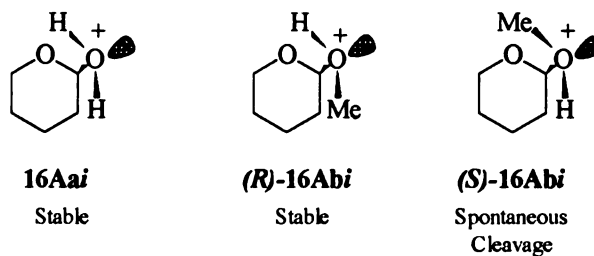


Figure 8.16. The six 60° rotomers for the protonated forms of equatorial 2-methoxy-THP. **16Ebi** is an intermediate form produced by minimization of several rotomers (see text).

cleaved. All forms of the equatorial and axial rotomers of the dimethyloxonium compounds **16A,E** cleaved.



These results show that, at least in terms of the number of stable conformers, the equatorial is more stable than the axial. The unprotonated

1950

hemiacetals and methylacetals are subject to the anomeric effect with the axial form more stable than the equatorial, which was recently reaffirmed by Salzner and Schleyer¹⁸ with high-level *ab initio* calculations; our semi-empirical methods (in PM3) reproduce the difference in ΔH_f found for various rotomers in the six-membered series. Because of the possibility of the so-called "reverse" anomeric effect--or as Perrin has pointed out recently,¹⁹ the lack of it in certain nitrogen compounds--we computed PM3 ΔH_f for the "generic" stable forms of **16Ea,b** and **16Aa,b** in which the anomeric carbon-oxygen bond length was constrained to 1.58Å, the distance of this bond in the stable forms, and then minimized in MM2 and PM3. In **16a**, the axial isomer is more stable by 0.9 kcal/mol, but in **16b** the equatorial isomer is more stable by 0.4 kcal/mol. Thus there is no "reverse" anomeric effect for **16a** but there is a slight reverse anomeric effect for **16b**, which matches the differences in reactivity measured by ΔH_R (Table 8.1) and the stability of the ion-dipole complexes (see below). Because the difference in energy is so small and because it is possible that Perrin's explanation¹⁹ of electrostatic repulsion as a possible cause for the "reverse" anomeric is entirely reasonable, we do not wish to make too stringent a case for this effect to explain our results. An additional 18 cases have been examined computationally,²⁰ and the energy differences between equatorial and axial forms of various nitrogen, oxygen, and sulfur compounds vary between 0.1 and 4.2 kcal/mol, with no apparent pattern in conformational preference.

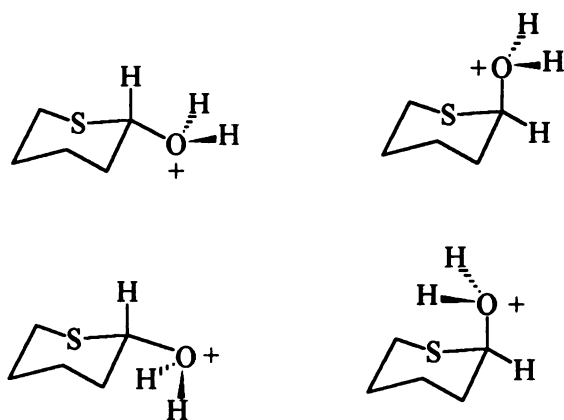
The energy profiles for **16Ea,Aa** (Figure 8.13) were generated in PM3 as described for the 5-membered compounds. Both gave low but distinct transition states, with $\Delta H^\ddagger = 0.3$ kcal/mol for **16Aa** and 0.1 kcal/mol for **16Ea**. The ion-dipole complexes showed the same pattern, with the complex more stable for **16Ea** (-2.4 kcal/mol) than for **16Aa** (-1.4 kcal/mol).

MINI

USA

MEMPHIS

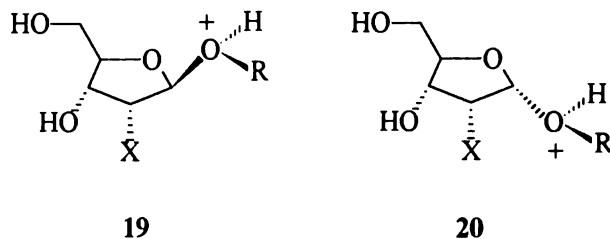
1950



All undergo spontaneous cleavage

series, ΔH_R was much more exothermic for the thio analogs, with a slight preference for equatorial cleavage (Table 8.1).

Ribofuranosides. These compounds (**19**, **20**; R = H, Me) show essentially the same behavior as found for the THF substrates with either water or methanol as the leaving group. The 2-deoxy compounds (**19aH** and **19aMe**) cleave from all



X = H, **a**; NH₂, **b**; OH, **c**; F, **d**

rotomers, however. The protonated β -methylriboside **19cMe** is more stable than the protonated α -methylriboside **20cMe** by 5.7 kcal/mol, a "reverse" anomeric effect. The α -methylriboside cleavage reaction is more exothermic by the same amount, a consequence of the ground-state energies. In the 2-deoxy compounds **19aMe** and **20aMe**, however, the protonated α -methylriboside is more stable by 1.5 kcal/mol. These differences are not the result of the formation of hydrogen bonds as found for the hydroxy THF derivatives, however; no hydrogen bonds are

MEMPHIS

452

formed in the most stable minimized forms, presumably because the rotomers necessary to form hydrogen bonds all have significant orbital-orbital repulsion.

The effect of substituents α to the anomeric carbon were examined. Plots of ΔH_R and ΔH^\ddagger vs. σ_I are linear for the cleavage of protonated 2-substituted (X = H, NH₂, OH, F) β -methylribosides **19a-dMe** (Figure 8.17), the same order as found

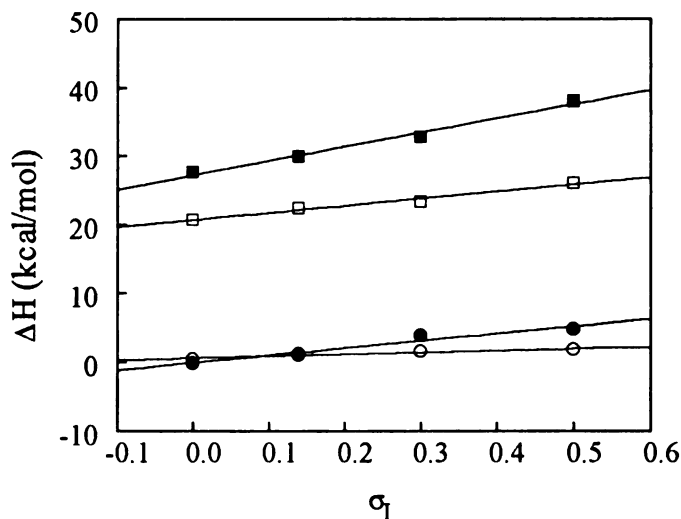


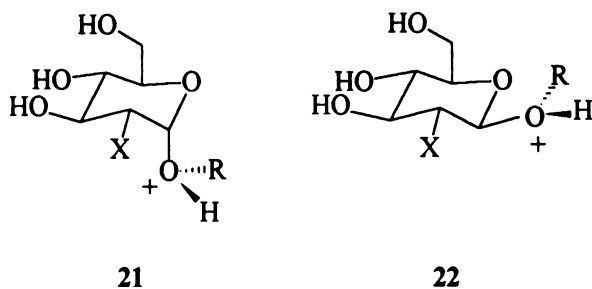
Figure 8.17. Plots of PM3 ΔH^\ddagger (open symbols) and ΔH_R (closed symbols) for C-O bond cleavage in **19a-d** with R = Me (circles) and the corresponding β -nicotinamide arabinosides (squares, from Ref. 17) vs σ_I . The correlation coefficients are: ■, $r = 0.994$; □, $r = 0.991$; ●, $r = 0.974$; ○, $r = 0.963$.

for hydrolysis²² and gas-phase dissociation¹⁷ of β -nicotinamide arabinosides and hydrolysis of β -nicotinamide ribosides²³ bearing the same 2 substituents. The barriers to dissociation are low; for the 2'-F compound, which has the least stable ion-dipole complex and oxocarbenium ion, $\Delta H^\ddagger = 1.8$ kcal/mol. Comparison with the results for the 2-substituted glucosides is given below. The ribosides are a well-behaved system.

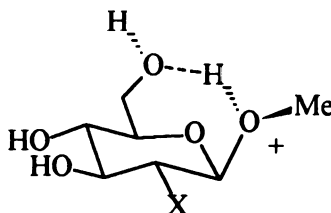
Methyl glucopyranosides. These compounds show the same rotomer dependence as found for the riboside/THF compounds. Unlike the ribosides,

1951

1952



however, all β anomers of the protonated species (22) are more stable than the α anomers (21), which is the opposite of the trends found for the unprotonated compounds.¹⁸ As a consequence, reactions of all β anomers are more exothermic, often by substantial amounts (Table 8.2). The cause of this effect is the formation of hydrogen bonds between the protonated leaving group and the 5-oxygen, which, because of differences in ring geometry, is not possible in the β -methyl ribosides.



The effects of substituents α to the anomeric carbon (H, NH₂, OH, and F) is very much like that found for the β -methyl ribosides, with one exception. In the α -methyl glucopyranoside series (Figure 8.18), the points for the fluoro compounds are significantly off the correlation lines for the other three substituents, which is no doubt the result of a fluorine anomeric effect on the α compound that would stabilize the ground state and decrease both enthalpies. Fluorine in either the α or β position has little effect on the relative values of ΔH_R , but has a substantial effect on the relative values of ΔH^\ddagger .

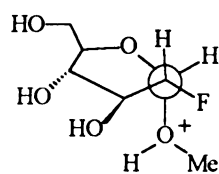
For the β -methyl glucopyranosides, plots of ΔH_R and ΔH^\ddagger vs. σ_I are linear (Figure 8.18), which parallels the results of Marshall²⁴ for the acid-catalyzed

1951

1952

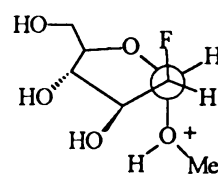
Table 8.2. PM3 ΔH_f , ΔH^\ddagger , and ΔH_R (kcal/mol) for 2-substituted α and β Methylglucosides

Substituent		MeOH	ΔH_f	ΔH^\ddagger	ΔH_R
2'-deoxy	22a	α	-29.7	0	-3.9
	21a	β	-38.9	0.1	5.3
α -2'-amino	22b	α	-26.6	0.8	-1.6
	21b	β	-34.4	1.2	6.2
α -2'-hydroxy	22c	α	-74.2	1.0	4.2
	21c	β	-78.8	1.4	8.8
α -2'-fluoro	22d	α	-67.1	0	3.1
	21d	β	-75.8	2.2	12.8
β -2'-fluoro		α	-64.2	1.1	3.3
		β	-74.0	4.5	11.0



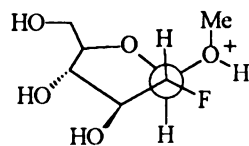
$$\Delta H^\ddagger \quad 0$$

$$\Delta H_R \quad 3.1$$



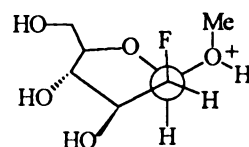
$$1.1$$

$$3.3$$



$$\Delta H^\ddagger \quad 2.2$$

$$\Delta H_R \quad 12.8$$



$$4.5$$

$$11.0$$

MEMPHIS

1950

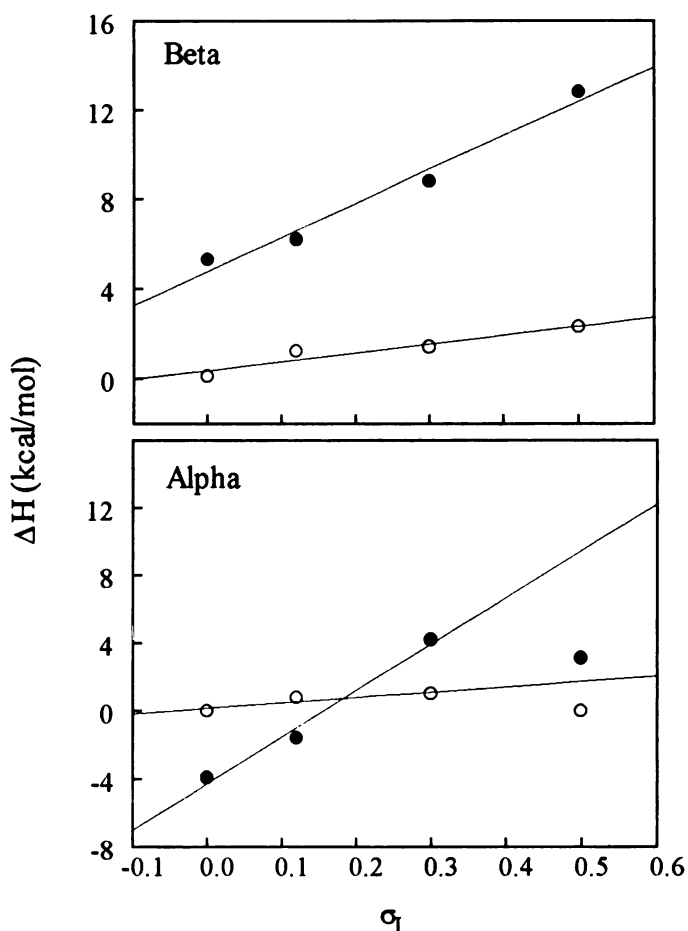


Figure 8.18. Plots of PM3 ΔH^\ddagger (○) and ΔH_R (●) for C-O bond cleavage in 2'-substituted β (22a-d) and α (21a-d) methylglucosides. The points for 21d are off the correlation line for the other substituents, presumably because of a fluorine anomeric effect. The correlation coefficients are: Beta: ●, $r = 0.987$; ○, $r = 0.954$. Alpha (ignoring F): ●, $r = 0.992$; ○, $r = 0.901$.

hydrolysis of the corresponding compounds. In fact, the correlation between $\log k_H^+$, the rate constant for the specific-acid catalyzed reaction, and the PM3 ΔH^\ddagger for Marshall's series of compounds is excellent (Figure 8.19), which provides further confirmation that our methods reproduce accurately the relative energies involved in glycosyl bond cleavage, including the effects of substituents α to the reaction center.

Oxygen vs. Sulfur Substrates. Methyl 5-thioxylopyranosides undergo specific-acid catalyzed hydrolysis 10-15 fold faster than the corresponding oxygen

1951

1951

compounds.^{1a,c} The corresponding ribosides show the same pattern of reactivity. This rate difference has been ascribed to increased proton affinity in the

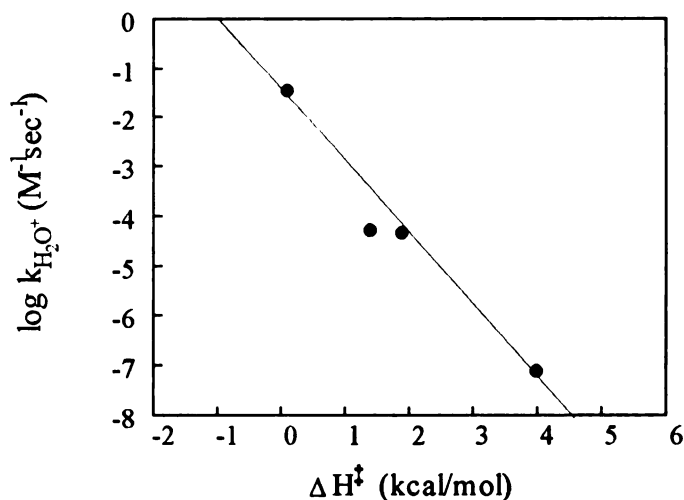


Figure 8.19. Plot of the log of the second-order rate constants for specific-acid catalyzed hydrolysis at 25°C of Marshall's series of 2-substituted β -methylglucosides²⁴ vs. the PM3 ΔH^\ddagger ($r = 0.980$). Left to right the points are for **21a,b,f,d**.

anomeric oxygen and not to a greater stability of the thio- over the oxocarbenium ion. In Chapter 7 we showed that $HO=CH_2^+$ was more stable than $HS=CH_2^+$ by 2.4 kcal/mol in PM3, but that $MeS=CH_2^+$ was more stable than $MeO=CH_2^+$ by 1.5 kcal/mol in PM3, with the same relative difference found in the experimental²⁵ and *ab initio*²⁶ (MP3/6-31G*) energies (see Table 2 of Reference 12). For the RPy⁺ compounds with R = 2-THF or 2-tetrahydrothiophene, the AM1 ΔH^\ddagger was greater for the thio compound (by 1.4 kcal/mol), but ΔH_R was more exothermic for the thio compound (by 12.5 kcal/mol).

Both the 2-MeOTHP compound (**S**)-**13Abvi** and the 2-MeO-thio-THP compound (**S**)-**17Abvi** cleave with no barrier; the ion-dipole complex of the thio compound is 9.5 kcal/mol more stable than the ion-dipole complex of the oxo compound, and ΔH_R is 24.1 kcal/mol more exothermic for the thio compound, which shows that the thermodynamic driving force greatly favors the thiocarbenium ion. Unlike the pyridiniums, however, the ion-dipole complex for the thio-THP does not have a bridged structure (see Figure 2 in Reference 12).

MEMPHIS

1950

These results suggest that, contrary to the commonly held view, in linear and cyclic secondary aliphatic systems there is substantial resonance participation of the sulfur with the cationic center. Indeed, between the ground state and ion-dipole complex for *(S)*-13Abvi and *(S)*-17Abvi, the change in charge on sulfur ($\delta q = 0.489$) is much greater than on oxygen ($\delta q = 0.183$), and the charge at the cationic center is actually more negative for the sulfur compound ($\delta q = -0.064$) than for the oxygen compound ($\delta q = 0.125$). This does not appear to be a computational artifact because correlations of semi-empirical ΔH^\ddagger for cleavage of 4-MeS-ArCRR'X (R = R' = Me or H; R = H, R' = Me; X = H₂O, EtOH, MeOH, N₂) substrates fall where expected on correlation lines against either σ^+ or ΔG° , a gas-phase stability scale based on *t*-cumyl carbenium ions.²⁷ Our findings are also in accord with the recent *ab initio* results of Wiberg and Rablen²⁸ for thioformamide that showed greater resonance stabilization for H₂N⁺=C-S⁻ than for H₂N⁺=C-O⁻ and a substantial σ stabilization for the C-S bond that is largely Coulombic in character. The latter effect may account for the large difference in the magnitude and sign of the charge on the cationic center between the sulfur and oxygen analogs in our series.

Alkyl glucosides in which the glycosidic oxygen is replaced by sulfur invariably react more slowly than the oxygen compounds; the effect is more dramatic in aryl glucosides.^{1a,c} This is clearly the result of the reduced proton affinity of SR compared to OR. Anti- and syn-periplanar effects are also important, however, and may be the dominant factor. This is shown by the finding that 13c undergoes spontaneous cleavage regardless of stereochemistry, while 16 is stable. In 13c there is a good LG with either or both anti- and syn-periplanar effects in any rotomer. The same effect is seen between the pyridinium and methyl ribosides, which is discussed below.

1951

USF

Comparison of mechanisms.

A-1 vs. A-2. The spontaneous cleavage, or cleavage with very low barriers, of protonated leaving groups in the linear and cyclic compounds is consistent with the A-1 mechanism that produces oxocarbenium ion intermediates, either as distinct species or elements of ion-dipole complexes. For linear pyridinium and dimethylanilinium substrates that show no distinct transition states, reactions with nucleophiles probably proceed through concerted displacement reactions. This is not the case for cyclic pyridinium compounds, which cleave to produce ion-dipole complexes.^{12,17}

Whether or not gas-phase results can be used to predict behavior in solution depends on the system. For instance, we have shown that gas-phase dissociation benzyl dimethylsulfoniums and pyridiniums⁸ occurs by direct, rate-limiting dissociation to ion-dipole complexes (with the exception of [4-nitrobenzyl] pyridiniums, which dissociate directly to the carbenium ion and LG without the formation of an intermediate). The computational results match this reactivity, including the disparity of the (4-nitrobenzyl) pyridiniums. The experimental results in water, however, show that (4-methoxybenzyl)dimethylsulfonium hydrolyzes by an S_N1 mechanism²⁹ but all other benzyldimethylsulfonium bearing less electron-donating groups react by solvent displacement,³⁰ and that all benzyl pyridiniums react by direct solvent displacement.³¹ In solution, the entropy of solvation of the leaving group--or the lack of it for SMe₂--appears to control the rate.^{29,31} Thus the computational results accurately predict reactivity in the gas-phase but fail miserably for condensed-phase reactions.

On the other hand, the computed reaction profiles for β -nicotinamide arabinosides show dissociation to ion-dipole complexes, and both the experimental gas-phase and solution results are consistent with this mechanism.¹⁷ The arabinosides react faster in the gas-phase and in solution than either the

MEMPHIS

1950

dimethylsulfoniums or pyridiniums, which may reflect the increased stability of the ribosyl oxocarbenium ions compared with 4-substituted benzyl carbenium ions^{8,17}; certainly the calculated energies for the ion-dipole complexes show this difference.³² Moreover, the computed ΔH^\ddagger and ΔH_R correlate well with $\log k_{H_2O}$ and ΔG^\ddagger , ΔH^\ddagger , and ΔS^\ddagger for the solution reactions. For xylo- and glucopyranosyl pyridiniums, the computed ΔH^\ddagger correlates with ΔH^\ddagger and ΔS^\ddagger for the solution reactions.¹² Model studies with pyridinium LGs in 3-substituted THF substrates show an excellent correlation of the computed ΔH^\ddagger with σ_I .⁸ As shown above, the computed ΔH^\ddagger correlates very well with k_{H^+} for specific-acid catalyzed hydrolysis of Marshall's series of 2-substituted methylglucosides (Figure 8.19), and there is an excellent correlation of the computed ΔH^\ddagger and ΔH_R with σ_I for 2-substituted methyl ribosides (Figure 8.17) and for α and β methylglucosides (Figure 8.18). These results suggest that comparisons can be made for ribosides and glucosides between the gas and condensed phases.

They also suggest that there is no particular reason, based on intrinsic energies, that ribosides and glucosides should not react by the same mechanism in solution. This is not in accord with the commonly-held view that the mechanism of hydrolysis is different for the two classes, a judgment made primarily from a consideration of ΔS^\ddagger values. Schlager and Long³³ have emphasized the dangers inherent in the use of ΔS^\ddagger values to differentiate among mechanisms; nonetheless, for compounds of similar structures and reactions of similar energies, if used with caution and with other supporting evidence, ΔS^\ddagger is a reasonable criterion. For the methyl pyranosides, ΔS^\ddagger are high and positive,^{1a} which is consistent with rate-limiting bond cleavage of a preprotonated substrate--the A-1 mechanism. Methyl furanosides, however, invariably react with negative values of ΔS^\ddagger , which has led some workers to suggest that the protonated alcohol moiety is displaced by water

MEMPHIS

USF

in the A-2 mechanism.^{ia-c} A rate analysis using Bunnett's ω -scale supports the A-2 mechanism for furanosides.³⁴

For the pyridinium substrates, however, ΔS^\ddagger values are high and positive for both β -nicotinamide ribosyl and arabinosyl compounds ($\Delta S^\ddagger = 1.6$ - 13.2 gibbs/mol) and β -pyridinium glucosyl, xylosyl, and galactosyl compounds ($\Delta S^\ddagger = 15$ - 31 gibbs/mol). Shuber³⁵ has shown that hydrolysis of a series of NAD^+ analogs with different pyridine LGs has a β_{LG} value of -1.11 . We have shown that the ribosyl oxocarbenium ion is more stable in the gas phase than the 4-methoxybenzyl carbenium ion,³¹ a species known to be a solvent-equilibrated intermediate in solvolysis reactions of neutral³⁶ and positively-charged substrates.²⁹ Taken with the computational profiles, gas-phase results, and other correlations, the entropy results are consistent with a common dissociative mechanism for both classes of compounds. As shown below, it is possible that the entropy differences reflect the mode of proton transfer and not a change in mechanism from direct dissociation to displacement of the protonated LG by water.

Specific vs. General-Acid Catalysis. As Handlon and Oppenheimer²² have pointed out, one difference between the pyridinium substrates and methyl ribosides and glucosides is that the former bear a formal positive charge in the ground state, while the latter must be protonated before reaction can occur. The compounds studied here do not undergo general acid catalysis (or the so-called $A_{\text{SE}2}$ mechanism) in solution, so the reactive intermediate must form in a preequilibrium $\text{ROR}' + \text{H}_3\text{O}^+ \rightleftharpoons \text{ROR}'\text{H}^+ + \text{H}_2\text{O}$; for the simple A-1 mechanism, dissociation of the protonated intermediate (k_2) is rate-limiting. In this case, $k_{\text{obsd}} = K_a k_2$. Cordes and Bull^{1b} have pointed out that reasonable values of k_2 can be calculated using k_{obsd} and measured values of K_a for acetals.

MEMPHIS

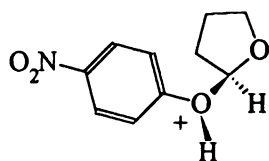
US

For simple acetals, the proton affinity is affected by either R or R'. For R containing the potential oxocarbenium ion, the orientation of OR' relative to the α oxygen affects the proton affinity of the LG because of $n\sigma^*$ interactions, an idea first suggested by Deslongchamps¹⁶ and confirmed by Andrews, et al.,¹⁴ in their study of **6**. Our results support this contention. Inductive effects on the R' group also affect proton affinity. Alkyl groups are much more basic (pK_a MeOH = 15.5) than phenols (pK_a 4-NO₂-phenol = 7.2), yet compounds such as **23** and **25** undergo general-acid catalyzed and "spontaneous" hydrolysis reactions. Invoking Jencks's "libido rule," which states (roughly) that general-acid catalysis would be expected for systems in which the pK of the catalyst is intermediate between the site being protonated and the final product,³⁷ Cordes and Bull^{1b} point out that acetals (or ketals or orthoesters) with phenol LGs would be expected to undergo general-acid catalysis. They also argue that within a series, it would be expected that substrates containing potentially stable carbenium ions should undergo general-acid catalysis in an order that depends on carbenium ion stability.

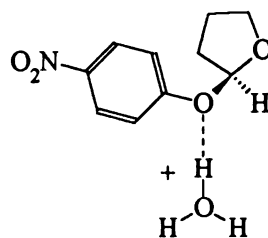
We attempted to model this effect with hydronium as the general acid in **24**, **26**, and **28**, all of which are known to undergo general-acid catalysis in solution. With the RO---H---⁺OH₂ bond constrained to linearity, **24** and **26** were stable, but **28** underwent spontaneous cleavage. In **24** and **26**, the proton remained bound to the water, which prevents cleavage. Attempts to reduce the proton affinity of the water oxygen by hydrogen bonding two waters to the remaining hydronium protons in **26** did not alter the reaction profile, even in a structure with an anti-periplanar orbital interaction. This is of course a *very* crude approximation of solvent stabilization. In **28**, starting with a hydronium structure with three equal H-O bond lengths of 0.96Å and an H-LG oxygen bond length of 1.8Å, minimization leads to transfer of the proton from the water to the phenol oxygen with a concomitant increase in the length of the reaction coordinate bond. (Note that if

USF
LIBRARY

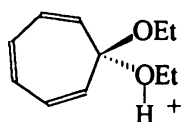
the phenol in **23** and **24** is replaced by OEt, the preprotonated compound undergoes spontaneous cleavage, but the hydronium-bound species is stable.)



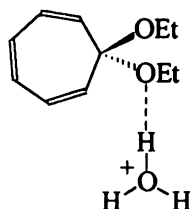
23



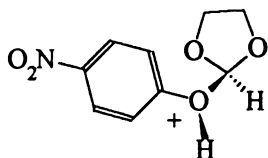
24



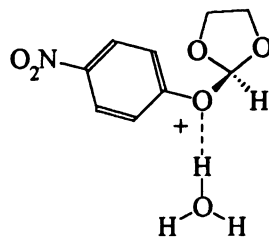
25



26



27



28

These results show that the LG is more important than the carbenium ion for this effect. The order is counterintuitive, however, because values of ΔH_R for reaction of **23**, **27**, and **25**, all of which undergo spontaneous cleavage upon minimization, are -13.1, -14.6, and -26.2 kcal/mol, respectively, with tropyllium heavily favored. In fact, the relative rate for hydration of the ethoxytropyllium carbenium ion derived from **25** and the dioxolane oxocarbenium ion³⁸ derived from **27** is 10^{11} in favor of tropyllium! From the trends in this series, we can predict that **29** and **30** will have the highest ΔH_R and will undergo hydronium ion

MS
1971

REMI

USF

constant for HOAc catalysis is ca. 10^{-5} lower than the hydronium rate constant, so the effect is not large and difficult to detect above small salt effects. We have examined this series and find that no substrate cleaves with hydronium as a general acid. An interesting finding, however, is that the energies (in kcal/mol) of the ion-dipole complexes relative to the starting structures, which were given the same stereochemistry as *(S)*-17Abvi, for specific-acid catalyzed cleavage have similar values (MeOH = -12.7; EtOH = -11.5; MeO-CH₂CH₂, -12.4; propargyl = -10.2; phenol = -10.6) except for the TFE compound (-23.9). (The equatorial compounds show the same trends.) The ion-dipole complexes for the "normal" alcohols all have the structure R⁺-----OHR', while the TFE ion-dipole complex has the structure R⁺---F₃CCH₂OH. Such a dipolar structure has been suggested by Richard and Jencks⁴¹ for an α -phenylethyl carbenium ion-TFE encounter complex and by Jencks and Banidit⁰⁰ for the solvolysis reaction of fluoroglucose in TFE. This structure was found to be important for carbenium ion combination reactions of benzyl, α -phenylethyl, and *t*-cumyl carbenium ions.³² While the complex would not affect the bond-breaking step, it would have an enormous effect on the recombination reaction, increasing the ΔH_{k-1}^\ddagger by ca. 12 kcal/mol based on the expected value obtained by extrapolation of the plot shown in Figure 8.20.

Aryloxy- vs. Pyridinium THF Substrates. While solution data are not available to allow a strict comparison, the relative rates between a protonated phenol and a pyridine as LGs can be obtained by crude extrapolation of Lathi's data⁴² for the specific-acid catalyzed hydrolysis of 2-aryloxy-THF substrates and from Handlon's rate constant²² for the hydrolysis of β -nicotinamide-2'-deoxyriboside. We estimate that **31** (pK_a LG = 4.1) hydrolyzes $\sim 3.6 \times 10^3$ faster than β -nicotinamide-2'-deoxyriboside (pK_a LG = 3.33) at 37°C. This large difference is also reflected in the energies for bond cleavage of **31** and **32**, relatively simple computational systems with LGs of approximately the same pK_a.

MEMPHIS

MS

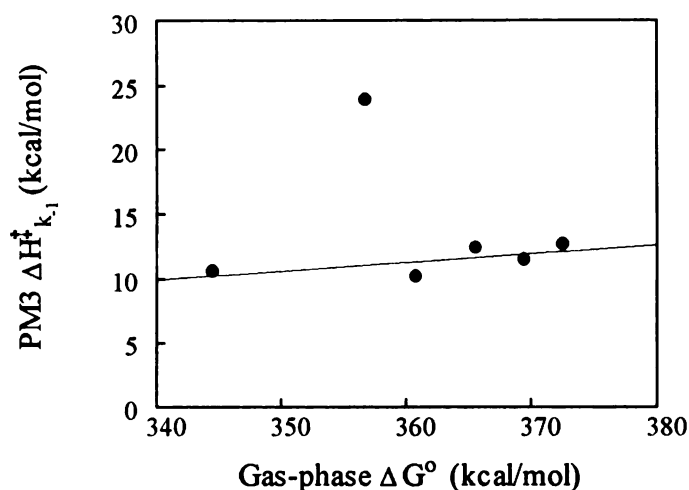
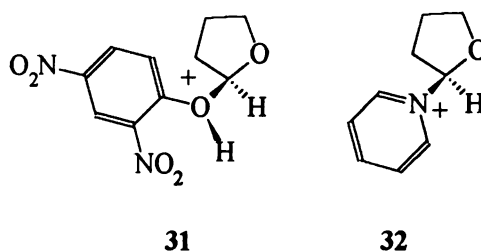


Figure 8.20. Plot of the PM3 ΔH^\ddagger_{k-1} (kcal/mol), the difference between the ground state and ion-dipole complex structures that is also ΔH^\ddagger for the addition of alcohols to the carbenium ion, vs. the absolute gas-phase ΔG° (kcal/mol) for the alcohols (from Bartmess, J.E.; Scott, J.A.; McIver, R.T. Jr., *J. Am. Chem. Soc.* 1979, 101, 6046-6056). The value of ΔG° for propargyl alcohol was estimated from a plot of ΔG° vs. pK_a of the other alcohols ($r = 0.994$). *Left to right* the points are for phenol, TFE, propargyl alcohol, 2-methoxyethanol, ethanol, and methanol.

(The AM1 energies for **32** were reported in Chapter 7, and the energies for **31** were calculated in this method.) The values $\Delta\Delta H^\ddagger \sim 22.7$ kcal/mol and



pK _a LG	4.09	5.25
ΔH^\ddagger (kcal/mol)	~ 0	22.7
ΔH_R (kcal/mol)	-8.9	34.1

$\Delta\Delta H_R = 43.0$ kcal/mol show the same trends found in the crude comparison of water rate constants. It is readily apparent that the difference is the result of the anti- or syn-periplanar interactions of the LG and ring oxygens in **31** that are not

MEMPHIS

USF

32. Thus while the gas-phase mechanisms are the same--dissociative to a stable ion-dipole complex--the driving forces and energies are clearly different and favor the phenol over the pyridinium. Here, too, however, the ΔS^\ddagger have different signs. Lathi⁴² found $\Delta S^\ddagger = -6.4 \pm 0.7$ gibbs/mol for 2-(4-phenoxy)THF, while Handlon⁴³ found $\Delta S^\ddagger = 9.5 \pm 2.5$ gibbs/mol for β -D-glucosylamide-2'-deoxyriboside. Given this profile, it is doubtful that **31** reacts in an A-2 mechanism, with the negative ΔS^\ddagger arising from direct displacement of the LG by water. It seems more probable, given the results for **23**, that the negative ΔS^\ddagger arises because the activated complex is organized from substrate and hydronium in a mechanism in which proton transfer is rate limiting.

References and Notes

- (1) Leading and recent reviews: (a) Capon, B. *Chem. Rev.* **1969**, *69*, 407-498. (b) Cordes, E.H.; Bull, H.G. *Chem. Rev.* **1973**, *73*, 581-603. (c) Sinnot, M.L. In *The Chemistry of Enzyme Action*; Page, M.I., Ed.; Elsevier: Amsterdam, 1984; pp 389-431.
- (2) Lönnberg, H; Poljola, V. *Acta Chem. Scand. A* **1976**, *30*, 669-670.
- (3) Fife, T.H.; Jao, L.K. *J. Am. Chem. Soc.* **1968**, *90*, 4081-4085; Fife, T.H.; Brod, L.H. *J. Am. Chem. Soc.* **1970**, *92*, 1681-1684; Craze, G-A.; Kirby, A.J. *J. Chem. Soc. Perkin Trans. II* **1978**, 354-356.
- (4) Anderson, E.; Fife, T.H. *J. Am. Chem. Soc.* **1969**, *91*, 7163-7166.
- (5) Ahmad, M.; Bergstrom, R.G.; Cashen, M.J.; Chiang, Y.; Kresge, A.J.; McClelland, R.A.; Powell, M.F. *J. Am. Chem. Soc.* **1979**, *101*, 2669-2677.
- (6) Chiang, Y.; Kresge, A.J.; Salomaa, P.; Young, C.I. *J. Am. Chem. Soc.* **1974**, *96*, 4494-4499.

1951

USF

- (7) Knier, B.L.; Jencks, W.P. *J. Am. Chem. Soc.* **1980**, *102*, 6789-6798.
- (8) Buckley, N.; Maltby, D.; Burlingame, A.L.; Oppenheimer, N.J., submitted (Chapter 6).
- (9) Ichikawa, H.; Harrison, A.G. *Org. Mass. Spectrom.* **1978**, *13*, 389-396.
- (10) Schröder, S.; Buckley, N.; Oppenheimer, N.J.; Kollman, P.A., *J. Am. Chem. Soc.* **1992**, *114*, 8231-8238.
- (11) Caserio, M.C.; Souma, Y.; Kim, J.K. *J. Am. Chem. Soc.* **1981**, *103*, 6712-6716.
- (12) Buckley, N.; Oppenheimer, N.J., submitted (Chapter 7).
- (13) Wipff, G. *Tetrahedron Lett.* **1978**, 3269-3270.
- (14) Andrews, C.W.; Bowen, J.P.; Fraser-Reid, B. *J. Chem. Soc. Chem. Commun.* **1989**, 1913-1916. These authors provide a review of earlier work.
- (15) Jeffrey, G.A.; Pople, J.A.; Radom, L. *Carbohydrate Res.* **1974**, *38*, 81-95.
- (16) Deslongchamps, P. *Stereoelectronic Effects in Organic Chemistry*; Pergamon: New York, 1983; p. 30, pp. 34-35. For the view in favor of these effects in these systems, see Kirby, A.J. *Acc. Chem. Res.* **1984**, *17*, 305-311. For the view against, see Hosie, L.; Marshall, P.J.; Sinnott, M.L. *J. Chem. Soc. Perkin II* **1984**, 1121-1131.
- (17) Buckley, N.; Handlon, A.L.; Maltby, D.; Burlingame, A.L.; Oppenheimer, N.J. *J. Org. Chem.* **1994**, *59*, 3609-3615.
- (18) Salzner, U.; Schlyer, P. v.R. *J. Org. Chem.* **1994**, *59*, 2138-2155.
- (19) Fabian, M.A.; Perrin, C.L.; Sinnott, M.L. *J. Am. Chem. Soc.* **1994**, *116*, 8398-8399; Perrin, C.L.; Armstrong, K.B.; Fabian, M.B. *J. Am. Chem. Soc.* **1994**, *116*, 715-722; Perrin, C.L.; Armstrong, K.B. *J. Am. Chem. Soc.* **1993**, *115*, 6825-6834.
- (20) Buckley, N. Unpublished results.

MEMPHIS

US

- (21) Fraser-Reid, B.; Merritt, J.R.; Handlon, A.L.; Andrews, C.W. *Pure Appl. Chem.* **1993**, *65*, 779-786; Woods, J.R.; Andrews, C.W.; Bowen, J.P. . *J. Am. Chem. Soc.* **1992**, *114*, 859-864.
- (22) Handlon, A.L.; Oppenheimer, N.J. *J. Org. Chem.* **1991**, *56*, 5009-5010.
- (23) Handlon, A.L.; Xu, C.; Müller-Steffner, H.-M.; Schuber, F.; Oppenheimer, N.J. *J. Am. Chem. Soc.* **1994**, *116*, 12087-12088.
- (24) Marshall, R.D. *Nature* **1963**, *199*, 998-999.
- (25) Taft, R.W.; Martin, R.H.; Lampe, F.W. *J. Am. Chem. Soc.* **1965**, *87*, 2490-2497.
- (26) Apeloig, Y.; Karni, M. *J. Chem. Soc. Perkin Trans. II* **1988**, 625-636.
- (27) Taft, R.W.; Topsom, R.D. *Prog. Phys. Org. Chem.* **1987**, *16*, 2-83.
- (28) Wiberg, K.B.; Rablen, P.R. *J. Am. Chem. Soc.* **1995**, *117*, 2201-2209.
- (29) Buckley, N.; Oppenheimer, N.J. *J. Org. Chem.* **1994**, *59*, 5717-5723.
- Kevill, D.N.; Ismail, N.H.J.; D'Souza, M.J. *J. Org. Chem.* **1994**, *59*, 6303-6312.
- (30) Friedberger, M.P.; Thornton, E.R. *J. Am. Chem. Soc.* **1976**, *98*, 2861-2865.
- (31) Buckley, N.; Oppenheimer, N.J., submitted.
- (32) One of us (N.B.) has found that the $\text{PM}_3 \Delta H^\ddagger$ for the reaction $\text{R}^+ + \text{R}'\text{OH} \rightarrow \text{ROHR}^+$ and ΔH_{R} for the reverse reaction give excellent correlations with the respective measured rate constants for $\text{R} = \alpha$ -phenylethyl, *t*-cumyl, 4,4,5,5-tetramethyldioxolane, and diethoxymethyl cation ions. (Buckley, N., unpublished results.)
- (33) Schaleger, L.L.; Long, F.A. *Adv. Phys. Org. Chem.*, **1963**, *1*, 1-34.
- (34) Bunnett, J.F. *J. Am. Chem. Soc.* **1961**, *83*, 4978-4983.
- (35) Tarnus, C.; Schuber, F. *Bioorg. Chem.* **1987**, *15*, 31-42; Tarnus, C.; Muller, H.M.; Schuber, F. *Bioorg. Chem.* **1988**, *16*, 38-51.

MEMPHIS

1951

- (36) Amyes, T.L.; Richard, J.P. *J. Am. Chem. Soc.* **1990**, *112*, 9507-9512.
- (37) Jencks, W.P. *Chem. Rev.* **1972**, *72*, 705-718.
- (38) The rate constant for the hydration of the ethoxy tropyllium carbenium ion is from McClelland, R.A.; Ahmad, M. *J. Am. Chem. Soc.* **1978**, *100*, 7027-7031. The rate constant for hydration of the unsubstituted dioxolane oxocarbenium ion ($1.7 \times 10^9 \text{ M}^{-1}\text{sec}^{-1}$) was estimated from ratios of rate constants for the 2-Me 3,3,4,4-protio and tetramethyl dioxolanes and the 2-H 3,3,4,4-tetramethyl dioxolane oxocarbenium ions: Steenken, S.; McClelland, R.A.. *J. Am. Chem. Soc.* **1989**, *111*, 4967-4973.
- (39) Schowen, R.L. *Prog. Phys. Org. Chem.* **1972**, *9*, 275-000.
- (40) Jensen, J.L.; Wuhrman, W.B. *J. Org. Chem.* **1983**, *48*, 4686-4691.
- (41) Richard, J.P.; Jencks, W.P. *J. Am. Chem. Soc.* **1984**, *106*, 1373-1383.
- (42) Lahti, M.; Lindström, R.; Lönnberg, H. *J. Chem. Soc. Perkin Trans. II* **1989**, 603-605. The rate constant for the specific-acid catalyzed hydrolysis of **31** was estimated from the Hammett ρ value of -0.97 for reaction at 25°C; this was extrapolated to 35°C by a simple ratio with the respective rate constants for 2-(3-chloroaryl)oxy)THF, which is based on the reasonable assumption that the Eyring plots for these substrates have the same slopes.
- (43) Handlon, A.L. Ph.D. Dissertation, University of California, San Francisco, 1991.

RENT

US

Chapter 9
Summary and Conclusions

USF
1212

"The centre cannot hold."

Yeats

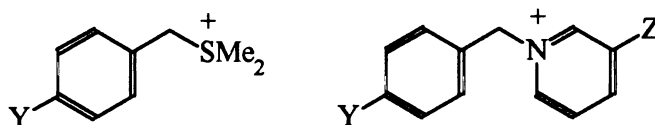
The results presented above allow direct comparison of the kinetics of heterolysis and nucleophilic substitution reactions of charged benzyl substrates in solution and the gas phase. With the potential energy surfaces for dissociation of these and related compounds, direct comparison comparison can be made of the intrinsic energies and mechanism in the two phases. Taken together, they provide a complete and consistent picture of these reactions, and allow comparisons *between* compounds of vastly different structures.

Heterolytic Cleavage in Charged Benzyl Substrates

"Mere anarchy is loosed upon the world,..."

Yeats

In the gas phase, benzyl pyridiniums (with the exception of the 4-nitro-benzyl substrates 2-4e) and sulfoniums 1a-e undergo a dissociative reaction. The energy profiles follow the intrinsic stabilities of the carbenium ions (Chapter 6). In



1

2, Z = CN

3, Z = CONH₂

4, Z = H

Y = MeO, a; Me, b; H, c; Cl, d; NO₂, e

the absence of solvent, the primary entropy change is translational, which should be approximately the same for loss of SMe₂ or the various substituted pyridines. Thus $T\Delta S^\ddagger$ is favorable (ΔG^\ddagger is more positive), and differences among and between the two series must be related to ΔH^\ddagger for the strength of the benzyl-

1941

1941

leaving group bond, which is borne out by the computed energy profiles. The sulfoniums dissociate more rapidly than the pyridiniums, but the difference in reactivity is not large. (Comparison of the relative rates with the β -nicotinamide arabinosides is given below.)

An entirely different pattern is found in solution. In the sulfonium series, the 4-methoxybenzyl substrate **1a** hydrolyzes by an S_N1 mechanism,^{1,2} while other members of the series with less electron-donating substituents react by direct displacement of SMe_2 by solvent (Chapters 3 and 4). In the pyridinium series, all substrates react by direct displacement by solvent (Chapter 2). It is interesting to compare the relative rates for these reactions (Table 9.1), in this case obtained by

Table 9.1. Relative Rates for the Hydrolysis of Benzyldimethylsulfoniums and Benzylpyridiniums in D_2O at $70^\circ C$

Substrates	k_{rel}
1. 4-MeO ϕ CH ₂ SMe ₂ ⁺ / ϕ CH ₂ SMe ₂ ⁺ (1a/1c)	6.4×10^4
2. 4-MeO ϕ CH ₂ -3'CN-Py ⁺ / ϕ CH ₂ -3'CN-Py ⁺ (2a/2c)	7.7
3. 4-MeO ϕ CH ₂ SMe ₂ ⁺ / 4-MeO ϕ CH ₂ -3'CN-Py ⁺ (1a/2a)	1.9×10^3
4. ϕ CH ₂ SMe ₂ ⁺ / ϕ CH ₂ -3'CN-Py ⁺ (1c/2c)	2.2

comparing the 4-methoxy with the 4-protio substrates. These results show an enormous variation in rate among (entry 1) and between (entry 3) the series, clearly dominated by the mechanism. From the gas-phase results, however, it is not clear why there should be such a large difference in rate, especially when it is realized that the difference in rate of the bimolecular reaction with azide is quite small ($k_{rel} = 2.5$ for **1a/2a** under identical conditions at $80^\circ C$). If the difference in

MINI

USA

ΔS^\ddagger for the azide reaction for the 4-methoxy substrates, -15 gibbs/mol, is a crude measure of the effect of solvation of the leaving group that could be applied to the to the solvolysis reaction as well,¹ it seems clear that a very unfavorable entropy of solvation of the pyridinium is sufficient to raise ΔG^\ddagger for the unimolecular reaction of the pyridinium such that the bimolecular reaction with water is more favorable. This is more astonishing because the solution ΔH^\ddagger for the azide reaction of the pyridinium is 4.6 kcal/mol more favorable than for the dimethylsulfonium, which, because it includes contributions from solvation, does not parallel the gas-phase relative ΔH^\ddagger .

It is also true, however, that solvent can change the reactivity of pyridiniums. Results from Katritzky's system,³ which we have shown does not involve ion-dipole complex intermediates (Chapter 2), show that (4-methoxybenzyl)pyridiniums with highly arylated or alkylated leaving groups can undergo unimolecular dissociation in solvent chlorobenzene, which is much less polar and has a much lower dielectric than water, conditions that favor ionization of charged substrates. Data for the sulfoniums have not been obtained in chlorobenzene.

Solvation effects alone cannot be the exclusive source of these effects, however. For **1a**, the rates of the hydrolysis and azide substitution reaction are comparable, a consequence of the S_N1 mechanism for hydrolysis of **1a**. As shown by Swain and his colleagues,⁴ the rates of hydrolysis for **1b**, **1c**, and the *m*-Cl analog are significantly slower than the rates of the azide substitution reaction (by more than two orders of magnitude), which is consistent with direct solvent displacement in the hydrolysis reaction for the less electron donating groups. Thus the Hammett plots for both hydrolysis and the azide reaction in the sulfonium series show breaks with no minimum, but the source of the break is different for the two reactions: a change in mechanism for the hydrolysis reaction, and a change in the structure of the activated complex for the azide reaction.

MEMPHIS

USF

For the pyridiniums, however, the relative rates of the hydrolysis reaction *by direct solvent displacement* and the azide substitution reaction are a function of the basicity of the pyridine. For the least basic pyridine (**2a-e**), the rate for the azide reaction is much greater than the rate for solvent displacement; this is also true for the methyl analog **2Me**. For the nicotinamide substrates **3a-e** and the methyl analog **3Me**, however, the rates of the bimolecular reactions with both solvent and azide are comparable. The flat Hammett plot for the azide reactions of **2a-e** show little change in charge at the transition state across the series, which is in accord with a constant "looseness" across the series. Despite this, as the basicity of the pyridine increases ($4 > 3 > 2$), the Hammett plots become V-shaped. The Hammett plot for the hydrolysis reaction changes from linear with a ρ of -1.25 for **2a-e** to flat for **3a-e**. As shown in Chapter 2, these differences are the result of the mixing of different valence bond forms for neutral and negative nucleophiles as described by Pross and Shaik⁵ and not of a change in mechanism. In fact, the finding that β_{LG} is very large for the azide reaction ("loose" activated complex) but probably very small for the hydrolysis reaction ("tight" activated complex) is consistent with the Pross-Shaik avoided crossing model.

Having said all this, it is still not immediately clear why **1a** should be the odd compound out, with the only S_N1 reaction and a much faster azide substitution reaction than predicted by the otherwise regular Hammett relation. Frontier orbital theory⁶ provides a hint. Before a definitive conclusion can be reached, the potential energy surfaces for the bimolecular reaction with azide will have to be computed. Nonetheless, an examination of the ground and transition states for heterolytic cleavage of the benzyl-leaving group bond suggests an explanation.

Shown in Figure 9.1 are the LUMOs (positive lobes shown for clarity) for the fully PM3 minimized structures⁷ for the ground states and activated complex

USF
LUMINA

for heterolytic cleavage for **1a**, **1c**, and **2a**. Similarities and differences are immediately apparent. First, the LUMOs of the ground states are different. Only

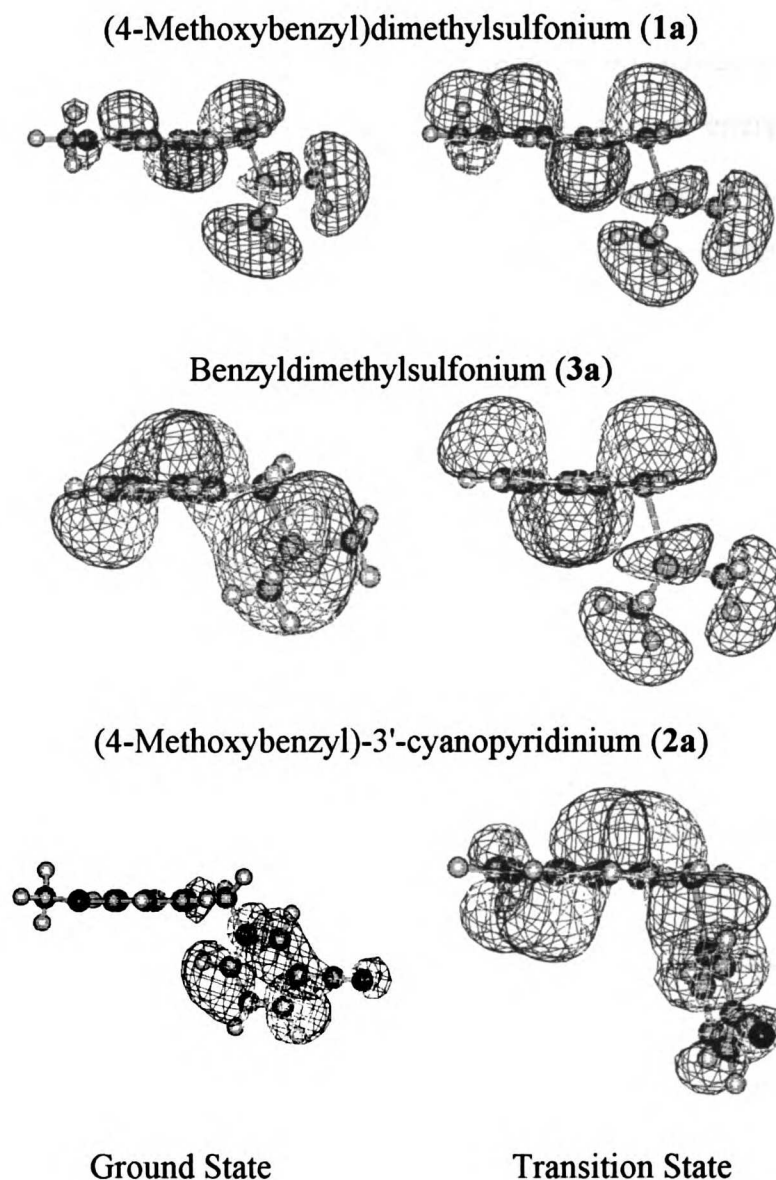


Figure 9.1. LUMOs from the fully minimized PM3 structures for **1a**, **1c**, and **2a**.

the LUMO for **1a** has a lobe at the backside of the reaction center. Thus a nucleophile with the proper HOMO energy for overlap can interact directly with the ground state structure without the need to perturb the LUMO. Because this will be a lower energy process, the rate of reaction of **1a** with azide should be greater

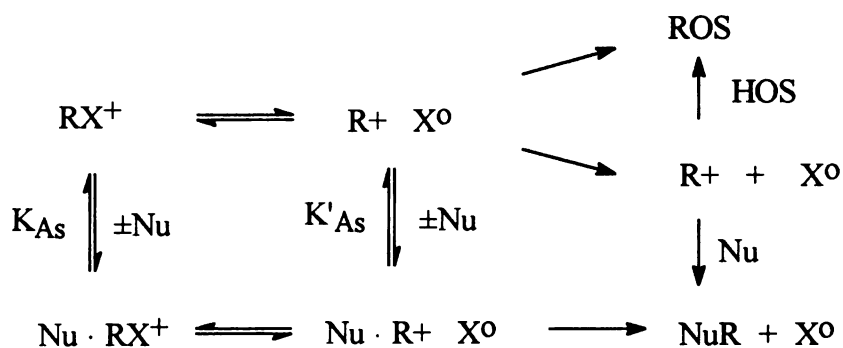
USF
LIT
M
M

than the rate for reaction with **1c**, which nicely accounts for the Hammett plot for the azide reaction. (The LUMOs for the **1b,d,e** all have the same form as that for **1c**.) The LUMO for the ground and transition states for **1a** are the same; thus to achieve the transition state for the S_N1 reaction requires no change in orbital symmetry relative to the ground state, which should be a lower energy process than that required by **1c**, which has different symmetries for the ground and transition states. Note that this is pattern is not limited to these systems. The same relative shapes and symmetries of orbitals between ground states and cations is seen between 2-arylpropenes and the corresponding *t*-cumyl carbenium ions obtained by protonating the olefins, the relative free energies of which are the basis of the $\delta\Delta G^\circ$ gas-phase substituent scale.⁸ This provides a rationale for the fit of the gas-phase dissociation data to this scale and the equivalent solution scale, σ^+ . For **2a**, the LUMO is localized on the pyridine, and achieving the transition state for heterolytic cleavage requires extensive orbital reorganization, which may also be a factor that prevents the S_N1 reaction from occurring. In the gas phase, this energy requirement would not prevent the reaction, it would merely slow it down, which is the effect seen (Chapter 6).

These results also provide the basis for a challenge to the Jencks scheme⁹ (Scheme 9.1). Jencks has argued that a concerted bimolecular reaction (lower pathway) will take place only when the *alternative* unimolecular pathway (upper pathway) is unfavorable because the lifetime of the intermediate is so short that a concerted reaction is enforced, and that stabilization in an enforced exploded transition state is provided by the interaction of the nucleophile and leaving group with the cationic center (Nu · R+ X^o). None of these criteria is met in our system.

First, the solvolysis of **1a**, the 4-sulfobenzoate and the work of Aymes and Richard¹⁰ on the corresponding chloride and benzoates show that the 4-methoxybenzyl carbenium ion is a solvent equilibrated intermediate in pure water or highly

USF
LIBRARY



Scheme 9.1

aqueous systems. Second, SMe_2 is a much better nucleophile than 3-cyanopyridine, but in the reaction of **1a** and **2a** with azide under identical conditions the rates are essentially the same, which suggests either that the nucleophiles and leaving groups are stabilizing the transition state to the same extent, which seems highly unlikely, or that the "tickling" effect does not operate in this system. The LUMOs of the activated complexes for heterolytic bond cleavage, the frontier orbital with which a nucleophile would combine in the Jencks scheme, are the same for **1a** and **2a** (Figure 9.1). Thus a nucleophile would find the same orbitals with the same symmetries to tickle, and any enhanced stabilization would be the result of the interaction of the leaving group with the reaction center. Because of the difference in nucleophilicities, it is doubtful that leaving group tickling can account for the similar rates. Moreover, the β_{LG} values for **2a-4a** show a large amount of bond-breaking at the transition state, but the fact that the 4-methoxybenzyl and methyl substrate have the same value of β_{LG} shows that the geometry of the activated complex is not related to the stability of the putative intermediate. While data are not available to calculate β_{LG} in the sulfonium series, Swain, et al.¹¹ have shown that the activated complex for the reaction of benzylmethylphenylsulfoniums with hydroxide gets "tighter" as the substituent on the benzyl becomes less electron donating. With the orbital symmetry arguments

1941

USF

made above, this Hammond argument is consistent with the curved Hammett plot for the azide reaction of the sulfoniums.

There are theoretical reasons to doubt the Jencks mechanism as well. Jorgensen,¹² among others, has shown with *ab initio* and Monte Carlo methods that the familiar double-well potential energy surface for a gas-phase S_N2 identity reaction $X^- + RX \rightarrow XR + X^-$ is lost as solvent is included explicitly in the

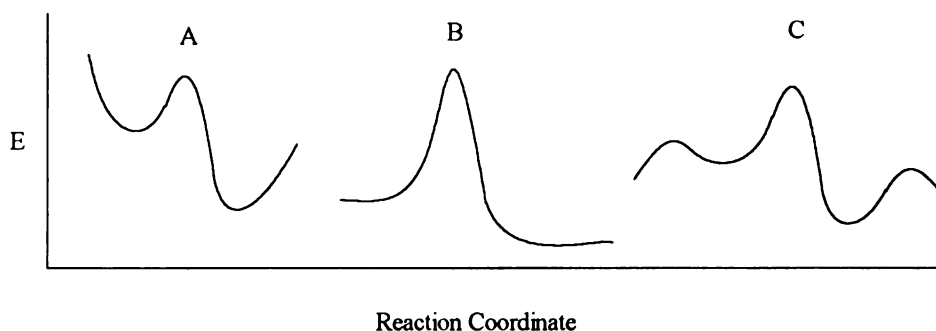


Figure 9.2. Two-dimensional potential energy surfaces for gas-phase displacement reactions. A, unsymmetrical; B, reaction in A with solvent included explicitly; C, reaction A in which there is a strong attraction between nucleophile and substrate.

computation with a concomitant increase in the reaction barrier. For $Cl^- + MeCl$, Jorgensen's methods accurately reproduce the experimental values of ΔG^\ddagger for the gas-phase and solution reactions. The surfaces shown in Figure 9.2 are for an unsymmetrical reaction ($X + RY$) but the principles and conclusions remain the same. The double potential wells in Surface A, which represent formation of ion-dipole complexes between nucleophile and reactant, are damped out in Surface B because the favorable energy of formation for the complexes is offset by the energy needed to desolvate the nucleophile. A third possibility is shown in surface C, in which the energy of desolvation and the ion-dipole attraction are significant, but are out of phase.

It seems reasonable that the general case described by Jencks fits Surface B for the reaction of a negative nucleophile with a neutral substrate, for which the

NOV 19 1951

USF

energy of formation of the ion-dipole complex should be much less than the energy needed to desolvate the nucleophile. Surface C, however, is a reasonable description of the reactions of 1a with negative nucleophiles, in which both the substrate and nucleophile would be strongly solvated in water and have a significant Coulombic attraction. Indeed, the non-salt effect breaks in the second-order rate plots and the fit of the selectivity data to the equation for this preassociation mechanism are entirely consistent with this energy profile, in which the ion pair is a distinct intermediate leading to the transition state for the concerted reaction (Chapter 4). Moreover, the fact that there is no difference, either in nonlinearity of second-order plots or of a change in rate constant, for reaction of 1a with the neutral nucleophile pyridine-d₅ is consistent with a simple S_N2 mechanism that proceeds along Surface B through an encounter complex that is not an intermediate on the reaction coordinate. Thus this system provides good kinetic evidence for a preassociation mechanism, but it is not Jencks's.

Heterolytic Cleavage of the Nicotinamide-Ribosyl Bond

*"The blood-dimmed tide is loosed, and everywhere
the ceremony of innocence is drowned."*

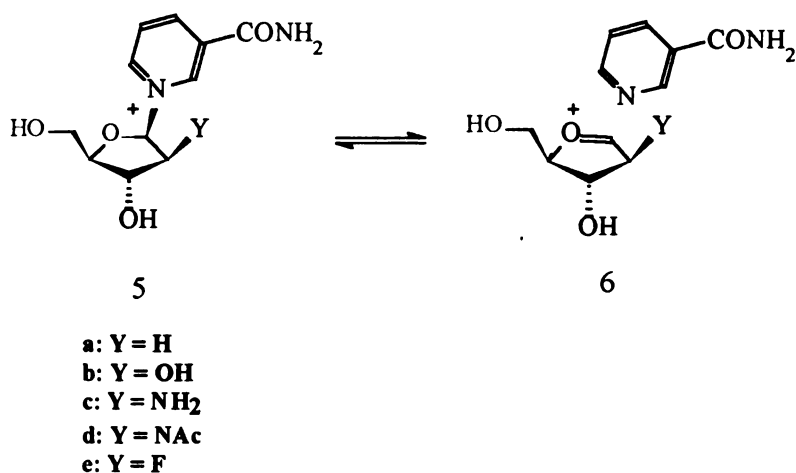
Yeats

Handlon's work¹³ with β -nicotinamide ribosides and arabinosides showed that the hydrolysis reaction occurs with a large difference in charge between the ground and transition states ($\rho_F = -6.7$) and that ΔS^\ddagger values were positive for all substrates studied (except the *trans* NAc compounds that undergo anchimerically assisted cleavage of the nicotinamide-ribosyl bond). Recent work showed that the Taft plot for enzyme-catalyzed cleavage of NAD⁺ analogs with 2' substituents paralleled the plots for the ribo and ara compounds.¹⁴ Ta-Shma¹⁵ found that the rate of hydrolysis of NAD⁺ in the presence of 2.5M azide was increased only by

UCSF
LIBRARY

20% compared to the hydrolysis in water alone. All of these results are consistent with unimolecular dissociation of the bond with formation of either an ion-dipole complex or a solvent-equilibrated oxocarbenium ion. By analogy with the estimated lifetime of the methoxymethyl carbenium ion, however, Young and Jencks¹⁶ have argued that the glycosyl oxocarbenium ion is too unstable to exist as solvent-equilibrated intermediate. Thus we have reached a conundrum.

The resolution of it is relatively straightforward. The gas-phase dissociation of the β -nicotinamide arabionsides **5a-e** occurs with formation of an ion-dipole



Scheme 9.2

complex (Chapter 5). The relative rates follow the Taft equation, and the computed ΔH^\ddagger correlate well with the solution values of ΔH^\ddagger and ΔG^\ddagger . Moreover, the relative rates are all greater than the relative rates for **3a** measured under identical conditions (Chapter 6). Therefore, in the gas-phase, the arabinosyl oxocarbenium ions are intrinsically more stable than the 4-methoxybenzyl carbenium ion.

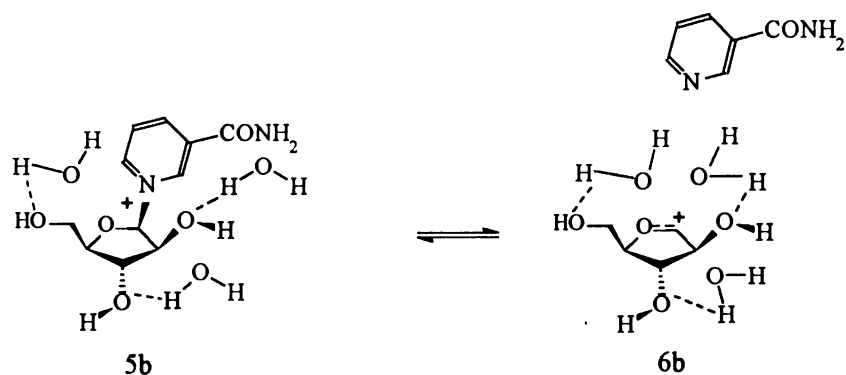
In their original estimate of the lifetime of the glycosyl oxocarbenium ion, Young and Jencks¹⁶ noted that the relative rates for the specific-acid catalyzed hydrolysis of formaldehyde dimethyl acetal was 10^4 greater than the rate for hydrolysis of methyl glucoside, and concluded that the lifetime of the intermediate

1951

USF

oxocarbenium ion must therefore be much less than the lifetime of the methoxy-methyl oxocarbenium ion, which they estimated to be 10^{-17} sec. With the measured rate constants available now for **3a**, we can make the same comparison: hydrolysis of **5a** is 10^4 faster than **3a**, and, because the 4-methoxybenzyl carbenium ion is a solvent-equilibrated intermediate, the arabionosyl and ribosyl oxocarbenium ions are also solvent-equilibrated intermediates.

This comparison of *solution* relative rates in this way is of course nonsense. If we have shown anything in this work it is that solvation is of utmost importance for determining mechanism. In this we follow the wise counsel of Arnett¹⁷ and Ritchie.¹⁸ The ordering of solvent about the essentially hydrophobic benzyl substrates will be vastly different than the ordering of solvent about the hydrophilic sugars. The reordering of solvent as each reaches the activated complex for heterolytic bond cleavage will therefore be different both in enthalpy and entropy, and the rates of these processes will be controlled by different arrays of solvent within the first and second solvation shells. These effects can be dramatic. For instance, we have shown that the difference between ΔS^\ddagger for hydrolysis of **1a** in H_2O^2 (13.4 ± 1.7 gibbs/mol) and in D_2O^3 (7.1 ± 1.0 gibbs/mol) is the result of a mere 5-7% difference in the strength of hydrogen bonds between H_2O and D_2O (Chapter 3). Imagine, then, the fanciful process--analogous to a similar fanciful drawing in the famous paper by Arnett and Reich¹⁷--shown in Scheme 9.3, in which the waters hydrogen-bonded to the arabionsyl hydroxyls undergo minor positional shifts after cleavage of the bond to form a stabilizing "solvation shell" about the oxocarbenium ion center. This would require little entropic deficit compared to the relative large changes in solvation about the 4-methoxybenzyl carbenium ion, in which the developing charges on the methoxy and ring would have to be solvated (solvent reorganization about the reaction center, which is already positively charged, should be relatively minor) with a



Scheme 9.3

substantial loss of entropy. Because it is nearly impossible to deconvolute the source of entropic changes in these complex systems, direct comparison of the rates for the different substrates, especially if they react by different mechanisms, is fraught with danger.

In the *gas phase*, however, the only significant entropic change would be translational, and should be essentially the same for cleavage of the substrate-nicotinamide bond in either **3a** or **5b**. The measure of the relative stabilities of the intermediates would then be reflected in the relative rates of dissociation, which favors **5b**.

To examine this further, potential energy surfaces were computed using semi-empirical methods for a wide variety of substrates with different leaving groups that contain potentially stable oxocarbenium intermediates (Chapters 7 and 8). While some of the results obtained are extremely complex--see the dependence on rotomers for dissociation of methyl ribosides and glucosides, for instance--the general conclusions are relatively straightforward.

In a set of experiments designed to test the intermediate lifetime hypothesis, Knier and Jencks¹⁹ studied the substitution reactions of $\text{MeOCH}_2\text{NMe}_2\text{Ar}^+$. They concluded that these substrates reacted with nucleophiles by a concerted mechanism and not through either an ion-dipole complex or solvent-equilibrated

1951

USF

carbenium ion. Our results for the heterolytic cleavage of the substrate agree with this assessment: in AM1 and PM3, these substrates dissociate directly to the oxocarbenium ion and dimethylaniline without a distinct transition state (Chapter 7). Cleavage of $\text{MeOCH}_2\text{OR}_2^+$ ($\text{R} = \text{H}, \text{Me}$ in various proportions), however, proceeds with formation of an intermediate ion-dipole complex (Chapter 8). For tetrahydrofuranyl, tetrahydropyranyl, ribosyl, and glucosyl substrates, those with pyridinium or ROR leaving groups all dissociate with formation of an ion-dipole complex. In systems for which experimental data are available, this computational pattern is matched exquisitely by large, positive ΔS^\ddagger for bond cleavage, consistent with a dissociative mechanism to either the ion-dipole complex containing an oxocarbenium ion or to the naked oxocarbenium ion. Thus, as we found for the direct comparison of stabilities in the gas phase, these results tend to support the idea that oxocarbenium ions are sufficiently stable to be intermediates in these reactions.

These computations provide no reason to suspect that ribosides undergo specific-acid catalyzed bond cleavage by an A-2 mechanism, in which the protonated leaving group is displaced by water. Indeed, the patterns found for ribosides match those found for glucosides, which hydrolyze by an A-1 mechanism.²⁰ The mechanisms were based on negative ΔS^\ddagger for ribosides and positive ΔS^\ddagger for glucosides, but as noted above, solvation effects may determine these values and may not necessarily reflect a change in mechanism.

Enzyme Catalysis of NAD^+

"Surely some revelation is at hand."

Yeats

Calf spleen NAD^+ glycohydrolase "catalyzes" the cleavage of the ribosyl-nicotinamide bond with a rate increase of ca. 10^4 relative to the solution reaction

REMI

USF

(from $\log V_{\max}$ compared with $\log k_w$).¹⁴ While the formation of the diol anion of NAD^+ itself is important,²¹ the relative rates are essentially the same independent of the presence of an ionizable group at the 2'-position of the riboside. This raises an interesting question: how can an enzyme "catalyze" a first-order reaction? There are several possibilities.

One is that the enzyme stabilizes the intermediate sufficiently that its formation is favored; this could be accomplished by having an ionized carboxyl under the oxocarbenium center in the active site that would stabilize the charge electrostatically without formation of an substrate-enzyme acyl intermediate. This mechanism has been advocated for stabilization of glucosyl oxocarbenium ions in enzymes such as lysozyme. Nonetheless, Czarnik and his colleagues²² have shown that placing a carboxy group under the oxocarbenium ion center in a riboside has no more stabilizing effect than bulk water, at least as measured by relative rates of dissociation of a protonated purine leaving group.

The results obtained in this work offer an alternative view. As noted above, the difference in ΔS^\ddagger for the azide substitution reaction of **1a** and **2a** is ca. 15 gibbs/mol, which is apparently the difference in solvation entropy between the hydrophobic SMe_2 and a pyridine. If upon binding NAD^+ in the enzyme active site the leaving group is desolvated--that is, if that part of ΔS^\ddagger in the solution reaction that is related to solvation of the nicotinamide is released upon binding, it becomes part of the ΔS° term in ΔG° for K_m --then the subsequent bond cleaving reaction would take place without the retarding entropic effect seen in solution. The rate acceleration²³ expected for a $\Delta\Delta S^\ddagger$ of ca. 15 gibbs/mole is about 5×10^3 , which is in excellent agreement with the 10^4 difference in rate reported by Handlon, et al.¹⁴ for the calf spleen NAD^+ glycohydrolase. While this comparison is of course relatively crude--it assumes, for instance, that ΔH^\ddagger is constant, which is a

RECEIVED
MAY 11 1961
USF

reasonable but unproven assumption--it does suggest that enzyme "catalysis" of NAD⁺ bond cleavage is merely a solvent entropic effect.

References and Notes

- (1) Buckley, N.; Oppenheimer, N.J. *J. Org. Chem.* **1994**, *59*, 5717-5723.
- (2) Kevill, D.N.; Ismail, N.H.J.; D'Souza, M.J. *J. Org. Chem.* **1994**, *59*, 6303-6312.
- (3) Reviewed in Katritzky, A.R.; Brycki, B.E. *Chem. Soc. Rev.* **1990**, *19*, 83-105, and elsewhere.
- (4) Swain, C.G.; Thornton, E.R. *J. Org. Chem.* **1961**, *26*, 4808-4809;
Swain, C.G.; Rees, T.; Taylor, L.J. *J. Org. Chem.* **1963**, *28*, 2903;
- (5) Pross, A. *Adv. Phys. Org. Chem.* **1985**, *21*, 99-196; Pross, A.; Shaik, S.S. *Acc. Chem. Res.* **1983**, *16*, 363-370.
- (6) Klopman, G. *J. Am. Chem. Soc.* **1968**, *90*, 223-234. Salem, L. *J. Am. Chem. Soc.* **1968**, *90*, 543-552.
- (7) Computed as described in Buckley, N.; Handlon, A.L.; Maltby, D.; Burlingame, A.L.; Oppenheimer, N.J., *J. Org. Chem.* **1994**, *59*, 3609-3615, and Chapters 5,7, and 8.
- (8) Taft, R.W.; Topsom, R.D. *Prog. Phys. Org. Chem.* **1987**, *16*, 2-83.
- (9) Jencks, W.P. *Acc. Chem. Res.* **1980**, *13*, 161-169; Jencks, W.P. *Chem. Soc. Rev.* **1981**, *10*, 345-375. The "exploded" transition state concept has been challenged: Schröder, S.; Buckley, N.; Oppenheimer, N.J.; Kollman, P.A. *J. Am. Chem. Soc.* **1992**, *114*, 8232-8238.
- (10) Amyes, T.L.; Richard, J.P. *J. Am. Chem. Soc.* **1990**, *112*, 9507-9512.
- (11) Swain, C.G.; Burrows, W.D.; Schowen, B.J. *J. Org. Chem.* **1968**, *33*, 2534-2536.

USF
LIBRARY

(12) Chandrasekhar, J.; Smith, S.F.; Jorgensen, W.L.. *J. Am. Chem. Soc.* **1985**, *107*, 154-163.

(13) Handlon, A.L.; Oppenheimer, N.J. *J. Org. Chem.* **1991**, *56*, 5009-5010. Handlon, A.L. Ph.D. Dissertation, The University of California, San Francisco, 1991.

(14) Handlon, A.L.; Xu, C.; Müller-Steffner, H.-M.; Schuber, F.; Oppenheimer, N.J. *J. Am. Chem. Soc.* **1994**, *116*, 12087-12088.

(15) Ta-Shma, R.; Oppenheimer, N.J., in preparation.

(16) Young, P.R.; Jencks, W.P. *J. Am. Chem. Soc.* **1977**, *99*, 8238-8248.

(17) Arnett, E.M.; Reich, R. *J. Am. Chem. Soc.* **1980**, *102*, 5892-5902.

"[M]any attempts to deduce detailed structures for bimolecular transitions states in displacement, addition, or elimination reactions are seriously overextended [because] the energetics of the reaction are dominated by solvation dynamics into which there is only the most primitive insight at present."

(18) Ritchie, C.D. In *Solute-Solvent Interactions*; Coetzee, J.F., Ritchie, C.D., Eds.; Marcel Dekker: New York, 1976, Vol. 2; p. 265. "All patterns of reactivity and selectivity arise primarily from solvent effects, and not from some inherent property of the solute reactant."

(19) Knier, B.L.; Jencks, W.P. *J. Am. Chem. Soc.* **1980**, *102*, 6789-6796.

(20) Capon, B. *Chem. Rev.* **1969**, *69*, 407-498. (b) Cordes, E.H.; Bull, H.G. *Chem. Rev.* **1973**, *73*, 581-603.

(21) Johnson, R.W.; Marschner, T.M.; Oppenheimer, N.J. *J. Am. Chem. Soc.* **1988**, *110*, 2257-2263.

(22) Cherian, X.M.; Van Arman, S.A.; Czarnik, A.W. *J. Am. Chem. Soc.* **1990**, *112*, 4490-4498.

(23) Lowry, T.H.; Richardson, K.S. *Mechanism and Theory in Organic Chemistry*; Harper & Row: New York, 1981, Second Ed., p. 196.



For reference

Not to be taken
from the room.

6441763



3 1378 00644 1763

